

The Role of the Neuropeptides

NPF, sNPF, ITP and PDF in the Circadian Clock of *Drosophila melanogaster*

Die Rolle der Neuropeptide

NPF, sNPF, ITP und PDF in der Circadianen Uhr von *Drosophila melanogaster*



Doctoral thesis for a doctoral degree
at the Graduate School of Life Sciences,
Julius-Maximilians-Universität Würzburg,

Section Neuroscience

submitted by

Christiane Luibl

née Hermann

from Eggenfelden

Würzburg, January 2014

Submitted on:

Office stamp

Members of the Thesis Committee (Promotionskomitee):

Chairperson: **Prof. Dr. Wolfgang Rössler**

Primary Supervisor: **Prof. Dr. Charlotte Förster**

Supervisor (Second): **Prof. Dr. Thomas Raabe**

Supervisor (Third): **Assistant Prof. Ori T. Shafer**

Date of Public Defence:

Date of Receipt of Certificates:

“Science is organized knowledge. Wisdom is organized life.”

Immanuel Kant (1724-1804)

Table of Contents

Table of Contents	1
Zusammenfassung	3
Summary.....	6
List of publications.....	8
1 Introduction.....	9
1.1 A Rhythmic World	9
1.2 The Circadian Clock of <i>Drosophila melanogaster</i>	11
1.3 Neuropeptide Circuits in Insects.....	16
1.4 Neuropeptides Expressed in <i>Drosophila</i> Clock Neurons	18
1.5 Aim of Study.....	22
2 Material and Methods.....	24
2.1 Material.....	24
2.1.1 Fly strains.....	24
2.1.2 Antibodies.....	26
2.2 Methods.....	28
2.2.1 The <i>GAL4/UAS</i> System.....	28
2.2.2 Molecular Methods	29
2.2.3 Immunocytochemistry	35
2.2.4 Behavioral Assay.....	37
2.2.5 Live Imaging	39
2.2.6 <i>In silico</i> Analysis	44
2.2.7 Statistics.....	44
3 Results.....	45
3.1 The Clock Network Is Conserved in Different <i>Drosophila</i> Species (Paper 1).....	45

Table of Contents

3.2	NPF ⁺ Clock Neurons Modify E Activity and Free-Running Period (Paper 2).....	47
3.3	ITP is a new functional clock neuropeptide (Paper 3, <i>submitted</i>)	48
3.4	The role of sNPF in circadian behavior	50
3.5	Clock neuron responsiveness to bath applied peptides	65
3.5.1	NPF Application	65
3.5.2	sNPF Application	70
3.5.3	NPFR1 and sNPFR1 expression.....	75
4	General Discussion	77
4.1	Importance and Conservancy of Neuropeptides in the Clock System	77
4.2	Neuropeptide F (NPF)	79
4.3	short Neuropeptide F (sNPF)	83
4.4	Ion Transport Peptide (ITP)	88
4.5	Final Conclusions	93
5	References.....	97
	Full text Paper 1	109
	Full text Paper 2	131
	Full Text Paper 3 (Manuscript, <i>submitted</i>).....	149
	Appendix.....	187
	Additional Material	187
	Abbreviations	190
	Acknowledgements.....	191
	Curriculum vitae	192
	Declarations.....	193

Zusammenfassung

Die meisten Organismen haben endogene Uhren entwickelt, mit deren Hilfe sie ihre Verhaltensweisen, ihren Metabolismus und auch ihre Physiologie an die periodisch wechselnden Umweltbedingungen auf unserer Erde anpassen können. Die sogenannten circadianen Uhren steuern dabei biologische Rhythmen, die an täglich wiederkehrende Umweltfaktoren angepasst sind. Schon seit Jahrzehnten wurden diese circadianen Uhren von Chronobiologen in verschiedensten Modellorganismen untersucht. Zu diesen gehört auch die Taufliege *Drosophila melanogaster*, welche im Rahmen dieser Doktorarbeit Verwendung fand.

Anatomisch besteht die circadiane Uhr der Taufliege aus etwa 150 sogenannten Uhrneuronen, die sich im dorsalen und lateralen Protocerebrum der Fliege befinden. Diese können anhand ihrer Position im Gehirn, ihrer Morphologie als auch ihrer neurochemischen Eigenschaften charakterisiert werden. Es wurde bereits in früheren Arbeiten gezeigt, dass einige dieser Uhrneuronen jeweils ein oder mehrere Neuropeptide exprimieren, welche mit großer Wahrscheinlichkeit die wichtigsten Signalmoleküle der Uhr darstellen. Dabei ist der „Pigment Dispersing Factor“ (PDF) wohl das Neuropeptid, welches bisher in Bezug auf seine Funktion in der Uhr die größte Aufmerksamkeit fand. Es ist daher auch das Neuropeptid, das bei Weitem am besten untersucht ist. So wurde bereits gezeigt, dass PDF die Oszillationen der Uhrneuronen untereinander synchronisiert und auch in Ausgangssignalwegen der Uhr zu nachgeschalteten Gehirnregionen eine Rolle spielt.

In Zusammenarbeit mit verschiedenen Kollegen, wurde im Rahmen dieser Doktorarbeit untersucht, welche Rolle drei andere Neuropeptide, welche in den Uhrneuronen exprimiert werden, in der Generierung von Verhaltensrhythmen spielen. Der Fokus lag dabei auf der Untersuchung des Neuropeptids F (NPF) des short Neuropeptids F (sNPF) und des Ion Transport Peptids (ITP). Wir konnten für manche dieser Peptide zeigen, dass ihre Verwendung im Uhrnetzwerk unterschiedlicher *Drosophila*-Arten konserviert zu sein scheint. Im Falle von PDF zeigten sich jedoch Unterschiede in der zellspezifischen Expression in Arten aus südlichen Breitengraden im Vergleich zu Arten aus nördlichen Breitengraden. Zusammen mit ergänzenden Verhaltensdaten anderer Arbeitsgruppen,

gehen wir davon aus, dass unterschiedliche Arten bestimmte Eigenschaften ihrer Uhr – wie etwa die Neuropeptid-Expression in bestimmten Zellen – verändert haben, um ihr Verhalten bestmöglich an ihr jeweiliges Habitat anzupassen.

Des Weiteren wurde in dieser Arbeit die Aktivitätsrhythmik in Fliegen untersucht, in welchen gezielt bestimmte Neuropeptid-Systeme auf genetischem Wege - entweder durch Zellablation oder RNA-Interferenz (RNAi) - manipuliert wurden. Wir konnten zeigen, dass wohl keines der untersuchten Peptide eine ähnlich große Rolle für die Aktivitätsrhythmik spielt wie PDF. Aus früheren Arbeiten geht hervor, dass PDF sowohl für die Aufrechterhaltung eines Rhythmus in konstanter Dunkelheit (DD), als auch für die Generierung der Morgenaktivität und für die richtige Phasenlage der Abendaktivität in Licht-Dunkel Zyklen (LD) essentiell ist. Ergebnisse der vorliegenden Arbeit zeigen nun, dass NPF und ITP die Abendaktivität in LD fördern, dass sie jedoch nicht die einzigen Faktoren sind, die dies bewerkstelligen. ITP scheint außerdem Aktivität während der Nacht zu hemmen. Des Weiteren stellen ITP und möglicherweise auch sNPF eine schwache Perioden verkürzende Komponente in DD dar, ganz im Gegensatz zu PDF, welches eine Perioden verlängernde Wirkung besitzt. Jedoch scheinen weder ITP, NPF noch sNPF für die generelle Aufrechterhaltung eines Rhythmus in DD nötig zu sein.

Vorhergehende Arbeiten wiesen bereits darauf hin, dass PDF wahrscheinlich rhythmisch an den dorsalen Nervenendigungen ausgeschüttet wird. Unsere jetzigen Ergebnisse zeigen desweiteren eine Oszillation in der ITP-Immunfärbung in den dorsalen Projektionen der ITP⁺ Uhrneuronen in LD, was auch auf eine rhythmische Ausschüttung dieses Peptids schließen lässt. Die rhythmische Freisetzung beider Peptide scheint für die Aufrechterhaltung eines Verhaltensrhythmus in DD wichtig zu sein, da eine konstant hohe Menge an ITP und PDF im dorsalen Gehirn den Freilauf-Rhythmus stören.

Die live-Imaging Experimente dieser Arbeit zeigten, dass sNPF auf manche Uhrneuronen inhibitorisch wirkt – auch auf einige, die durch PDF aktiviert werden können. sNPF könnte also als Signalmolekül innerhalb des Uhrnetzwerkes fungieren. Auch NPF führte zu inhibitorischen Zellantworten, jedoch waren diese äußerst schwach und betrafen nur wenige Uhrneuronen, was darauf schließen lässt, dass dieses Peptid wahrscheinlich am Signalausgang der Uhr beteiligt ist. Es war uns bisher nicht möglich dieselben live-Imaging Untersuchungen auch für ITP durchzuführen, jedoch zeigten Überexpressionsstudien mit

verschiedenen Treiberlinien, dass auch ITP mit großer Wahrscheinlichkeit im Signalausgang der Uhr fungiert.

Zusammenfassend lässt sich sagen, dass alle hier untersuchten Neuropeptide an der Kontrolle der rhythmischen Lokomotoraktivität von *Drosophila melanogaster* mitwirken. Dabei ist PDF eindeutig der dominierende Faktor, während die anderen Neuropeptide die Wirkung von PDF eher feinregulieren oder komplementieren. Aus den Daten kann geschlossen werden, dass die örtliche und zeitliche Funktionsweise dieser verschiedenen Peptide sehr komplex ist, um sowohl die Prozessierung von Signalen innerhalb des Uhrnetzwerkes als auch in den weitgehend noch unbekanntem Ausgangswegen der Uhr zu gewährleisten.

Summary

Organisms have evolved endogenous clocks which allow them to organize their behavior, metabolism and physiology according to the periodically changing environmental conditions on earth. Biological rhythms that are synchronized to daily changes in environment are governed by the so-called circadian clock. Since decades, chronobiologists have been investigating circadian clocks in various model organisms including the fruitfly *Drosophila melanogaster*, which was used in the present thesis.

Anatomically, the circadian clock of the fruitfly consists of about 150 neurons in the lateral and dorsal protocerebrum, which are characterized by their position, morphology and neurochemistry. Some of these neurons had been previously shown to contain either one or several neuropeptides, which are thought to be the main signaling molecules used by the clock. The best investigated of these neuropeptides is the Pigment Dispersing Factor (PDF), which had been shown to constitute a synchronizing signal between clock neurons as well as an output factor of the clock.

In collaboration with various coworkers, I investigated the roles of three other clock expressed neuropeptides for the generation of behavioral rhythms and the partly published, partly unpublished data are presented in this thesis. Thereby, I focused on the Neuropeptide F (NPF), short Neuropeptide F (sNPF) and the Ion Transport Peptide (ITP). We show that part of the neuropeptide composition within the clock network seems to be conserved among different *Drosophila* species. However, the PDF expression pattern in certain neurons varied in species deriving from lower latitudes compared to higher latitudes. Together with findings on the behavioral level provided by other people, these data suggest that different species may have altered certain properties of their clocks - like the neuropeptide expression in certain neurons - in order to adapt their behavior to different habitats.

We then investigated locomotor rhythms in *Drosophila melanogaster* flies, in which neuropeptide circuits were genetically manipulated either by cell ablation or RNA interference (RNAi). We found that none of the investigated neuropeptides seems to be of equal importance for circadian locomotor rhythms as PDF. PDF had been previously shown to be necessary for rhythm maintenance in constant darkness (DD) as well as for

the generation of morning (M) activity and for the right phasing of the evening (E) activity in entrained conditions. We now demonstrate that NPF and ITP seem to promote E activity in entrained conditions, but are clearly not the only factors doing so. In addition, ITP seems to reduce nighttime activity. Further, ITP and possibly also sNPF constitute weak period shortening components in DD, thereby opposing the effect of PDF. However, neither NPF or ITP, nor sNPF seem to be necessary in the clock neurons for maintaining rhythmicity in DD.

It had been previously suggested that PDF is released rhythmically from the dorsal projection terminals. Now we discovered a rhythm in ITP immunostaining in the dorsal projection terminals of the ITP⁺ clock neurons in LD, suggesting a rhythm in peptide release also in the case of ITP. Rhythmic release of both ITP and PDF seems to be important to maintain rhythmic behavior in DD, since constantly high levels of PDF and ITP in the dorsal protocerebrum lead to behavioral arrhythmicity.

Applying live-imaging techniques we further demonstrate that sNPF acts in an inhibitory way on few clock neurons, including some that are also activated by PDF, suggesting that it acts as signaling molecule within the clock network and has opposing effects to PDF. NPF did only evoke very little inhibitory responses in very few clock neurons, suggesting that it might rather be used as a clock output factor. We were not able to apply the same live-imaging approach for the investigation of the clock neuron responsiveness to ITP, but overexpression of ITP with various driver lines showed that the peptide most likely acts mainly in clock output pathways rather than inter-clock neuron communication.

Taking together, I conclude that all investigated peptides contribute to the control of locomotor rhythms in the fruitfly *Drosophila melanogaster*. However, this control is in most aspects dominated by the actions of PDF and rather only fine-tuned or complemented by the other peptides. I assume that there is a high complexity in spatial and temporal action of the different neuropeptides in order to ensure correct signal processing within the clock network as well as clock output.

1 Introduction

1.1 A Rhythmic World

Our world has several periodical characteristics, to which organisms ranging from primitive unicellular bacteria or protozoans up to plants and higher animals, including us humans, have adapted to. Thus, organisms have evolved biological rhythms in behavior, metabolism and physiology, which enable them to cope with their periodically changing environment. The research field of Chronobiology, which was founded by scientists like Halberg, Bünning, Aschoff and Pittendrigh, deals with the investigation of these biological rhythms since the 1930s.

The most prominent rhythms on our planet are the daily changes in light and temperature that are mediated by the rotation of the earth around its axis. To anticipate these periodic environmental changes, organisms have evolved endogenous clocks, which are able to autonomously generate a rhythm of approximately 24 hours. These clocks are therefore also called circadian clocks (from lat. circa = approximately; dies = day; Fig. 1). Receiving sensory input from the environment in terms of so-called Zeitgebers like light, temperature, humidity, food or social contacts, the oscillation of the circadian clock is synchronized to exactly 24 hours. This process is called entrainment. In today's modern world we sometimes experience a sudden phase shift in the occurrence of external stimuli, e.g. when travelling across time zones or even when changing from summer to winter time. The clock then needs to reentrain to the new environment, a phenomenon we know as jetlag. As soon as external Zeitgebers are completely absent, the oscillation of the clock would persist, but would free-run with its own endogenous circadian period length of approximately 24 hours.

The anatomical localization of the circadian clock within different organisms added to the understanding of its general working mechanism. Thus, it was found that unicellular organisms and plants contain an autonomous clock in every cell, whereas the clock in higher animals can be located to particular parts of the central nervous system (CNS). In mammals the nucleus suprachiasmaticus (SCN) of the Hypothalamus was identified as the master circadian pacemaker center, whereas the accessory medulla, a small neuropil between the optic lobe and the central brain, was identified as such in most insects.

Although several additional tissues in the animal body contain so-called peripheral clocks which are able to maintain autonomous oscillations, they are always governed by the master clock in the brain. Through various output pathways, which are by far not fully understood, the circadian clock creates rhythms in behavior, which allow an organism to optimally time its activity within the 24 hour cycle. Thus, organisms have not only specialized for life in different spatial ecological niches, but also for life in temporal niches, being active either at night (nocturnal), during the day (diurnal) or at twilight (crepuscular). Further, the master clock coordinates daily rhythms in physiological processes, such as the core body temperature or hormone levels, as well as rhythms in metabolism either directly or indirectly through peripheral clocks (Fig. 1).

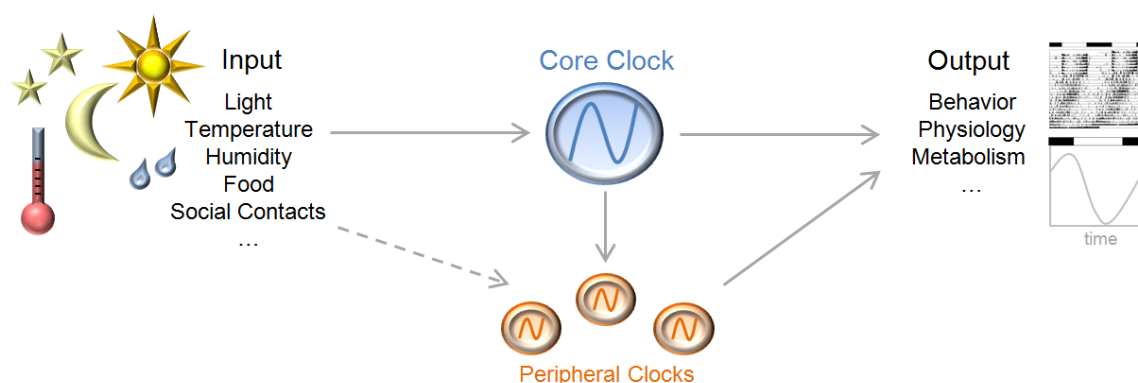


Figure 1: Schematic overview of the clock system. The core clock in the brain receives input from the environment through Zeitgebers like light, temperature, humidity, food or social contacts. The endogenous circadian rhythm is thus synchronized to the environment (entrainment). Through different output pathways, the core clock regulates rhythms in behavior, physiology or metabolism either directly or by governing the action of peripheral clocks in various body tissues.

But daily (also called diurnal) rhythms are not the only periodic changes occurring on our planet, which organisms have adapted to. The different seasons for example, which we experience every year, reflect an annual periodism in the change of average temperature and day length. Being able to anticipate seasonal changes in environment allows different organisms to time actions or processes, which are essential for survival. The right timing of flowering or growth in plants, and the right timing of reproduction, hibernation or migration in long-living animals would be examples for such adaptations. Further, there are organisms that have synchronized their behavior to lunar or also tidal rhythms, which both depend on the moon phases. How time measurement in these non-diurnal rhythms is achieved and whether the circadian clock plays a role in this mechanism is only at the

beginning of our understanding. The present thesis, however, will mostly deal with questions concerning diurnal rhythms. (reviewed by Helfrich-Förster, 2002, 2004)

1.2 The Circadian Clock of *Drosophila melanogaster*

The first experiments investigating circadian periodicity were conducted in plants followed by investigations in mammals including even humans. The discovery of the genetic basis of the circadian clock was, however, achieved by Konopka and Benzer in 1971 through their work on the fruitfly *Drosophila melanogaster*. Applying an EMS-based mutagenesis screen, they were able to identify the first gene controlling circadian rhythms, which they called *period*. Following studies on mosaic flies carrying the *per*⁰ mutation only in certain tissues and studies on anatomical brain mutants revealed that the circadian pacemaker center is located in the accessory medulla, a small neuropil in the lateral brain close to the optic lobes (Konopka et al., 1983; Helfrich, 1986; Dushay et al., 1989). This was in accordance with previous findings in the cockroach or the cricket (Page, 1982). The identification of more clock genes (see also below) and the generation of specific antibodies against their gene products allowed the identification and morphological characterization of the neuronal clock network as we know it today (e.g. Helfrich-Förster et al., 2007; for review see also Helfrich-Förster, 2002). Due to its genetic accessibility, short generation time, relative neuronal simplicity, and its numerous measurable clock output effects *Drosophila* serves as a model to study the circadian clock since the last forty years.

Clock Neuron Network

The clock of *Drosophila* consists of about 150 neurons in the lateral and dorsal brain, which are called clock neurons. These neurons can be divided into several clusters according to their location, size or neurochemical character (Fig. 2). The ventral lateral neurons (LNv) consist of four larger neurons, the so-called large LNv (lLNv), and five small neurons, the small LNv (sLNv). The latter group can be further divided into four sLNv, which express the neuropeptide Pigment Dispersing Factor (PDF) and are thus referred to be PDF-positive (PDF⁺; Helfrich-Förster, 1995), and a fifth sLNv, which is PDF-negative

(PDF⁻). Extensive neuroanatomical studies were conducted to reveal details of the projection pattern of these cells with the attempt to unravel the network properties of the neuronal clock system (Helfrich-Förster, 1995; Helfrich-Förster et al., 2007). According to these studies, the ILN_v send fibers into the ventral elongation of the ipsilateral accessory medulla and arborize in the outer layer of the ipsilateral and contralateral medulla, thereby allowing a coupling of both brain hemispheres. The PDF⁺ sLN_v also innervate the accessory medulla, but not its ventral elongation, and project into the dorsal protocerebrum through a prominent fiber bundle. The fifth sLN_v was shown to have a similar projection pattern, innervating the center of the accessory medulla and the dorsal protocerebrum. The more dorsally located group of the dorsal lateral neurons (LN_d) consists of six neurons of approximately the same size. They were shown to send out projections into the dorsal protocerebrum, which even reach to the contralateral side. Further, there are fibers splitting off of these projections, which run down innervating the ipsilateral accessory medulla. The last group of lateral neurons is the group of the lateral posterior neurons (LPN), of which the projection pattern is unknown so far. (Helfrich-Förster et al., 2007)

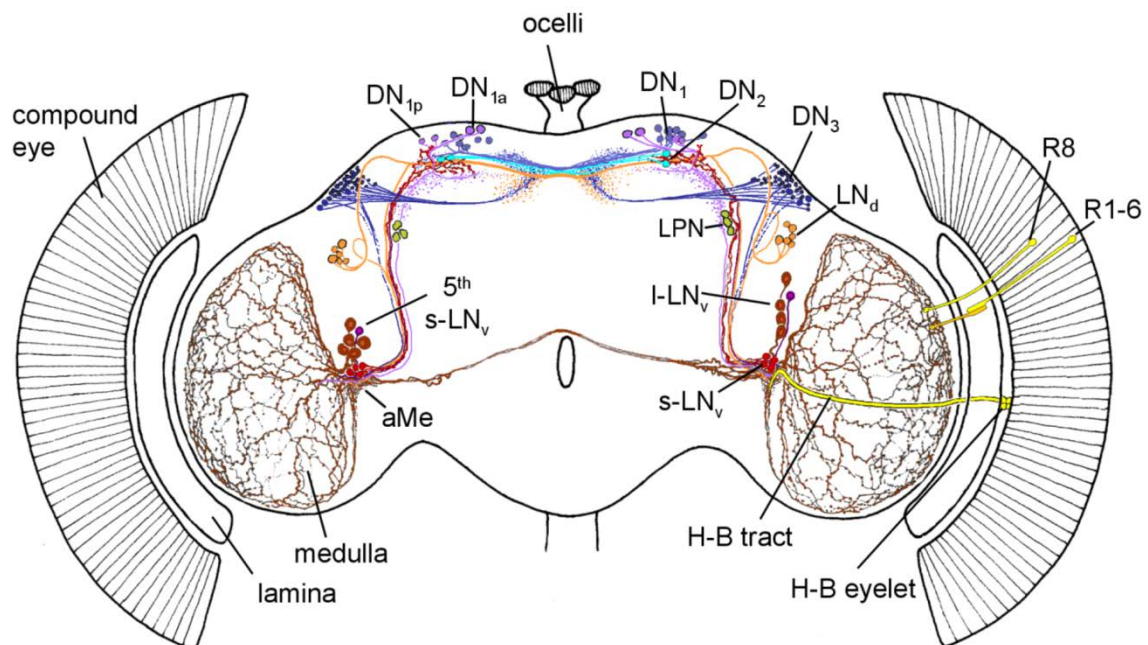


Figure 2: Schematic overview of the neuronal clock network in the adult *Drosophila* brain. The clock neurons are divided into seven different clusters: the sLN_v, ILN_v, LN_d and LPN in the lateral brain and the DN1, DN2 and DN3 in the dorsal protocerebrum. The DN1 can be further divided into DN1a and DN1p, while the sLN_v can be divided into four PDF⁺ neurons and a fifth PDF⁻ sLN_v. (For details see text. Adapted from Helfrich-Förster et al., 2007)

The dorsal clock neurons (DN) can be divided into three groups: the DN1 (further separated into the more anterior DN1a and the more posterior DN1p), DN2 and DN3. All three groups project into the dorsal protocerebrum, while some of the DN1 and DN3 also arborize into the ipsilateral accessory medulla. Taking together, all clock neuron groups innervate the dorsal protocerebrum and most of them the accessory medulla, where their fibers largely overlap, allowing not only potential clock output at these sites, but also inter-clock-neuron communication. (Helfrich-Förster et al., 2007)

Molecular Clock Mechanism

The molecular mechanism of the clock consists of two interlocked negative and positive feedback loops, in which clock genes are transcribed rhythmically within the clock neurons and the resulting proteins influence their own transcription (Fig. 3). The key components in this machinery are the two clock proteins CLOCK (CLK) and CYCLE (CYC), which form heterodimers and act as transcriptional activators recognizing a certain DNA-motif, the so-called E-box, in the promoter region of clock controlled genes (*ccg*; Fig. 3, Allada et al., 1998; Darlington et al., 1998; Rutila et al., 1998). Thus, CLK and CYC activate the transcription of the two clock genes *period* (*per*) and *timeless* (*tim*). Both mRNAs are then translocated to the cytoplasm, where they are translated and the PER and TIM proteins accumulate. PER and TIM form heterodimers, thereby enhancing PER protein stability (Price et al., 1998). The heterodimers enter the nucleus and inhibit their own transcription by an interaction between PER and CLK, which prevents the CLK/CYC dimer from further binding to the E-boxes (Lee et al., 1999). This oscillation is synchronized to the surrounding light-dark (LD) cycle by the action of the blue-light sensitive protein CRYPTOCHROME (CRY), which is expressed in most clock neurons (Emery et al., 1998; Yoshii et al., 2008). In the morning CRY is activated by light and leads to the degradation of TIM (Lin et al., 2001), which also destabilizes PER. Thus, the inhibiting action of PER and TIM decreases during the day together with PER/TIM protein levels and the CLK/CYC heterodimers can activate *per* and *tim* transcription again. During the night, when CRY is not activated, PER and TIM will again accumulate until the cycle restarts in the morning.

In the second feedback loop, the CLK/CYC heterodimer activates the transcription of the two clock genes *vri* (*vri*) and *Par domain protein 1* (*Pdp1*; Blau and Young, 1999; Cyran et al., 2003). Both VRI and PDP1 proteins then feed back to their own transcription by regulating the transcription of the *clock* (*clk*) gene, whereby VRI is repressing and PDP1 is activating. Thus, both feedback loops are interlocked on the level of *clk* expression, which is timed reciprocally to the *per/tim* expression in the 24 hour cycle.

In fact, this description is a rather simplified representation of the whole mechanism, since there are more components involved regulating e.g. protein stabilities or interactions (especially different kinases and phosphatases; details were reviewed by Peschel and Helfrich-Förster, 2011). However, these details are of no particular relevance for the present thesis.

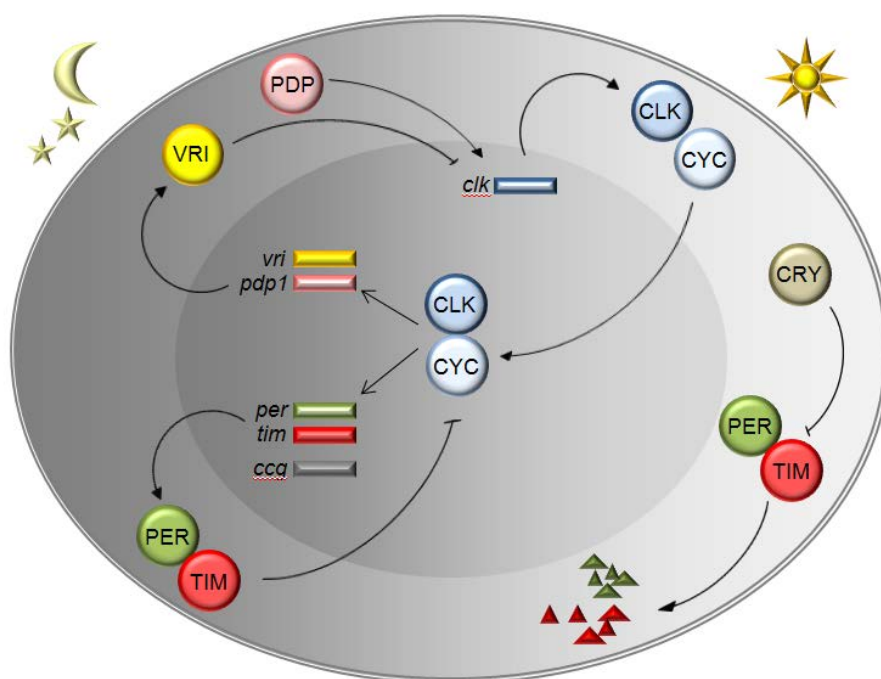


Figure 3: Simplified model of the molecular clock mechanism of *Drosophila*. The transcription factors CLOCK (CLK) and CYCLE (CYC) activate the transcription of the clock genes *period* (*per*), *timeless* (*tim*), *vri* (*vri*) and *par domain protein 1* (*pdp1*) and other clock controlled genes (*ccg*). After translation, the clock proteins PER, TIM, VRI and PDP1 accumulate in the cytoplasm and feed back on their own transcription by influencing the action of CLK or the *clk* expression. The resulting oscillation in RNA and protein levels is synchronized to the 24 hour LD cycle by the action of the blue light photoreceptor Cryptochrome (CRY), which leads to TIM and PER degradation upon light stimulation. See text for details.

Behavioral Rhythms

Drosophila melanogaster shows various measurable types of circadian behavior, like eclosion, feeding, courtship or oviposition. The most prominent, however, is the circadian rhythm in locomotor activity, which can be efficiently measured photoelectrically under various simulated light or temperature conditions. In constant darkness (DD) *Drosophila* maintains robust locomotor rhythms reflecting its endogenous period length of approximately 24 hours. In entrained conditions like an LD cycle *Drosophila* is a crepuscular animal, showing two robust activity peaks: a morning (M) peak and an evening (E) peak, which are separated by a midday siesta. In accordance with the proposed dual oscillator model by Pittendrigh and Daan (1976), who suggested that there are two different oscillators present in nocturnal rodents controlling M activity and E activity, *Drosophila melanogaster* was the first organism in which an M oscillator and E oscillator were anatomically attributed to different clock neuron clusters. Thus, it was shown that the four PDF⁺ sLN_v mainly control the M activity, while three CRY⁺ LN_d and the fifth PDF⁻ sLN_v control the E activity (Grima et al., 2004; Stoleru et al., 2004; Rieger et al., 2006; Picot et al., 2007; reviewed by Yoshii et al., 2012). However, further studies suggested that this regulation is rather plastic and depends on the environmental conditions (e.g. Rieger et al., 2009; Zhang et al., 2010).

How sensitive the clock system is to environmental changes, which occur for example also in the course of annual seasons, is of growing interest in the research field and quite some work has been conducted recently (e.g. Yoshii et al., 2009; Rieger et al., 2012; Vanin et al., 2012; Menegazzi et al., 2013). Under long photoperiods, which would occur during summer time, the two activity peaks of *Drosophila melanogaster* move further apart tracking the timing of dusk and dawn, mediated by an acceleration of the clock in the M cells and a deceleration of the clock in the E cells (e.g. Rieger et al., 2007; Yoshii et al., 2009). Vice versa, in shorter photoperiods M and E peak move closer together. However, these changes in phase angle between M and E peak were shown to have limitations, in that dusk and dawn under extreme photoperiods (e.g. LD 20:04 or LD 04:20) cannot be completely followed anymore. Rieger et al. (2012) nicely showed that wildtype *Drosophila melanogaster* strains deriving from more northern habitats were less limited in increasing their phase angle than flies from southern habitats, indicating that this behavior might be

based on adaptation to local conditions. Nevertheless, the general limitation in phase angle indicates that the M and E peak are coupled and not acting independently of each other (Rieger et al., 2003; 2012).

1.3 Neuropeptide Circuits in Insects

Insect Neuropeptides

Neuropeptides are neuromodulatory molecules that can be found from the most primitive to highly evolved animal nervous systems. They are synthesized by neurons and endocrine cells and act on targets within the central nervous system or on peripheral targets, either by direct innervation or by release as hormones into the circulation. Neuropeptides arise through enzymatic cleavage of large precursor peptides (prepropeptides) that are encoded in the genome. The completion of the whole genome sequence of *Drosophila* allowed a good estimation of the actual number of putative insect neuropeptide precursors (Hewes and Taghert, 2001). Thus, around 25 of them have been identified so far, each of which giving rise to sometimes numerous different mature neuropeptide isoforms. Additional precursor genes were identified in other insect species through direct isolation. The prepropeptides enter the secretory pathway, during which they undergo maturation. This process includes cleavage of the precursor in smaller peptides as well as posttranslational modifications. The mature neuropeptides are then transported to their release sites in so called large dense cored vesicles. (Reviewed by Nässel, 2002 and Bendena et al., 2012)

A general feature of insect neuropeptides is that different peptide types largely vary in their expression pattern and that the expression is usually restricted to distinct subsets of neurons or sometimes even single cells. This spatial specificity would indicate a rather narrow functional area for each neuropeptide. But in fact, most of them appear to be multifunctional. In contrast to classical neurotransmitters, which are released at synapses and directly act on ligand-gated ion channels, neuropeptides can be released also non-synaptically on both axons and dendrites. This broadens their field of action, in that they can on one hand act on precise targets, when released at classical synapses. On the other hand the peptide containing vesicles are stored along the neuronal projections within

varicosities and can thus be released upon neuronal stimulation as local neurohormone with a broader distribution. (Reviewed by Nässel, 2002 and Bendena et al., 2012)

Neuropeptide Signaling and Function

Most neuropeptides, that have been studied so far, activate a large family of receptors, the so-called G-protein coupled receptors (GPCRs), which can be further divided into several subfamilies. GPCRs are composed of 7 transmembrane domains with an N-terminal ligand binding site in the extracellular matrix as well as a cytoplasmic oriented C-terminus that interacts with a GTP binding protein (G-protein). Through these G-proteins the receptor initiates a signal transduction cascade within the adenylate cyclase or the phospholipase c pathway, thereby regulating intracellular levels of either cyclic AMP (cAMP) or inositoltriphosphate (IP3), diacylglycerol (DAG), and calcium (Ca^{2+}). Downstream processes of these signaling pathways include the activation of kinases or phosphatases, ion channel activation, protein synthesis or transcriptional regulation. Thus neuropeptides elicit rather slow responses, also considering that they are not always released in a localized fashion (synaptically), but travel longer distances to reach their target receptor, either as local neurohormone in a paracrine fashion or as neurohormone travelling within the circulation system. Neurons quite often express a neuropeptide together with a classical fast neurotransmitter that directly influences the opening or closing of ion channels in its target cell. The coexpressed neuropeptide can then modulate the cellular response through its activation of the corresponding GPCR. (Reviewed by Nässel, 2002 and Caers et al., 2012)

About 44 genes encoding putative neuropeptide GPCRs were identified in the genome of *Drosophila melanogaster* (Hewes and Taghert, 2001). About three quarters of them have been assigned to their corresponding neuropeptides by now, while the remaining orphan receptors are still waiting for the identification of their ligands. In contrast to the expression patterns of different neuropeptides, which have been extensively characterized in most cases, much less is known about the precise expression pattern of most neuropeptide receptors. Antibodies are often not available and reporter lines are sometimes unspecific. Nevertheless, newly developed tools employing optogenetics or

electrophysiology are used nowadays to search for target sites of different neuropeptides or classical neurotransmitters *in vivo*.

As mentioned earlier, most neuropeptides are multifunctional. The same peptide sometimes fulfills completely different tasks when acting in the central nervous system compared to the periphery. In general, neuropeptides are involved in the regulation of homeostasis, different developmental processes, neuronal modulation, and the coordination of various types of behavior. (Hewes and Taghert, 2001; Nässel, 2002; Caers et al., 2012)

1.4 Neuropeptides Expressed in *Drosophila* Clock Neurons

Neuropeptides are divided into families according to their structural relationship. Thus, a neuropeptide family usually consists of members with similar amino acid sequences. A nice overview of insect neuropeptide families and their functions is provided in relevant reviews, e.g. by Nässel (2002), Bendena et al. (2012) or Taghert and Nitabach (2012). Therefore, I will restrict my descriptions here to neuropeptides that are expressed in the clock neurons of *Drosophila*.

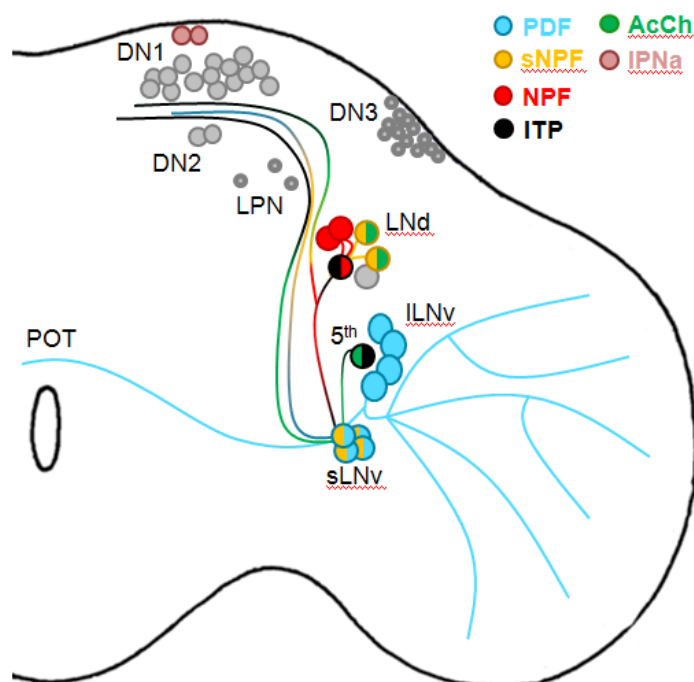


Figure 4: Neurochemistry of the clock neurons of *Drosophila melanogaster* (reviewed by Peschel and Förster, 2011). Four sLNv and the ILNv express PDF (blue), while the fifth sLNv is PDF⁻. NPF is expressed in three LNd (red) and sNPF was found in the four PDF⁺ sLNv as well as in two NPF⁻ LNd (yellow). ITP is

expressed in the fifth sLNv and in one NPF⁺ LNd (black). Further, IPNamide was found within the DN1a (purple) and there are hints for the presence of Acetylcholine in the sNPF⁺ LNd and the fifth sLNv (green).

The neurochemical characterization of the *Drosophila* clock neurons is of great interest, since it is a first step towards understanding the network properties of the clock system as well as clock output pathways. Fig. 4 shows the neurochemistry of the different clock neurons as it was reviewed in Peschel and Helfrich-Förster (2011). As mentioned earlier, the large and small LNv express the neuropeptide PDF (Helfrich-Förster, 1995). Later Shafer et al. (2006) found the expression of IPNamide in the DN1a neurons. Further, three of the LNd were found to contain Neuropeptide F (Lee et al. 2006). And finally in 2009, the study by Johard et al. even added two more peptides: short Neuropeptide F (sNPF), which is expressed in all four PDF⁺ sLNv and in two NPF⁻ LNd, and the Ion Transport Peptide (ITP), which was found in the fifth sLNv and in one NPF⁺ LNd. The same study revealed the presence of the Choline-Acetyltransferase in the fifth PDF⁻ sLNv as well as in the two sNPF⁺ LNd, suggesting that these cells contain Acetylcholine (AcCh).

In the following I will introduce those neuropeptides that were examined in the course of this PhD project.

Pigment Dispersing Factor (PDF)

Mature PDF is an 18 amino acid amidated neuropeptide and is related to a peptide family of crustaceans, the pigment dispersing hormones (PDH), which regulate the pigment migration in crab chromatophores (Rao and Riehm, 1993). However, PDF was found to fulfill no such function within insects, but to be an important component of the circadian clock. This was extensively shown for *Drosophila melanogaster* (e.g. Helfrich-Förster 1995; Renn et al., 1999), but also in other insect species PDF was found in putative clock neurons (reviewed by Helfrich-Förster, 2009 and Tomioka and Matsumoto, 2010). The PDF receptor (PDFR) was discovered in 2005 and was shown to be expressed mainly in CRY⁺ clock neurons and in additional cells outside of the clock network (Hyun et al., 2005; Mertens et al., 2005; Im and Taghert, 2010; Im et al., 2011). Thus, most clock neurons in explanted adult brains respond to bath applied PDF with robust increases in cAMP (Shafer et al., 2008). It is further known that PDF has the ability to speed up the clock in certain

clock neurons while slowing it down in others (Yoshii et al., 2009). These studies assume that PDF acts as a synchronizing signal within the clock network. Recent work, however, identified PDF target sites outside of the clock network in the ellipsoid body, confirming the general opinion of PDF being also an important output factor of the circadian clock (Pérez et al., 2013). Impairment of the PDF/PDFR circuit leads to arrhythmicity or shortened free-running rhythms in DD, as well as to reduced M activity and advanced E activity in entrained conditions (Renn et al., 1999). PDF from the sLN_v seems to be responsible for maintaining rhythmicity in general and for generating M activity, while PDF from the ILN_v influences the length of the free-running period as well as the E peak timing in LD (Shafer and Taghert, 2009).

Neuropeptide F (NPF)

The first invertebrate NPF was found in a tapeworm and was thought to be related to the vertebrate Neuropeptide Y (Maule et al., 1991). More peptides identified in mollusks and insects followed. The mature *Drosophila melanogaster* NPF was characterized as a 36-residue amidated peptide that is expressed in few neurons in the brain and in endocrine cells of the midgut in both larvae and adults (Brown et al., 1999). A receptor for *Drosophila* NPF, NPFR1, was identified by Garczynski et al. (2002) and *in vitro* studies showed that it acts via an inhibitory G-protein, thus inhibiting adenylate cyclase activity and likely also decreasing intracellular Ca²⁺ (Xu et al., 2010). NPFR1 was localized by *in situ* hybridization to neurons in the brain, ventral nerve chord and to midgut cells in larvae (Garczynski et al., 2002; Wu et al., 2003), and by *GAL4* driven GFP expression to very few cells in the adult brain (Wen et al., 2005). Major functions of NPF signaling include the regulation of feeding and courtship behavior, metabolism, alcohol sensitivity, aggression as well as learning and memory (Shen and Cai, 2001; Wu et al., 2003, 2005; Wen et al., 2005; Dierick and Greenspan, 2007). The discovery of NPF within three LNd clock neurons (Lee et al., 2006; Hamasaka et al., 2010) allowed the assumption that NPF might also be involved in the circadian system of the fly. Indeed, the ablation of the NPF⁺ neurons altered the phase and the shape of the E activity of male adult flies in entrained conditions (Lee et al., 2006). (For detailed review see Nässel, 2002 and Nässel and Wegner, 2011.)

short Neuropeptide F (sNPF)

sNPFs were so far only found in arthropod species and are best characterized in insects. Many species express multiple isoforms of sNPF, which derive from one precursor that is encoded by one gene. In *Drosophila* four different amidated isoforms were predicted based on the genome data (sNPF-1, sNPF-2, sNPF-3 and sNPF-4), however biochemical analysis employing mass spectrometry revealed divergences of the actually occurring sNPF peptides in comparison to what was predicted. Especially sNPF-1 and sNPF-2 were shown to mainly occur in a much shorter truncated form (sNPF-1⁴⁻¹¹, reviewed by Nässel and Wegener, 2011). The expression pattern of sNPF is best characterized in *Drosophila* and is very broad in both larvae and adults. sNPF⁺ cells were identified in the brain (a large proportion within the mushroom bodies), the ventral nerve chord as well as some endocrine cells in the midgut in larvae (Veenstra, 2009). Also in adult flies, sNPF is present in a large number of cells including Kenyon cells of the mushroom body, olfactory sensory neurons, neurosecretory cells in the protocerebrum as well as many other unidentifiable interneurons (e.g. Johard et al., 2008; reviewed by Nässel and Wegener, 2011). The sNPF receptor (sNPF_{R1}), which was first identified in *Drosophila*, seems to be expressed widely in the CNS and other tissues, although only little is known so far about details (Mertens et al. 2002, Feng et al. 2003, Reale et al., 2004). According to its relationship to the vertebrate NPY receptor and a study conducted on the sNPF receptor in *Anopheles* (Garczynski et al., 2007), the sNPF_{R1} of *Drosophila* is suggested to inhibit adenylate cyclase activity. The broad distribution of sNPF and its receptor suggests multiple functions in the brain, the gut and actions as endocrine hormone system. These functions include regulation of feeding and growth, metabolic stress, locomotion, learning and hormone release (Lee et al., 2004, 2008; Johard et al., 2008; Nässel et al., 2008; Kahsai et al., 2010a, b; Knapek et al., 2013). A function for sNPF in circadian rhythms was suggested, when Johard et al. (2009) discovered sNPF expression within certain clock neurons, although no experimental proof had been provided so far. (For detailed review see Nässel, 2002 and Nässel and Wegener, 2011.)

Ion Transport Peptide (ITP)

ITP was first identified in the corpora cardiaca of the desert locust *Schistocerca gregaria*. It was shown to fulfill antidiuretic functions and to be related to crustacean hyperglycemic hormones (CHH; Audsley et al., 1992). Later the analysis of the *Drosophila* genome revealed a gene encoding a peptide that is structurally similar to the locust ITP and to CHH (Hewes and Taghert, 2001). The study of Dircksen et al. (2008) showed that long and short *Drosophila* ITP isoforms derive from alternative splicing of one *itp* gene, just like it had been shown before for locusts and moths (Meredith et al., 1996; Dai et al., 2007). The short amidated isoform, ITP, stimulates chloride transport within the hindgut, while the two long carboxylated isoforms, ITP-L1 and ITP-L2, are thought to act as competitive inhibitors on the so far unknown ITP receptor (reviewed by Dircksen, 2009). Recent studies on *Schistocerca gregaria* ITP suggest signaling through a GPCR as well as a membrane bound guanylate cyclase, which increase intracellular cAMP and cGMP levels (Audsley et al., 2012). By immunohistochemical analysis and *in situ* hybridization ITP expression in *Drosophila* was localized to only few cells in larvae and adults (Dircksen et al., 2008). Among these are pars lateralis neurosecretory cells, which most probably release ITP into the haemolymph, hindgut innervating neurons in abdominal ganglia, and different types of interneurons, which include the fifth sLNv clock neuron and one LNd (Dircksen et al., 2008; Johard et al., 2009). Recently, a clock related function of ITP was proposed by Damulewicz and colleagues (Damulewicz and Pyza, 2011; Damulewicz et al., 2013) for the regulation of circadian rhythms in morphological plasticity of lamina monopolar cells and the oscillation in abundance of the catalytic subunit of a sodium/potassium pump in glia cells of the lamina. However, no clock related function in behavior was so far shown for ITP.

1.5 Aim of Study

The general aim of this PhD project was to investigate possible yet unknown functions of different neuropeptides for the circadian clock of *Drosophila melanogaster*. Thereby, I focused on NPF, sNPF and ITP since they had been previously shown to be expressed in the lateral pacemaker neurons of the fly (LN_s; Helfrich-Förster, 1995; Lee et al., 2006; Johard et al., 2009), which are important for rhythm generation in behavior.

One goal was to verify the neuropeptide expression pattern by immunohistochemistry in *Drosophila melanogaster* and to compare it in part among different *Drosophila* species to gain evolutionary insight into its importance for the clock system. Investigation of the neuropeptide PDF ought to be included in this study, since a recent work by Bahn et al. (2009) had shown remarkable differences in the PDF expression pattern of *Drosophila virilis* in comparison to *Drosophila melanogaster*. This part of the thesis also includes the characterization of the neuronal clock network of different *Drosophila* species in general as well as characterization of the CRY expression.

The second and probably main aim of this thesis was the investigation of effects on circadian locomotor behavior, after manipulation of neuropeptide signaling by specifically directed RNA-interference (RNAi), cell ablation, the use of mutants or overexpression. Also here, effects of PDF are often co-examined, to reveal possible interactions between different neuropeptide signaling pathways.

Using the example of Shafer et al. (2008), in which the effect of bath applied PDF on clock neurons had been investigated employing optogenetic second messenger sensors, the third goal of this thesis was to examine, whether the three peptides function in inter-clock-neuron communication, i.e. targeting clock neurons. Part of this topic was consequently the examination of the expression pattern of the respective neuropeptide receptors within the clock network using available *GAL4* lines and GFP reporters.

2 Material and Methods

2.1 Material

2.1.1 Fly strains

In Table 1 all fly strains that were used in the course of this thesis are listed with information on source (from whom they were obtained) and literature reference. Flies were reared on cornmeal/agar medium containing 0.8% agar, 2.2% sugar beet molasses, 8.0% malt extract, 1.8% yeast, 1.0% soy flour, 8.0% corn flour and 0.3% hydroxybenzoic acid. All flies were kept in LD 12:12 during the whole time of development either on 18°C for long-term maintenance or on 25°C before conducting experiments. Humidity was kept between 60 and 65%.

Table 1: Fly strains used in this thesis. DSSC: *Drosophila* Species Stock Center, San Diego. BL: Bloomington Stock Center. VDRC: Vienna *Drosophila* RNAi Center. DGRC: *Drosophila* Genetic Resource Center, Kyoto Institute of Technology, Japan.

Genotype	Source	Reference/Comments
Wildtypes, Mutants and Balancer		
<i>Canton S (CS)</i>	S. Schneuwly	Lindsley and Grell, 1968; <i>D. melanogaster</i>
<i>D. simulans</i>	DSSC	Drosophila species
<i>D. yakuba</i>		
<i>D. ananassae</i>		
<i>D. triauraria</i>		
<i>D. pseudoobscura</i>		
<i>D. willistoni</i>		
<i>D. virilis</i>		
<i>D. littoralis</i>	A. Hoikkala	
<i>D. ezoana</i>	A. Hoikkala	
<i>yw</i>	stock collection	for control crosses
<i>w¹¹¹⁸</i>	stock collection	for control crosses

<i>w;CyO/Sco</i>	from BL #3703	Balancer
<i>w;+;TM6B/MKRS</i>	from BL #3703	Balancer
<i>w;CyO/Sco;TM6B/MKRS</i>	BL #3703	Double-Balancer
GAL4/GAL80-driver and UAS-responder lines		
<i>yw;pdf-GAL4;+</i>	J. C. Hall	Renn et al, 1999
<i>w;tim(UAS)-GAL4;+</i>	M. W. Young	Blau and Young, 1999
<i>w;tim-GAL4/CyO;+</i>	M. Kaneko	Emery et al., 1998
<i>yw;per-GAL4;+</i>	M. Kaneko	Plautz et al. 1997
<i>w;clk856-GAL4;+</i>	O. T. Shafer	Gummadova et al., 2009
<i>w;cry-GAL4^{#39}/+</i>	F. Rouyer	Klarsfeld et al., 2004
<i>yw;snpf-GAL4;+(NP6301)</i>	DGRC	Nässel et al., 2008; Johard et al., 2009
<i>yw;snpfR1-GAL4</i>	C. Wegener	e.g. Hong et al., 2012
<i>yw;+;npf-GAL4</i>	Prof. Jae H. Park	Wu et al., 2003
<i>w;npfR1-GAL4</i>	P. Shen	Wen et al., 2005
<i>sNPF^{c00448}, sNPF^{hypp}</i>	O. T. Shafer	Lee et al., 2008
<i>w;elav-GAL4/CyO;+</i>	BL #8765	Dimitroff et al., 2012
<i>w;386y(amon)-GAL4</i>	C. Wegener	Taghert et al., 2001
<i>yw;+;cry-GAL80_{2e3m}/TM6B,D³</i>	M. Rosbash	Stoleru et al., 2004
<i>yw;pdf-GAL80_{96A}</i>	M. Rosbash	Stoleru et al., 2004
<i>w;UAS-hid¹⁴/CyO;+</i>	H. Steller	Zhou et al, 1997
<i>w;+;UAS-GFP-S65t</i>	BL #1522	Siegmund and Korge, 2001
<i>w,UAS-dicer2;+;+</i>	VDRC #60012	Dietzl et al., 2007
<i>w;+;UAS-pdf-RNAi</i>	VDRC #4380	Shafer and Taghert, 2009
<i>w;+;UAS-npf-RNAi</i>	VDRC #108772	Hermann et al., 2012
<i>w;+;UAS-snpf-RNAi^{Lee}</i>	R. Costa	Lee et al., 2008
<i>w;+;UAS-snpf-RNAi^{Bloo}</i>	BL #25867	Shang et al., 2013
<i>w;+;UAS-snpfR-RNAi</i>	BL #27507	-
<i>w;+;UAS-itp-RNAi</i>	VDRC #43848	Damulewicz and Pyza 2011

<i>w</i> ;+;UAS-ITP ² /TM3		present thesis
<i>w</i> ;UAS- <i>Epac1camps</i> ^{50A} ;+	O. T. Shafer	Shafer et al., 2008
<i>w</i> ;UAS- <i>GCaMP3.0</i> ;+	O. T. Shafer	Lelito and Shafer, 2012

2.1.2 Antibodies

Table 2 lists all primary and secondary antibodies that were used in this thesis and gives information on the exact Immunogen, the donor animal, dilution and reference. “Source” refers to the person from whom the antibody was obtained. Antibodies were stored at 4°C or in 50% Glycerol at -20°C. For the working solution antibodies were diluted in PBT to the appropriate concentration. 0.02% NaN₃ was added to primary antibody solutions to prevent bacterial growth. Like this it was possible to use the primary antibody solutions several times. Detailed production procedures of primary antibodies can be found in the material and methods sections of Hermann et al. (2012, 2013) and in other given references.

Table 2: Primary and secondary antibodies used in this thesis.

Prim. Antibody	Immunogen	Donor animal	Dilution	Reference/Source
anti-TIM	Polyhistidine fused TIM fragment expressed in <i>E. coli</i> (amino acids 222–577)	rat, poly	1:1000	Sidote et al., 1998 / I. Edery
anti-PDP1	GST-fused bacterially purified PDP1 α	rabbit, poly	1:1000	Cyran et al., 2003 / J. Blau
anti-VRI	Histidine fused VRI (coding region) expressed in Sf9 insect cells	guinea pig, poly	1:3000	Glossop et al., 2003 / P. Hardin
anti-CRY	Polyhistidine fused full-length <i>Drosophila</i> CRY expressed in <i>E. coli</i>	rabbit, poly	1:1000	Yoshii et al., 2008 / T. Todo
anti-PER	Baculovirus expressed full length <i>Drosophila</i> PER protein	rabbit, poly	1:1000	Stanewsky et al., 1997 / R. Stanewsky
anti-PDF-C7	amidated <i>Drosophila</i> PDF peptide (NSELINSLLSLPKNMNDA-NH ₂)	mouse, mono	1:1000	DSHB, J. Blau

nb33 (PDF)	<i>Drosophila melanogaster</i> head extracts	mouse, mono	1:100	Hofbauer et al., 2009 / A. Hofbauer
anti-βPDH	βPDH conjugated to bovine thyroglobulin (NSELINSILGLPKVMNDA-NH ₂)	rabbit, poly	1:2000	Dirksen et al., 1987 / H. Dirksen
anti-NPF	mature <i>Drosophila</i> NPF (SNSRPPRKNDVNTMADAYKFLQDLDTYYGDRARVRFV-NH ₂)	rabbit, poly	1:300	Shen and Cai, 2001 / J. Park
anti-sNPFp	part of the sNPF precursor protein (DPSLPQMRRTAYDDLREL)	rabbit, poly	1:3000	Johard et al., 2008; Nässel et al., 2008 / J. Veenstra
anti-ScgITP-C1	Gly-extended peptide of short ScgITP (GGGDEEEKFNQ)	rabbit, poly	1:4000	Ring et al, 1998; Dirksen et al., 2008 / H. Dirksen
anti-ITP-R1	<i>Drosophila melanogaster</i> ITP specific C-terminal fragment CEMDKYNEWRDTL-NH ₂	rabbit, poly	1:10000	Dirksen et al., <i>in prep.</i> ; Hermann-Luibl et al., <i>submitted</i> / H. Dirksen
Sec. Antibody	Immunogen	Dilution	Source	
Alexa Fluor 488	goat anti-rabbit	1:200	Molecular Probes (Invitrogen)	
	goat anti-guinea pig			
Alexa Fluor 555	goat anti-rabbit			
	goat anti-rat			
Alexa Fluor 532	goat anti-rabbit			
Alexa Fluor 635	goat anti-mouse			

All further Material used for the experiments included in this thesis is listed in the Appendix.

2.2 Methods

2.2.1 The *GAL4/UAS* System

The most basic method in this thesis is the *GAL4/UAS* binary expression system, which was first described by Brand and Perrimon in 1993. This system can be used to direct the expression of certain gene constructs in a spatially controlled manner *in vivo*. The principle of this system involves two different transgenic fly lines, the so-called driver or *GAL4*-line, and the responder or *UAS*-line. The driver line contains the genetic sequence of *GAL4*, a transcriptional activator of yeast, which is cloned downstream of a particular promoter sequence of interest. By using tissue or cell specific promoter sequences the *GAL4* expression can be directed to almost any anatomical structure in the animal. The responder fly line contains the so-called upstream-activating-sequence (*UAS*), which is the target sequence of the *GAL4* transcriptional activator. This *UAS* sequence is cloned upstream of any kind of effector gene (e.g. reporter genes, RNAi constructs, cell death genes etc.). By crossing flies of the driver line with flies of the responder line, the resulting progeny contains both transgenic constructs. *GAL4* will then be synthesized under the control of the tissue or cell specific promoter and will activate the expression of the effector gene by binding to the *UAS* sequence. Thus, this system allows the expression of an effector gene in any tissue or cell group of interest. (Fig. 5A)

The work of Lee and Luo (1999) added another useful tool to the system – *GAL80*, another transcriptional regulator of yeast. In contrast to *GAL4*, *GAL80* is an inhibitory element, which can bind to the active domain of the *GAL4* protein, thereby preventing its binding to the *UAS* sequence. A third class of transgenic fly lines contains the *GAL80* sequence again under the control of a tissue or cell specific promoter. As soon as all three transgenic constructs (*GAL4*, *UAS* and *GAL80*) are combined in one fly, tissue specific *GAL4* expression will activate the effector gene downstream of *UAS*, but only in cells in which *GAL80* is not simultaneously expressed. In cells in which promoter activity allows both *GAL4* and *GAL80* expression, *GAL4* activity will be inhibited and the effector gene will not be expressed. (Fig. 5B)

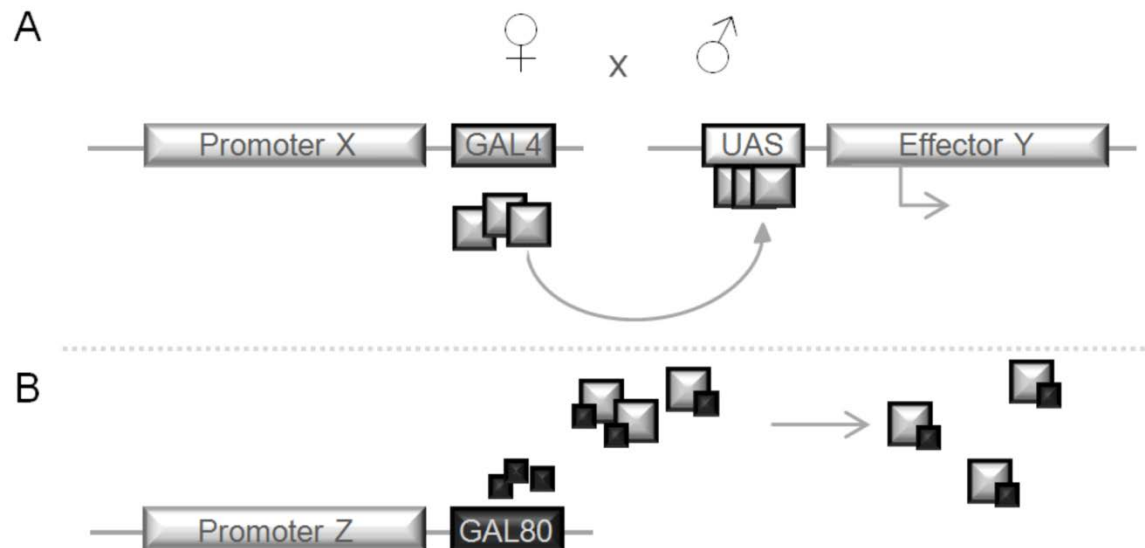


Figure 5: The *GAL4/UAS* System. (A) *GAL4* is expressed under the control of a tissue specific promoter X. In presence of the *UAS*-sequence, *GAL4* will bind to it and will activate the transcription of the effector gene Y. (B) In case a promoter Z allows in addition the expression of *GAL80*, it will bind to *GAL4* and prevent the activation at the *UAS*-sequence. Thus, cells containing only *GAL4* will express the effector Y, while cells containing both *GAL4* and *GAL80* will not. For details see text.

2.2.2 Molecular Methods

2.2.2.1 Generation of *UAS-itp* lines

The whole process of generating the *UAS-ITP* lines will be described in the following. A list of all used kits and reagents can be seen in the Appendix of this thesis.

RNA Extraction

For RNA Extraction I used the ZYMO Quick-RNATM MicroPrep Kit. Five *Drosophila melanogaster* Canton S heads were quickly removed from the fly bodies on ice and were directly transferred into RNA Extraction Buffer. A hand-held electrical homogenizer was used to break up the heads. The washing and centrifugation steps were performed according to the manufacturer's protocol. Finally the RNA was eluted from the column with 8µl of RNase free water.

Reverse Transcription (RT)

For cDNA synthesis 6µl of the eluted RNA were treated with the QuantiTect Reverse Transcription Kit. First, 1µl of gDNA wipe-out was added to the RNA and was incubated at 42°C for 2 min. Subsequently a mastermix containing 0.5µl Reverse Transcriptase Enzyme,

2µl of RT Buffer, 0.5µl of RT Primer Mix was added to the RNA and the sample was placed into a PCR machine to perform the following temperature steps: 42°C for 30 min, 95°C for 3 min and subsequently cooling down to 4°C. The resulting cDNA sample was finally diluted 1:2 in water.

ITP PCR

To amplify full length *itp* cDNA, I used the ITP-PE primer pair (see table 11 in the Appendix) which would create restriction enzyme sites for EcoRI and XbaI. Primers were diluted to 5µM in water before use. Table 3 shows the contents of the PCR reaction and the PCR program of the Mastercycler gradient machine (Eppendorf).

Table 3: PCR program applied for ITP PCR.

PCR reaction	PCR program
1µl cDNA	90°C 30sec
2µl 5µM ITP-PE Primer Mix (5´and 3´Primer)	62°C 20sec
7µl water	72°C 20sec
10µl VWR Taq DNA Polymerase Master Mix	72°C 5min
20µl total	4°C hold

34x

Gel Electrophoresis and DNA Extraction

The PCR products were then split up by agarose gel electrophoresis (1% gel) and the bands of the different *itp* isoforms were cut out from the gel with razor blades. The band of the ITP-PE isoform (~500kb) was used for the cloning procedure to generate the ITP-pUAST vector. Therefore, the ITP-PE DNA was extracted from the gel slice using the innuPREP DOUBLEpure Kit. The procedure was done according to the manufacturer’s protocol and finally the DNA was eluted with 20µl of water.

Amplification of the pUAST vector (Midi-Prep)

To amplify the pUAST vector (containing an Ampicillin resistance gene and a mini-white gene (kindly donated by A. Fiala) for cloning, overnight cultures of pUAST containing *E. coli* were incubated at 37°C. The cultures were centrifuged and the pUAST DNA was extracted from the bacterial pellets using the SIGMA GenElute™ Plasmid Midiprep Kit. All

steps were conducted following the manufacturer's protocol and the elution volume at the end was 0.5ml. For DNA precipitation 0.5ml of the eluate were incubated at -20°C for 30 min, after adding 150µl of Na-Acetate (pH 5.2) and 1000µl of isopropanol, and were subsequently centrifuged at 4°C for 30 min with maximum speed. The DNA pellet was washed with 800µl of 70% Ethanol (centrifugation at 4°C for 10 min), dried at 37°C for 30 min, resuspended in 100µl of water and again incubated at 37°C for 10 min. DNA concentration was subsequently measured with a spectrophotometer Nanodrop 2000c (Thermo Scientific; Peqlab).

Digestion with Restriction Enzymes

To obtain sticky DNA ends for ligation the pUAST vector DNA and the ITP-PE cDNA were digested with the two restriction enzymes EcoRI and XbaI. The following Table 4 shows the contents of the digestion reactions.

Table 4: Digestion reactions applied on pUAST vector and ITP cDNA.

pUAST digest	cDNA digest
5µl pUAST DNA	20µl ITP-PE cDNA
2µl EcoRI	2µl EcoRI
2µl XbaI	2µl XbaI
2µl Buffer (2x)	3µl Buffer (2x)
9µl water	3µl water
20µl total	30µl total

Digestion reactions containing pUAST vector DNA and no restriction enzyme or either EcoRI or XbaI served as controls. All reactions were incubated at 37°C over night. A small part of the digestion reactions was then observed on a 1% agarose gel to confirm the success of the digestion.

Phosphatase Reaction and Ligation

Prior to ligation the digested pUAST and ITP-PE DNA were purified using the MSB®Spin PCRapace (250) Kit according to the protocol and the DNA concentration was measured using the Nanodrop. To prevent self-ligation of the pUAST vector 10µl of vector DNA

(~1µg) were incubated with 2µl of 10x Buffer, 1µl of Fast APTM Phosphatase and 7µl of water at 37°C for 10 min and subsequently at 75°C for 5 min. 1µl of phosphatase treated pUAST DNA (~50ng) was then incubated with 9µl of the digested ITP-PE DNA, 2µl of T4 DNA Ligase Buffer, 1µl of T4 DNA Ligase and 7µl of water at 22°C (room temperature) for 30 min.

Transformation

NEB 10-beta competent *E. coli* cells were incubated with the ligated ITP-pUAST vector for 20 min on ice. Then the cells were heat shocked at 42°C for 1 min and afterwards bacteria were allowed to grow in 200µl of LB₀ medium for 1 hour at 37°C to recover from the heat shock. Then the cells were dispersed on selective LB_{Amp} plates to allow growth only to those bacteria, which had incorporated the vector with the Ampicillin resistance. The plates were then incubated at 37°C over night.

Single colony PCRs

Single bacterial colonies from the LB_{Amp} plates were picked with pipette tips and were used to inoculate 500µl of liquid LB_{Amp} medium. The cultures were then incubated for 30-90 min at 37°C on a shaker. 5µl of each culture were then incubated at 95°C for 10 min to kill the bacteria. To test which bacterial clone contained the vector including the ITP-PE insert, PCRs were performed using the ITP-PE primers (Mastercycler gradient, Eppendorf). For this a mastermix containing 3µl of water, 2µl of 0.5M ITP-PE Primer Mix and 10µl of VWR Taq DNA Polymerase Master Mix was added to the 5µl of bacterial culture. The PCR reactions were running with the same PCR program as the ITP PCR, which was performed before to amplify the *itp* cDNA. All tested clones contained the ITP-PE insert.

Amplification of the ITP-PE pUAST Vector

Several tested bacterial clones were used to inoculate 70ml of LB_{Amp} medium and were incubated over night at 37°C. After centrifugation the vector DNA was extracted from the bacterial pellets according to the protocol of the SIGMA GenEluteTM Plasmid Midiprep Kit. The DNA was precipitated as described above for the pUAST vector alone. A small sample of vector DNA was then digested with EcoRI and XbaI to verify again the presence of the ITP-PE insert on a 1% agarose gel.

Sequencing and Microinjection

Four different ITP-PE pUAST vectors from four different bacterial clones were sequenced using the ITP-pUAST Fw Primer (Table 11 in the Appendix). After the sequence of the insert was verified, one of the four vectors (Fig. 6) was sent to BestGene for microinjection into w^{1118} flies. 10 different *UAS-ITP* lines were obtained from BestGene after three months.

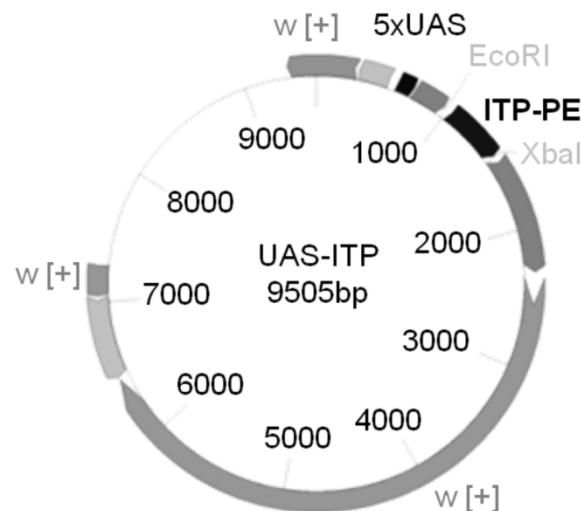


Figure 6: The ITP-PE pUAST vector. The vector contains a mini-white gene (w^+) and five copies of the UAS-sequence upstream of the ITP-PE sequence.

2.2.2.2 qPCR to verify RNAi efficiency

RNA Extraction

For RNA extraction, flies were killed in liquid nitrogen and heads and bodies were separated by vortexing. Five heads were transferred into the RNA Extraction Buffer and homogenized. RNA was extracted according to the protocol of the ZYMO Quick-RNA™ MicroPrep Kit. Three biological replicates were prepared for each genotype.

Reverse Transcription

The Reverse Transcription reaction was performed as described above. The obtained cDNA was diluted 1:5 in water and stored at -20°C .

qPCR

All three biological replicates were tested at the same time in two technical replicates with the Primers of interest and Primers against the housekeeping protein Tubulin (Table 11 in the Appendix). The RNA amount of interest was later calculated relative to the Tubulin-RNA amount (see below). qPCR reactions were performed in a Rotor-Gene Q PCR machine using the SensiFAST™ SYBR No-ROX Kit. The reaction components and the PCR program were as follows (Table 5).

Table 5: PCR program used for qPCR.

PCR reaction	PCR program	
1µl cDNA	95°C 2min	
4µl 0.5µM Primer Mix (5' and 3' Primer)	95°C 5sec	40x
5µl water	60°C 2min	
10µl SensiFAST™ SYBR-Green No-ROX-Mix (2x)	72°C 15min	
20µl total	4°C hold	

qPCR Data Analysis

Raw data were depicted as amplification curves showing the SYBR-Green fluorescence signal in each PCR cycle. A threshold for the fluorescence signal was set close to the base of the exponential amplification phase. Then the PCR cycle numbers at the threshold (cycle threshold, Ct) were extracted from the raw data for all samples. Within one biological replicate the Ct values of all technical replicates for Tubulin were subtracted from the Ct values of all technical replicates of interest. Since the obtained ΔCt values are inversely correlated to the actual amount of RNA in the sample (high values mean that more PCR cycles were necessary to gain the same amount of amplicon, i.e. mean low RNA levels at the beginning) all ΔCt values were subtracted from an arbitrary value, which was set higher than the highest ΔCt value of the experiment. This was done to later depict high amounts of amplicon as high values in the histogram. Finally, the ΔCt values of all technical replicates were pooled for each biological replicate. Values of the biological

replicates were averaged across genotypes and standard deviation and standard error were calculated.

2.2.3 Immunocytochemistry

2.2.3.1 Entrainment and Tissue Fixation

For immunohistochemical analysis 5-7 days old flies were entrained in an LD 12:12 cycle for at least four days prior to dissection. The entrainment was done in light tight boxes equipped with white light LEDs (Lumitronix, LED-Technik, Hechingen, Germany), which were set to an intensity of 100 lux. 20-25 male flies were housed in glass vials with normal fly food (see above) during the whole time of entrainment. At the appropriate ZT or CT, the flies were transferred through a funnel into 4% PFA in PB with 0.1% TrX-100. This was done under red light illumination and samples collected at dark time points were wrapped in aluminum foil to prevent light exposure prior to fixation. Whole *D. melanogaster* flies were fixed for 2.5 hours at room temperature on a shaker, while fixation times in other *Drosophila* species varied from 2.5-4 hours (see Material and Methods of Hermann et al., 2013). GFP expressing flies were fixed in 4% PFA in PB without TrX-100 for 3 hours in the same way. After fixation time was reached, the flies were washed 3 times 10 min in PB.

2.2.3.2 Staining protocol

Adult brains were dissected from the whole fly in cold PB in a black block dish under a stereo microscope using two sharp forceps (Fig. 7A). After separating the head from the fly body the eyes, the head capsule and most of the trachea were removed from the brain. The brains were kept in PBT (0.5% TrX-100) until the dissection of all flies was complete. Short-cut pipette tips glued to a tissue mesh served as collection baskets, in which the brains of each genotype were transferred (Fig. 7B). These collection baskets optimally fit into the wells of 96-well plates, in which all following incubation and washing steps were conducted (Fig. 7C).

To change the incubation solution the basket was simply placed into the next well in a row and the new incubation solution was applied. First, the brains were incubated in the blocking solution (5% Normal Goat Serum (NGS) in PBT (0.5% TrX-100)) for two hours at room temperature or overnight at 4°C. Then the primary antibody solution containing 1-3 different primary antibodies in the appropriate concentration and 5% NGS in PBT (0.5% TrX-100) was applied and the brains were incubated for 1-2 nights, depending on the primary antibody. Unbound antibody was then washed away by rinsing the brains 5 times for 10 min with PBT (0.5% TrX-100). Subsequently, fluorescence-conjugated secondary antibodies were applied in a concentration of 1:200 in PBT (0.5% TrX-100) containing 5% NGS for three hours at room temperature or overnight at 4°C. After washing the brains again 5 times with PBT (0.5% TrX-100), they were transferred into PBT with 0.1% TrX-100. The brains were then removed from the baskets and placed on SuperFrost glass slides in the same orientation along the anterior-posterior and dorsal-ventral axes. Excess buffer was removed and the brains were absorbed in a droplet of Vectashield, which was then covered by a thin glass slip. The cover slip edges were then sealed with Fixogum and the preparations were stored at 4°C.

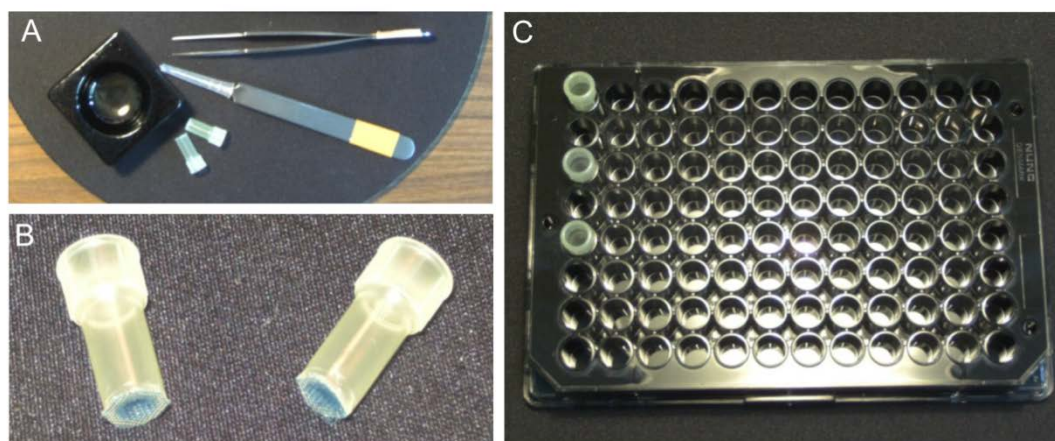


Figure 7: Tools for immunohistochemistry. (A) Flies were dissected with sharpened forceps within a black block dish containing PBS. (B) Brains were transferred into self-made collection baskets. (C) Baskets with brains were placed into 96-well plates, in which all washing and incubation steps were conducted.

2.2.3.3 Microscopy and Image Analysis

Imaging of immunofluorescent brains was conducted with two different confocal laser scanning microscopes. Images for the NPF-cell ablation experiments from Hermann et al. (2012) were taken with a Zeiss LSM 510 Meta (Carl Zeiss MicroImaging, Jena, Germany),

whereas for all other confocal images a Leica TCS SPE (Leica, Wetzlar, Germany) was used. In both cases I obtained confocal stacks with 2 μm layer thickness by sequentially scanning with two to three different laser lines to excite the fluorophores of the secondary antibodies in double and triple labeling. The three laser excitation channels with 488 nm, 532/555 nm and 635 nm were later depicted in green/yellow, magenta and cyan/blue, respectively. Image visualization and editing was done with the Zeiss LSM Image Browser (v. 4,2,0,121) for the Zeiss pictures and with the ImageJ distribution Fiji (<http://fiji.sc/wiki/index.php/Fiji> or <http://rsb.info.nih.gov/ij/>) for the Leica pictures. I cropped the stacks, compiled maximum projections, adjusted brightness and contrast, but applied no other manipulations on the images.

To quantify the number of particular neurons, I investigated single optical layers of each stack in Fiji and counted the cells, after identifying them according to their location, immunostaining and morphology. Usually both hemispheres of 7-13 brains were analyzed in that way and the values were then averaged for each brain and across genotypes. For the quantification of the staining intensity a square shaped area of 9 pixels (3x3 pixels) was placed on the brightest spot of each cell of interest in the Fiji software and the average pixel intensity was measured in one focal plane. The cells of 5-7 different hemispheres were analyzed and the intensity values were first background corrected and then averaged for each neuronal group across genotypes.

Quantification of staining in peptidergic neuronal projection terminals is described in Hermann-Luibl et al. (*submitted*; starting from page 153).

2.2.4 Behavioral Assay

2.2.4.1 *Drosophila* Activity Monitoring (DAM) System

The behavioral assay performed in this thesis was exclusively the measurement of the flies' locomotor activity in certain light conditions. This was done with the commercially available *Drosophila* Activity Monitoring (DAM) System from TriKinetics (TriKinetics, Waltham MA, USA). Being under CO₂-anesthesia 3-5 days old flies were individually placed into glass tubes, which were filled by one third with food (2% agar, 4% sucrose; Fig. 8A) and closed on the other end with an air permeable plug. 32 of these glass tubes

were placed into each activity monitor in a way that the integrated infrared light beam was approximately in the middle of each tube (Fig. 8B). Moving back and forth within the glass tube the flies disrupt the infrared light beam when being active. The number of light beam disruptions per minute was then registered by the DAMSystem Collection Software for each fly and the raw data were read out as text files.

To simulate certain light conditions for the flies, the activity monitors were placed into house-made light-tight boxes, which were equipped with white light LEDs (Lumitronix, LED-Technik, Hechingen, Germany; Fig. 8C). Light intensity and light sequence were set using the Lichtorgel software (G. Stöckl, Regensburg). To maintain constant temperature of 20°C during the experiment the whole recording system was installed either inside an incubator or in a climate chamber.

In this thesis, I used only male flies for behavior experiments – if not explicitly stated otherwise (in Hermann et al., 2012). All experiments started with 7 days of LD 12:12 followed by either constant conditions (DD for at least 14 days) or changing photoperiods (long days: 7 days LD 16:08, 7 days LD 20:04; short days: 7 days LD 08:16, 7 days LD 04:20). Thus, flies were usually recorded for at least 21 days within one experiment. Light intensity during light phases of each experiment was set to 100 lux.

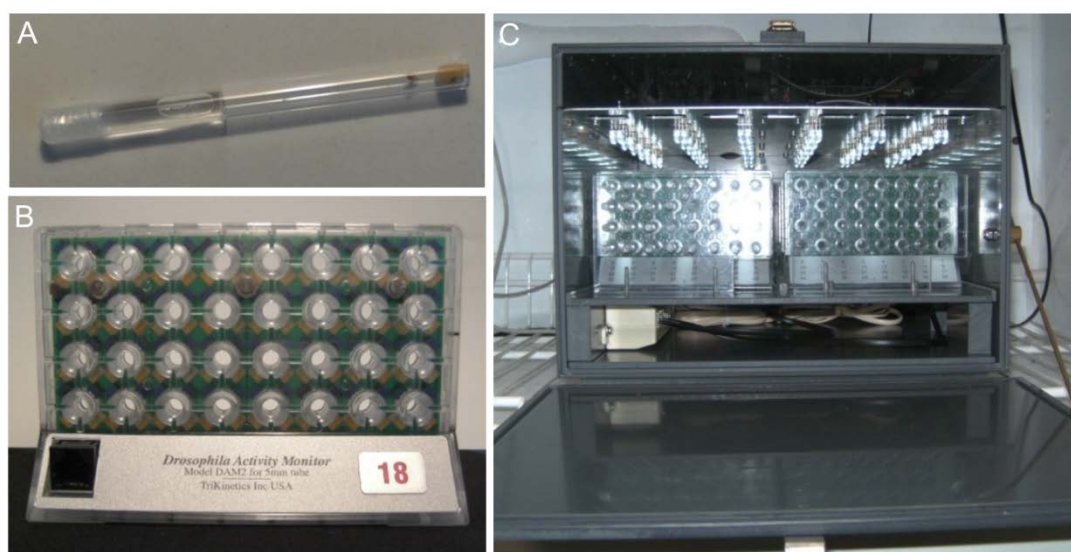


Figure 8: *Drosophila* Activity Monitoring. (A) Flies were individually placed into glass tubes with sugar/agar food. (B) Tubes were placed into *Drosophila* Activity Monitors of TriKinetics with infrared light beams measuring individual beam crosses per minute. (C) Light boxes equipped with white light LEDs were used to simulate various light conditions. Temperature was kept constant at 20°C.

2.2.4.2 Data Analysis

For data analysis the raw data text files were edited in Microsoft Excel. The data of the first day of the experiment were always discarded, because during this time the flies recover from the CO₂-anesthesia and adapt to their new environment. Single fly actograms of the whole experiment were compiled using the software El Temps (Diez-Noguera, Barcelona, 1999; upper limit 5) or the Fiji Plugin ActogramJ (Schmid et al., 2011). To depict the flies' locomotor activity under entrained conditions (LD), average activity profiles were calculated. For this, the activity of each minute during the last five days of each entrainment condition was averaged for each fly. The single fly data were then averaged for each genotype and finally the curves of the activity profile and the standard error of the mean (SEM) were smoothed by a moving average of 11 values. The average activity profiles were then normalized, whereby the highest activity count was set to 1. Average activity levels were calculated from mean activity counts of single flies in certain time intervals relative to the average beam crosses over the whole day, if not stated otherwise.

DD data were used to determine the flies rhythmicity and internal free-running period of locomotor activity. The period length during 10 days in DD was determined by chi²-periodogram analysis for each single fly. Values were then averaged across genotypes and standard deviation and standard error of the mean were calculated.

For the sleep analysis, I used data that were collected during LD 12:12. Sleep was defined as the amount of time, in which the flies did not cross the infrared light beam for more than 10 consecutive minutes. Average sleep profiles were calculated as the mean sleep time during each hour of the day. Total sleep was calculated for daytime and nighttime during LD 12:12.

2.2.5 Live Imaging

2.2.5.1 The Epac1camps sensor and the GCaMP sensor

Cellular excitation upon stimulation is reflected in rapid changes in intracellular Ca²⁺ and/or cAMP levels. Measuring cellular changes in cAMP or Ca²⁺ levels *in vivo* employing

optogenetic tools is a powerful way to investigate the responsiveness of single neurons to various stimuli.

To examine neuronal cAMP responses to bath applied neuropeptides I used the ratiometric cAMP sensor Epac1camps. The core of this sensor is a truncated Epac protein (**E**xchange **P**rotein **D**irectly **A**ctivated by **c**AMP), which is fused to two fluorophores: cyan fluorescent protein (CFP) and yellow fluorescent protein (YFP). The Epac protein binds cAMP as a monomer and therefore shows quite rapid kinetics in its activation (Nikolaev et al., 2004). The truncated form of Epac present in this sensor is of advantage, because it contains only the cAMP binding site, thus decreasing the risk of any other cellular functionality. When intracellular cAMP levels are low, the two fluorophores are in close proximity (Fig. 9A). Excitation of CFP with light of 440 nm leads to high Fluorescence Resonance Energy Transfer (FRET) from CFP to YFP, resulting in low CFP and high YFP emission. When cAMP levels rise within the cell, a single molecule of cAMP will bind to Epac and cause a conformational change, whereby the two fluorophores move further apart (Fig. 9B). This leads to a loss in FRET with high CFP, but low YFP emission.

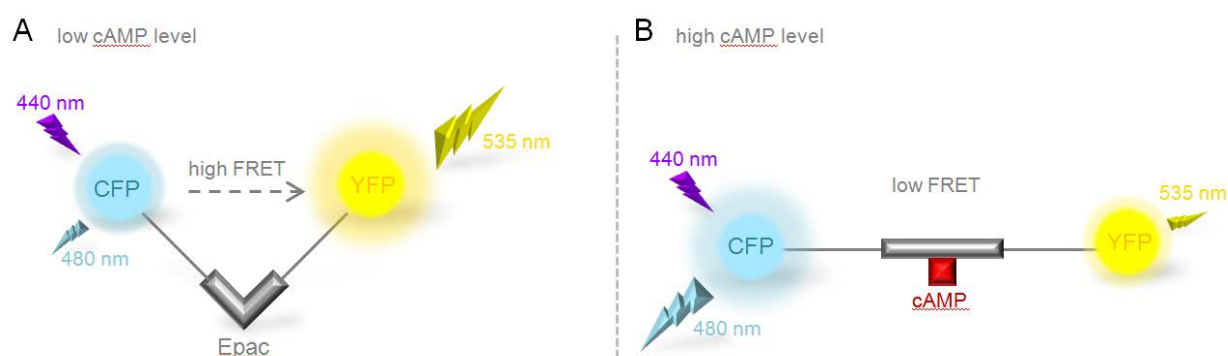


Figure 9: The Epac1camps sensor. (A) At low intracellular cAMP levels, the two fluorophores CFP and YFP are in close proximity, resulting in high FRET upon excitation of CFP. **(B)** In the presence of cAMP, the Epac protein changes its conformation, thus CFP and YFP move further apart. This leads to a loss in FRET.

For the investigation of intracellular Ca^{2+} levels, I used the GCaMP3.0 sensor (Tian et al., 2009), which is a fusion protein of green fluorescent protein (GFP) and Calmodulin. In the absence of Ca^{2+} , fluorescence of this sensor is only dim. When Ca^{2+} is present and binds to Calmodulin, GFP undergoes a conformational change, which increases its fluorescence. Expressed within cells, GCaMP fluorescence intensity thus directly reflects intracellular Ca^{2+} levels.

With the help of the *GAL4/UAS* system, both sensors can be expressed in the fly with any *GAL4*-line available (e.g. Shafer et al., 2008; Lelito and Shafer, 2012). In all imaging data shown in this thesis, I used a *clk856-GAL4* line (Gummadova et al., 2009), which shows an expression pattern quite specific to the clock neurons (*clk856G4>Epac1camps50A* and *clk856G4>GCaMP3.0*; see also Yao et al., 2012).

2.2.5.2 Dissection and Mounting

5-7 days old male flies were anesthetized on ice and brains were quickly dissected in cold Hemolymph-like saline (HL3; Stewart et al., 1994). I carefully removed all parts of the retina, lamina and ocelli to exclude any neuronal responses upon light stimulation of the photoreceptive organs. The brain was then mounted in a 35 mm FALCON petri dish (Becton Dickenson Labware, Franklin Lakes, NJ) in 405 μ l of HL3 in the center of a ring shaped silicone insert, which was used to reduce the working volume to 450 μ l (Fig. 10A). Depending on which neurons were intended to be imaged, the brain was either mounted with the anterior side up (for sLNv, lLNv and lNd) or with the dorsal side up (for DN). The surface of the petri dish was adherent enough for mounting without the use of tissue glue. All brains were allowed to recover from the dissection and mounting at least 10 min prior to imaging.

2.2.5.3 Confocal Live-Imaging and Applied Solutions

For all imaging experiments present in this thesis, I used an Olympus FV1000 laser scanning confocal microscope (Olympus, Center Valley, PA; Fig. 10B) in the laboratory of Prof. Orié T. Shafer, which was equipped with a 60x (1.10 N/A W, FUMFL N) objective with a dipping cone (Olympus, Center Valley, PA; Fig. 10C) and a 20x (0.50 N/A W, UMPlan FL N) objective. The petri dish containing the brain was placed below the objective and the cells were first brought into focus with the help of epifluorescent illumination for GFP excitation.

For cAMP imaging time lapse frames were scanned with a 440 nm laser at a 60x magnification and a frequency of 0.2 Hz for a total recording duration of 10 min. Regions of interest (ROI) were defined on single cell bodies in one focal plane, which was chosen

in the center of the somata of interest. The emission of CFP and YFP fluorophores was separated by a SDM510 dichroic mirror and the mean pixel intensities for each ROI were collected over time by the Olympus Fluoview software (v. 10). Clock neuron clusters were imaged separately in different brains, except for DN1a and DN1p, which were usually caught within the same frame.

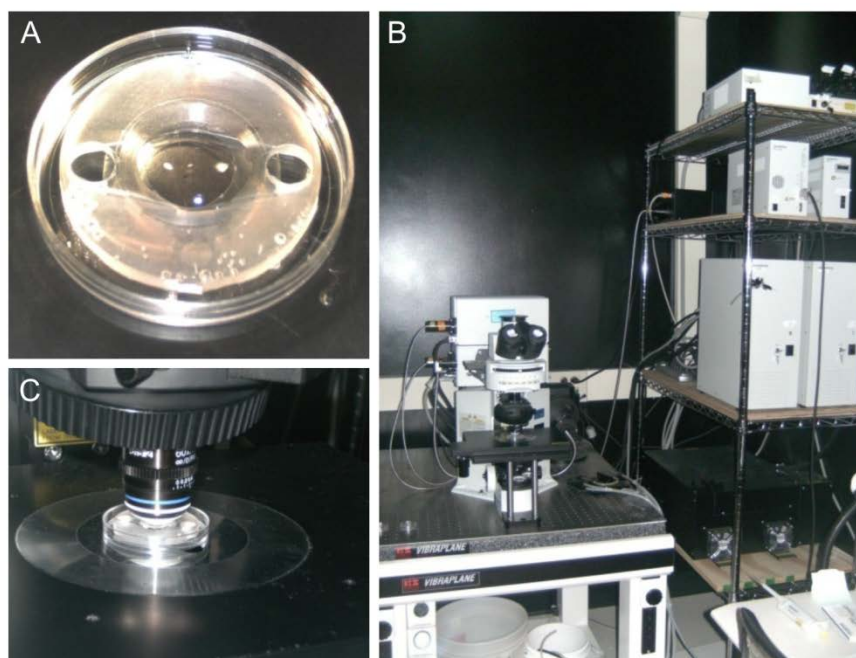


Figure 10: Confocal live-imaging Setup. (A) Brains were mounted in a petri dish with silicone insert. (B) Imaging was conducted using an Olympus FV1000 laser scanning confocal microscope (in the lab of Prof. Ori T. Shafer). (C) For single clock neuron imaging a 20x or 60x water objective was used.

For Ca^{2+} imaging I scanned time lapse frames with a 488 nm laser at a frequency of 1 Hz. The total recording duration was 7 minutes. Regions of interest were defined in the same way as for cAMP imaging experiments. GFP emission was detected using standard GFP optics and the mean pixel intensity for each ROI was measured over time. Since the 20x objective was used in this case, several clock neuron clusters were usually imaged within one brain (e.g. sLNv, ILNv and/or LNd together).

Applications of reagents were done using a 100 μl pipette, adding 45 μl of a 10x solution drop-wise between recording second 30 and 40, to end up with a 1x end concentration in 450 μl working volume. As positive controls I used the adenylate cyclase activator Forskolin in an end concentration of 20 μM (in HL3 + 0.1% DMSO) for cAMP imaging and Carbamylcholine (Carbachol) in an end concentration of 10^{-4}M for Ca^{2+} imaging. HL3 with

0.1% DMSO (end concentration) alone was applied as negative control (named HL3 in all figures). All peptides were weighed with a special accuracy weighing machine into low binding tubes, the small amount of peptide powder was then absorbed within a droplet of DMSO (end concentration 0.1%) and the solution was diluted in HL3 (end concentration of peptides, see Table 6). All concentrations given in figure legends refer to the end concentration after application.

Table 6: Peptides used for live imaging experiments.

Peptide Name	Sequence	End Concentration	Source
NPF	H-SNSRPPRKNDVNTMADAYKFLQDLDTYYGDRARVRFV-NH ₂	10 ⁻⁴ M	PolyPeptide Laboratories, San Diego
sNPF-1	H-AQRSPSLRLRF-NH ₂		
sNPF-2	H-VFGDVNQKPIRSPSLRLRF-NH ₂		
PDF	H-NSELINSLLSLPKNMNDA-NH ₂	10 ⁻⁵ M	

2.2.5.4 Data Analysis

For cAMP imaging experiments raw CFP and YFP fluorescence data were further processed in Microsoft Excel. CFP spillover into the YFP channel was measured as 0.444 for the used imaging setup. Consequently, raw YFP intensities were corrected by subtracting the CFP spillover at each time point: $YFP_{corr} = YFP - (CFP * 0.444)$. Then both CFP and YFP intensity traces were normalized to the mean intensity during the first 20 seconds of recording (baseline). Relative inverse FRET changes were then calculated as the ratio of normalized CFP/YFP_{corr} to directly reflect changes in cAMP and were transformed to percentaged traces of ratio change (Δ CFP/YFP). Traces for all regions of interest (ROIs) were averaged for the same cell group and stimulation, and the mean and standard error curves were finally smoothed by a moving average of 5. For quantification and statistical analysis of the cellular responses, maximal inverse FRET changes (Δ_{max} CFP/YFP) were calculated as the maximal (positive or negative) ratio deflection from baseline between recording second 30 and 300. For all cell groups positive and negative controls were conducted from neurons of at least 5 different brains, and data of peptide applications from at least 7 different brains.

Also for Ca²⁺ imaging we used Microsoft Excel to further process raw GFP fluorescence values. Single fluorescence values of each time point (F_n) were transformed into percentages of fluorescence change relative to baseline (F_0) by the following equation: $(F_n - F_0)/F_0 * 100$. Each neuronal trace thus depicts the percentage of fluorescence change from baseline ($\Delta F/F_0$), which directly reflects changes in intracellular Ca²⁺. Neuronal traces were averaged for the same cell group and treatment, and the mean and standard error curves were smoothed by a moving average of 5. For quantification and statistical analysis of the Ca²⁺ responses maximal changes in relative GFP fluorescence ($\Delta_{\max} F/F_0$) were calculated as the maximal (positive or negative) fluorescence deflection from baseline after recording second 60. Data were obtained from at least 5 different brains for each cell group and treatment.

2.2.6 *In silico* Analysis

To compare neuropeptide and clock protein sequences among different *Drosophila* species for our publication Hermann et al. (2013), Dr. Pingkalai R. Senthilan performed *in silico* analyses using sequence data bases and software, which are available online. The details of the method can be obtained from the Material and Methods section of Hermann et al. (2013).

2.2.7 Statistics

Statistical analysis was done with the software SYSTAT (v 11.00.01, Systat 11, SPSS, Chicago, IL). Data were first tested for normal distribution applying a one-sample Kolmogorov-Smirnov test. Normally distributed data were subsequently tested for significant differences using a one-way ANOVA followed by a post-hoc pairwise comparison with Bonferroni correction. The equivalent for not normally distributed data was the Kruskal-Wallis test followed by Wilcoxon analysis. Data were considered as significantly different with $p < 0.05$, indicated by *, and as highly significant with $p < 0.001$, indicated by ** in most graphic charts. Otherwise significant differences are indicated by a letter code, in which different lettering reflects significances.

3 Results

In the following, I will shortly describe the key findings of the publications included in this thesis as well as of a new manuscript, which has been submitted to the Journal of Neuroscience (3.1, 3.2 and 3.3). The full text versions of the papers and the manuscript can be read starting from page 109. In addition, I will present data obtained during this PhD project (3.4 and 3.5), which are so far not part of a manuscript.

3.1 The Clock Network Is Conserved in Different *Drosophila* Species (Paper 1)

In this study we were interested in the properties of the neuronal clock network in different *Drosophila* species. We chose 10 species with fully or partly sequenced genome, which were distributed along the *Drosophila* phylogenetic tree (including species of the subgenera *Sophophora* and *Drosophila*). *In silico* analyses of protein sequences revealed high similarity and identity values for canonical clock protein homologues (PER, TIM, VRI, PDP1 and CRY) of the different fly species. To investigate the morphology of the neuronal clock network, we immunostained brains of the different species with antibodies against VRI, PDP1 and CRY, and showed that all clock neuron clusters, that are described for *Drosophila melanogaster*, are also present in the investigated species. However, species of the *Drosophila* subgenus and *Drosophila pseudoobscura* did not express CRY in the ILNv. Since Bahn et al. (2009) had shown first results on the expression of PDF in *Drosophila virilis* and had found that these flies lack PDF in the sLNv we extended this study to the other species. In addition, we included the neuropeptide ITP into the investigation. Both mature peptides showed high sequence similarities and identities in the *in silico* analysis, indicating a high structural conservation within the *Drosophila* genus. Immunostaining with anti-ITP showed that the peptide is present in the fifth sLNv and in one LNd in all investigated species, like it was reported for *Drosophila melanogaster* (Johard et al., 2009). Anti-PDF staining revealed that investigated species of the *Drosophila* subgenus and *Drosophila pseudoobscura* have reduced PDF expression in the sLNv. Considering the flies' natural habitat, we thus found that species distributed up to higher latitudes (investigated species of the *Drosophila* subgenus and *Drosophila*

pseudoobscura) lack CRY in the ILNv and PDF in the sLNv, which might be interpreted as an adaptation to cold temperatures and extreme photoperiods in the north.

(For details see results section of Hermann et al., 2013.)

3.2 NPF⁺ Clock Neurons Modify E Activity and Free-Running Period (Paper 2)

Based on previous studies, in which NPF⁺ neurons have been successfully ablated (Lee et al., 2006; Hamasaka et al., 2010), we aimed to investigate the role of NPF for circadian locomotor rhythms. First, we reevaluated the NPF expression pattern in adult *Drosophila melanogaster* brains using anti-NPF as well as *npf-GAL4* (*npfG4*) mediated GFP expression. We found NPF expression in three LN_d, which had been reported before (Lee et al., 2006), but identified in addition the fifth sLN_v and 2-3 ILN_v as NPF⁺. Lee et al. (2006) had shown that the ablation of the NPF⁺ neurons has an effect on the phase and the shape of the E activity in entrained conditions. We found in addition that NPF-ablated flies (*npfG4>UAS-hid*) significantly prolong their circadian free-running period in DD. To address these phenotypes to either the absence of the NPF⁺ clock neurons or NPF⁺ non-clock neurons, we additionally introduced a *cry-GAL80* (*cryG80*) construct to prevent cell ablation in all clock cells. Like this we were able to rescue the observed phenotypes, indicating that the NPF⁺ clock neurons are involved in the control of the E activity and the free-running rhythms in DD. Using *pdfG80* instead of *cryG80* we were able to only rescue the PDF⁺ clock neurons from the cell ablation. This experiment showed only partial rescue phenotypes in behavior. Thus, we conclude that the PDF⁻ NPF⁺ clock neurons (the fifth sLN_v and the NPF⁺ LN_d) modify E activity and free-running period.

To investigate whether the observed phenotypes derive from the absence of NPF itself or the absence of the whole neurons, we expressed a genetically encoded *npf-RNAi* construct in the clock neurons using *tim(UAS)G4* and tested these NPF-knockdown flies under the same conditions as the NPF-ablated flies. We found no effect on locomotor rhythms. However, immunocytochemical analysis revealed that the RNAi-construct was not working efficiently and NPF was still detectable in the clock cells. Nevertheless, double knockdown of NPF and PDF seemed to slightly repress E activity compared to control flies and PDF-single-knockdown flies.

(For details see results section of Hermann et al., 2012.)

3.3 ITP is a new functional clock neuropeptide (Paper 3, submitted)

Previous studies had shown that the Ion Transport Peptide (ITP) is expressed in the fifth sLNv and in one LNd (Dircksen et al., 2008; Johard et al., 2009). Thus, we were interested, whether ITP plays a role in the control of circadian behavior. We first showed that ITP is continuously present in clock neuron cell bodies in LD, while its immunostaining cycles within the dorsal projections into the Pars intercerebralis (PI), indicating that ITP is released rhythmically there. Further, *Clk^{AR}* mutants, but not *per⁰¹* mutants showed reduced ITP immunostaining, indicating that the *itp* gene is under direct or indirect CLK control.

We then employed a genetically encoded RNAi-construct to specifically knock down ITP only in the two ITP⁺ clock neurons and gave proof of its efficiency by immunohistochemistry. We found that ITP-knockdown flies were not impaired in the phasing of the activity peaks and their general ability to entrain to LD cycles of different photoperiods. However, the E activity of ITP-knockdown flies was reduced in amplitude when examined relative to the M peak amplitude and relative night activity was enhanced. Investigating free-running rhythms in DD we found that the knockdown of ITP in the clock neurons doesn't affect rhythmicity in general, but significantly prolongs the flies' free-running period.

To investigate the effects of high amounts of ITP in the brain and to figure out putative regions of ITP action, we developed a *UAS-ITP* construct and ectopically expressed the peptide with different *GAL4 (G4)* driver lines. We found that flies get arrhythmic in DD and show a slight dampening of PER cycling within the sLNv and the LNd, when ITP is overexpressed with *tim(UAS)G4*. In addition, flies were similarly arrhythmic in behavior when ITP was overexpressed with another *timG4* line. With all other tested driver lines, however, flies were behaviorally normal. Examining ITP immunostaining in overexpressing flies in detail, we tried to identify particular regions in the brain, where ITP⁺ projections seemed especially enriched in the arrhythmic overexpressing strains (*tim(UAS)>ITP²/timG4>ITP²*) in comparison to the rhythmic ones. We found that especially *tim(UAS)G4>ITP²* and *perG4>ITP²* have strong ITP staining in the clock neurons and their projections into the PI. Interestingly, we discovered that the rhythm in ITP-immunostaining in the projections into the PI is lost in behaviorally arrhythmic

tim(UAS)G4>ITP² flies, while it is still present in behaviorally rhythmic *perG4>ITP²* flies. Further, in 60% of *tim(UAS)G4>ITP²* flies the ILNv were sending misled fibers into the dorsal protocerebrum, in which PDF was expressed constantly high. Thus, we assume that constantly high levels of both ITP and PDF evoke arrhythmicity in *tim(UAS)G4>ITP²* flies.

When we knocked down ITP in conjunction with PDF, flies showed an advanced E peak phase in LD, which is typical for PDF-knockdown flies. Further, E activity was reduced relative to the M activity and night activity was enhanced, as it was observed in ITP-knockdown flies. Thus ITP/PDF-knockdown flies showed both PDF-knockdown specific and ITP-knockdown specific characteristics in LD. In DD, ITP/PDF-knockdown flies showed enhanced activity levels and were almost completely arrhythmic or showed several free-running components, which made the determination of the period length impossible.

(For details see results section of Hermann-Luibl et al., *submitted*.)

3.4 The role of sNPF in circadian behavior

sNPF is expressed in the sLNv and in two LNd

The first part of this section deals with the reevaluation of the expression pattern of sNPF in adult *Drosophila melanogaster* brains. Since Johard et al. (2009) had shown that sNPF is expressed in certain clock neurons I focused on these cells in my investigation. First, I used a *snpf-GAL4 (snpfG4)* line and expressed a *UAS-GFP* reporter construct (Fig. 11A, B, C). GFP was broadly expressed within the brain showing especially strong signals in the mushroom bodies and the lateral brain (Fig. 11A). To visualize the clock neurons I counterstained GFP expressing brains with anti-TIM and anti-PDF. In accordance with Johard et al. (2009) the GFP signal overlapped with anti-TIM in two LNd (Fig. 11B) and with anti-TIM and anti-PDF in four sLNv (Fig. 11C).

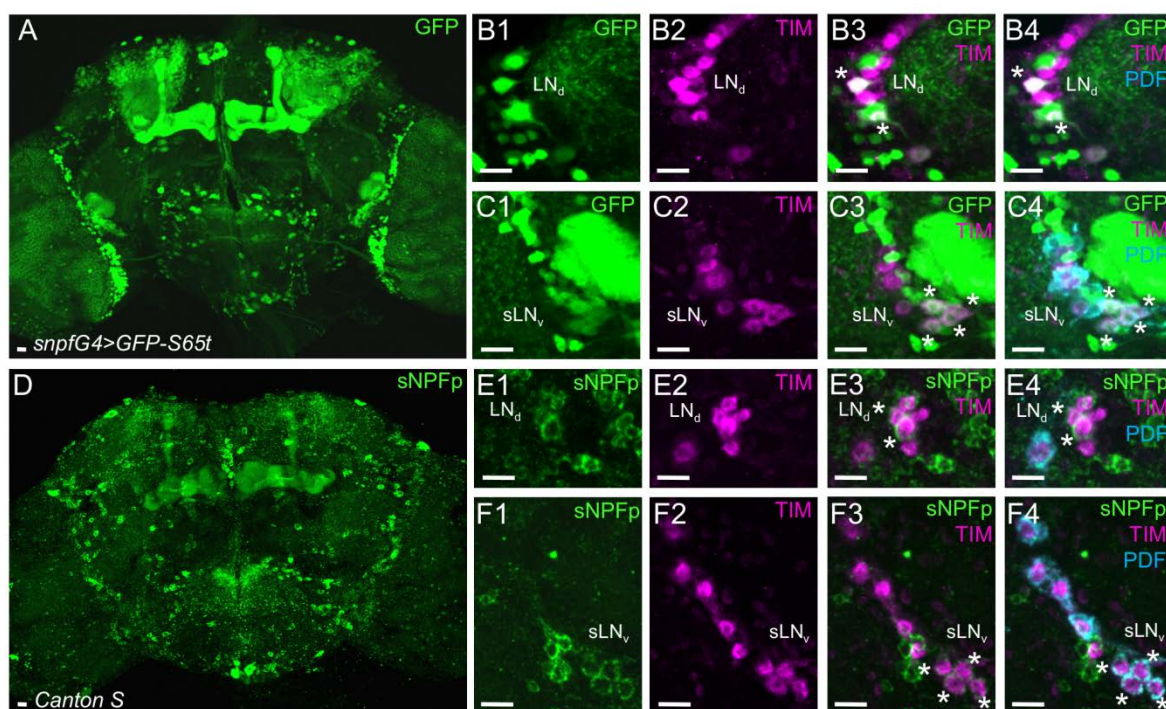


Figure 11: sNPF expression in clock neurons of adult *Drosophila melanogaster* brains. (A) Overview of *snpf-GAL4 (snpfG4)* mediated GFP expression in the whole brain. (B) Detailed view of LNd clock neurons. GFP expression (green) overlaps with anti-TIM staining (magenta) in two cells (asterisks). (C) Detailed view of sLNv, which express GFP and are colabeled with anti-TIM and anti-PDF (blue; asterisks). (D) Overview of anti-sNPFp (green) staining in the whole CS brain. (E) anti-sNPFp and anti-TIM (magenta) staining overlaps in two LNd (stars). (F) sLNv are stained with anti-sNPFp, anti-TIM and anti-PDF (blue). Scale bars = 10µm.

To directly prove the presence of the sNPF peptide, I additionally stained *Canton S (CS)* brains with an antibody against part of the sNPF precursor peptide (sNPFp; Fig. 11D, E, F; Johard et al., 2008; Nässel et al., 2008). The anti-sNPFp staining showed similarly broad

staining as the GFP signal had revealed. Further, it overlapped with costained anti-TIM in two LNd (Fig. 11E) and with anti-TIM and anti-PDF in the sLNv (Fig. 11F). Thus, both *GAL4* driven GFP expression and antibody staining confirmed the sNPF expression pattern in the two clock neuron groups as it was shown by Johard et al. (2009).

Expression of $snpf$ -RNAi^{Lee} within clock neurons fails to knock down $snpf$ expression

With the attempt to investigate the role of sNPF in circadian behavior, I obtained a *UAS-snpf-RNAi^{Lee}* construct (Lee et al., 2004) and expressed it under the control of *tim(UAS)-GAL4* (*tim(UAS)G4*) together with *UAS-dicer2* (*dcr2*). With this combination I expected a knockdown of sNPF within the sNPF⁺ clock neurons. To verify this, I immunostained brains of putative sNPF-knockdown flies (*tim(UAS)G4>dcr2;snpf-RNAi^{Lee}*) with the sNPFp antibody and counterstained with anti-VRI and anti-PDF to identify the clock neurons. I immediately realized, that the knockdown was not complete and that there was still sNPF⁺ staining within the clock cells. To determine, whether there was at least a signal reduction, I quantified the staining intensity in the sLNv and the two LNd and compared it to the data of equally treated control flies (*tim(UAS)G4>dcr2* and *dcr2;snpf-RNAi^{Lee}*). This quantification showed that there was no significant reduction of sNPF staining intensity in the sNPF-knockdown flies compared to controls (Fig. 12). I repeated this staining and quantitative analysis several times, but never found a significant reduction of sNPF within the clock neurons (data not shown). These results indicate that the *UAS-snpf-RNAi^{Lee}* construct is not working properly inside the clock neurons.

Since these results were in conflict to the work of Lee et al. (2004), which had demonstrated the efficiency of the *UAS-snpf-RNAi^{Lee}* construct by qPCR, I also tried to verify the sNPF-knockdown on the RNA level. Therefore I expressed the *RNAi*-construct with the panneuronal driver line *elav-GAL4* (*elavG4*) and performed qPCR analysis of adult male fly heads. Nevertheless, also this experiment did not prove the functionality of the *snpf-RNAi^{Lee}* construct (Fig. 13).

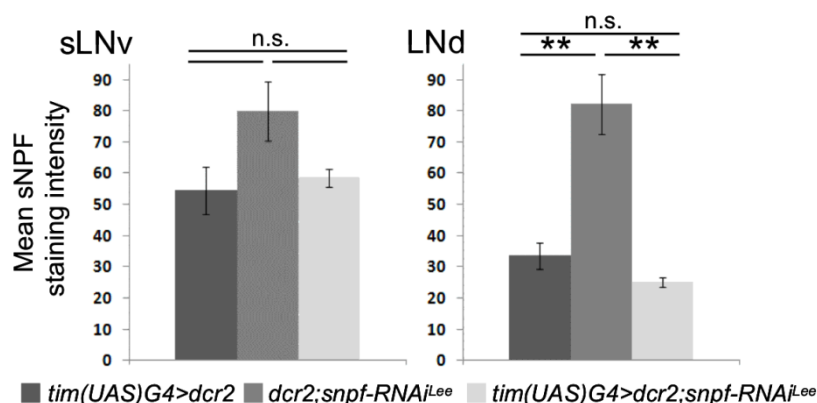


Figure 12: Quantification of sNPFp staining intensity in sLNv and LNd clock neurons in putative sNPF-knockdown flies. Staining intensity in sNPF-“knockdown” flies (light gray) was not reduced in comparison to both control genotypes (darker gray bars) in sLNv and LNd. ** indicate $p < 0.001$; n.s. = not significant; error bars depict SEM.

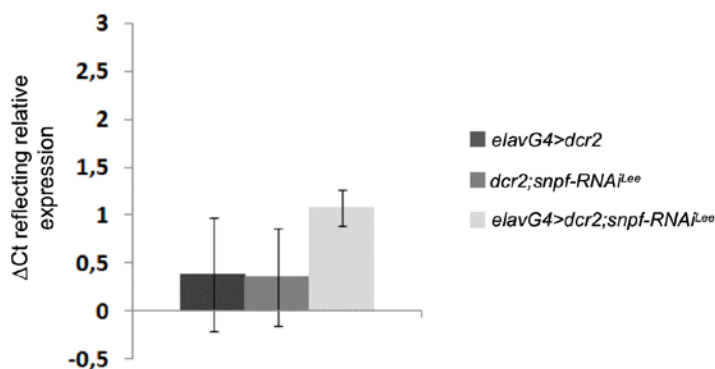


Figure 13: qPCR data of putative sNPF knockdown flies using *elav-GAL4* (*elavG4*) in comparison to controls. RNA was extracted from whole heads for qPCR analysis in two technical replicates for 3 biological replicates. Ct values of *tubulin* were subtracted from Ct values of *snpf* and the resulting Δ Ct values were subtracted from an arbitrary value (3) to depict lower RNA amounts as lower bars and higher RNA amounts as higher bars in the graph. Putative sNPF-knockdown flies and controls differed by less than 1 cycle, indicating that the sNPF-RNA levels were similar. I did not perform statistics on the data, since the n of the biological replicates is only 3. Error bars depict SEM.

snpf-RNAi^{lee} expressed in clock neurons decreases relative daytime activity in certain entrained conditions and increases nighttime activity

Although the immunohistochemistry did not lead to satisfying results concerning the *snpf-RNAi^{lee}* efficiency, I tested sNPF-“knockdown” flies and the respective controls (see above) in the locomotor activity assay. To investigate the flies’ behavior in entrained conditions, I monitored the different strains in LD conditions.

Since effects on the activity peak timing can sometimes be better observed, when the peak does not occur exactly at the time of the light transition, I recorded the flies not only

in LD 12:12, but also in longer and shorter photoperiods (LD 16:08, LD 20:04; Fig. 14 or LD 08:16, LD 04:20; Fig. 15). The normalized average activity profiles revealed no striking differences in general shape between sNPF-“knockdown” flies and controls in long days (Fig. 14) or short days (Fig. 15). The peak timing for example doesn’t seem to be affected by the expression of the *snpf-RNAi^{Lee}* construct. (Compare the E peak timing of the different genotypes in Fig. 14 and the M peak timing of the different strains in Fig. 15).

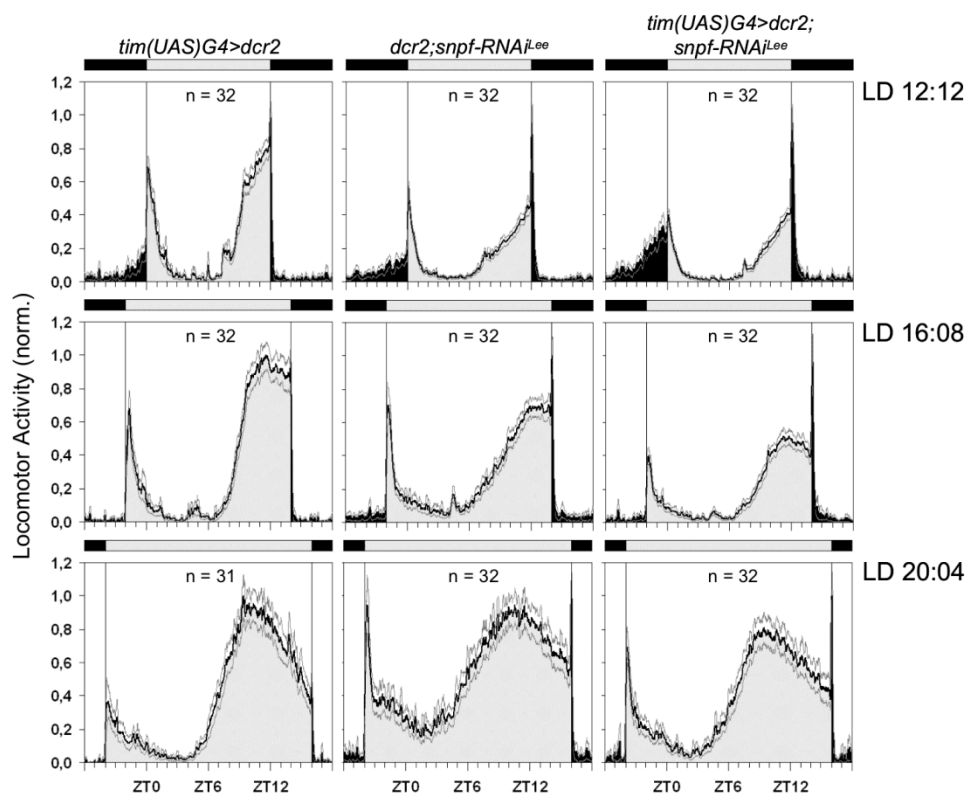


Figure 14: LD behavior of putative sNPF-knockdown flies and controls in LD 12:12 and longer photoperiods. Average activity profiles were calculated for each genotype and light condition and were normalized to the highest activity value to better visualize the shape of the profile. No differences in the shape of the bimodal activity pattern of sNPF-“knockdown” flies and controls were visible in the different conditions. n = number of investigated flies; black areas indicate darkness, gray areas indicate light of 100 lux; black line = mean, gray lines = SEM; T = 20°C.

When examining activity levels during the light phase and the dark phase relative to the total activity of the flies over the whole day, I found that sNPF-“knockdown” flies are significantly less active during daytime compared to controls in LD 12:12 and in short photoperiods, however not in long photoperiods (Fig. 16). The relative nighttime activity showed the opposite: sNPF-“knockdown” flies were significantly more active during the night compared to control flies (Fig. 17).

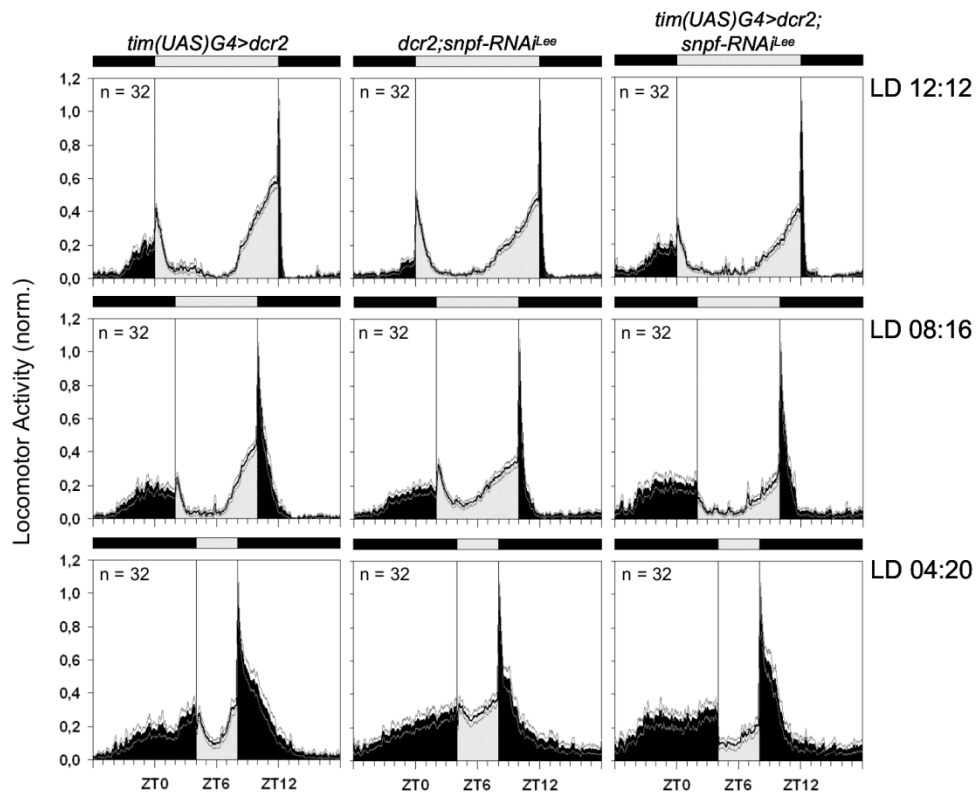


Figure 15: LD behavior of putative sNPF-knockdown flies and controls in LD 12:12 and shorter photoperiods. Average activity profiles were calculated for each genotype and light condition and were normalized to the highest activity value to better visualize the shape of the profile. No differences in the shape of the bimodal activity pattern of sNPF-“knockdown” flies and controls were visible in the different conditions. n = number of investigated flies; black areas indicate darkness, gray areas indicate light of 100 lux; black line = mean, gray lines = SEM; $T = 20^{\circ}\text{C}$.

snpf-RNAi^{Lee} expressed in clock neurons prolongs the free-running period in constant darkness

Next, I tested the flies in DD after seven days of entrainment to LD 12:12, to determine the endogenous rhythm of sNPF-“knockdown” flies compared to controls. Representative single actograms of the three genotypes show, that the flies are normally rhythmic in DD (Fig. 18; see also Table 7). I found highly significant differences in the free-running period length, with sNPF-“knockdown” flies having longer rhythms than both controls (Fig. 18; see also Table 7). This effect was, however, not reproducible: in a second experiment with the same light condition and genotypes, the period length of sNPF-knockdown flies lay in between the period lengths of the two controls (sNPF-knockdown flies 23.9 h, *GAL4*-control 24.3 h, *RNAi*-control 23.4 h).

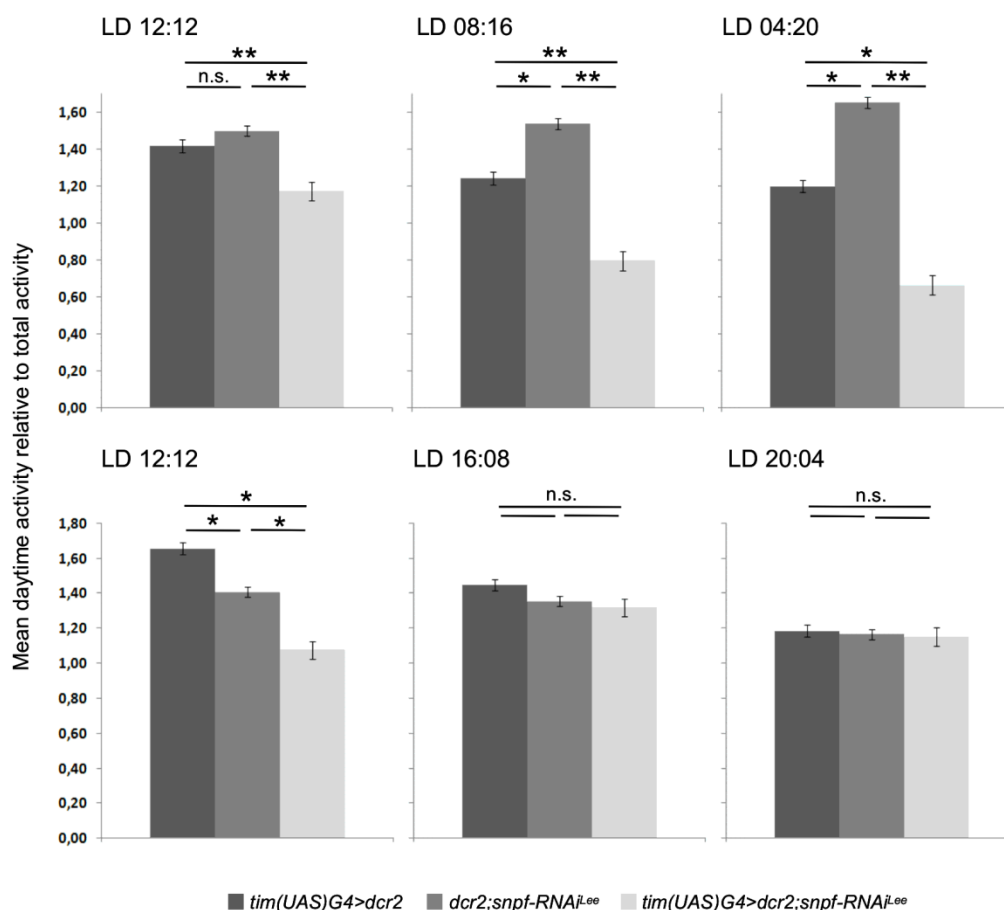


Figure 16: Relative daytime activity levels of putative sNPF-knockdown flies (light gray) and controls (darker gray) in LD 12:12, long and short photoperiods. Activity levels were calculated as the average of beam crosses per minute during the light phase relative to the average of total beam crosses over the whole day. sNPF-“knockdown” flies show a relative reduction in daytime activity in LD 12:12 and shorter photoperiods. * indicates $p < 0.05$; ** indicates $p < 0.001$; n.s. = not significant; error bars depict SEM.

snpf-RNAi^{lee} expressed in PDF-knockdown flies reduces daytime activity and enhances nighttime activity

To investigate possible interaction effects of sNPF and PDF, I investigated flies in which I expressed the *snpf-RNAi^{lee}* construct, while simultaneously knocking down PDF. I recorded sNPF-“knockdown” flies, PDF-knockdown flies and sNPF/PDF-knockdown flies together with the respective control flies in LD 12:12 (Fig. 19). The normalized average activity profile of sNPF-“knockdown” flies showed again no difference in shape or peak timing compared to controls, while PDF-knockdown flies showed an advanced E activity as described previously (Fig. 19A; Renn et al., 1999). When expressing both RNAi constructs together, the flies still had an advanced E activity as it was seen in PDF-knockdown flies (Fig. 19A).

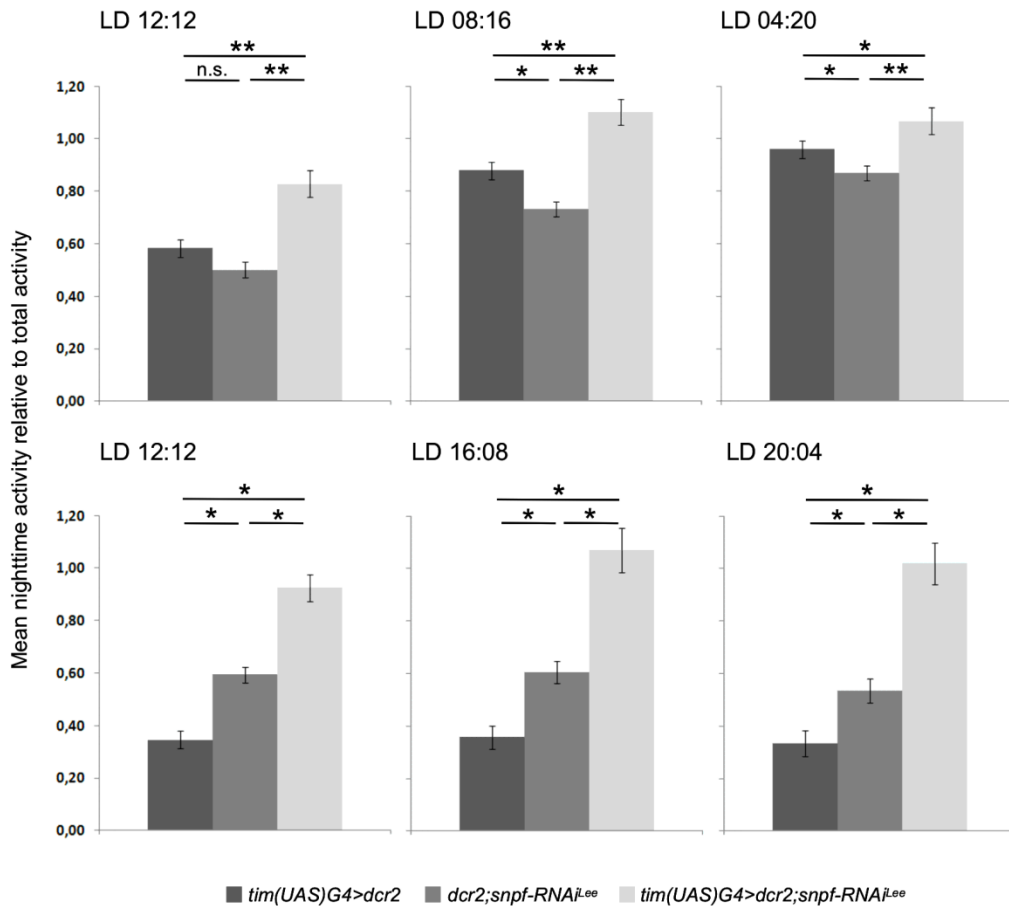


Figure 17: Relative nighttime activity levels of putative sPNF-knockdown flies (light gray) and controls (darker gray) in LD 12:12, long and short photoperiods. Activity levels were calculated as the average of beam crosses per minute during the dark phase relative to the average of total beam crosses over the whole day. sPNF-“knockdown” flies show a relative increase in nighttime activity in all conditions. * indicates $p < 0.05$; ** indicates $p < 0.001$; n.s. = not significant; error bars depict SEM.

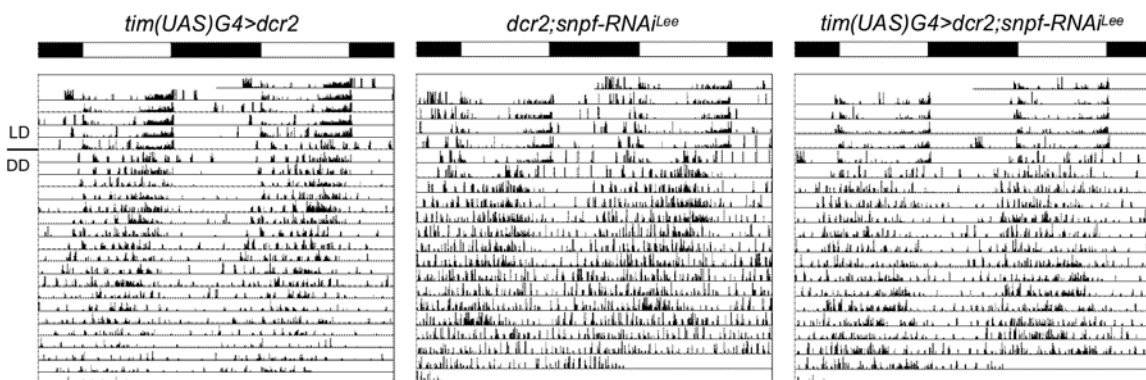


Figure 18: Representative individual double plotted actograms of putative sPNF-knockdown flies and controls in LD 12:12 followed by DD. sPNF-“knockdown” flies have a significantly prolonged free-running period in DD. Black and white bars indicate the light regime in LD 12:12 (100 lux); T = 20°C.

Table 7: Rhythmicity data of putative sNPF-knockdown flies, sNPF/PDF-knockdown flies and controls in constant darkness. ** indicates $p < 0.001$.

genotype	period (SEM) in h (n rhythmic flies)	power (SEM)	rhythmicity in % of all tested flies
<i>dicer2;tim(UAS)G4/+</i>	23.7 (0.05) (32)	22.8 (0.68)	100
<i>dicer2;+;snpf-RNAi^{Lee}/+</i>	23.5 (0.10) (27)	25.1 (1.54)	90
<i>dicer2;tim(UAS)G4/+;snpf-RNAi^{Lee}/+</i>	24.0 (0.06) (28) ** ¹⁾	31.3 (1.80)	90
<i>dicer2;+;pdf-RNAi/+</i>	23.8 (0.06) (31)	36.1 (2.29)	100
<i>dicer2;tim(UAS)G4;pdf-RNAi/+</i>	23.7 (0.16) (10)	16.9 (0.79)	31**
<i>dicer2;tim(UAS)G4;pdf-RNAi/snpf-RNAi^{Lee}</i>	24.4 (0.06) (29) * ²⁾	22.2 (1.18)	94

Data for *tim(UAS)G4>dcr2*, *dcr2;pdf-RNAi* and *tim(UAS)G4>dcr2;pdf-RNAi* are from Hermann-Luibl et al., submitted. ¹⁾ ** to *dicer2;timG4/+* and *dicer2;+;snpf-RNAi^{Lee}/+*; ²⁾ * to all genotypes, except *dicer2;timG4;pdf-RNAi/+*

I again calculated relative activity levels during the light phase and the dark phase of the different tested strains. sNPF-“knockdown” flies were again significantly less active during daytime than controls (Fig. 19B upper panel). PDF-knockdown flies showed a tendency towards a higher daytime activity level, which is not surprising, considering that the E peak is very much advanced in these flies. Nevertheless, when expressing the *snpf-RNAi^{Lee}* construct in addition, the daytime activity level was decreased to the same level as in sNPF-“knockdown” flies alone, although the much more efficient *pdf-RNAi* construct would rather increase daytime activity (Fig. 19B upper panel). When comparing nighttime activity levels of the different genotypes, we found again a significant increase in sNPF-“knockdown” flies (Fig. 19B lower panel) as it had been the case in the previous long and short day experiments (Fig. 17). Further, sNPF/PDF-knockdown flies showed the same increase in nighttime activity as sNPF-“knockdown” flies alone, while nighttime activity in PDF-knockdown flies was not affected (Fig. 19B lower panel).

Since I had found these differences in activity levels in sNPF-“knockdown” flies and sNPF/PDF-knockdown flies, we wondered, whether sleep would also be affected in these strains. Therefore I utilized the same data set that is depicted in Fig. 19 and calculated the average sleep for each hour in LD 12:12, whereby sleep is defined as the amount of time, in which the flies did not cross the infrared light beam for at least 10 minutes. The average sleep traces are quite similar in sNPF-“knockdown” flies compared to controls

during daytime, while sNPF/PDF-knockdown flies clearly show less daytime sleep (Fig. 20A). In addition, both genotypes sleep less than the other strains especially in the second half of the night (Fig. 20A).

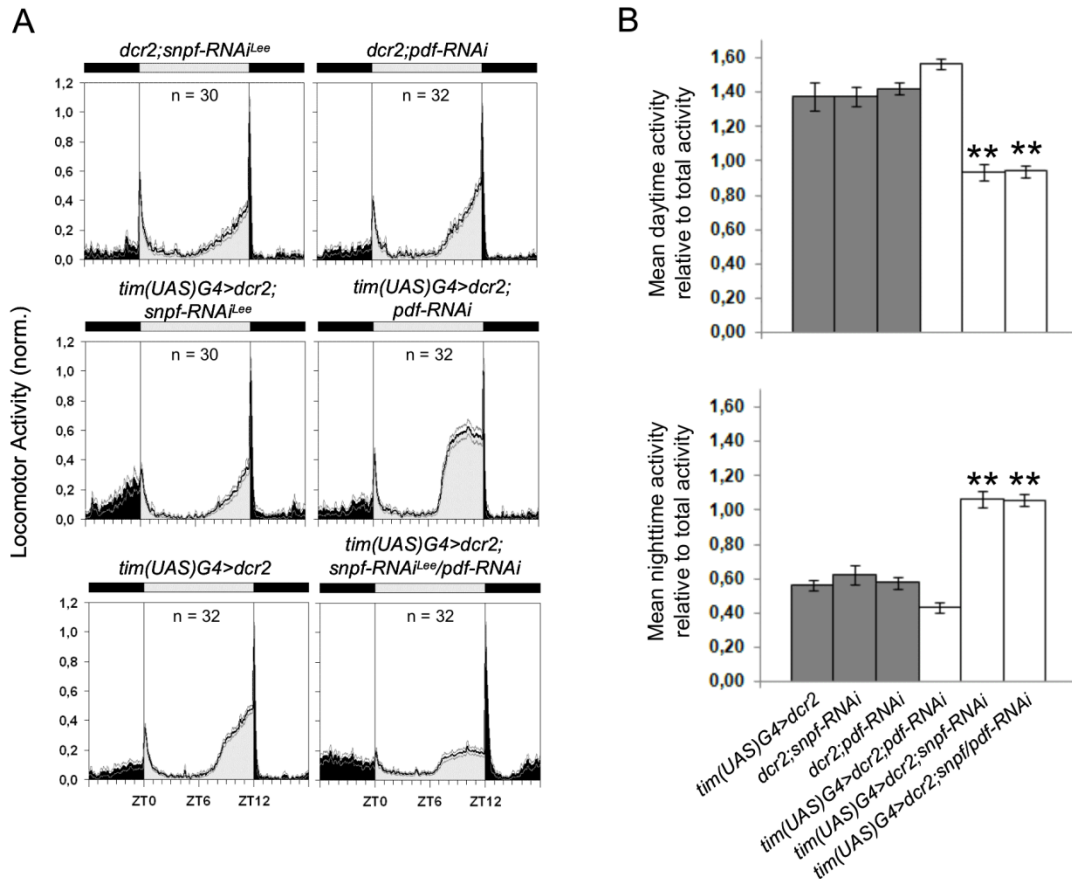


Figure 19: Average activity profiles and relative activity levels of sNPF/PDF-knockdown flies and controls in LD 12:12. (A) Average activity profiles were calculated for each genotype and light condition and were normalized to the highest activity value to better visualize the shape of the profile. n = number of investigated flies; black areas indicate darkness, gray areas indicate light of 100 lux; black line = mean, gray lines = SEM; T = 20°C **(B)** Relative activity levels were calculated as the average of beam crosses per minute during the light phase (upper panel) or the dark phase (lower panel) relative to the average of total beam crosses over the whole day. ** indicates p<0.001; n.s. = not significant; error bars depict SEM. Data for *tim(UAS)G4>dcr2*, *dcr2;pdf-RNAi* and *tim(UAS)G4>dcr2;pdf-RNAi* are from Hermann-Luibl et al., *submitted*.

To quantify this, I calculated the total amount of sleep during the day and the night in all genotypes. Total nighttime sleep was significantly decreased in sNPF-“knockdown” and sNPF/PDF-knockdown flies compared to the other genotypes, but the two genotypes did not differ from each other (Fig. 20B). Daytime sleep was unaffected in sNPF-“knockdown” flies, but was also significantly decreased in comparison to all other genotypes in

sNPF/PDF-knockdown flies (Fig. 20B). This was surprising, considering that lower daytime activity levels in sNPF/PDF-knockdown flies correlated with lower amounts of sleep.

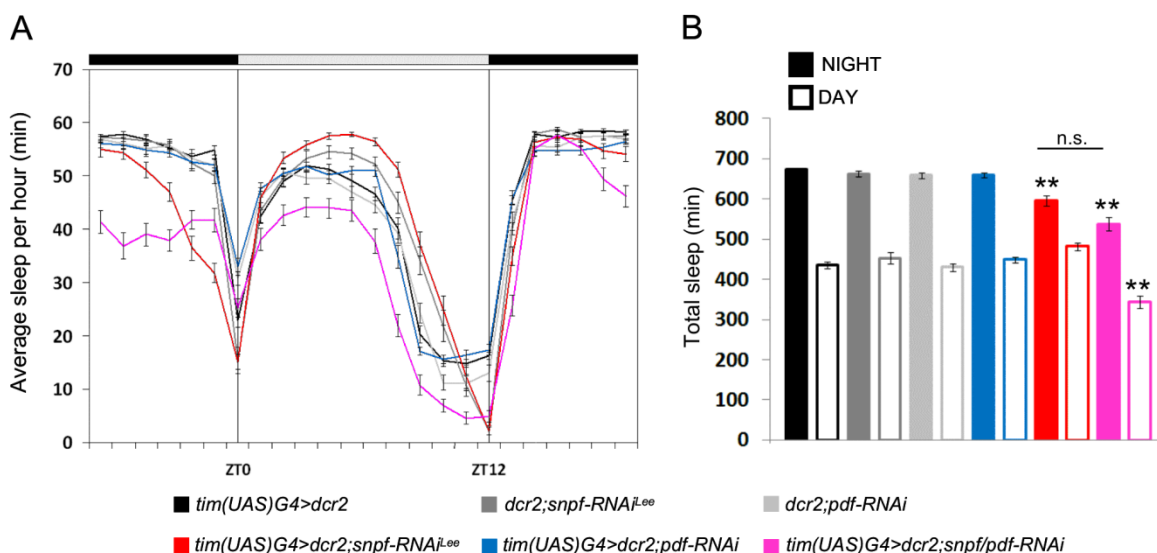


Figure 20: Daily averaged sleep profile and total sleep of putative sNPF-knockdown flies and sNPF/PDF-knockdown flies in LD 12:12. Sleep was defined as the average amount of time, in which the flies did not cross the infrared light beam for at least 10 consecutive minutes. **(A)** Daily average sleep profiles of putative sNPF-knockdown flies (red), PDF-knockdown flies (blue), sNPF/PDF-knockdown flies (magenta) and controls (different grays). sNPF-“knockdown” flies and sNPF/PDF-knockdown flies sleep less in the second half of the night and sNPF/PDF-knockdown flies also during the day. **(B)** Total amount of sleep during nighttime (full bars) and daytime (empty bars). sNPF-“knockdown” flies and sNPF/PDF-knockdown flies have a significantly decreased nighttime sleep compared to controls, while sNPF/PDF-knockdown flies have in addition decreased daytime sleep. ** indicates $p < 0.001$, n.s. = not significant; error bars depict SEM. Data for *tim(UAS)G4>dcr2*, *dcr2;pdf-RNAi* and *tim(UAS)G4>dcr2;pdf-RNAi* are from Hermann-Luibl et al., *submitted*.

In accordance with previous studies (Shafer and Taghert, 2009), PDF-knockdown flies showed very low percentages in rhythmicity, when recorded in DD (38% rhythmic flies; Table 7). Surprisingly, when coexpressing the *snpf-RNAi^{Lee}* construct, a high number of flies were again rhythmic (94%; Table 7). In addition, the free-running period of these flies was significantly longer than the period of the other genotypes, except of PDF-knockdown flies, to which there was no statistical difference (Table 7).

Alternative manipulations of the sNPF circuit had no or different effects on rhythmic behavior

Since the knockdown of sNPF with the *snpf-RNAi^{Lee}* construct by Lee et al. (2004) was not efficient, but still showed some phenotypes in rhythmic behavior, we wondered, whether

the knockdown was too weak for detection. Therefore, I decided to test a second independent *snpf-RNAi* line, which I obtained from the Bloomington stock collection (*snpf-RNAi^{Bloo}*). I again expressed this construct with the *tim(UAS)G4* line in the presence of *UAS-dicer2* and tested the flies in locomotor activity experiments in LD cycles and constant darkness. In addition, I investigated the effects of an RNAi construct against the sNPF receptor, sNPF1 (*snpfR-RNAi*) using the same driver line. Further, I used the hypomorph sNPF mutant, *sNPF^{c00448}*, from now on referred to as *sNPF^{hypo}*, in which overall sNPF levels should be lower compared to *CS* (Lee et al., 2008; Chen et al., 2013).

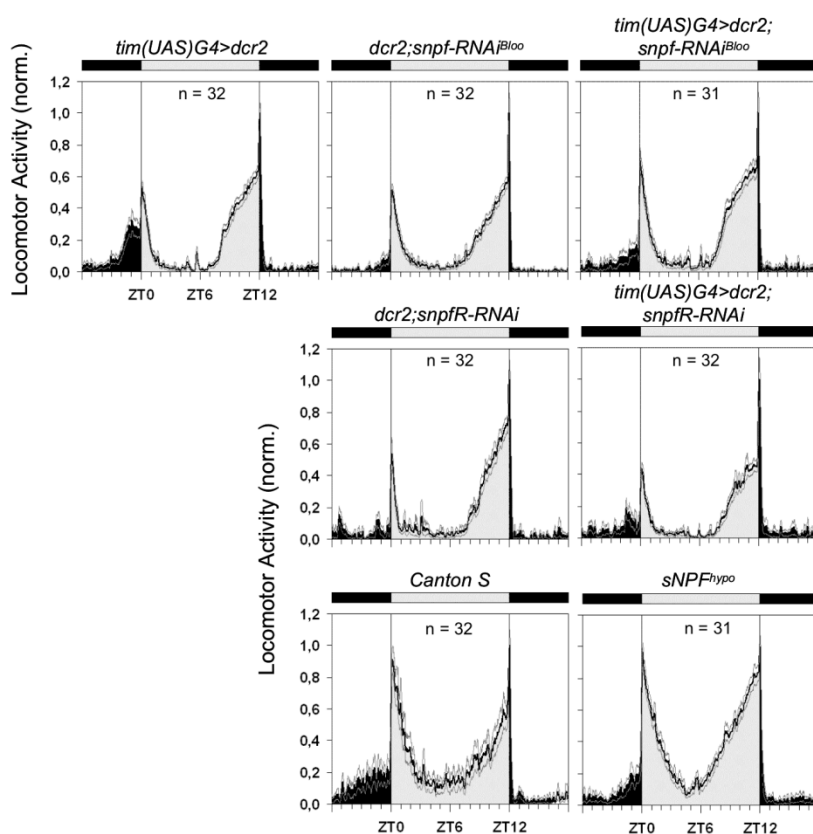


Figure 21: Average activity profiles of putative sNPF-knockdown, sNPF1-knockdown, *sNPF^{hypo}* flies and respective controls in LD 12:12. Activity profiles were calculated for each genotype and light condition and were normalized to the highest activity value to better visualize the shape of the profile. No obvious phenotypes were observed in LD behavior in any of the investigated genotypes. n = number of investigated flies; black areas indicate darkness, gray areas indicate light of 100 lux; black line = mean, gray lines = SEM; T = 20°C

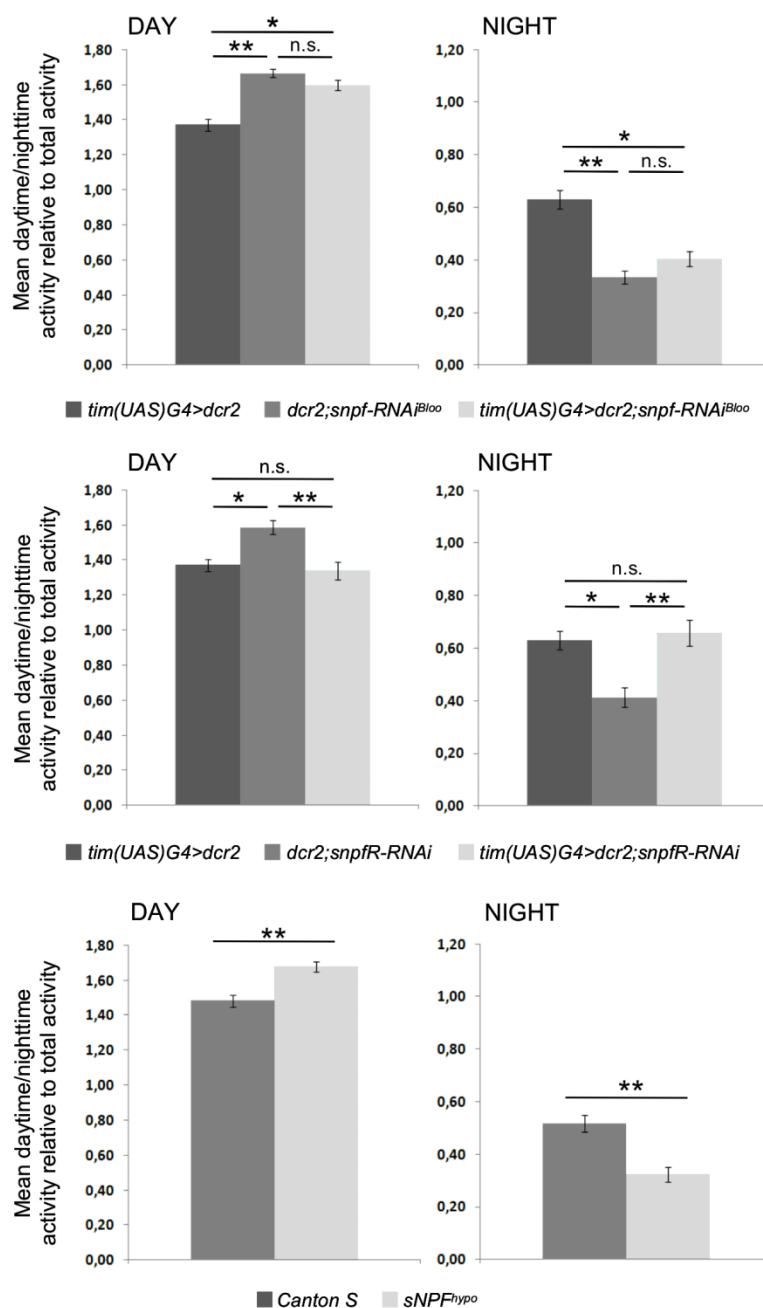


Figure 22: Relative activity levels of putative sNPF-knockdown, sNPFR-knockdown, *sNPF^{hypo}* flies and controls during day and night in LD 12:12. Activity levels were calculated as the average of beam crosses per minute during the light phase or the dark phase relative to the average of total beam crosses over the day. Experimental flies of RNAi-strains did not show significantly enhanced or reduced activity during the light phase or the dark phase. *sNPF^{hypo}* flies showed significantly more relative activity during the day and less relative nighttime activity compared to CS. * indicates $p < 0.05$; ** indicates $p < 0.001$; n.s. = not significant; error bars depict SEM.

When recording the flies in LD 12:12, I did not observe any phenotypes in sNPF-knockdown, sNPFR-knockdown or *sNPF^{hypo}* flies in comparison to the respective control flies with regard to the shape of the daily activity profile (Fig. 21). I then calculated the relative activity levels during the light phase and the dark phase (Fig. 22). Activity was not

significantly enhanced or reduced in both sNPF-knockdown flies and sNPFR-knockdown flies compared to controls; neither during daytime, nor nighttime. Also sleep was not affected in these genotypes (Fig. 23A, B). However, daytime activity was significantly increased in *sNPF^{hypo}* flies compared to CS, which correlated with a decrease in sleep (Fig. 23C, D). Nighttime activity in these flies was decreased compared to CS, but without affecting sleep (Fig. 23C, D).

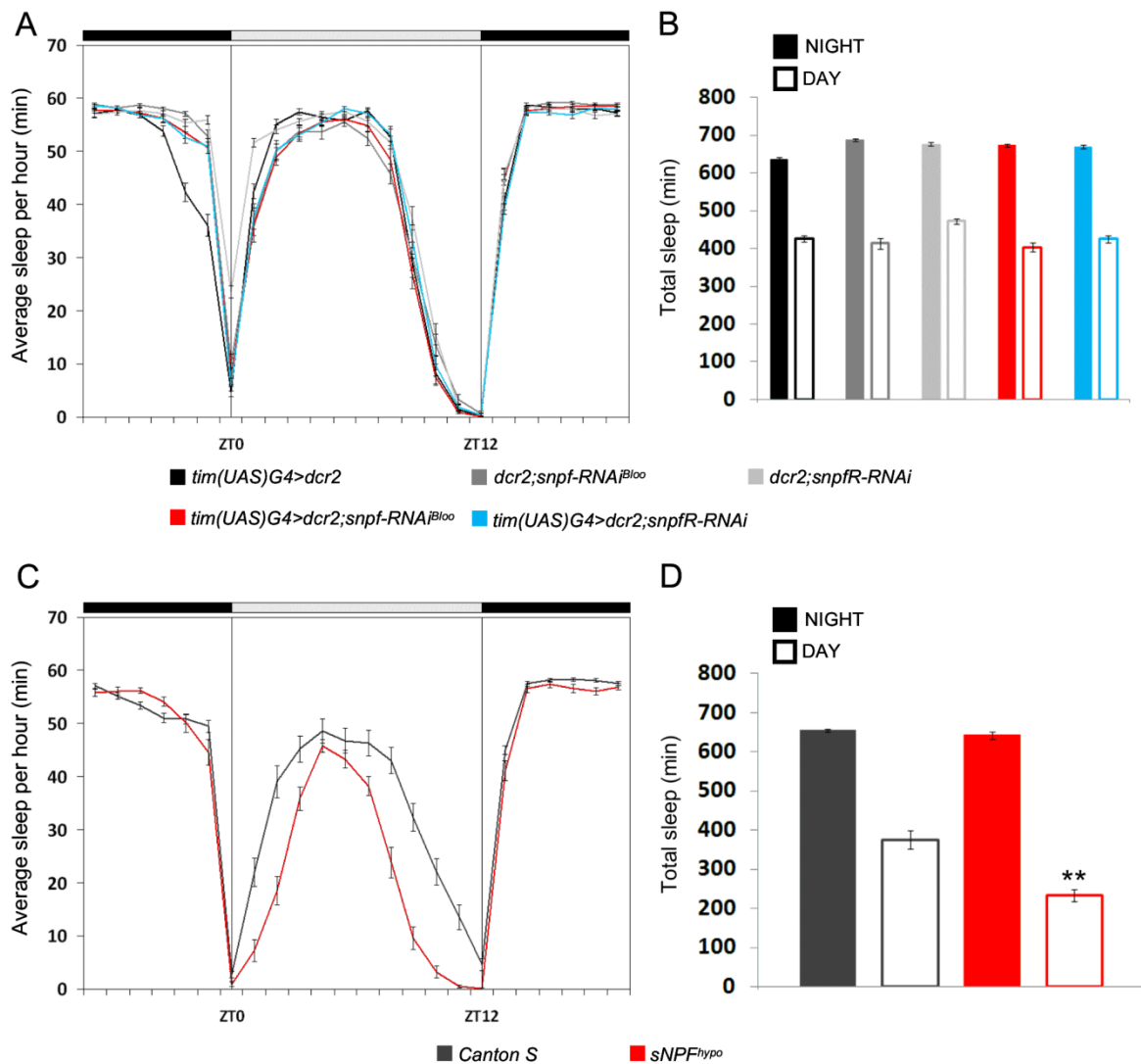


Figure 23: Sleep analysis in putative sNPF-knockdown, sNPFR-knockdown, *sNPF^{hypo}* flies and controls in LD 12:12. Sleep was defined as the average amount of time, in which the flies did not cross the infrared light beam for at least 10 consecutive minutes. **(A)** Daily average sleep profiles of putative sNPF-knockdown (red) and sNPFR-knockdown (blue) flies. No differences to control flies (grays) are observed. **(B)** Total amount of sleep during nighttime (full bars) and daytime (empty bars) of putative sNPF-knockdown and sNPFR-knockdown flies. **(C)** Daily average sleep profiles of *sNPF^{hypo}* (red) and *Canton S* control flies (gray). *sNPF^{hypo}* flies sleep less than CS during daytime. **(D)** Total amount of sleep during nighttime (full bars) and daytime (empty bars). *sNPF^{hypo}* flies show a significantly decreased daytime sleep compared to CS, while nighttime sleep is unaffected. ** indicates $p < 0.001$, n.s. = not significant; error bars depict SEM.

The recording in DD showed that both *sNPF*-knockdown flies and *sNPF_R*-knockdown flies are able to generate rhythmic behavior in constant conditions (Fig. 24, Table 8). Rhythmicity was, however, reduced in both genotypes (Table 8). I did not find a significant period lengthening with the *snpf-RNAi^{Bloo}* line, as it had been the case for the *snpf-RNAi^{Lee}* line. The expression of *snpfR-RNAi* within the clock neurons had also no effect on the period length. *sNPF^{hypo}* flies showed no significant reduction in rhythmicity, but they had a significantly shortened free-running period compared to *CS* (Table 8).

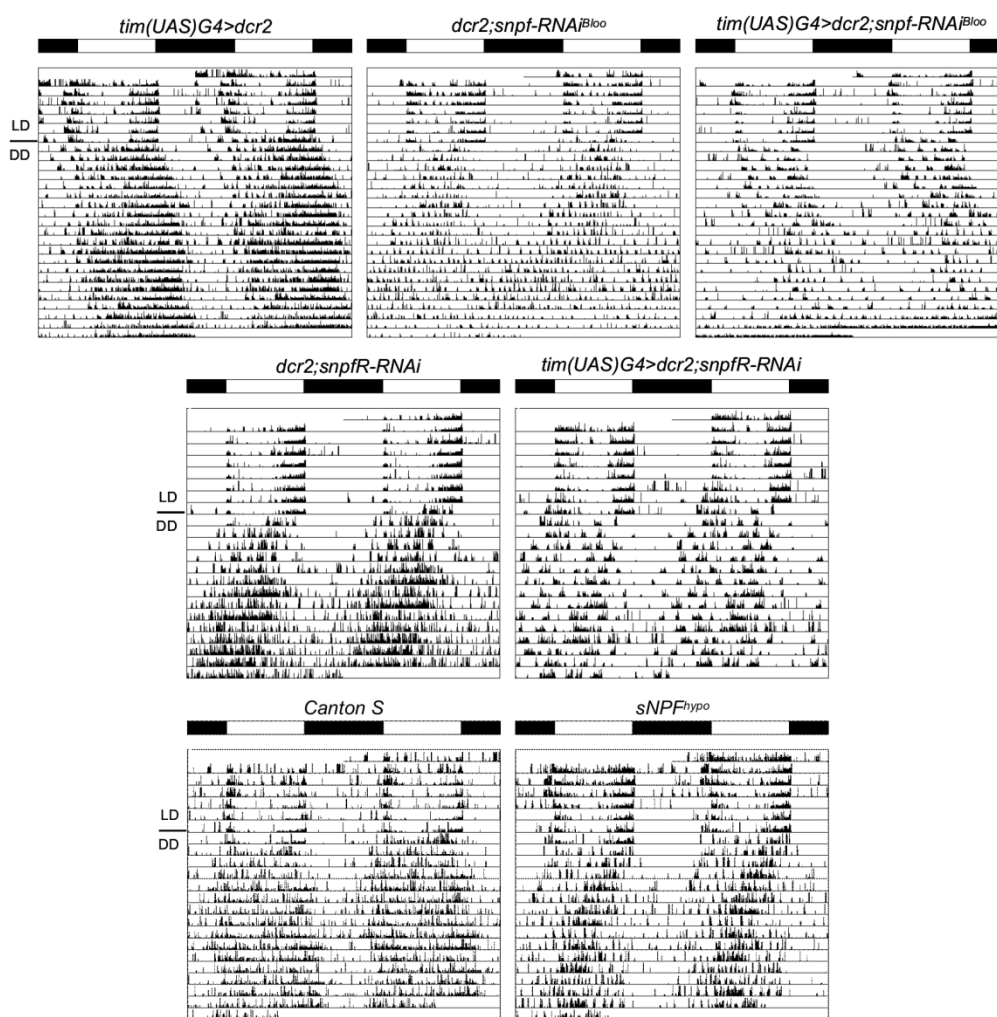


Figure 24: Representative individual double plotted actograms of *sNPF*-knockdown, *sNPF_R*-knockdown, *sNPF^{hypo}* flies and controls in LD 12:12 followed by DD. Both *sNPF*-knockdown flies and *sNPF_R*-knockdown flies show normal rhythms in DD. Black and white bars indicated the light regime in LD 12:12 (100 lux); T = 20°C.

Taking together, the expression of *snpf-RNAi^{Lee}* within the clock neurons led to a lengthening of the free-running period in DD, a reduction in daytime activity and an increase in nighttime activity. The reduction in daytime activity seems to be independent

Results

of sleep, while the increase in nighttime activity was accompanied by a reduction in sleep in these flies. Expression of the alternative independent *snpf-RNAi^{Bloo}* construct or a *snpfR-RNAi* construct had no significant effects on rhythmic behavior or sleep, except for a slight reduction of rhythmicity. In contrast, *sNPF^{hypo}* flies showed enhanced daytime activity, reduced nighttime activity and a shortened free-running period in DD, which was exactly the opposite of what sNPF-knockdown flies with *snpf-RNAi^{Lee}* had shown.

Table 8: Rhythmicity data of putative sNPF-knockdown, sNPFR-knockdown and sNPF^{hypo} flies and controls in constant darkness. * indicates p<0.05 when comparing experimental flies to the respective controls.

genotype	period (SEM) in h (n rhythmic flies)	power (SEM)	rhythmicity in % of all tested flies
<i>dicer2;timG4/+</i>	24.3 (0.05) (31)	45.1 (2.38)	100
<i>dicer2;+;snpf-RNAi^{Bloo}/+</i>	23.6 (0.10)	23.6 (1.86)	91
<i>dicer2;timG4/+;snpf-RNAi^{Bloo}/+</i>	24.4 (0.16) (24)	18.5 (1.08)	77*
<i>dicer2;+;snpfR-RNAi/+</i>	23.6 (0.08) (25)	22.8 (1.15)	78
<i>dicer2;timG4;snpfR-RNAi/+</i>	23.7 (0.16) (17)	22.8 (1.62)	55*
CS	24.6 (0.19) (29)	19.9 (1.13)	91
<i>sNPF^{hypo}</i>	23.7 (0.25) (26)*	26.8 (2.54)	84

3.5 Clock neuron responsiveness to bath applied peptides

The aim of this part of the thesis was to investigate the effect of other neuropeptides (different from PDF) on cAMP and Ca²⁺ levels within single clock neurons. Explanted adult brains were treated with bath applications of peptides, as it was described for PDF by Shafer et al. (2008). I expressed the ratiometric cAMP sensor *UAS-Epac1camps* or the Ca²⁺ sensor *UAS-GCaMP.3.0* with a clock neuron specific driver line, *clk856-GAL4 (clk856G4)*, and recorded single neuronal CFP and YFP traces or GFP fluorescence, respectively. FRET changes for cAMP imaging and changes in GFP fluorescence for Ca²⁺ imaging were examined upon application of full length mature and amidated NPF (H-SNSRPPRKNVDVNTMADAYKFLQDLDTYYGDRARVRFV-NH₂) and sNPF-1 (H-AQRSPSLRLRF-NH₂). Effects of sNPF-2 (H-VFGDVNQKPIRSPSLRLRF-NH₂) were only investigated in cAMP imaging experiments. Unfortunately I was not able to test responses to ITP, since the mature peptide has a length of 73 amino acids, which makes peptide synthesis extremely difficult. The sLNv, ILNv, LNd, DN1a and DN1p were investigated for both cAMP and Ca²⁺ responses, while the DN3 cluster was only tested in cAMP imaging experiments. The DN2 neurons were hard to distinguish from DN1 cells, so they were not included in this study.

3.5.1 NPF Application

cAMP

All neuronal clusters responded to 20μM Forskolin with robust increases in cAMP (increase of inverse FRET values), proving that the neurons were functional after the dissection and mounting process (Fig. 25). Application of HL3 with 0.1% DMSO (named only HL3 in all figures) did not elicit responses in any of the neurons. When I applied NPF in a concentration of 10⁻⁴M (with 0.1% DMSO), I did not observe obvious FRET responses in any of the tested cell groups either (Fig. 25).

To quantify the cellular responses, I calculated the maximal FRET changes from baseline level (Δ_{\max} CFP/YFP) in positive and/or negative direction (Fig. 26). As expected, the maximal positive FRET change with Forskolin was significantly different from the HL3 control in all tested cell groups. Since the NPF receptor (NPFR1) was shown to act through an inhibitory pathway *in vitro* (Garczynski et al., 2002), I would have expected to see

decreases in cAMP upon receptor activation and therefore calculated maximal FRET changes in negative direction, reflecting inhibitory reactions. When comparing maximal FRET changes between HL3 and NPF application, I found significant differences for the sLN_v and ILN_v. However, these differences were very close to the significance level and single neuronal YFP and CFP traces were not clearly showing a typical change, but were quite shaky (especially in the sLN_v).

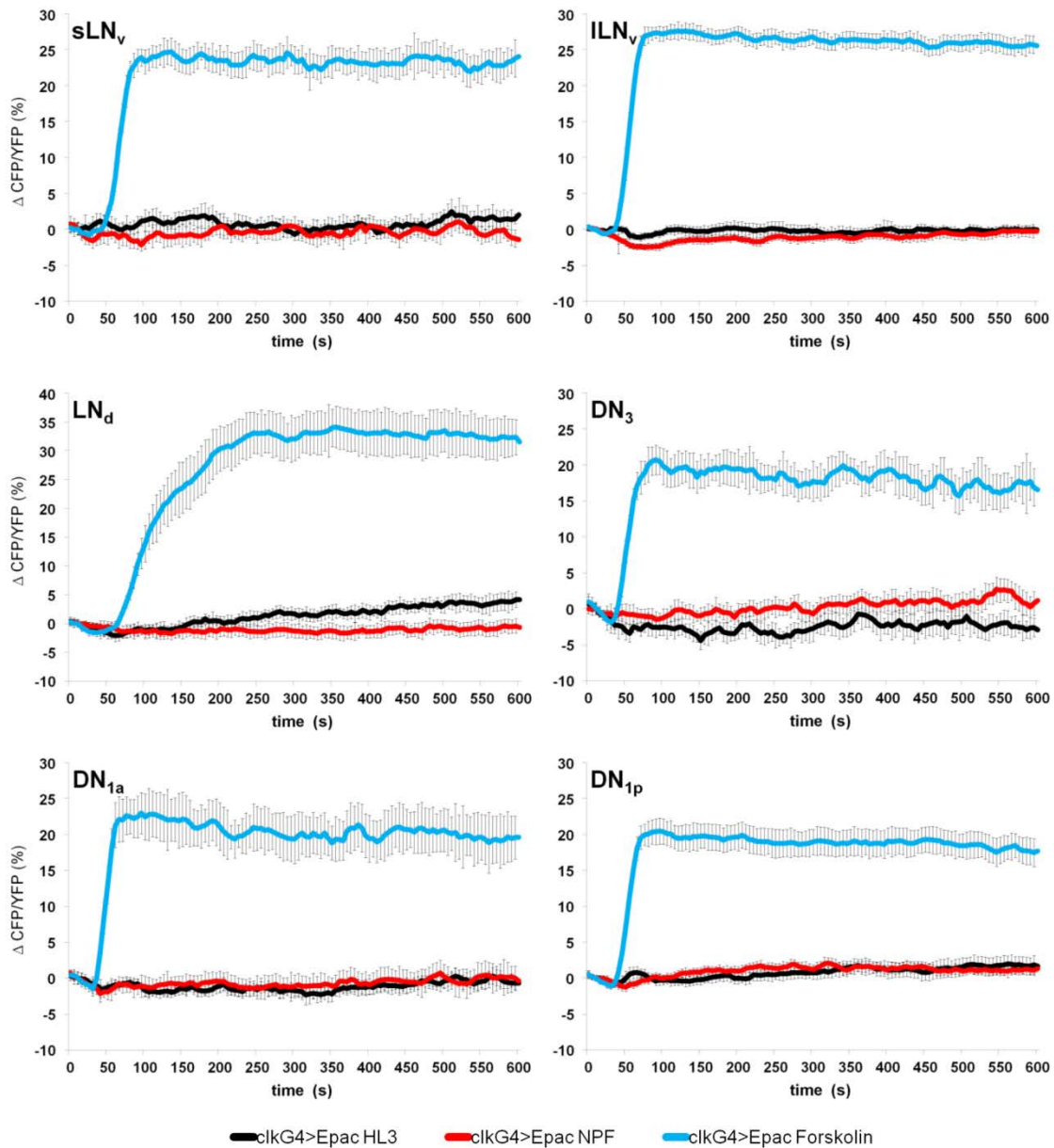


Figure 25: Averaged clock neuron traces of inverse FRET changes reflecting changes in cAMP upon application of NPF. Pharmacons were applied on *clk856G4>Epac1camps* brains between recording second 30 and 40. 20μM Forskolin served as positive control (blue), application of HL3 served as negative control (black). NPF was applied at a concentration of 10⁻⁴ M (red). Error bars depict SEM.

We wondered whether the Epac sensor was suitable to reliably measure inhibitory responses, therefore I tested a coapplication of NPF together with PDF as an excitatory stimulus on the sLNv (Fig. 27). The neurons showed robust increases in cAMP upon application of 10^{-5} M PDF (Fig. 27; blue; in accordance with Shafer et al., 2008). Coapplication of 10^{-5} M PDF together with 10^{-4} M NPF showed the same increase in cAMP as the PDF application alone, although NPF was applied in a 10x higher concentration (Fig. 27; red).

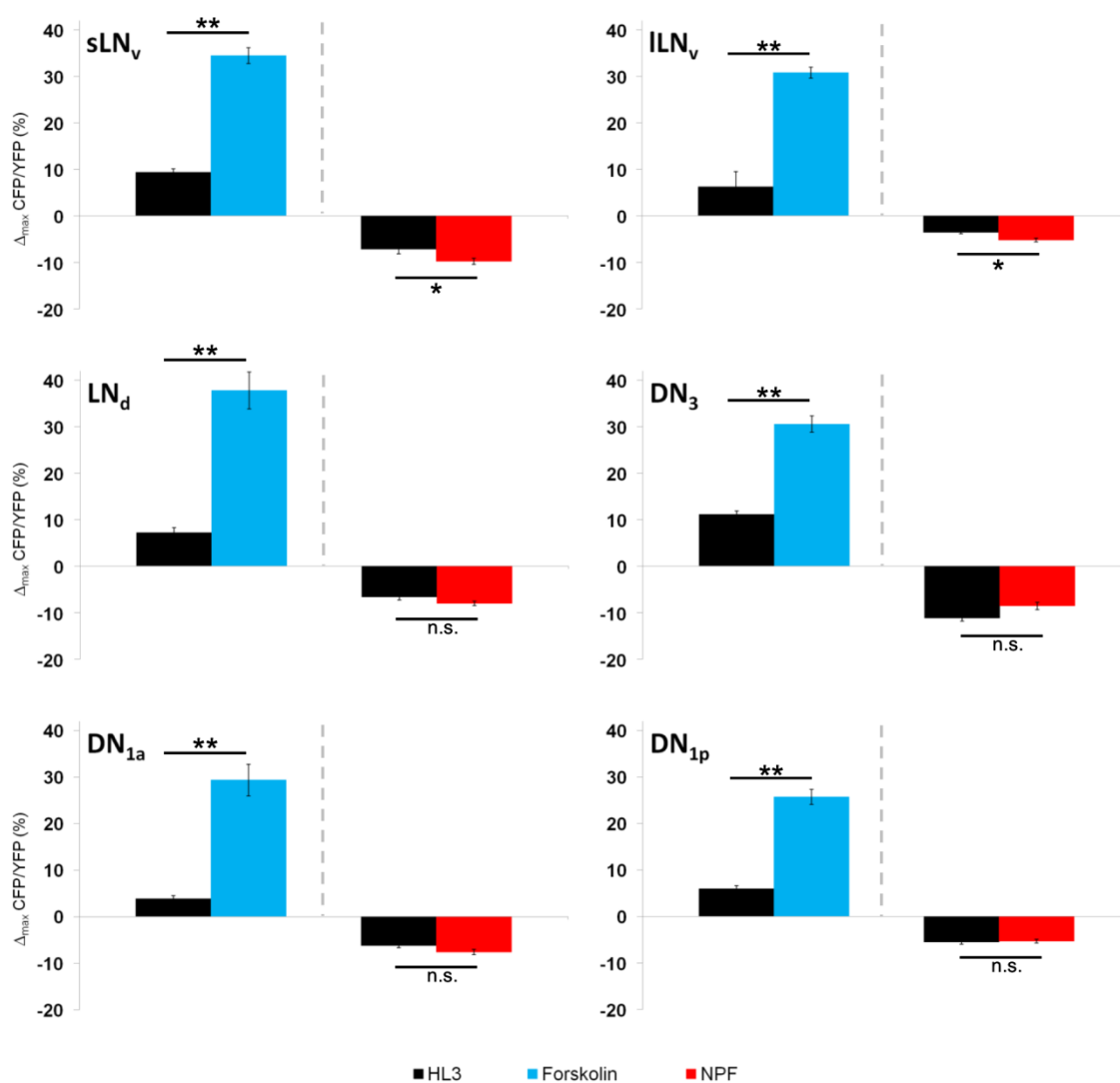


Figure 26: Mean maximum inverse FRET changes in clock neurons upon application of Forskolin or NPF. Left of gray dashed line in each panel: comparison of maximum inverse FRET changes in positive direction after application of $20\mu\text{M}$ Forskolin (blue) or HL3 (black). Right of gray dashed line in each panel: comparison of maximum inverse FRET changes in negative direction after application of 10^{-4} M NPF (red) or HL3 (black). Data are calculated as the mean maximum deflection from baseline level from recording second 30 to 300 of the neuronal traces depicted in Fig. 25. * indicates $p < 0.05$; ** indicates $p < 0.001$; n.s. = not significant; error bars depict SEM.

Ca^{2+}

Very recently, Lelito and Shafer (2012) showed that sLNv and ILNv clock neurons respond to application of the cholinergic agonist Carbachol with robust increases in cAMP and Ca^{2+} levels. I was able to reproduce the Ca^{2+} responses in both neuronal groups and observed in addition significant Ca^{2+} increases in the other clock neuron clusters (Fig. 28; blue). The quantification revealed that the responses were different from control HL3 application with high significance in all cell groups (Fig. 29; Carbachol blue, HL3 black). The application of 10^{-4} M NPF showed small, but significant decreases in Ca^{2+} levels in ILNv, DN1a and DN1p (Fig. 28, Fig. 29, red). Since it was shown before, that the GCaMP sensor is insufficiently sensitive to detect inhibitory Ca^{2+} responses in imaging experiments (Lelito and Shafer, 2012), I again investigated application of NPF together with an excitatory stimulus (Fig. 28 and Fig. 29; magenta), to see whether coapplication would diminish the responses that are elicited by the excitatory stimulus. Therefore, I coapplied 10^{-4} M NPF together with 10^{-4} M Carbachol. Compared to Carbachol alone, the coapplication of both compounds showed a significant reduction in the response amplitude only in the LNd and DN1p.

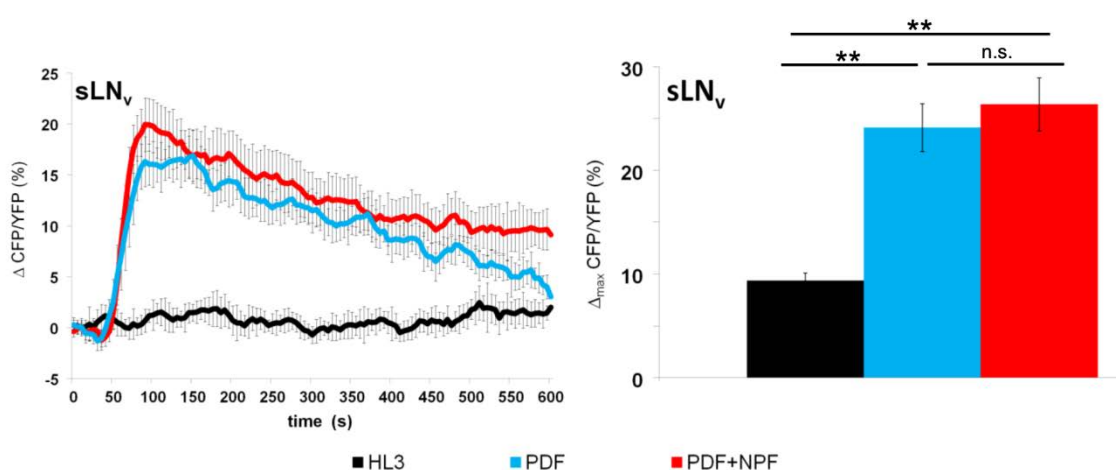


Figure 27: Averaged inverse FRET changes in sLNv reflecting changes in cAMP upon coapplication of PDF and NPF. (Left) Inverse FRET traces of *clk856G4>Epac1camps* sLNv upon application of HL3 (black), 10^{-5} M PDF (blue) or 10^{-5} M PDF + 10^{-4} M NPF (red). **(Right)** Mean maximum inverse FRET changes (same color code as in left panel). ** indicates $p < 0.001$; n.s. = not significant; error bars depict SEM.

Taking together, all clock neuron clusters responded to Forskolin with increases in cAMP and to Carbachol with increases in Ca^{2+} . Further, NPF led to small decreases in cAMP in the LNV, but did not diminish PDF responses, at least not in the sLNV. Ca^{2+} levels were decreased in ILNV, DN1a and DN1p upon application of NPF, but only in DN1p, the response was strong enough to diminish excitatory neuronal responses to Carbachol.

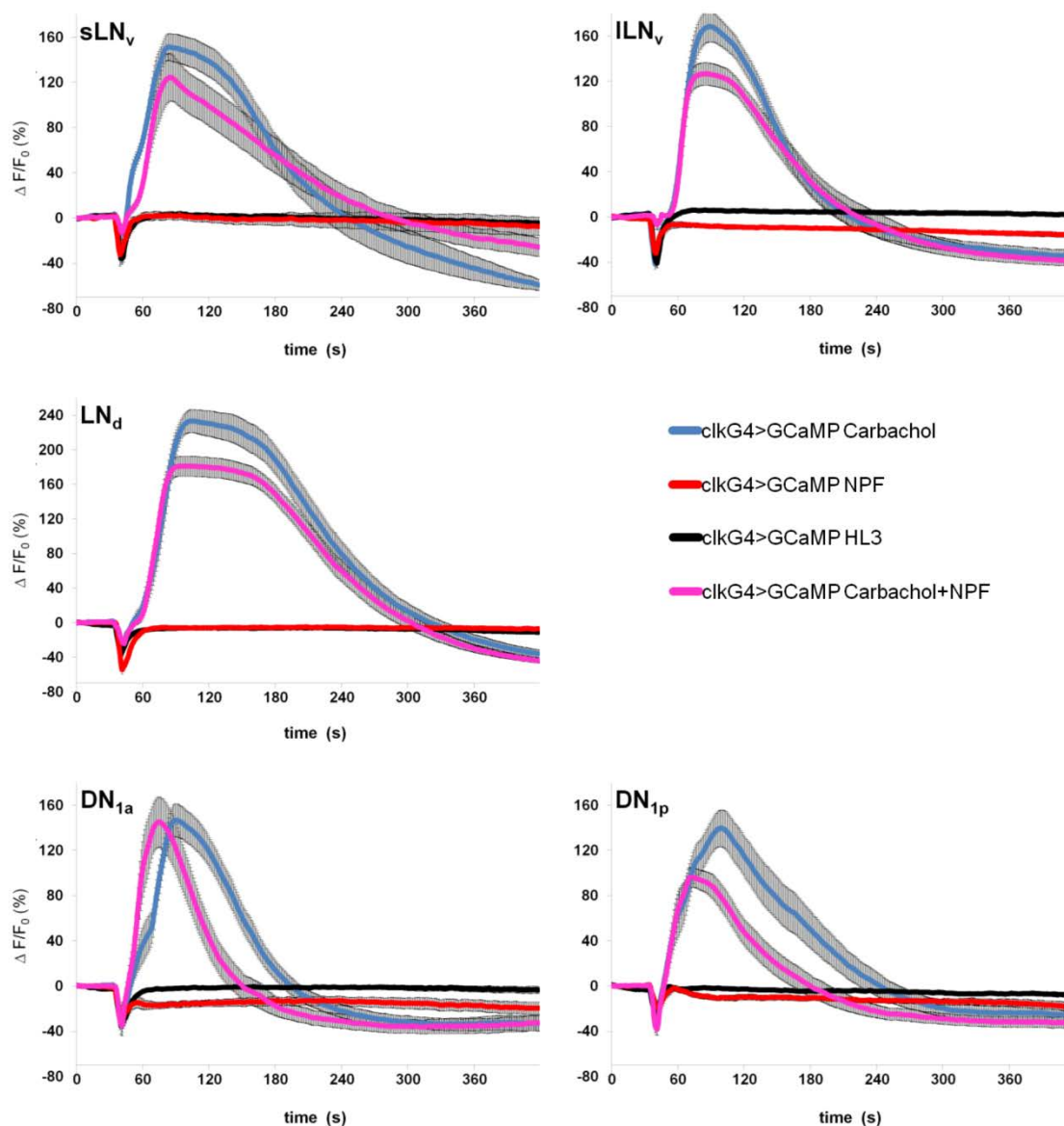


Figure 28: Averaged clock neuron traces of GCaMP fluorescence reflecting changes in Ca^{2+} levels upon application of Carbachol and/or NPF. Pharmacons were applied on *clk856G4>GCaMP3.0* brains between recording second 30 and 40. Application of HL3 served as negative control (black). 10^{-4} M Carbachol (blue) or 10^{-4} M NPF (red) were applied separately or coapplied (magenta). Error bars depict SEM.

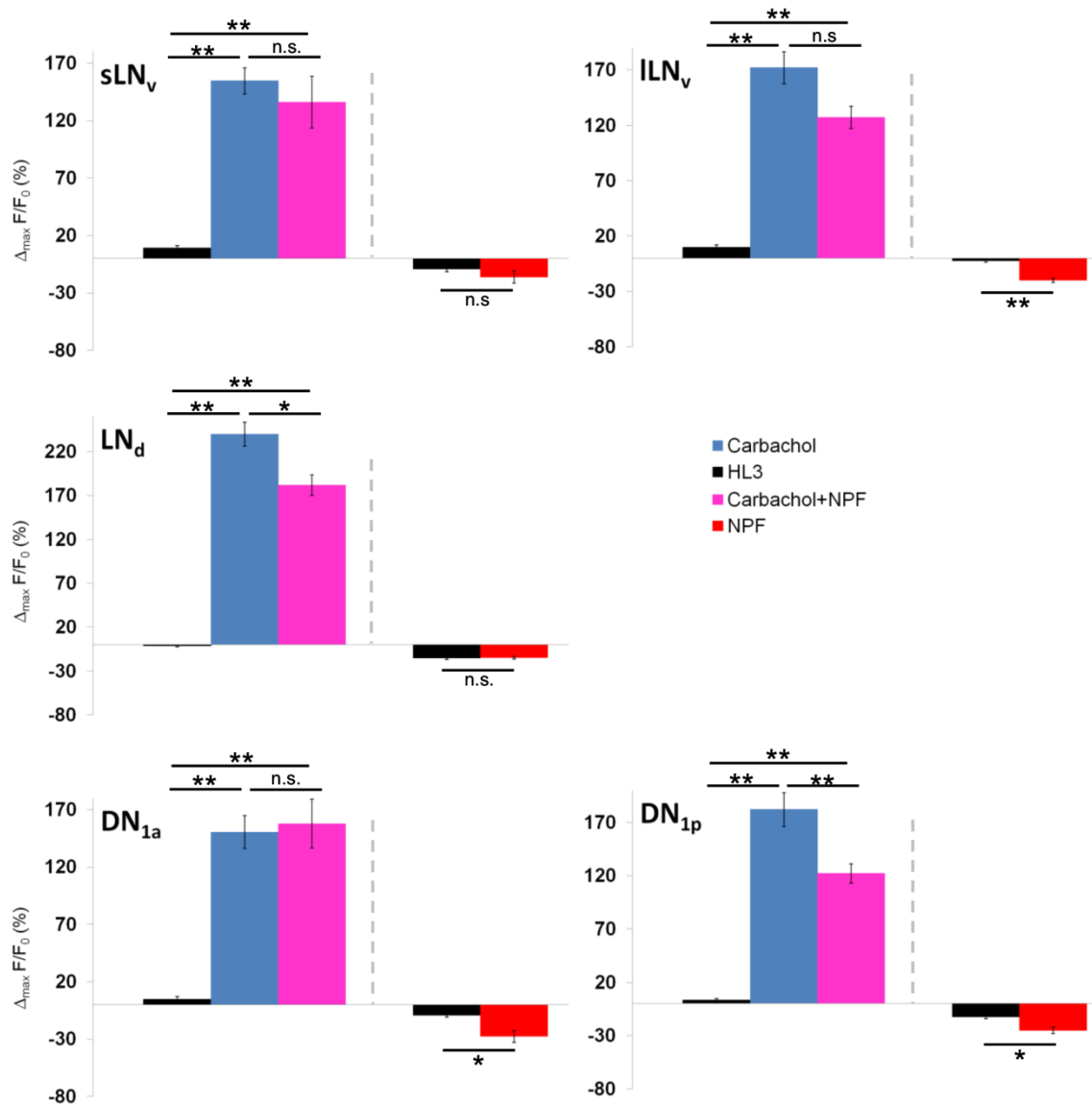


Figure 29: Mean maximum changes in GCaMP fluorescence upon application of Carbachol and/or NPF. Left of dashed line in each panel: comparison of maximum fluorescence change in positive direction after application of HL3 (black), 10^{-4} M Carbachol (blue) or 10^{-4} M Carbachol + 10^{-4} M NPF (magenta). Right of dashed line: comparison of maximum fluorescence change in negative direction after application of HL3 (black) or 10^{-4} M NPF (red). Data are calculated as the mean maximum deflection from baseline level from recording second 60 of the neuronal traces depicted in Fig. 28. * indicates $p < 0.05$; ** indicates $p < 0.001$; n.s. = not significant; error bars depict SEM.

3.5.2 sNPF Application

cAMP

I performed the same cAMP imaging experiments for the application of sNPF-1 and sNPF-2 (Fig. 30). The neuronal traces for Forskolin and HL3 depicted in Fig. 30 are the same as depicted in Fig. 25. The mean inverse FRET traces show small rather transient decreases

in cAMP in the ILNv, and quite long lasting inhibitory responses in the DN1a and DN1p upon application of 10^{-4} M sNPF-1 and/or sNPF-2 (Fig. 30; red and orange, respectively).

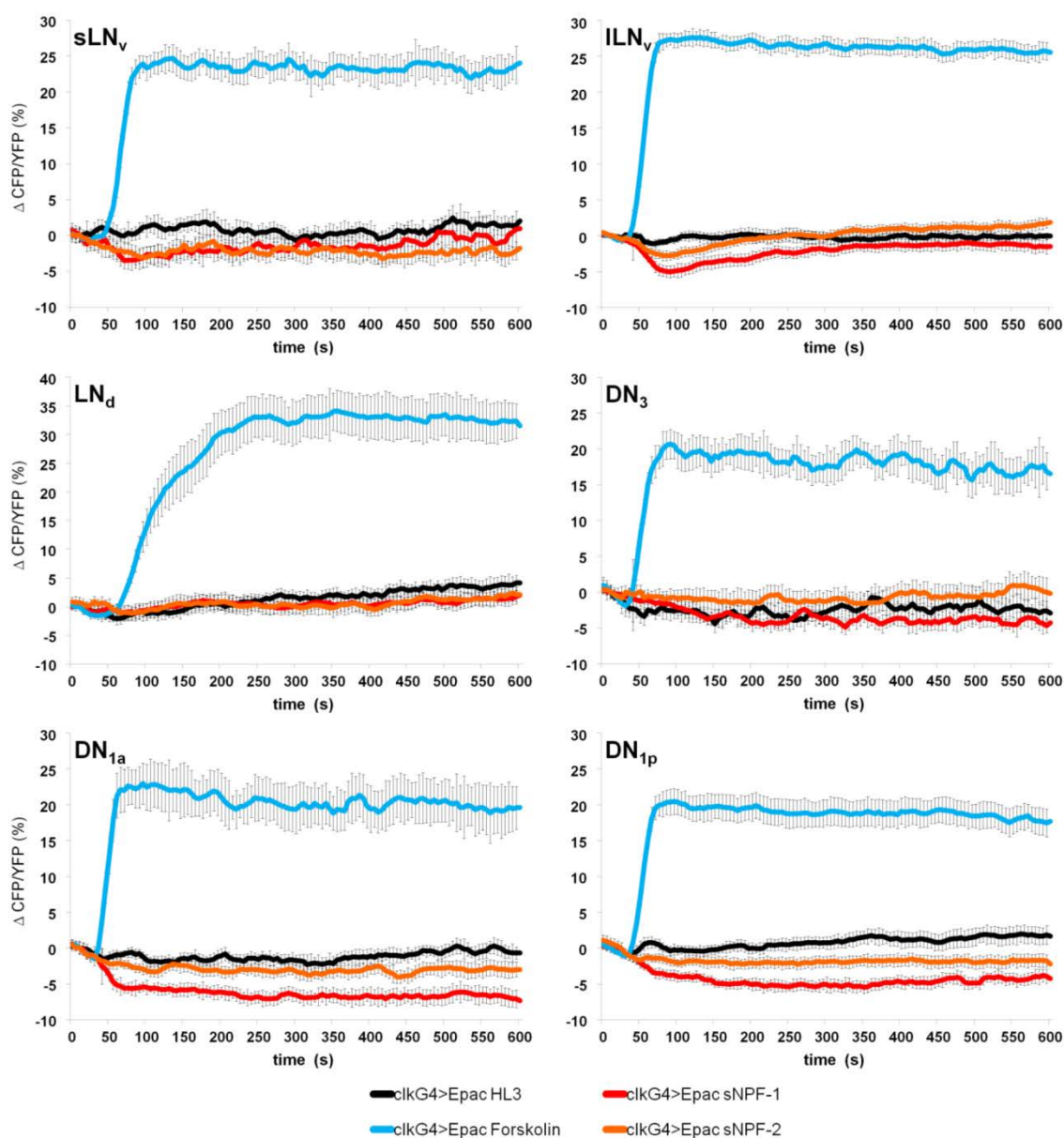


Figure 30: Averaged clock neuron traces of inverse FRET changes reflecting changes in cAMP upon application of sNPF. Pharmacons were applied on *clk856G4>Epac1camps* brains between recording second 30 and 40. Data after application of 20 μ M Forskolin (blue) and HL3 (black) are the same as depicted in Fig. 25 and served as positive and negative controls, respectively. sNPF-1 (red) and sNPF-2 (orange) were applied at a concentration of 10^{-4} M. Error bars depict SEM.

I again quantified the responses by calculating the maximal negative FRET changes (Fig. 31). There was a significant difference between the applications of sNPF-1 and the HL3 control in the ILNv. Both DN1a and DN1p responded significantly to sNPF-1, the DN1p in

addition also to sNPF-2. The inhibitory responses are in accordance with *in vitro* studies on the *Anopheles* sNPF-R (Garczynski et al., 2007).

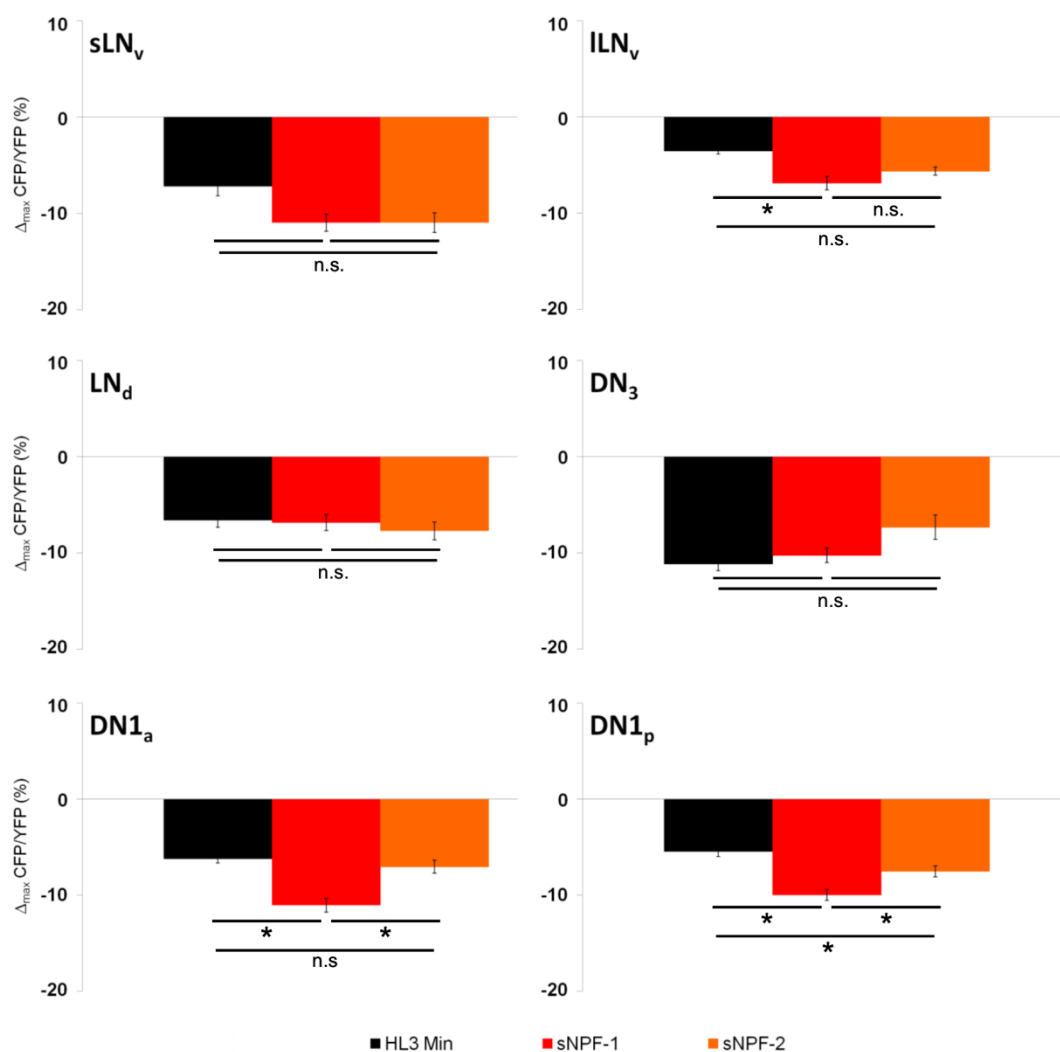


Figure 31: Mean maximum inverse FRET changes in clock neurons upon application of sNPF. Comparisons of maximum inverse FRET changes in negative direction after application of HL3 (black), 10^{-4} M sNPF-1 (red) or 10^{-4} M sNPF-2. Data are calculated as the mean maximum deflection from baseline level from recording second 30 to 300 of the neuronal traces depicted in Fig. 30. Data for HL3 are the same as depicted in Fig. 26. * indicates $p < 0.05$; ** indicates $p < 0.001$; n.s. = not significant; error bars depict SEM.

I further tested the coapplication of 10^{-5} M PDF and 10^{-4} M sNPF-1 on the DN1a and DN1p neurons (Fig. 32; red). PDF alone led to robust increases in cAMP, as expected (Fig. 32; blue; see also Shafer et al., 2008). Since sNPF had shown decreases in cAMP in these neurons, I expected that coapplication with PDF would possibly diminish the PDF response. However, there was no difference in the response amplitude between PDF application alone and PDF/sNPF coapplication.

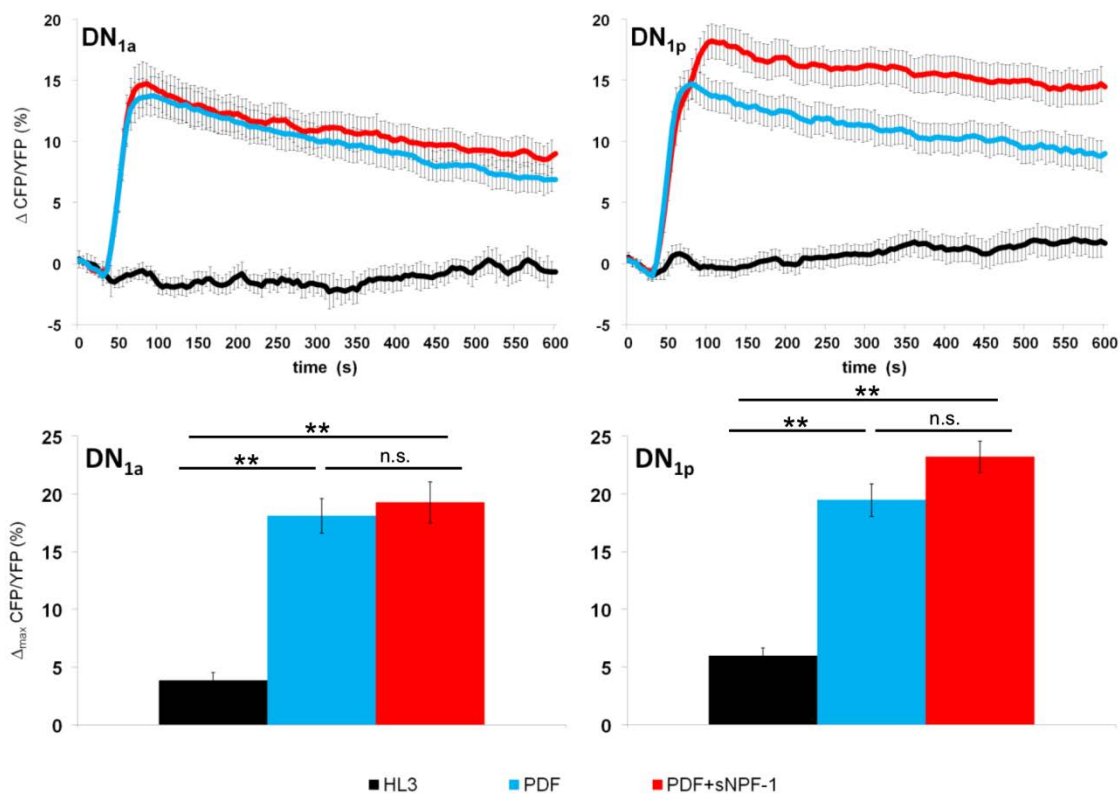


Figure 32: Averaged inverse FRET changes in DN1a and DN1p reflecting changes in cAMP upon coapplication of PDF and sNPF-1. (Upper panels) Inverse FRET traces of *clk856G4>Epac1camps* DN1a and DN1p upon application of HL3 (black), 10^{-5} M PDF (blue) or 10^{-5} M PDF + 10^{-4} M sNPF-1 (red). **(Lower panels)** Mean maximum inverse FRET changes in DN1a and DN1p (same color code as in upper panels). ** indicates $p < 0.001$; n.s. = not significant; error bars depict SEM.

Ca^{2+}

The same imaging data for Carbachol and HL3 applications that were depicted in the experiments with NPF (Fig. 28 and Fig. 29) served as positive and negative controls in the experiments with sNPF-1. When sNPF-1 was applied in a concentration of 10^{-4} M, no obvious effects on Ca^{2+} levels were visible in the average neuronal traces (Fig. 33; red). Statistical comparison of the maximal changes in fluorescence, however, revealed that sNPF-1 slightly decreased Ca^{2+} levels in the ILNv (Fig. 34; red). I again tested a coapplication of 10^{-4} M Carbachol together with 10^{-4} M sNPF-1 on the different clock neuron clusters (Fig. 33 and Fig. 34; magenta). Carbachol mediated increase in Ca^{2+} was reduced upon coapplication of sNPF-1 only in the LNd and DN1p, where sNPF-1 alone had no effect (Fig. 34). There was a tendency towards a reduction in the ILNv, but the difference was not significant (Fig. 34).

In summary, either sNPF-1 or sNPF-2 decreased cAMP levels within the ILN_v, DN1a and DN1p, but did not influence DN responses to PDF. Further, sNPF-1 seems to slightly decrease Ca²⁺ levels in the ILN_v and potentially also in the LN_d and DN1p.

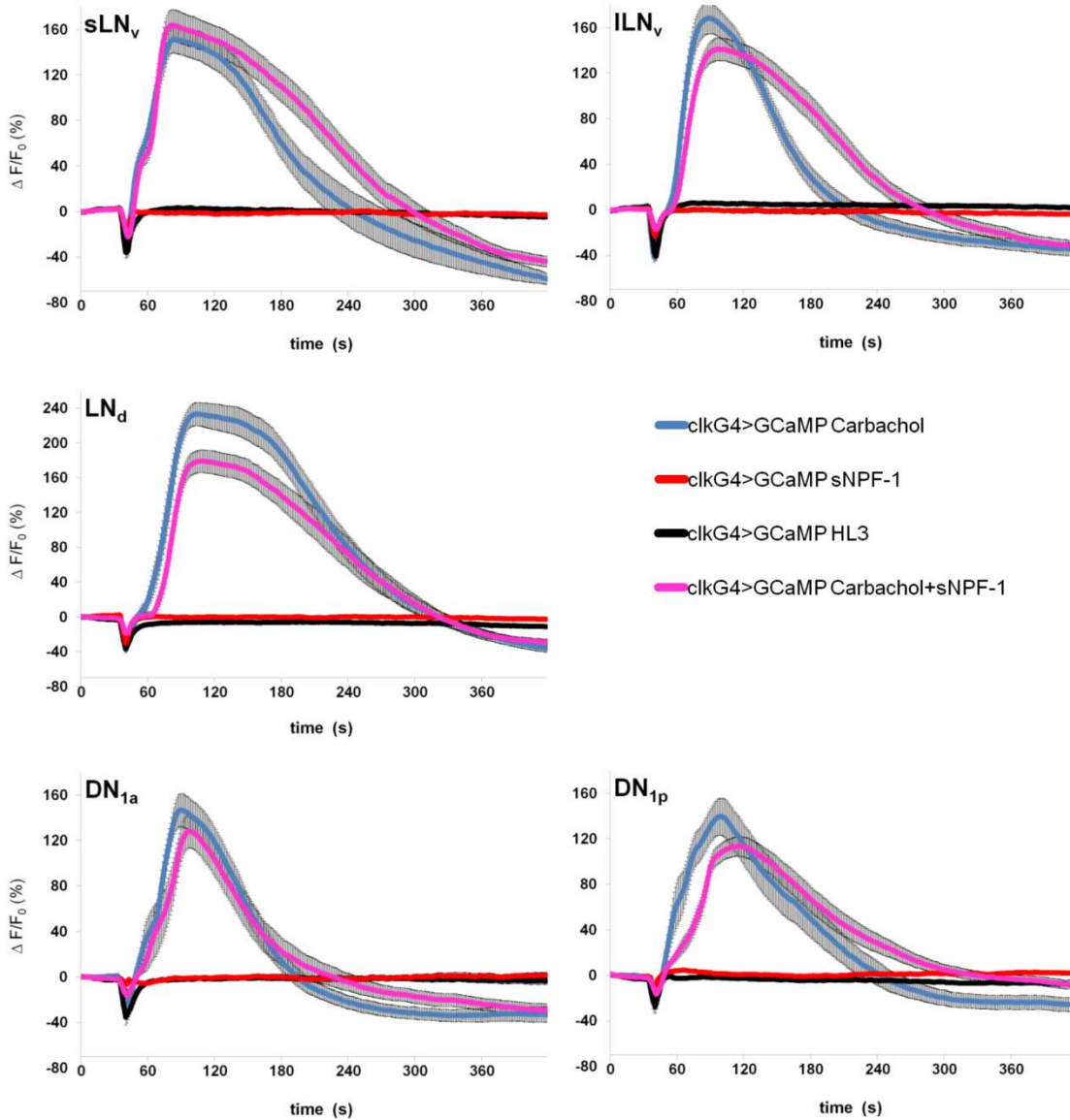


Figure 33: Averaged clock neuron traces of GCaMP fluorescence reflecting changes in Ca²⁺ levels upon application of Carbachol and/or sNPF. Pharmacons were applied on *clk856G4>GCaMP3.0* brains between recording second 30 and 40. Data after application of HL3 (black) and 10⁻⁴ M Carbachol (blue) are the same as depicted in Fig. 28. 10⁻⁴ M sNPF-1 (red) was applied either alone (red) or was coapplied with 10⁻⁴ M Carbachol (magenta). Error bars depict SEM.

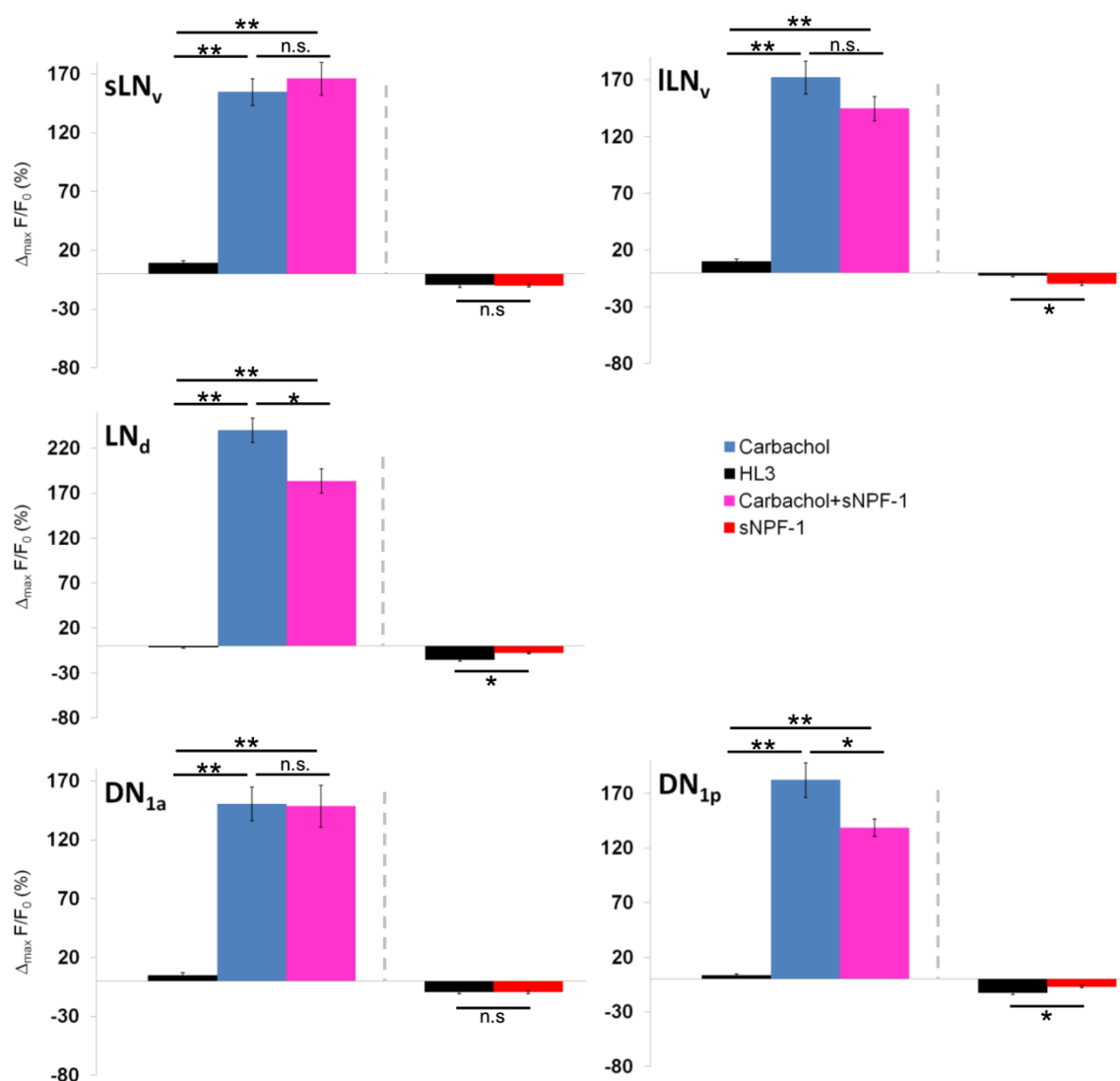


Figure 34: Mean maximum changes in GCaMP fluorescence upon application of Carbachol and/or sNPF-1. Left of dashed line in each panel: comparison of maximum fluorescence change in positive direction after application of HL3 (black), 10^{-4} M Carbachol (blue) or 10^{-4} M Carbachol + 10^{-4} M sNPF-1 (magenta). Right of dashed line: comparison of maximum fluorescence change in negative direction after application of HL3 (black) or 10^{-4} M sNPF-1 (red). Data for HL3 and Carbachol are the same as depicted in Fig. 29. Data are calculated as the mean maximum deflection from baseline level from recording second 60 of the neuronal traces depicted in Fig. 33. * indicates $p < 0.05$; ** indicates $p < 0.001$; n.s. = not significant; error bars depict SEM.

3.5.3 NPFR1 and sNPFR1 expression

To further strengthen the obtained imaging results, I aimed to characterize the expression pattern of both NPFR1 and sNPFR1 by *GAL4* mediated GFP expression with regard to the clock network.

For the investigation of NPFR1, I obtained an *npfr1G4* line that was used in the study of Wen et al. (2005). Wen and colleagues had shown that this *GAL4* construct drives GFP expression in one neuron per hemisphere in the dorso-lateral protocerebrum as well as in some neurons in the subesophageal ganglion (SOG). Unfortunately, the very same *GAL4* line did not produce any GFP signal in my hands (data not shown).

Investigation of *GAL4* mediated GFP expression using an *snpfr1G4* line (Hong et al., 2012) revealed a lot of staining in the whole brain (Fig. 35A). Especially the mushroom bodies and the ellipsoid body were strongly stained by GFP. When applying a costaining with anti-TIM, I did, however, not find any clear overlap with the GFP signal in any of the clock neuron groups (Fig. 35B, C).

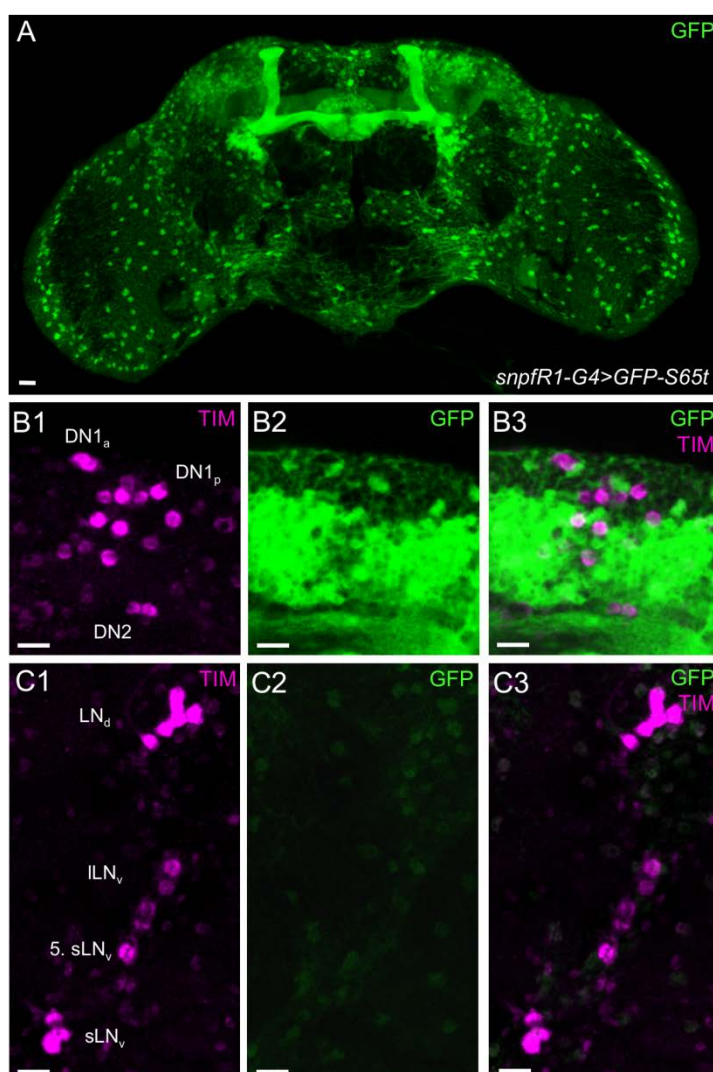


Figure 35: *snpfr1-GAL4* (*snpfr1-G4*) mediated GFP expression in adult male brains. (A) The *GAL4* line shows a broad expression pattern (green) within the whole brain with very prominent staining in the mushroom bodies and the ellipsoid body. Counterstaining with anti-TIM did not show a colabeling with the GFP signal in the dorsal clock neurons (B) or the lateral clock neurons (C). Scale bars = 10µm

4 General Discussion

In this thesis, I have presented data characterizing the roles of the neuropeptides NPF, sNPF, ITP and PDF with regard to circadian behavior in *Drosophila melanogaster*. Parts of these data have been published or are currently submitted for publication and have therefore already been extensively discussed. (See full text papers and manuscript starting from page 109.) Nevertheless, I will again briefly discuss these data here in the context of unpublished results and the current literature, since some very recent publications were not yet taken into account in the previous discussion sections.

4.1 Importance and Conservancy of Neuropeptides in the Clock System

The accessory medulla and the dorsal protocerebrum represent the circadian pacemaker center in insect species, while the SCN fulfills the same function in mammals. Neuropeptides constitute the majority of signaling molecules within the mammalian SCN. The well characterized accessory medulla of cockroaches was further shown to be invaded mainly by peptidergic fibers. As described earlier, most of the clock neurons in *Drosophila* were shown to contain either one or multiple neuropeptides and to project into the accessory medulla or the dorsal protocerebrum, indicating that also in the fruitfly the circadian clock employs mainly neuropeptides as signaling molecules. (Reviewed by Helfrich-Förster, 2004, 2005)

The best investigated neuropeptide fulfilling functions in the clock system of insects is PDF. Direct proof for its function in other insect species than *Drosophila melanogaster* is rare so far, however, its presence in putative pacemaker centers was shown for insects like cockroaches, crickets, blow-flies, blood sucking bugs and others (reviewed by Helfrich-Förster, 2009; Tomioka and Matsumoto, 2010). In our study of 2013 (Hermann et al., 2013) we had aimed to investigate the conservation of PDF and ITP within the clock network of different *Drosophila* species. By immunohistochemical and *in silico* analyses, we first of all showed that the morphology of the neuronal clock network and the structure of canonical clock proteins are highly conserved within the *Drosophila* genus. We further found high sequence similarities and identities of mature PDF and ITP

peptides of the different species, suggesting also a high structural conservation in the peptidergic systems. Bahn et al. (2009) had previously reported that *Drosophila virilis* lacks M activity in entrained conditions and had correlated this behavior with the lack of the sLNv clock neurons or the lack of PDF immunostaining within these cells, which are known to constitute the M oscillator in *Drosophila melanogaster*. We have shown with our immunohistochemical study that these flies do actually not lack the sLNv, but that PDF is not expressed in them. Further, other species of the *Drosophila* subgenus, presumably those that derived from habitats at higher latitudes on the northern hemisphere also showed a lack of PDF immunostaining in these cells. A recent study by Kauranen et al. (2012) reported the same for another northern fly species, *Drosophila montana*. Also here a reduction in M activity was observed, when flies were recorded in entrained conditions. Flies of the *Sophophora* subgenus that derived from more southern regions on the northern hemisphere showed normal PDF expression within the sLNv (Hermann et al., 2013) and seemed to show M activity in locomotor behavior (Saccon, 2010 unpublished; Domnik, 2011 unpublished; Prabhakaran and Sheeba, 2012). All these results together suggest that PDF seems to be conserved in its function in promoting M activity. Further, species that are distributed in northern regions have probably evolved a reduction of PDF in the M cells to be able to avoid activity at times, when temperatures are too cold.

ITP had been shown to be expressed in the fifth sLNv and one LNd in *Drosophila melanogaster* (Johard et al., 2009). According to previous studies, these neurons constitute the flies' most important E oscillator neurons (Grima et al., 2004; Stoleru et al., 2004; Rieger et al., 2006; Picot et al., 2007; Rieger et al., 2009). Our study showed that ITP is expressed in these two cells in all *Drosophila* species, we had investigated. Behavioral analyses further showed that all of these species have prominent E activity peaks (Saccon, 2010 unpublished; Domnik, 2011 unpublished). This already suggests that the E neurons might promote E activity through an ITP mediated pathway. However, previous studies on ITP had not investigated its function in relation to circadian behavior.

Whether the expression of other neuropeptides, which are present in the clock network of *Drosophila melanogaster*, is equally well conserved within the *Drosophila* genus has not been investigated in the course of this thesis. It has further not been investigated,

whether any of these neuropeptides are present in putative clock neurons of other insect species. Since NPFs and sNPFs have already been comparatively well described in their functions and structure (reviewed by Nässel and Wegener, 2011), and since fairly good antibodies are existing, both might be interesting tasks for future studies in this direction.

(See also discussion section of Hermann et al., 2013)

4.2 Neuropeptide F (NPF)

Lee et al. (2006) were the first to investigate a possible role for NPF in circadian behavior, by ablating NPF⁺ cells and recording locomotor activity in these flies. In our work of 2012 (Hermann et al., 2012), we aimed to refine previous findings of Lee et al. (2006) in both clock related behavior and NPF expression within the clock network of *Drosophila melanogaster*.

NPF expression in the clock network

Lee et al. (2006) had discovered NPF expression in a male-specific fashion within three of the LN_d clock neurons, employing both *GAL4* driven GFP expression and anti-NPF staining. A later study by Hamasaka et al. (2010) suggested that also the fifth sLN_v might be NPF⁺, showing its occasional ablation, when the cell death gene *head involution defective (hid)* was expressed under the control of the *npf* promoter (*npf-GAL4*, from now on referred to as *npfG4*). In our study (Hermann et al., 2012), we employed the same *npfG4* line the previous investigators had used and the same anti-NPF serum Lee et al. (2006) had applied. Besides the three LN_d neurons, we were able to clearly identify the fifth sLN_v as NPF⁺ as well as 2-3 of the ILN_v both by *GAL4* driven GFP expression and antibody staining. Our results are strengthened by our neuronal counting in NPF-ablated flies (*npfG4>hid*), in which the exact cell numbers were absent that had been shown to express NPF. Further, it was shown before that *npf* mRNA is enriched within the ILN_v (Kula-Eversole et al., 2010). Differences in our findings compared to the previous studies, could possibly be explained by the fact that NPF immunostaining or GFP expression was clear, but quite weak especially in the ILN_v and the detection thus probably largely depends on the sensitivity of the microscopic setup. A very recent study by He et al.

(2013a) even showed NPF immunostaining in the sLNv, but in this study a different NPF antibody was used, which could explain differences in the staining pattern. This finding is, however, not supported by the study of Kula-Eversole et al. (2010), which had reported that *npf* mRNA is not enriched in the sLNv. He et al. (2013a) further showed that NPF immunostaining is oscillating within cell bodies in LD, peaking at the end of the light phase. Kula-Eversole et al. (2010) had also reported a cycling in *npf* mRNA in the lLNv.

The role of NPF in circadian behavior

The most striking difference between our work on the NPF⁺ neurons (Hermann et al., 2012) and the work of Lee et al. (2006) is that we were able to address the observed phenotypes in behavior to the ablation of the NPF⁺ clock neurons. Lee et al. (2006) had found subnormal E activity in NPF-ablated male flies and had addressed it to the absence of the NPF⁺ LN_d, without discussing the possibility that also the NPF⁺ non-clock neurons might play a role in this effect. We have discovered a similar phenotype in LD with NPF-ablated male and female flies showing a reduction in E peak amplitude at the very end of the light phase. In addition, we newly found that NPF-ablated flies significantly prolong their circadian free-running period in DD. When we employed a *cry-GAL80* and a *pdf-GAL80* construct to rescue different subsets of clock neurons from the cell ablation, we were able to nail these phenotypes down to the lack of mainly the NPF⁺ PDF⁻ clock neurons, meaning the fifth sLNv and three LN_d, which were shown to partly constitute the E oscillator of the *Drosophila* clock (e.g. Grima et al., 2004; Stoleru et al., 2004). This experiment convincingly showed that the NPF⁺ non-clock neurons do not play a role in the observed clock-related phenotypes. Interestingly, when we ablated NPF⁺ and PDF⁺ neurons at the same time, we discovered additive effects in LD. The E peak phase was even more advanced than in PDF-ablated flies alone and was reduced in amplitude as it was the case in NPF-ablated flies. We concluded that PDF⁺ and NPF⁺ clock neurons are both necessary for the right phasing of the E activity, however, both neuronal types probably mediate this function through different mechanisms. While the ablation of the PDF⁺ neurons speeds up the clock in the E neurons (Lin et al., 2004; Yoshii et al., 2009), the ablation of the NPF⁺ neurons leads to a reduction of activity at the very end of the day and both these effects result in an earlier occurring E peak.

Another important aspect of our work (Hermann et al., 2012) in comparison to the work of Lee et al. (2006) is that we were trying to correlate the phenotypes we found to the lack of NPF itself. Since the NPF⁺ neurons were shown to contain e.g. also ITP (Johard et al., 2009), we assumed that these cells could also fulfill functions that are independent of the NPF signaling pathway. We tried to achieve this by expressing an *npf-RNAi* construct in the clock neurons and expected to find similar phenotypes, in case that NPF signaling was truly involved. However, we were not able to knockdown NPF completely by RNAi and consequently did not observe any phenotypes in behavior. Only when knocking down NPF together with PDF we observed a similar phenotype as in NPF/PDF-ablated flies, indicating a possible role for NPF in the control of the E activity. In accordance to this, the recent study of He et al. (2013a) demonstrated that a knockdown of NPF in all NPF⁺ cells (and also a knockdown of NPFR1 in NPFR1⁺ cells) using a different RNAi-construct also reduces E activity. The knockdown had, however, no effect on the free-running period in DD (He et al., 2013a). In consistence with our results, He et al. (2013a) had discovered the effect on the E activity in both male and female flies, indicating that this phenotype is not sex-specific. In a second recently published study, He et al. (2013b) further showed that NPF overexpression promotes sleep especially during the night in male flies. This is quite interesting, since it would mean that on the one hand NPF promotes activity late in the day to control the phasing of the E peak, while on the other hand it has the opposite effect during the night promoting sleep. Another recent study by Shang et al. (2013) had, however, demonstrated that activation of all NPF⁺ neurons does not affect sleep.

Taking all results together I conclude that NPF - mainly deriving from the E oscillator clock neurons - seems to participate in the control of the E activity in both male and female flies, possibly by promoting activity late in the day, but that it doesn't seem to be involved in the control of the free-running period (Lee et al., 2006; Hermann et al., 2012; He et al., 2013a). Further, NPF might promote sleep during the night (He et al., 2013b).

(See also discussion section of Hermann et al., 2012)

Clock neuron responsiveness to NPF

After the characterization of the effects of NPF on behavioral rhythms (Hermann et al., 2012; He et al., 2013a, 2013b), the question arises, whether NPF might mediate some of these effects by direct action on the clock system or by targeting other regions of the brain acting as output factor of the clock. In collaboration with Prof. Orié Shafer (University of Michigan, USA), I was able to investigate the effects of bath applied NPF on intracellular cAMP and Ca²⁺ levels in different clock neuron clusters, to shed some light on this question. The whole method employing the optogenetic sensors *UAS-Epac1camps* and *UAS-GCaMP* had been successfully applied in several previous studies on *Drosophila* adult brains (Shafer et al., 2008; Shang et al., 2011; Lelito and Shafer, 2012; Yao et al., 2012), thus I assumed that this method was suitable for this purpose. The NPF receptor (NPFR1) had been shown to act through an inhibitory pathway *in vitro* (Garczynski et al., 2002), thus I expected to see decreases in cAMP and/or Ca²⁺ upon application of NPF, in case that the receptor was present. The results showed that NPF evoked very small decreases in cAMP in the sLNv and ILNv and small decreases in Ca²⁺ in the ILNv, DN1a and DN1p. All responses were, however, quite weak (max. 5-10% for cAMP FRET responses and max. 25-30% for changes in GCaMP fluorescence reflecting Ca²⁺). Nevertheless, the Ca²⁺ responses in the DN1p seemed to be strong enough to significantly decrease excitatory responses, when NPF was coapplied with Carbachol. Thus, I assume that the DN1p, the sLNv and the ILNv are the most likely candidates to respond to application of NPF. Whether these responses occur directly through NPFR1 activation on the clock neurons or through the activation of NPFR1 on interneurons, which subsequently target the clock neurons, cannot be clarified with my data set. To answer this question, the experiments would have to be repeated in the presence of a blocker of neuronal firing (e.g. Tetrodotoxin). An alternative possibility would be to prove the presence of NPFR1 on the respective clock neurons. Previous studies had shown NPFR1 expression in larval brains and ventral nerve cords by *in situ* hybridization and antibody staining (Garczynski et al., 2002; Wu et al., 2003). Wen et al. (2005) had used *npfR1G4* mediated GFP expression to show one neuron in the dorso-lateral protocerebrum and some neurons in the SOG to express NPFR1. I have used the very same *npfR1G4* line with the attempt to investigate putative expression inside the clock system, but was not able to reproduce the data of Wen et al. (2005) in several trials (data not shown). The *GAL4* construct did not

evoke GFP signals in my hands, not even at higher temperatures. He et al. (2013a) had recently claimed to observe NPFR1 immunostaining in DN1 and LNd clock neurons by staining with anti-NPFR1 on GFP expressing brains using *clk8.0G4*. However, the specificity of the antiserum was not convincingly proven in this study and the confocal pictures indicate that the colabeling of GFP and anti-NPFR1 signal is located in non-clock neurons, that lie close to the DN1 and LNd cells and that are included in some of the *clk-GAL4* lines. The study of Kula-Eversole et al. (2010) had reported that *npfr1* mRNA is enriched within the sLNv and the lLNv, supporting my finding that both neuronal groups weakly respond to NPF.

4.3 short Neuropeptide F (sNPF)

sNPF is widely distributed in the nervous system of the fly and has been previously shown to fulfill functions like regulation of feeding and growth, metabolic stress, locomotion, learning and hormone release (Lee et al., 2004, 2008; Johard et al., 2008; Nässel et al., 2008; Kahsai et al., 2010a, 2010b; Knappek et al., 2013; reviewed by Nässel and Wegener, 2011). The discovery, that sNPF is expressed in the sLNv and two LNd clock neurons (Johard et al., 2009) had also suggested a possible clock-related function for the peptide, although no proof had been provided so far. Investigating locomotor activity in flies, in which the sNPF circuit was manipulated, I aimed to shed light on the putative role of the neuropeptide in circadian rhythms.

The role of sNPF in circadian behavior

The most important issue that needs to be discussed at the beginning of this section concerns the efficiency of the *snpf-RNAi^{lee}* construct that I expressed using *tim(UAS)G4* to knock down sNPF in the clock neurons. Lee et al. (2004) had described the creation of this construct and had proven its efficiency on the RNA level, when expressed in sensory neurons. However, my attempts to do so in case of the clock neurons gave different results. I assumed that immunohistochemistry would be the most direct way to verify a lack of the peptide within the clock neurons, which would be reflected by the loss of immunostaining. This had for example nicely been shown for the knockdown of PDF and

ITP (Shafer and Taghert, 2009; Hermann et al., 2012; Hermann-Luibl et al., *submitted*). However, since the signal given by the antibody certainly does not provide information about the absolute protein level within the cell, it might be that small decreases in peptide amount can just not be detected in this way. Thus, I tried to also investigate the RNAi efficiency on the RNA level expressing the construct with *elavG4* and ensuring at the same time, that the primers were not recognizing the RNAi construct itself. But also this attempt did not show a reduction in expression level. Considering the fact that at least six other published studies had used this very same RNAi construct – although in most cases only vaguely verifying its efficiency - (Lee et al., 2004; Lee et al., 2008; Kahsai et al., 2010; Chen et al., 2013; Knappek et al., 2013; Shang et al., 2013), I nevertheless decided to present the behavioral data of sNPF-“knockdown” flies in this thesis.

When recording sNPF-“knockdown” flies in LD cycles of different photoperiods, they showed a normal bimodal activity pattern in each condition. There was no sign, whatsoever, that flies had difficulties in entrainment, adapting to different photoperiods or the activity peak timing. The only differences I found were that relative activity levels during daytime were decreased compared to control flies, especially during short photoperiods. Sleep analysis showed, that total sleep was not significantly different from controls at that time, but was decreased during the night. This decrease in nighttime sleep correlated with a significant increase in relative nighttime activity. Two very recent studies of other groups produced completely contradicting results regarding the function of sNPF in sleep regulation: while Shang et al. (2013) claimed that sNPF is a sleep-promoting factor, Chen et al. (2013) reported the opposite, showing that sNPF deficient flies sleep more. Shang et al. (2013) had demonstrated that activation of all sNPF⁺ neurons dramatically increases sleep. By selectively excluding different subsets of sNPF⁺ cells from this experiment, they were able to address this phenotype to the action of the sNPF⁺ sLN_v, suggesting that sNPF deriving from the sLN_v promotes sleep. They further showed that knockdown of sNPF via RNAi (using *snpf-RNAi^{Lee}* or *snpf-RNAi^{Bloo}*) in the sLN_v leaves daytime sleep unchanged, while it significantly decreases nighttime sleep. This is in complete accordance with my findings for the sNPF-“knockdown” in LD.

When I investigated flies in which sNPF was knocked down in conjunction with PDF, I found again a decrease of relative daytime activity and an increase of relative nighttime

activity. Since PDF-knockdown alone did not show these phenotypes, while sNPF-“knockdown” did, I assume that this effect derives from the expression of the *snpf-RNAi^{Lee}* construct. Both phenotypes were further accompanied by a decrease in daytime and nighttime sleep in PDF/sNPF-knockdown flies. PDF knockdown alone did not influence sleep, while sNPF-“knockdown” alone had also decreased nighttime sleep (see above). Thus, reduction of sleep in sNPF/PDF-knockdown flies at this time of the day most probably derives from the sNPF-“knockdown”. A reduction in daytime sleep was, however, neither observed in PDF-knockdown nor sNPF-“knockdown” flies. Thus, this effect could derive from the disruption of a putative interplay of both sNPF and PDF.

Another phenotype observed in sNPF-“knockdown” flies in my experiments was a significantly prolonged free-running period in DD. This is quite interesting, considering that the sLN_v clock neurons express both PDF and sNPF (Helfrich-Förster, 1995; Johard et al., 2009). Flies deficient of PDF signaling (*Pdf⁰¹* mutants, PDF-ablated or PDF-knockdown flies) are either arrhythmic in DD or show a shortened free-running period (Renn et al., 1999; Shafer and Taghert, 2009). Taking together, this means that the same subset of clock neurons, the sLN_v, produces both a period lengthening factor (PDF) and a period shortening factor (sNPF). Shafer and Taghert (2009) had, however, shown that PDF from the ILN_v is already sufficient to generate a wildtype like period length and had suggested that PDF from the ILN_v might regulate both PDF and sNPF signaling of the sLN_v to other clock neurons to control the period length. One could assume that a differentially timed production or release of the two peptides thus fine-tunes clock neuron synchronization or clock output. Though PDF was shown not to be expressed in a rhythmic manner, it was demonstrated that it is rather rhythmically released (Park et al., 2000), while there are indications that sNPF is rhythmically expressed within the sLN_v (Kula-Eversole et al., 2010).

The additional investigation of the effects of another independent *snpf-RNAi^{Bloo}* construct and a *snpfR1-RNAi* construct using the same driver line as in the previous experiments (*tim(UAS)G4*), as well as the investigation of locomotor rhythms in the hypomorph *sNPF^{hypo}* flies were conducted to possibly strengthen the previous findings. However, the results of these experiments were quite contradicting. Expression of the *snpf-RNAi^{Bloo}* construct did not show any phenotype in activity levels, free-running period and also not

in sleep. Shang et al. (2013) had found the decrease in nighttime sleep also with this RNAi line. Since they had further claimed, that sNPF promotes sleep through signaling from the sLNv to the ILNv (see also below), one would further expect a similar phenotype, when the sNPF receptor, sNPFR1, is knocked down within the clock neurons. However, also the expression of the *snpfR1-RNAi* construct did not show any significant phenotype, whatsoever. This was in accordance with Shang et al. (2013) showing that the expression of a dominant negative variant of the sNPFR1 in the clock neurons had also no effects on sleep. These results indicate that multiple sites in the brain are responsible for sNPF mediated sleep control. The *sNPF^{hypo}* flies showed a reduction in sleep not during the night but during the day, which was accompanied by increased activity levels. Further, these flies showed a significantly shortened free-running rhythm in DD instead of a long period. A reason for these differences could be that in *sNPF^{hypo}* flies overall sNPF levels are reduced (Lee et al., 2008; Chen et al., 2013), while in case of the knockdown only sNPF within the clock neurons is putatively affected. This could again indicate that also sNPF⁺ non-clock neurons contribute to the control of sleep and the free-running period.

Taking together, the most critical point in these results is the functionality of the *snpf-RNAi^{Lee}* construct. If one assumes that it is not functional, then the observed phenotypes could be off-target effects of the RNAi construct. The fact, that the second RNAi construct did not show the same phenotypes, would strengthen this possibility. When I blasted the sequence of the *snpf-RNAi^{Lee}* construct against the *Drosophila* genome, I found no matches with other gene sequences that were larger than ~25bp. It is, however, conceivable that also small matches could lead to a down regulation of the respective gene expression. If one believed all the previous studies that were employing this *snpf-RNAi^{Lee}* construct and one assumed that it is functional, then my results support the findings of Shang et al. (2013), that clock neuron derived sNPF promotes sleep and they further indicate that sNPF has opposing effects to PDF in the control of the free-running period in DD.

Clock neuron responsiveness to sNPF

Again, I aimed to investigate whether sNPF has any effect on intracellular cAMP or Ca²⁺ levels within the clock neurons, to get an idea, whether it is involved in clock input, inter-

clock neuron communication or clock output. In collaboration with Prof. Shafer, I decided to investigate the effects of bath applied sNPF-1 and sNPF-2. All four sNPF isoforms had been previously shown to activate sNPFR1 in cellular expression systems (Mertens et al., 2002; Feng et al., 2003; Reale et al., 2004). Garczynski et al. (2006) had further reported that the longer sNPF isoforms (sNPF-1 and sNPF-2) had a higher affinity to the receptor than the shorter isoforms including the truncated sNPF-1⁴⁻¹¹. Thus, I assumed that the application of sNPF-1 and sNPF-2 might be most suitable for our purpose.

My results showed that the ILNv, the DN1a and the DN1p respond to applications of sNPF with decreases in cAMP levels, while Carbachol mediated Ca²⁺ responses were reduced in the LNd and the DN1p. I had expected inhibitory responses according to previous studies by Garczynski et al. (2007) on the *Anopheles* sNPF receptor. The cAMP responses in the DN1 appeared quite long lasting in comparison to the rather transient cAMP responses in the ILNv, indicating either differences in the receptor amount, its sensitivity or differences in intracellular signaling components. It had been previously shown that the ILNv respond to application of Dopamine with robust increases in cAMP thereby promoting wakefulness (Shang et al., 2011). A recent study by the same group had further demonstrated that this Dopamine mediated excitatory response in the ILNv is diminished by coapplication of sNPF, supporting my finding (Shang et al. 2013). The authors thus concluded that the excitatory dopaminergic input to the ILNv on the one hand and the inhibitory input via sNPF from the sLNv probably coordinates the timing of sleep (Shang et al., 2013).

The sLNv send very prominent projections into the dorsal protocerebrum that were previously shown to release PDF, which then evokes excitatory cAMP responses in the DN1 clock neurons (Park et al., 2000; Shafer et al., 2008). It is thus possible, that sNPF from the sLNv is released at the same or similar sites to act in an inhibitory way on the same cells to participate in the control of rhythmic parameters like the period length. My results indicate that sNPF indeed reduces cAMP levels within the DN1 clock neurons. When coapplied with PDF, sNPF – although applied in a 10x higher concentration - did not reduce the excitatory response mediated by PDF. This could be an indication that both peptides have to be released at different times *in vivo*, in order to enable sNPF to fulfill its inhibitory action.

Just like in the case of NPF, these experiments do not provide proof that the responses I observed within the clock neurons are direct cellular reactions to the application of sNPF. Again, usage of tetrodotoxin would allow the exclusion of a possible indirect response mediated by signaling via interneurons. Alternatively, I have investigated the expression pattern of a *snpfR1G4* line using GFP (Hong et al., 2012). Clock neuron specific counterstaining with anti-TIM did, however, not reveal any colabeling inside the clock neurons. Since *GAL4* lines do not always reflect the exact expression pattern of the respective genes, this result does not necessarily mean that there is no sNPFR1 expression inside the clock neurons. Kula-Eversole et al. (2010) did further not find an enrichment of *snpfR1* mRNA within the sLNv or the lLNv. However, these expression data were obtained relatively to the expression within all other brain neurons. Given the fact, that sNPFR1 seems to be very broadly expressed within the nervous system, it is quite reasonable that its mRNA was not especially enriched within the PDF cells and that it was therefore not discovered in this kind of expression study.

4.4 Ion Transport Peptide (ITP)

Previous studies had shown that ITP contributes to the regulation of circadian rhythms in cellular plasticity and the abundance of the catalytic subunit of a sodium/potassium pump in the lamina (Damulewicz and Pyza, 2011; Damulewicz et al., 2013). However, clock related functions of ITP on the behavioral level have been investigated for the first time in the course of this thesis and the resulting manuscript, which is currently submitted for publication (Hermann-Luibl et al., *submitted*).

The role of ITP in circadian behavior

Since ITP had been previously shown to be expressed not only in two clock neurons but also in non-clock cells (Dirksen et al., 2008), we employed a genetically encoded *itp-RNAi* construct, which enabled us to knock down ITP expression specifically within the two clock cells without affecting ITP in the other cells. The same RNAi construct had been successfully used in a recent study that was conducted at the same time as the present thesis (Damulewicz et al., 2013). Further, our immunohistochemical analysis confirmed

the high efficiency of this RNAi construct. Thus, I am quite confident that the effects we observed on the behavioral level are indeed deriving from a lack of ITP within the two clock cells.

Our locomotor experiments in LD showed that ITP-knockdown flies can normally entrain to different photoperiods and are not at all impaired in activity peak timing. However, we did observe effects on the activity level. The E peak amplitude was reduced relative to the morning activity and nighttime activity was enhanced in these flies. As mentioned previously, the fifth sLNv and the ITP⁺ LNd constitute the flies' most important E oscillator neurons (Grima et al., 2004; Stoleru et al., 2004; Rieger et al., 2006; Picot et al., 2007; Rieger et al., 2009). Further, ablation of these cells using *npfG4* had also led to a reduction in E peak amplitude (Hermann et al., 2012). Thus, these cells clearly promote E activity and ITP signaling seems to be involved in this process, albeit possibly in conjunction with NPF (see above and Hermann et al., 2012).

When recording ITP-knockdown flies in DD, we observed a slightly, but significantly prolonged free-running period. This effect was only very small and reminded us of a similar effect when the NPF⁺ neurons are ablated (Hermann et al., 2012). Since the knockdown of NPF had not resulted in a prolonged free-running period, we assume that this effect indeed derives from the knockdown of ITP. Thus, ITP seems to be a weak period shortening component in DD opposing the effect of PDF as a period lengthening factor on the behavioral level.

To investigate possible interaction effects of ITP and PDF we simultaneously knocked down both peptides. Also this RNAi was very efficient as it was proven by immunohistochemistry. The behavior of ITP/PDF-knockdown flies in LD very much resembled the behavior of PDF-knockdown flies, showing a clearly advanced E peak phase. The E activity was, however, again reduced in amplitude relative to the M activity and nighttime activity was enhanced, similarly to ITP-knockdown flies. Thus, ITP/PDF-knockdown flies combined both PDF-deficient and ITP-deficient characteristics in LD behavior. In addition, sleep was significantly reduced during daytime and nighttime in ITP/PDF-knockdown flies, which was not the case in the ITP- and PDF-single-knockdown flies, indicating that both peptides seem to cooperate in the control of sleep.

We had found only mild effects of ITP-knockdown on the free-running rhythm in DD (see above). Clearly, rhythmicity in general was not affected in these flies. PDF-deficient flies on the other hand are known to show only weak rhythms in DD, which run with a shortened period (Renn et al., 1999; Shafer and Taghert, 2009). Interestingly, when both peptides were knocked down, flies showed complex rhythms in DD with more than one free-running component, thus, having a more severe phenotype than the single-knockdown flies. This indicates that PDF and ITP constitute the main output factors of the clock, which maintain rhythmicity in DD.

ITP expression and putative target sites

The severe reduction of ITP immunostaining in *Clk^{AR}* mutants suggests that the *itp* gene is under CLK control. When we searched the upstream sequence of the *itp* gene, we did, however, not discover any indications for the presence of E-boxes whatsoever (data not shown). Thus, we assume that the clock controlled regulation probably occurs in an indirect way. However, ITP immunostaining did not cycle within the clock neuron cell bodies, meaning that the peptide is present in a high amount at all times of the day anyway. This indicates that a putative rhythm in *itp* expression and/or ITP stability is at least of such minor nature, that it is undetectable by immunohistochemistry. This is a quite similar situation as in the case of PDF. The only difference is that here E-boxes were indeed discovered in the upstream regulatory region of the *pdf* gene, but mRNA levels did nevertheless not cycle (Park et al., 2000). Further, PDF immunostaining was constantly high in the LN cell bodies, indicating that the amount of peptide did not significantly change in the course of the day. However, when Park and colleagues (2000) investigated PDF immunostaining in the terminals of the PDF⁺ dorsal projection, they discovered a cycling in staining signal peaking at the beginning of the light phase in LD. Staining was decreasing then during the rest of the light phase and stayed low in the first half of the night (Park et al., 2000). This decrease in immunostaining was interpreted as a loss in peptide amount, which would come about by the release of PDF from the dense cored vesicles (Park et al., 2000). Thus, PDF very likely acts in a rhythmic manner by being released rhythmically at the axon terminals.

We wondered, whether the same would be true for ITP, whether we would be able to detect rhythms in peptide release. Since the ITP⁺ projection pattern is, however, much more complex than the PDF⁺ projections, we were unsure at first, where to look at. We then decided to quantify the ITP immunostaining in the dorso-medial projection terminals that are close to the Pars intercerebralis (PI), since these were most consistently shaped and seemed to contain only fibers from the two ITP⁺ clock cells. We found that ITP immunostaining peaked in the middle of the light phase and in the middle of the dark phase and showed troughs at around lights-on and lights-off. Assuming that the peptide is released at the time, when staining intensity decreases, these results would indicate that ITP is released in the second half of the night and in the second half of the day. Since we had found effects on the E activity and the nighttime activity in behavior, we assume that ITP release in the second half of the day promotes E activity, while it may reduce activity during the night.

Investigation of ITP target sites within the brain turned out to be extremely difficult. First of all, the ITP receptor is still unknown. We assume that it is quite probable that this receptor belongs to the family of GPCRs, but further information on its physiology is so far unpredictable. The only hints are provided by a recent study on *Schistocerca gregaria* ITP suggesting signaling through a GPCR as well as a membrane bound guanylate cyclase, which increase intracellular cAMP and cGMP levels (Audsley et al., 2012). Our live imaging assay would have offered a first opportunity to investigate the effects of ITP on *Drosophila* brain neurons *in vivo*. In collaboration with Prof. H. Dirksen (University of Stockholm) we aimed to synthetically produce *Drosophila melanogaster* ITP, which could have been used in this investigation. Unfortunately, the synthesis of this 73aa peptide turned out to be extremely difficult and time consuming, especially considering that the tertiary structure of the obtained peptide needs to be faultless in order to allow receptor activation. This was demonstrated by King et al. (1999), where it was shown that synthetically produced locust ITP is only biologically active in the gut of the insect, when it is properly folded. Thus, until now we were not able to produce enough ITP for the live imaging assay, but this will be one of our desired future goals.

Aiming for an alternative way to identify possible target sites for ITP in the brain, we studied circadian behavior of flies, in which ITP was overexpressed with different driver

lines. This approach had been previously conducted by Helfrich-Förster et al. (2000) to identify putative target sites for PDF, before its receptor was even identified. Thus, we generated a *UAS-ITP* construct containing the sequence of the short *itp* isoform ITP-PE, which is thought to be expressed in the fly head (H. Dircksen, personal communication). Our results first of all showed that ITP can be ectopically expressed in quite a lot of neurons in the brain, including all clusters of clock neurons. This is quite remarkable, considering that the whole peptide processing machinery needs to be present in the cells to end up with the mature peptide, which is exclusively recognized by the antibody that we used (Dircksen et al., *in prep.*; Hermann-Luibl et al., *submitted*). Further, we showed that flies get completely arrhythmic when ITP is overexpressed with two different *tim-GAL4* lines, *timG4* and *tim(UAS)G4*, while they are behaviorally normal with any of the other tested driver lines. Even overexpression with *perG4* did not impair rhythmicity, although similar subsets of neurons should be targeted by this driver. Detailed comparative analysis of the ITP staining pattern in behaviorally rhythmic and behaviorally arrhythmic ITP-overexpressing flies did not give us any hints, in which brain regions ITP signaling might be especially enhanced in the behaviorally arrhythmic flies compared to the rhythmic ones. Since we had only looked at brains in this examination, we cannot exclude that there are differences in expression in certain regions in the body of the flies. However, we consider these putative differences as being of minor role in the control of rhythmic locomotor activity. The fact that the amplitude of PER cycling seemed to be dampened in the sLN_v and the LN_d in the overexpression flies using *tim(UAS)G4* could indicate that ITP targets these clock neurons. Future live-imaging experiments could investigate, whether these two cell groups indeed respond to ITP. However, since there was still significant PER cycling present, but the flies were completely arrhythmic in DD, we assume that the major role of ITP lies in the output of the clock targeting other brain regions.

Interestingly, we found that in behaviorally arrhythmic *tim(UAS)G4>ITP²* flies the ITP cycling in the projection terminals in the PI was abolished, while it was still present in behaviorally rhythmic *perG4>ITP²* flies. Further, PDF⁺ projections from the ILN_v showed an abnormal pattern in the majority of the *tim(UAS)G4>ITP²* flies, arborizing into the dorsal protocerebrum. Thus, we concluded that probably constantly high amounts of both ITP and PDF in the PI led to behavioral arrhythmicity in *tim(UAS)G4>ITP²* flies.

(See also discussion section of Hermann-Luibl et al., *submitted*)

4.5 Final Conclusions

This PhD project had aimed to characterize the role of the neuropeptides NPF, sNPF and ITP in the circadian clock of *Drosophila melanogaster*. In collaboration with various helpful coworkers I have tried to exhaust the majority of available technical means to shed some light on this topic. I will draw my final conclusions of this work in the following.

A first achievement was the verification and refinement of the neuropeptide expression pattern within the *Drosophila melanogaster* clock neurons. Thus, Figure 4 of the introduction section can be adapted taking the recent findings of the NPF expression (Hermann et al., 2012) into account (Fig. 36). I can further conclude that the usage of neuropeptides as signaling molecules within the clock network is probably conserved within the *Drosophila* genus and maybe even among other insect species, although the network properties seem to have adapted differently to different environmental conditions in order to allow the animal to time its activity to the most suitable time (Hermann et al., 2013).

Knocking down a gene of interest in a spatially controlled manner via RNAi is nowadays probably the most elegant way to investigate the role of a certain protein or peptide in *Drosophila*. However, this approach is limited, in that the user depends on the functionality of the available RNAi constructs, which is probably up to various partly unknown factors. In the course of this thesis we were lucky having two very efficient RNAi constructs, *pdf-RNAi* and *itp-RNAi*, while the *npf-RNAi* and the *snpf-RNAi* constructs turned out to be only insufficiently functional. Thus, I would like to emphasize at this point that especially the results for the sNPF-knockdown should be regarded with care, since they very likely are the result of off-target effects of the RNAi construct. In case of NPF, we were able to draw further conclusions on its function from the cell ablation experiments. Such experiments were, however, not possible in the case of sNPF, since these flies would not be viable.

The most general conclusion from this work – also with regard to the current literature – is that especially ITP, most probably NPF and potentially also sNPF play a role in the

control of locomotor rhythms. However, none of these peptides seems to be of equal importance as PDF. The observed phenotypes were all rather small, when the peptides were knocked down. This implies that the major clock derived signal controlling locomotor rhythms is mediated by PDF, while signaling through the other peptides probably only fine-tunes the actions of PDF.

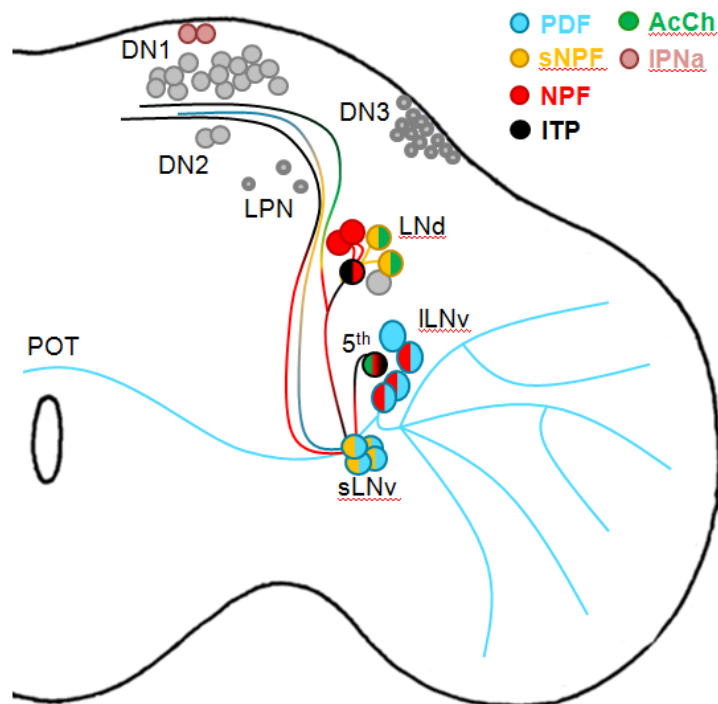


Figure 36: Updated neurochemistry of the clock neurons of *Drosophila melanogaster*. NPF (red) was newly discovered in the fifth sLNv and a subset of the ILNv in the course of this thesis. For further details, please refer to Figure legend 4 in the introduction section.

In LD behavior, PDF is necessary to promote M activity and necessary for the right E peak phase in that it delays the E activity to the end of the day by decelerating the clock in the E cells (Renn et al., 1999; Shafer and Taghert, 2009; Yoshii et al., 2009). The latter effect is important in the adaptation to longer photoperiods, in which the E activity needs to be delayed in order to follow the delay of dusk. It is assumed that the control of the M activity derives from sLNv PDF, while the E peak timing is most probably controlled by PDF from the ILNv (Shafer and Taghert, 2009; Yoshii et al., 2009). The amplitude of the E activity, however, seems to be promoted by the actions of ITP and NPF from the E oscillator cells (Hermann et al., 2012; Hermann-Luibl et al., *submitted*). Since the ablation of the NPF⁺ cells – which includes also the ITP⁺ clock neurons – did not completely abolish

the E peak (Hermann et al., 2012), it is clear that ITP and NPF are not the only factors promoting E activity. Indeed, the two NPF⁻CRY⁺ LN_d of the E oscillator are remaining, which could still fulfill this function. These neurons contain sNPF, but whether it indeed participates in the promotion of the E activity is unsure due to the inefficiency of the RNAi.

It is further very clear that of the investigated neuropeptides PDF seems to be also the major factor that maintains rhythmicity under constant conditions. Flies with a disruption in PDF signaling get either arrhythmic in DD or show a shortened free-running rhythm in behavior (Renn et al., 1999; Shafer and Taghert, 2009). It is believed that PDF signaling is required to synchronize the oscillations of different clock neurons and that PDF is further able to decelerate or accelerate the clock in different clock neurons (Yoshii et al., 2009). Behavioral arrhythmicity in DD in PDF-deficient flies was shown to be mainly caused by a desynchronization of the oscillations in individual sLN_v neurons, while the short free-running period results from the lack of PDF-mediated deceleration of the clock in the majority of pacemaker neurons (Yoshii et al., 2009). Disruption of clock neuron mediated signaling via the other investigated neuropeptides did not affect behavioral rhythmicity in general, indicating that they are not required for maintenance of a free-running rhythm in DD (Hermann et al., 2012; Hermann-Luibl et al., *submitted*). However, knockdown of ITP and PDF together had shown a more severe phenotype in DD than the PDF-knockdown alone, and constantly high ITP levels in the dorsal protocerebrum had impaired rhythmicity, clearly indicating a certain importance of ITP for the free-running rhythm. Further, it seems that ITP and possibly also sNPF constitute period shortening components opposing the effect of PDF. Thus, one could imagine that in wildtype flies the period lengthening component (PDF) and period shortening component(s) (ITP, sNPF) are in balance resulting in a free-running period of about 24 hours in DD. Disrupting either PDF signaling or ITP/sNPF signaling results then in a shorter period or longer period, respectively. And disrupting both PDF and ITP signaling from the clock neurons leads to complete arrhythmicity or complex rhythms showing more than one free-running component.

The question, whether this peptide mediated behavioral control is achieved via clock output pathways or signaling inside the clock network cannot yet be fully answered for

the different neuropeptides. Concerning the communication among clock neurons, it is very clear that also here PDF is the main signaling molecule. All clock neuron clusters, except the ILNv, had been shown to respond to applied PDF (Shafer et al., 2008) and further PDF is able to speed up or slow down the oscillation in certain clock neurons (Yoshii et al., 2009). Since PDF is intrinsic to the sLNv and ILNv in the adult brain and the neuronal responses had been shown to be PDFR dependent (Shafer et al., 2008) it is even clear in this case that there is indeed direct signaling from one set of clock neurons to others. Only few clock neurons were, however, responsive to sNPF and NPF, suggesting already that the function of both peptides in inter-clock neuron communication is of minor nature and that both might also be involved in clock output. The findings that PDF and ITP seem to be rhythmically released into the PI and the pars lateralis (PL; Park et al., 2000; Hermann-Luibl et al., *submitted*) suggest that there are not only spatial differences in neuropeptide action but also temporal differences. The latter can be of special importance when the same cells receive both excitatory and inhibitory stimuli as it seems to be the case for some DN, which were shown to respond both to PDF (Shafer et al., 2008) and sNPF, which very likely derive from the sLNv.

Dissecting clock related neuronal connectivity is of growing interest in our field of study to understand the pathways of clock input, input processing within the network and subsequent neuronal output. Especially the latter will be an interesting subject of further investigation in future studies. This work has provided a basis for the investigation of neuropeptide mediated signaling within the clock network as well as for the effects of neuropeptide mediated behavioral output.

5 References

- Allada R, White NE, So WV, Hall JC and Rosbash M (1998) A mutant *Drosophila* homolog of mammalian *Clock* disrupts circadian rhythms and transcription of *period* and *timeless*. *Cell* 93:791-804.
- Audsley N, Jensen D and Schooley DA (2012) Signal transduction for *Schistocerca gregaria* ion transport peptide is mediated via both cyclic AMP and cyclic GMP. *Peptides* 41:74-80.
- Audsley N, McIntosh C and Phillips JE (1992) Isolation of a neuropeptide from locust corpus cardiacum which influences ileal transport. *The Journal of experimental biology* 173:261-274.
- Bahn JH, Lee G and Park JH (2009) Comparative analysis of Pdf-mediated circadian behaviors between *Drosophila melanogaster* and *D. virilis*. *Genetics* 181:965-975.
- Bendena WG, Campbell J, Zara L, Tobe SS and Chin-Sang ID (2012) Select Neuropeptides and their G-Protein Coupled Receptors in *Caenorhabditis Elegans* and *Drosophila Melanogaster*. *Frontiers in endocrinology* 3:93.
- Blau J and Young MW (1999) Cyclic *vriille* expression is required for a functional *Drosophila* clock. *Cell* 99:661-671.
- Brand AH and Perrimon N (1993) Targeted gene expression as a means of altering cell fates and generating dominant phenotypes. *Development (Cambridge, England)* 118:401-415.
- Brown MR, Crim JW, Arata RC, Cai HN, Chun C and Shen P (1999) Identification of a *Drosophila* brain-gut peptide related to the neuropeptide Y family. *Peptides* 20:1035-1042.
- Caers J, Verlinden H, Zels S, Vandersmissen HP, Vuerinckx K and Schoofs L (2012) More than two decades of research on insect neuropeptide GPCRs: an overview. *Frontiers in endocrinology* 3:151.
- Chen W, Shi W, Li L, Zheng Z, Li T, Bai W and Zhao Z (2013) Regulation of sleep by the short neuropeptide F (sNPF) in *Drosophila melanogaster*. *Insect biochemistry and molecular biology* 43:809-819.
- Cyran SA, Buchsbaum AM, Reddy KL, Lin MC, Glossop NR, Hardin PE, Young MW, Storti RV and Blau J (2003) *vriille*, *Pdp1*, and *dClock* form a second feedback loop in the *Drosophila* circadian clock. *Cell* 112:329-341.
- Dai L, Zitnan D and Adams ME (2007) Strategic expression of ion transport peptide gene products in central and peripheral neurons of insects. *The Journal of comparative neurology* 500:353-367.

- Damulewicz M and Pyza E (2011) The clock input to the first optic neuropil of *Drosophila melanogaster* expressing neuronal circadian plasticity. *PLoS one* 6:e21258.
- Damulewicz M, Rosato E and Pyza E (2013) Circadian regulation of the Na⁺/K⁺-ATPase alpha subunit in the visual system is mediated by the pacemaker and by retina photoreceptors in *Drosophila melanogaster*. *PLoS one* 8:e73690.
- Darlington TK, Wager-Smith K, Ceriani MF, Staknis D, Gekakis N, Steeves TD, Weitz CJ, Takahashi JS and Kay SA (1998) Closing the circadian loop: CLOCK-induced transcription of its own inhibitors *per* and *tim*. *Science (New York, NY)* 280:1599-1603.
- Dierick HA and Greenspan RJ (2007) Serotonin and neuropeptide F have opposite modulatory effects on fly aggression. *Nature Genetics* 39:678-682.
- Dietzl G, Chen D, Schnorrer F, Su KC, Barinova Y, Fellner M, Gasser B, Kinsey K, Oppel S, Scheiblauer S, Couto A, Marra V, Keleman K and Dickson BJ (2007) A genome-wide transgenic RNAi library for conditional gene inactivation in *Drosophila*. *Nature* 448:151-156.
- Dimitroff B, Howe K, Watson A, Champion B, Lee HG, Zhao N, O'Connor MB, Neufeld TP and Selleck SB (2012) Diet and energy-sensing inputs affect TorC1-mediated axon misrouting but not TorC2-directed synapse growth in a *Drosophila* model of tuberous sclerosis. *PLoS one* 7:e30722.
- Dircksen H (2009) Insect ion transport peptides are derived from alternatively spliced genes and differentially expressed in the central and peripheral nervous system. *The Journal of experimental biology* 212:401-412.
- Dircksen H, Strauß J, Mandali A and Nässel DR (2014) Cell-type specific distribution of three ion-transport-peptide splice forms in the central and peripheral nervous system of larval and adult *Drosophila melanogaster*. *in prep*.
- Dircksen H, Tesfai LK, Albus C and Nassel DR (2008) Ion transport peptide splice forms in central and peripheral neurons throughout postembryogenesis of *Drosophila melanogaster*. *The Journal of comparative neurology* 509:23-41.
- Dircksen H, Zahnow CA, Gaus G, Keller R, Rao KR, Riehm JP (1987) The ultrastructure of nerve endings containing pigment dispersing hormone (PDH) in crustacean sinus glands: identification by an antiserum against synthetic PDH. *Cell Tissue Research* 250:377-387.
- Domnik L (2011) Uhrnetzwerk und Aktivitätsmuster verschiedener *Drosophila*arten. Bachelor Thesis, University of Würzburg
- Dushay MS, Rosbash M and Hall JC (1989) The *disconnected* visual system mutations in *Drosophila melanogaster* drastically disrupt circadian rhythms. *Journal of biological rhythms* 4:1-27.

- Emery P, So WV, Kaneko M, Hall JC and Rosbash M (1998) CRY, a *Drosophila* clock and light-regulated cryptochrome, is a major contributor to circadian rhythm resetting and photosensitivity. *Cell* 95:669-679.
- Feng G, Reale V, Chatwin H, Kennedy K, Venard R, Ericsson C, Yu K, Evans PD and Hall LM (2003) Functional characterization of a neuropeptide F-like receptor from *Drosophila melanogaster*. *The European journal of neuroscience* 18:227-238.
- Garczynski SF, Brown MR and Crim JW (2006) Structural studies of *Drosophila* short neuropeptide F: Occurrence and receptor binding activity. *Peptides* 27:575-582.
- Garczynski SF, Brown MR, Shen P, Murray TF and Crim JW (2002) Characterization of a functional neuropeptide F receptor from *Drosophila melanogaster*. *Peptides* 23:773-780.
- Garczynski SF, Crim JW and Brown MR (2007) Characterization and expression of the short neuropeptide F receptor in the African malaria mosquito, *Anopheles gambiae*. *Peptides* 28:109-118.
- Glossop NR, Houl JH, Zheng H, Ng FS, Dudek SM and Hardin PE (2003) VRILLE feeds back to control circadian transcription of *Clock* in the *Drosophila* circadian oscillator. *Neuron* 37:249-261.
- Grima B, Chelot E, Xia R and Rouyer F (2004) Morning and evening peaks of activity rely on different clock neurons of the *Drosophila* brain. *Nature* 431:869-873.
- Gummadova JO, Coutts GA and Glossop NR (2009) Analysis of the *Drosophila Clock* promoter reveals heterogeneity in expression between subgroups of central oscillator cells and identifies a novel enhancer region. *Journal of biological rhythms* 24:353-367.
- Hamasaka Y, Suzuki T, Hanai S and Ishida N (2010) Evening circadian oscillator as the primary determinant of rhythmic motivation for *Drosophila* courtship behavior. *Genes Cells* 15:1240-1248.
- He C, Cong X, Zhang R, Wu D, An C and Zhao Z (2013a) Regulation of circadian locomotor rhythm by neuropeptide Y-like system in *Drosophila melanogaster*. *Insect molecular biology* 22:376-388.
- He C, Yang Y, Zhang M, Price JL and Zhao Z (2013b) Regulation of sleep by neuropeptide Y-like system in *Drosophila melanogaster*. *PloS one* 8:e74237.
- Helfrich-Förster C (1995) The *period* clock gene is expressed in central nervous system neurons which also produce a neuropeptide that reveals the projections of circadian pacemaker cells within the brain of *Drosophila melanogaster*. *Proceedings of the National Academy of Sciences of the United States of America* 92:612-616.

- Helfrich-Förster C (2002) The circadian system of *Drosophila melanogaster* and its light input pathways. *Zoology (Jena, Germany)* 105:297-312.
- Helfrich-Förster C (2004) The circadian clock in the brain: a structural and functional comparison between mammals and insects. *J Comp Physiol A Neuroethol Sens Neural Behav Physiol* 190:601-613.
- Helfrich-Förster C (2005) Organization of endogenous clocks in insects. *Biochemical Society transactions* 33:957-961.
- Helfrich-Förster C (2009) Neuropeptide PDF plays multiple roles in the circadian clock of *Drosophila melanogaster*. *Sleep and Biological Rhythms* 7:130-143.
- Helfrich-Förster C, Shafer OT, Wülbeck C, Grieshaber E, Rieger D and Taghert P (2007) Development and morphology of the clock-gene-expressing lateral neurons of *Drosophila melanogaster*. *The Journal of comparative neurology* 500:47-70.
- Helfrich-Förster C, Tauber M, Park JH, Muhlig-Versen M, Schneuwly S and Hofbauer A (2000) Ectopic expression of the neuropeptide pigment-dispersing factor alters behavioral rhythms in *Drosophila melanogaster*. *Journal of Neuroscience* 20:3339-3353.
- Helfrich C (1986) Role of the optic lobes in the regulation of the locomotor activity rhythm of *Drosophila melanogaster*: behavioral analysis of neural mutants. *Journal of neurogenetics* 3:321-343.
- Hermann C, Saccon R, Senthilan PR, Domnik L, Dirksen H, Yoshii T and Helfrich-Förster C (2013) The circadian clock network in the brain of different *Drosophila* species. *The Journal of comparative neurology* 521:367-388.
- Hermann C, Yoshii T, Dusik V and Helfrich-Förster C (2012) Neuropeptide F immunoreactive clock neurons modify evening locomotor activity and free-running period in *Drosophila melanogaster*. *The Journal of comparative neurology* 520:970-987.
- Hermann-Luibl C, Yoshii T, Senthilan PR, Dirksen H and Helfrich-Förster C (2014) The Ion Transport Peptide is a new functional clock neuropeptide in the fruit fly *Drosophila melanogaster*. *submitted to Journal of Neuroscience*
- Hewes RS and Taghert PH (2001) Neuropeptides and neuropeptide receptors in the *Drosophila melanogaster* genome. *Genome research* 11:1126-1142.
- Hofbauer A, Ebel T, Waltenspiel B, Oswald P, Chen YC, Halder P, Biskup S, Lewandrowski U, Winkler C, Sickmann A, Buchner S and Buchner E (2009) The Würzburg hybridoma library against *Drosophila* brain. *Journal of neurogenetics* 23:78-91.
- Hong SH, Lee KS, Kwak SJ, Kim AK, Bai H, Jung MS, Kwon OY, Song WJ, Tatar M and Yu K (2012) Minibrain/Dyrk1a regulates food intake through the Sir2-FOXO-sNPF/NPY pathway in *Drosophila* and mammals. *PLoS genetics* 8:e1002857.

- Hyun S, Lee Y, Hong ST, Bang S, Paik D, Kang J, Shin J, Lee J, Jeon K, Hwang S, Bae E and Kim J (2005) *Drosophila* GPCR Han is a receptor for the circadian clock neuropeptide PDF. *Neuron* 48:267-278.
- Im SH, Li W and Taghert PH (2011) PDFR and CRY signaling converge in a subset of clock neurons to modulate the amplitude and phase of circadian behavior in *Drosophila*. *PLoS One* 6:e18974.
- Im SH and Taghert PH (2010) PDF receptor expression reveals direct interactions between circadian oscillators in *Drosophila*. *The Journal of comparative neurology* 518:1925-1945.
- Johard HA, Enell LE, Gustafsson E, Trifilieff P, Veenstra JA and Nässel DR (2008) Intrinsic neurons of *Drosophila* mushroom bodies express short neuropeptide F: relations to extrinsic neurons expressing different neurotransmitters. *The Journal of comparative neurology* 507:1479-1496.
- Johard HA, Yoishii T, Dirksen H, Cusumano P, Rouyer F, Helfrich-Förster C and Nässel DR (2009) Peptidergic clock neurons in *Drosophila*: ion transport peptide and short neuropeptide F in subsets of dorsal and ventral lateral neurons. *The Journal of comparative neurology* 516:59-73.
- Kahsai L, Kapan N, Dirksen H, Winther AM and Nassel DR (2010a) Metabolic stress responses in *Drosophila* are modulated by brain neurosecretory cells that produce multiple neuropeptides. *PLoS one* 5:e11480.
- Kahsai L, Martin JR and Winther AM (2010b) Neuropeptides in the *Drosophila* central complex in modulation of locomotor behavior. *The Journal of experimental biology* 213:2256-2265.
- Kauranen H, Menegazzi P, Costa R, Helfrich-Förster C, Kankainen A and Hoikkala A (2012) Flies in the north: locomotor behavior and clock neuron organization of *Drosophila montana*. *Journal of biological rhythms* 27:377-387.
- King DS, Meredith J, Wang YJ and Phillips JE (1999) Biological actions of synthetic locust ion transport peptide (ITP). *Insect biochemistry and molecular biology* 29:11-18.
- Klarsfeld A, Malpel S, Michard-Vanhée C, Picot M, Chélot E and Rouyer F (2004) Novel features of Cryptochrome-mediated photoreception in the brain circadian clock of *Drosophila*. *Journal of Neuroscience* 24(6):1468-1477.
- Knappek S, Kahsai L, Winther AM, Tanimoto H and Nässel DR (2013) Short neuropeptide F acts as a functional neuromodulator for olfactory memory in Kenyon cells of *Drosophila* mushroom bodies. *Journal of Neuroscience* 33:5340-5345.
- Konopka RJ and Benzer S (1971) Clock mutants of *Drosophila melanogaster*. *Proceedings of the National Academy of Sciences of the United States of America* 68:2112-2116.

- Konopka RJ, Wells S and Lee T (1983) Mosaic analysis of a *Drosophila* clock mutant. *Molecular and General Genetics* 190: 284–288.
- Kula-Eversole E, Nagoshi E, Shang Y, Rodriguez J, Allada R and Rosbash M (2010) Surprising gene expression patterns within and between PDF-containing circadian neurons in *Drosophila*. *Proceedings of the National Academy of Sciences of the United States of America* 107:13497-13502.
- Lee C, Bae K and Edery I (1999) PER and TIM inhibit the DNA binding activity of a *Drosophila* CLOCK-CYC/dBMAL1 heterodimer without disrupting formation of the heterodimer: a basis for circadian transcription. *Molecular and cellular biology* 19:5316-5325.
- Lee G, Bahn JH and Park JH (2006) Sex- and clock-controlled expression of the neuropeptide F gene in *Drosophila*. *Proceedings of the National Academy of Sciences of the United States of America* 103:12580-12585.
- Lee KS, Kwon OY, Lee JH, Kwon K, Min KJ, Jung SA, Kim AK, You KH, Tatar M and Yu K (2008) *Drosophila* short neuropeptide F signalling regulates growth by ERK-mediated insulin signalling. *Nature cell biology* 10:468-475.
- Lee KS, You KH, Choo JK, Han YM and Yu K (2004) *Drosophila* short neuropeptide F regulates food intake and body size. *The Journal of biological chemistry* 279:50781-50789.
- Lee T and Luo L (1999) Mosaic analysis with a repressible cell marker for studies of gene function in neuronal morphogenesis. *Neuron* 22:451-461.
- Lelito KR and Shafer OT (2012) Reciprocal cholinergic and GABAergic modulation of the small ventrolateral pacemaker neurons of *Drosophila's* circadian clock neuron network. *Journal of neurophysiology* 107:2096-2108.
- Lin FJ, Song W, Meyer-Bernstein E, Naidoo N and Sehgal A (2001) Photic signaling by cryptochrome in the *Drosophila* circadian system. *Molecular and cellular biology* 21:7287-7294.
- Lin Y, Stormo GD and Taghert PH (2004) The neuropeptide pigment-dispersing factor coordinates pacemaker interactions in the *Drosophila* circadian system. *Journal of Neuroscience* 24:7951-7957.
- Lindsley DL and Grell EH (1968) Genetic variation of *Drosophila melanogaster*. *Carnegie Institution of Washington Publication* No. 627.
- Maule AG, Shaw C, Halton DW, Thim L, Johnston CF, Fairweather I, et al. (1991) Neuropeptide F: a novel parasitic flat worm regulatory peptide from *Moniezia expansa* (Cestoda: Cyclophyllidea). *Parasitology* 102: 309–16.

- Menegazzi P, Vanin S, Yoshii T, Rieger D, Hermann C, Dusik V, Kyriacou CP, Helfrich-Förster C and Costa R (2013) *Drosophila* clock neurons under natural conditions. *Journal of biological rhythms* 28:3-14.
- Meredith J, Ring M, Macins A, Marschall J, Cheng NN, Theilmann D, Brock HW and Phillips JE (1996) Locust ion transport peptide (ITP): primary structure, cDNA and expression in a baculovirus system. *The Journal of experimental biology* 199:1053-1061.
- Mertens I, Meeusen T, Huybrechts R, De Loof A and Schoofs L (2002) Characterization of the short neuropeptide F receptor from *Drosophila melanogaster*. *Biochemical and biophysical research communications* 297:1140-1148.
- Mertens I, Vandingenen A, Johnson EC, Shafer OT, Li W, Trigg JS, De Loof A, Schoofs L and Taghert PH (2005) PDF receptor signaling in *Drosophila* contributes to both circadian and geotactic behaviors. *Neuron* 48:213-219.
- Nässel DR (2002) Neuropeptides in the nervous system of *Drosophila* and other insects: multiple roles as neuromodulators and neurohormones. *Progress in neurobiology* 68:1-84.
- Nässel DR, Enell LE, Santos JG, Wegener C and Johard HA (2008) A large population of diverse neurons in the *Drosophila* central nervous system expresses short neuropeptide F, suggesting multiple distributed peptide functions. *BMC neuroscience* 9:90.
- Nässel DR and Wegener C (2011) A comparative review of short and long neuropeptide F signaling in invertebrates: Any similarities to vertebrate neuropeptide Y signaling? *Peptides* 32:1335-1355.
- Nikolaev VO, Bunemann M, Hein L, Hannawacker A and Lohse MJ (2004) Novel single chain cAMP sensors for receptor-induced signal propagation. *The Journal of biological chemistry* 279:37215-37218.
- Page TL (1985) Clocks and circadian rhythms. *Comprehensive Insect Physiology Biochemistry and Pharmacology* 6: 557–653.
- Park JH, Helfrich-Förster C, Lee G, Liu L, Rosbash M and Hall JC (2000) Differential regulation of circadian pacemaker output by separate clock genes in *Drosophila*. *Proceedings of the National Academy of Sciences of the United States of America* 97:3608-3613.
- Peschel N and Helfrich-Förster C (2011) Setting the clock--by nature: circadian rhythm in the fruitfly *Drosophila melanogaster*. *FEBS letters* 585:1435-1442.
- Picot M, Cusumano P, Klarsfeld A, Ueda R and Rouyer F (2007) Light activates output from evening neurons and inhibits output from morning neurons in the *Drosophila* circadian clock. *PLoS biology* 5:e315.

- Pirez N, Christmann BL and Griffith LC (2013) Daily rhythms in locomotor circuits in *Drosophila* involve PDF. *Journal of neurophysiology* 110:700-708.
- Pittendrigh CS and Daan S (1976) A functional analysis of circadian pacemakers in nocturnal rodents. V. pacemaker structure: A clock for all seasons. *J Comp Physiol (A)* 106:333-355.
- Plautz JD, Kaneko M, Hall JC and Kay SA (1997) Independent photoreceptive circadian clocks throughout *Drosophila*. *Science (New York, NY)* 278:1632-1635.
- Prabhakaran PM and Sheeba V (2012) Sympatric *Drosophilid* species *melanogaster* and *ananassae* differ in temporal patterns of activity. *Journal of biological rhythms* 27:365-376.
- Price JL, Blau J, Rothenfluh A, Abodeely M, Kloss B and Young MW (1998) *double-time* is a novel *Drosophila* clock gene that regulates PERIOD protein accumulation. *Cell* 94:83-95.
- Rao KR and Riehm JP (1993) Pigment-dispersing hormones. *Annals of the New York Academy of Sciences* 680:78-88.
- Reale V, Chatwin HM and Evans PD (2004) The activation of G-protein gated inwardly rectifying K⁺ channels by a cloned *Drosophila melanogaster* neuropeptide F-like receptor. *The European journal of neuroscience* 19:570-576.
- Renn SC, Park JH, Rosbash M, Hall JC and Taghert PH (1999) A pdf neuropeptide gene mutation and ablation of PDF neurons each cause severe abnormalities of behavioral circadian rhythms in *Drosophila*. *Cell* 99:791-802.
- Rieger D, Fraunholz C, Popp J, Bichler D, Dittmann R and Helfrich-Förster C (2007) The fruit fly *Drosophila melanogaster* favors dim light and times its activity peaks to early dawn and late dusk. *Journal of biological rhythms* 22:387-399.
- Rieger D, Peschel N, Dusik V, Glotz S and Helfrich-Förster C (2012) The ability to entrain to long photoperiods differs between 3 *Drosophila melanogaster* wild-type strains and is modified by twilight simulation. *Journal of biological rhythms* 27:37-47.
- Rieger D, Shafer OT, Tomioka K and Helfrich-Förster C (2006) Functional analysis of circadian pacemaker neurons in *Drosophila melanogaster*. *Journal of Neuroscience* 26:2531-2543.
- Rieger D, Stanewsky R and Helfrich-Förster C (2003) Cryptochrome, compound eyes, Hofbauer-Buchner eyelets, and ocelli play different roles in the entrainment and masking pathway of the locomotor activity rhythm in the fruit fly *Drosophila melanogaster*. *Journal of biological rhythms* 18:377-391.
- Rieger D, Wülbeck C, Rouyer F and Helfrich-Förster C (2009) *Period* gene expression in four neurons is sufficient for rhythmic activity of *Drosophila melanogaster* under dim light conditions. *Journal of biological rhythms* 24:271-282.

- Ring M, Meredith J, Wiens C, Macins A, Brock HW, Phillips JE and Theilmann DA (1998) Expression of *Schistocerca gregaria* ion transport peptide (ITP) and its homologue (ITP-L) in a baculovirus/insect cell system. *Insect biochemistry and molecular biology* 28:51-58.
- Rutila JE, Suri V, Le M, So WV, Rosbash M and Hall JC (1998) CYCLE is a second bHLH-PAS clock protein essential for circadian rhythmicity and transcription of *Drosophila period* and *timeless*. *Cell* 93:805-814.
- Saccon R (2010) Comparative analysis of PDF-neurons and activity patterns of different *Drosophila* species. Master Thesis, University of Regensburg/Padova.
- Schmid B, Helfrich-Förster C and Yoshii T (2011) A new ImageJ plug-in "ActogramJ" for chronobiological analyses. *Journal of biological rhythms* 26:464-467.
- Shafer OT, Helfrich-Förster C, Renn SC and Taghert PH (2006) Reevaluation of *Drosophila melanogaster's* neuronal circadian pacemakers reveals new neuronal classes. *The Journal of comparative neurology* 498:180-193.
- Shafer OT, Kim DJ, Dunbar-Yaffe R, Nikolaev VO, Lohse MJ and Taghert PH (2008) Widespread receptivity to neuropeptide PDF throughout the neuronal circadian clock network of *Drosophila* revealed by real-time cyclic AMP imaging. *Neuron* 58:223-237.
- Shafer OT and Taghert PH (2009) RNA-interference knockdown of *Drosophila* pigment dispersing factor in neuronal subsets: the anatomical basis of a neuropeptide's circadian functions. *PLoS one* 4:e8298.
- Shang Y, Donelson NC, Vecsey CG, Guo F, Rosbash M and Griffith LC (2013) Short neuropeptide F is a sleep-promoting inhibitory modulator. *Neuron* 80:171-183.
- Shang Y, Haynes P, Pirez N, Harrington KI, Guo F, Pollack J, Hong P, Griffith LC and Rosbash M (2011) Imaging analysis of clock neurons reveals light buffers the wake-promoting effect of dopamine. *Nature neuroscience* 14:889-895.
- Shen P and Cai HN (2001) *Drosophila* neuropeptide F mediates integration of chemosensory stimulation and conditioning of the nervous system by food. *Journal of neurobiology* 47:16-25.
- Sidote D, Majercak J, Parikh V and Edery I (1998) Differential effects of light and heat on the *Drosophila* circadian clock proteins PER and TIM. *Molecular and cellular biology* 18:2004-2013.
- Siegmund T and Korge G (2001) Innervation of the ring gland of *Drosophila melanogaster*. *The Journal of comparative neurology* 431:481-491.
- Stanewsky R, Frisch B, Brandes C, Hamblen-Coyle MJ, Rosbash M and Hall JC (1997) Temporal and spatial expression patterns of transgenes containing increasing amounts of the *Drosophila* clock gene *period* and a lacZ reporter: mapping

- elements of the PER protein involved in circadian cycling. *Journal of Neuroscience* 17:676-696.
- Stewart BA, Atwood HL, Renger JJ, Wang J and Wu CF (1994) Improved stability of *Drosophila* larval neuromuscular preparations in haemolymph-like physiological solutions. *Journal of comparative physiology* 175:179-191.
- Stoleru D, Peng Y, Agosto J and Rosbash M (2004) Coupled oscillators control morning and evening locomotor behaviour of *Drosophila*. *Nature* 431:862-868.
- Taghert PH, Hewes RS, Park JH, O'Brien MA, Han M and Peck ME (2001) Multiple amidated neuropeptides are required for normal circadian locomotor rhythms in *Drosophila*. *Journal of Neuroscience* 21:6673-6686.
- Taghert PH and Nitabach MN (2012) Peptide neuromodulation in invertebrate model systems. *Neuron* 76:82-97.
- Tian L, Hires SA, Mao T, Huber D, Chiappe ME, Chalasani SH, Petreanu L, Akerboom J, McKinney SA, Schreiter ER, Bargmann CI, Jayaraman V, Svoboda K and Looger LL (2009) Imaging neural activity in worms, flies and mice with improved GCaMP calcium indicators. *Nature methods* 6:875-881.
- Tomioka K and Matsumoto A (2010) A comparative view of insect circadian clock systems. *Cellular and Molecular Life Sciences* 67:1397-1406.
- Veenstra JA (2009) Peptidergic paracrine and endocrine cells in the midgut of the fruit fly maggot. *Cell and tissue research* 336:309-323.
- Wen T, Parrish CA, Xu D, Wu Q and Shen P (2005) *Drosophila* neuropeptide F and its receptor, NPFR1, define a signaling pathway that acutely modulates alcohol sensitivity. *Proceedings of the National Academy of Sciences of the United States of America* 102:2141-2146.
- Wu Q, Wen T, Lee G, Park JH, Cai HN and Shen P (2003) Developmental control of foraging and social behavior by the *Drosophila* neuropeptide Y-like system. *Neuron* 39:147-161.
- Wu Q, Zhao Z and Shen P (2005) Regulation of aversion to noxious food by *Drosophila* neuropeptide Y- and insulin-like systems. *Nature neuroscience* 8:1350-1355.
- Xu J, Li M and Shen P (2010) A G-protein-coupled neuropeptide Y-like receptor suppresses behavioral and sensory response to multiple stressful stimuli in *Drosophila*. *Journal of Neuroscience* 30:2504-2512.
- Yao Z, Macara AM, Lelito KR, Minosyan TY and Shafer OT (2012) Analysis of functional neuronal connectivity in the *Drosophila* brain. *Journal of neurophysiology* 108:684-696.

-
- Yoshii T, Rieger D and Helfrich-Förster C (2012) Two clocks in the brain: an update of the morning and evening oscillator model in *Drosophila*. *Progress in brain research* 199:59-82.
- Yoshii T, Todo T, Wülbeck C, Stanewsky R and Helfrich-Förster C (2008) Cryptochrome is present in the compound eyes and a subset of *Drosophila's* clock neurons. *The Journal of comparative neurology* 508:952-966.
- Yoshii T, Wülbeck C, Sehadova H, Veleri S, Bichler D, Stanewsky R and Helfrich-Förster C (2009) The neuropeptide pigment-dispersing factor adjusts period and phase of *Drosophila's* clock. *Journal of Neuroscience* 29:2597-2610.
- Zhang Y, Liu Y, Bilodeau-Wentworth D, Hardin PE and Emery P (2010) Light and temperature control the contribution of specific DN1 neurons to *Drosophila* circadian behavior. *Current Biology* 20:600-605.
- Zhou L, Schnitzler A, Agapite J, Schwartz LM, Steller H and Nambu JR (1997) Cooperative functions of the *reaper* and *head involution defective* genes in the programmed cell death of *Drosophila* central nervous system midline cells. *Proceedings of the National Academy of Sciences of the United States of America* 94:5131-5136.

The Circadian Clock Network in the Brain of Different *Drosophila* Species

Christiane Hermann,¹ Rachele Saccon,^{1,2} Pingkalai R. Senthilan,¹ Lilith Domnik,¹ Heinrich Dircksen,³ Taishi Yoshii,^{1,4} and Charlotte Helfrich-Förster^{1*}

¹Neurobiology and Genetics, Theodor-Boveri Institute, Biocenter, University of Würzburg, Würzburg D-97074, Germany

²Department of Biology, University of Padova, 35100 Padova, Italy

³Department of Zoology, Stockholm University, S-10691 Stockholm, Sweden

⁴Graduate School of Natural Science and Technology, Okayama University, Okayama 700-8530, Japan

ABSTRACT

Comparative studies on cellular and molecular clock mechanisms have revealed striking similarities in the organization of the clocks among different animal groups. To gain evolutionary insight into the properties of the clock network within the *Drosophila* genus, we analyzed sequence identities and similarities of clock protein homologues and immunostained brains of 10 different *Drosophila* species using antibodies against vrille (VRI), PAR-protein domain1 (PDP1), and cryptochrome (CRY). We found that the clock network of both subgenera *Sophophora* and *Drosophila* consists of all lateral and dorsal clock neuron clusters that were previously described in *Drosophila melanogaster*. Immunostaining against CRY and the neuropeptide pigment-dispersing factor (PDF), however, revealed species-specific differences. All species of the *Drosophila* subgenus and

D. pseudoobscura of the *Sophophora* subgenus completely lacked CRY in the large ventrolateral clock neurons (ILN_{v,s}) and showed reduced PDF immunostaining in the small ventrolateral clock neurons (sLN_{v,s}). In contrast, we found the expression of the ion transport peptide (ITP) to be consistent within the fifth sLN_v and one dorsolateral clock neuron (LN_d) in all investigated species, suggesting a conserved putative function of this neuropeptide in the clock. We conclude that the general anatomy of the clock network is highly conserved throughout the *Drosophila* genus, although there is variation in PDF and CRY expression. Our comparative study is a first step toward understanding the organization of the circadian clock in *Drosophila* species adapted to different habitats. *J. Comp. Neurol.* 521:367–388, 2013.

© 2012 Wiley Periodicals, Inc.

INDEXING TERMS: circadian; clock neurons; cryptochrome; neuropeptide; immunostaining

During the last decades, the molecular, physiological, and morphological properties of circadian clocks have been extensively studied in various animal groups, especially in insects. By estimates, insects include more than 1 million different species, which are highly divergent in morphology because of spatial, but also temporal, adaptation to various environmental niches. Despite this diversity, there are striking similarities in the principal organization of circadian clocks among all species: The master clock in the brain seems to be composed of a neuronal network that utilizes mainly neuropeptides as signaling molecules (for review see Helfrich-Förster, 2004). The pigment-dispersing factor (PDF) is a well-conserved neuropeptide that is present in putative master clock neurons of all insects studied so far, ranging from apterygotes and orthopteroids to coleoptera, hymenoptera, lepi-

doptera, and diptera (for review see Helfrich-Förster, 2009; Tomioka and Matsumoto, 2010). In the fruit fly *Drosophila melanogaster*, PDF is considered to constitute a main output factor of the clock and was shown to act as a neuromodulatory and synchronizing signal between the different clock neuron clusters (Helfrich-Förster, 1998; Peng et al., 2003; Lin et al., 2004; Shafer et al., 2008;

Rachele Saccon's current address is Institute of Neurology, University College London, Queen Square House, Queen Square, London WC1N 3BG, United Kingdom.

Grant sponsor: Deutsche Forschungsgemeinschaft (DFG); Grant number: Fo 207/12-1.

*CORRESPONDENCE TO: Charlotte Helfrich-Förster, Neurobiology and Genetics, Theodor-Boveri Institute, Biocenter, University of Würzburg, 97074 Würzburg, Germany.
E-mail: charlotte.foerster@biozentrum.uni-wuerzburg.de

Received March 30, 2012; Revised May 22, 2012; Accepted June 21, 2012

DOI 10.1002/cne.23178

Published online June 27, 2012 in Wiley Online Library (wileyonlinelibrary.com)

© 2012 Wiley Periodicals, Inc.

Yoshii et al., 2009). Because of the availability of various genetic tools, including the Gal4/UAS-mediated expression of reporter genes, the clock network of *D. melanogaster* is the best characterized (Dushay et al., 1989; Ewer et al., 1992; Helfrich-Förster and Homberg, 1993; Helfrich-Förster, 1995; Kaneko et al., 1997; Kaneko and Hall, 2000; Shafer et al., 2006). In addition to two PDF-positive cell clusters, each consisting of four neurons, the clock network comprises seven additional PDF⁻ cell clusters, all located in the lateral or dorsal protocerebrum (for details see Fig. 1). Further neuropeptides used by the clock neurons are IPName (encoded by the gene *neuropeptide-like precursor 1*), neuropeptide F (NPF), short neuropeptide F (sNPF), and ion transport peptide (ITP; Lee et al., 2006; Shafer et al., 2006; Dirksen et al., 2008; Nässel et al., 2008; Johard et al., 2009; Nässel and Wegener, 2011; Hermann et al., 2012). Among these, the ITP⁺ clock neurons are most conspicuous, because only two cells in the lateral protocerebrum are clearly distinct from the PDF neurons (see Fig. 1; Johard et al., 2009).

Because the clock neuron clusters are differentially localized, display different arborization patterns, and were shown to contain different neurotransmitters, researchers have assumed that they are functionally distinct (see, e.g., Kaneko and Hall, 2000). Studies by Grima et al. (2004) and Stoleru et al. (2004) spotlighted the functions of different clock neuron clusters in the control of the flies' bimodal activity pattern, which consists of a morning (M) and an evening (E) activity peak. The authors demonstrated that ventral and dorsal clusters of clock neurons (the sLN_vs, LN_ds, and DN1s; Fig. 1) play distinct roles in the control of these two activity bouts, indicating that the so-called M and E oscillators are anatomically separated in the fly brain. Although this model is not as simple as expected, many *Drosophila* chronobiologists have been attracted by this subject (for review see Yoshii et al., 2012).

The Drosophilidae are a cosmopolitan family of dipterans, which diverged from other fly families between 80 and 100 million years ago, according to a study of the molecular evolution of a larval serum protein (Beverley and Wilson, 1984, 1985; Ashburner, 1989). Within the *Drosophila* genus, the subgenera *Drosophila* and *Sophophora* (see Fig. 2) are assumed to have separated from each other about 60–65 million years ago (for review see Spicer, 1988), and members of the *Drosophila* genus are found in different habitats all over the world. In 2009, Bahn et al. investigated the diurnal and circadian behavior of *D. virilis*, which live in colder habitats than *D. melanogaster*. They showed that *D. virilis* have a reduced morning activity, as do *D. melanogaster Pdf⁰¹* mutants (Renn et al., 1999). In addition, Bahn et al. (2009) found that the sLN_vs in *D. virilis* do not express PDF, indicating

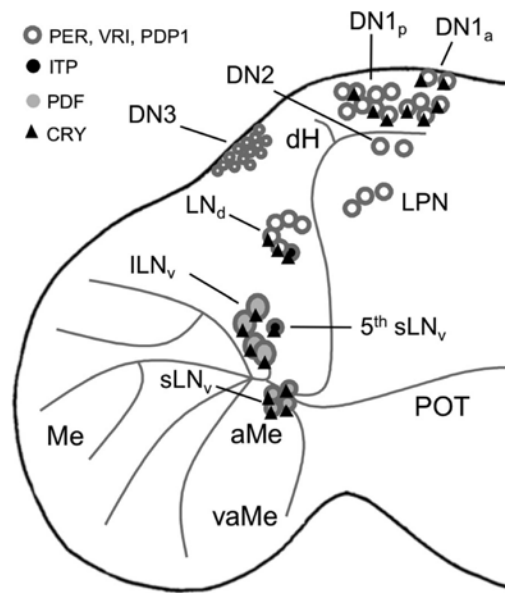


Figure 1. Schematic overview of the master clock of *D. melanogaster*. By antibody staining against the neuropeptide pigment-dispersing factor (PDF), the clock was localized to four large (ILN_v) and four small (sLN_v) PDF-immunoreactive neurons innervating the accessory medulla (aMe), a small neuropil between the medulla (Me) and the lobula (Lo; Helfrich-Förster, 1995). The ILN_vs send fibers through the posterior optic tract (POT) to the contralateral Me and arborize on the surface of the ipsilateral Me, whereas the sLN_vs project into the ipsilateral dorsal protocerebrum. Anti-period (PER) staining revealed six clock neurons in the dorsal-lateral brain (LN_d) as well as three neuron clusters in the dorsal brain (DN1, DN2, and DN3). The DN1 cluster can be further divided into two anterior neurons (DN1_a) and about 15 posterior neurons (DN1_p). A fifth PDF⁻ sLN_v per hemisphere and three lateral posterior neurons (LPN) were discovered later. The fifth sLN_v as well as one LN_d contain the neuropeptide ion transport peptide (ITP; Johard et al., 2009). CRY is expressed in all LN_ds, in three LN_ds, in both DN1_a, and in about six DN1_p (Yoshii et al., 2008). dH, Dorsal horn; vaMe, ventral dendritic elongation of the aMe.

that the observed behavior might indeed be attributed to the lack of PDF in these pacemaker cells. Considering differences in the flies' endemic habitats, the authors suggest that both species have evolved unique circadian clock systems that are most advantageous for their environment. In the case of *D. virilis* flies, a reduction of the morning activity is advantageous, because morning temperatures are rather low in their habitats.

The same would be true for other members of the *Drosophila* genus. For example, *D. yakuba*, which is distributed in more equatorial regions with only little fluctuation in temperature throughout the year, exhibits two activity peaks similarly to *D. melanogaster*, but, unlike the case in

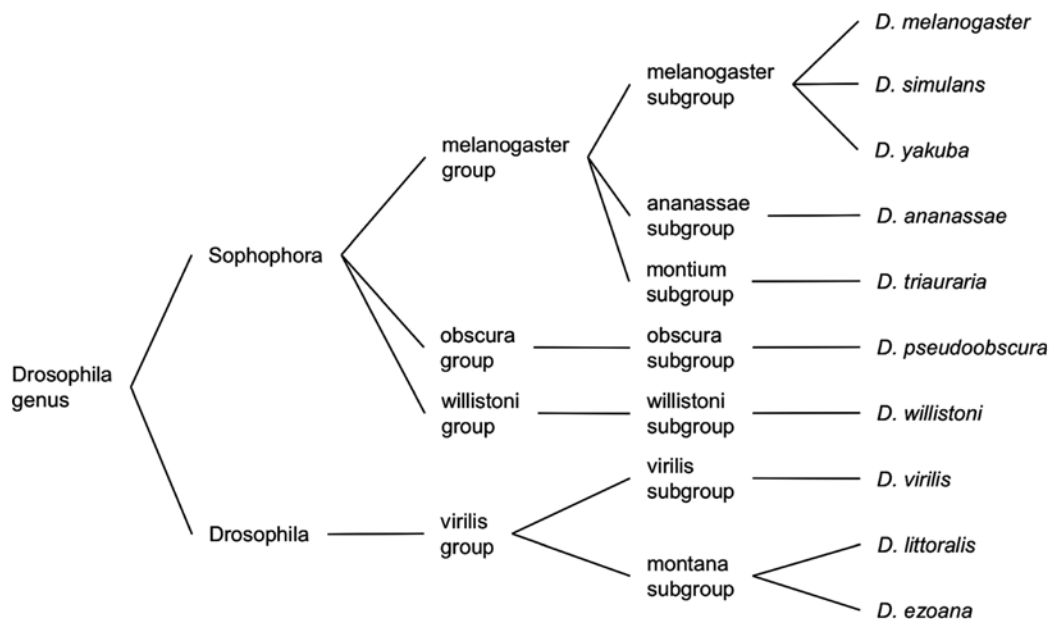


Figure 2. Phylogenetic relationship between all investigated *Drosophila* species according to Flybase (www.flybase.org). The *Drosophila* genus is divided into two subgenera, *Sophophora* and *Drosophila*. *D. melanogaster*, *D. simulans*, and *D. yakuba* are part of the melanogaster subgroup, which belongs to the melanogaster group in the *Sophophora* genus. *D. ananassae* from the ananassae subgroup and *D. triauraria* from the montium subgroup are also part of the melanogaster group. *D. pseudoobscura* is part of the obscura group, which is located between the melanogaster group and the willistoni group, with *D. willistoni* as one of its members. From the *Drosophila* subgenus we investigated *D. virilis* of the virilis subgroup and *D. ezoana* and *D. littoralis* of the montana subgroup. Lines do not represent phylogenetic distances.

D. melanogaster, the phases of the two peaks are rather insensitive to the ambient temperature level (Low et al., 2008), suggesting that the flies never had the need to adapt to temperature fluctuations and thus did not evolve this capability. The northern species, *D. littoralis*, *D. ezoana*, and *D. triauraria*, exhibit photoperiodic diapause, a physiological adaptation to the long and cold winters, which is not present in the southern species (Lankinen and Forsman, 2006; Yamada and Yamamoto, 2011). A comparison of mating activity times revealed even small differences between flies living in similar moderate habitats as *D. simulans*, *D. ananassae* and *D. melanogaster* (Sakai and Ishida, 2001; Nishinokubi et al., 2006). Thus, the different species display different circadian life styles, and the question arises of whether there is any correlation between differences in clock network morphology and changed circadian behavior, as was shown previously for *D. virilis*.

To gain a broader insight into the conservation of the clock system in different *Drosophila* species, we first compared the amino acid sequences of canonical core clock proteins as well as of the blue-light photoreceptor cryptochrome (CRY) and of the two neuropeptides PDF

and ITP in silico. Then we compared the clock network of nine *Drosophila* species with that of *D. melanogaster* by antibody staining against the clock proteins vriille (VRI) and PAR-domain protein 1 (PDP1), which are expressed in all clock neurons in *D. melanogaster* (Blau and Young, 1999; Reddy et al., 2000; Cyran et al., 2003; Glossop et al., 2003) and against CRY, which is expressed in most clock neurons of *D. melanogaster* (Yoshii et al., 2008; Benito et al., 2008). In addition, we examined the neuropeptide expression pattern by using antibodies against PDF and ITP.

MATERIALS AND METHODS

Fly strains

For immunohistochemistry, we used the *D. melanogaster* wild-type strain *Canton S* and nine other wild-type strains of the *Drosophila* genus, which we obtained mostly from the University of California San Diego *Drosophila* Species Stock Center (DSSC). We tried to choose species that are as representative as possible for the two subgenera *Drosophila* and *Sophophora* (Fig. 2), and we decided on species with already fully or at least partly

TABLE 1.
Primary Antibodies

Antibody	Immunogen	Donor animal, dilution
Anti-CRY	Polyhistidine fused full-length <i>Drosophila</i> (d) CRY expressed in <i>E. coli</i>	Rabbit polyclonal, 1:1,000
Anti-ScgITP-C1	Gly-extended peptide of short ScgITP (GGGDEEEKFNQ)	Rabbit polyclonal, 1:4,000
Anti-βPDH	βPDH conjugated to bovine thyroglobulin (NSELINSILGLPKVMNDAamide)	Rabbit polyclonal, 1:2,000
Anti-PDP1	GST-fused bacterially purified PDP1α	Rabbit polyclonal, 1:1,000
Anti-VRI	Histidine fused VRI (coding region) expressed in Sf9 insect cells	Guinea pig polyclonal, 1:3,000

sequenced genomes. All fly strains were reared on standard cornmeal/agar medium with yeast at 18° C. *Drosophila simulans* (DSSC; collection site (c.s.): Trento, Italy), *Drosophila yakuba* (DSSC; c.s.: Ivory Coast), *Drosophila ananassae* (DSSC; c.s.: Tamazunchale, San Luis Potosi, Mexico), *Drosophila triauraria* (DSSC; c.s.: Tokyo, Japan), *Drosophila pseudoobscura* (kindly donated by Stephan Schneuwly, University of Regensburg, Regensburg, Germany; unknown c.s.), *Drosophila willistoni* (DSSC; c.s.: Santa Maria de Ostuna, Nicaragua), *Drosophila virilis* (DSSC; unknown c.s.), and *Drosophila littoralis* (kindly donated by Anneli Hoikkala (University of Jyväskylä, Jyväskylä, Finland; c.s.: Viitasaari, Finland) were kept on a light-dark cycle of 12:12 hours (LD 12:12), whereas *Drosophila ezoana* (kindly donated by Anneli Hoikkala; c.s.: Oulanka, Finland) was reared in long photoperiods (LD 20:04) or constant light to avoid diapause. Male flies at the age of 4–7 days after eclosion were used for immunohistochemistry.

In silico clock protein and neuropeptide sequence analysis

All *D. melanogaster* sequences were obtained from Flybase, FB2012_02 (<http://flybase.org/>). Based on the annotated protein database and the blastp program in Flybase, BLAST (<http://flybase.org/blast/>), we identified protein homologues for the fully or partially sequenced *Drosophila* species mentioned above. Protein sequences were then exported and aligned by the Clustal-W algorithm in GENTle V.1.9.4. (<http://gentle.magnusmanske.de/>). Sequence identities and similarities were calculated with SIAS (Sequence Identities And Similarities, April, 2008; <http://imed.med.ucm.es/Tools/sias.html>). We chose the PID₃ method, in which gaps are taken into account, for the identity calculation. For the similarity calculation, the standard parameters offered by SIAS were chosen, in which all positively charged amino acids (Arg, Lys, and His), all negatively charged amino acids (Asp and Glu), and all aliphatic amino acids (Val, Iso, and Leu) were considered as similar. Additionally the aromatic amino acids Phe, Tyr, and Trp, the polar amino acids Asn and Gln, and the small amino acids Ala, Thr, and Ser were treated as similar.

Because sequences for multiple potential isoforms of the different proteins and peptides are not characterized for the other *Drosophila* species, we always selected the most conserved *D. melanogaster* protein isoform for the identity and similarity analysis in cases in which *D. melanogaster* genes encoded for multiple protein isoforms. This selection was made with the help of phylogeny.fr, One Click analysis (<http://www.phylogeny.fr/>; Dereeper et al., 2008). In the case of the neuropeptides ITP and PDF, we used the amino acid sequence of the mature peptide for the identity and similarity analysis. The ITP isoform expressed in the brain, ITP-PE, has not been characterized in all *Drosophila* species, so the corresponding ITP-PE sequence and its mature form were extracted from the genomic regions of ITP. The analyzed sequences are as follows.

- *D. melanogaster* CRY-PA: GD19278-PA, GE25590-PA, GF16541-PA, GA17677-PA, GK13802-PA, GJ24000-PA
- *D. melanogaster* PER-PA: GF20905-PA, GK19903-PA, GJ16682-PA
- *D. melanogaster* TIM-PB: GD22753-PA, GE14857-PA, GF14670-PA, GA16835-PA, GK14675-PA, GJ17601-PA
- *D. melanogaster* VRI-PA: GD23334-PA, GE25380-PA, GF14387-PA, GA12711-PA, GK24157-PA, GJ17539-PA
- *D. melanogaster* PDP1-PC/PDP1-PD: GD13032-PA, GE20386-PA, GF24150-PA, GA28498-PA, GK10510-PA, GJ11425-PA
- *D. melanogaster* PDF-PA: GD18135-PA, GE10630-PA, GF18882-PA, GA19638-PA, GK11356-PA, GJ23022-PA
- *D. melanogaster* ITP-PE: GD11871, GE14416, GF13627, GA12379, GK19672, GJ20243

Characterization of primary antibodies

Information for all primary antibodies is summarized in Table 1. Polyclonal antiserum against *D. melanogaster* (d) CRY was generated by immunizing rabbits with a full-length *Drosophila* (d)CRY protein fused to a histidine tag and purified from *Escherichia coli* extracts. The antibody was first described by Yoshii et al. (2008) and was provided by Takeshi Todo (Osaka University, Osaka, Japan). The specificity of the antibody was proofed using the cry null mutant *cry^{out}*; no specific signal was detected in immunohistochemical staining of these flies.

The polyclonal antiserum against ITP (anti-ScgITP-C1) was raised against the Gly-extended peptide GGGDEEEKFNQ of the desert locust *Schistocerca gregaria* short ITP (ScgITP) coupled to keyhole limpet hemocyanin (Ring et al., 1998). Part of this peptide sequence is the so-called C1 fragment, a specific octapeptide of *Schistocerca gregaria* ITP (DEEEKFNQ, ScgITP-C1). The antiserum specifically recognized ScgITP on Western blots of desert locust corpora cardiaca extracts (Ring et al., 1998) and *Drosophila* ITP in Western blots of both *Drosophila* third-instar larval CNS/ring gland extracts and adult brain/retrocerebral complex extracts. It further reliably recognized a high-performance liquid chromatography (HPLC)-purified fraction containing short, amidated DmITP, as confirmed by mass spectrometry (Dirksen et al., 2008). Controls were performed by preabsorption with the sequences DEEEKFNQ or GGGDEEEKFNQ (Dirksen et al., 2008). Neurons labeled with the ScgITP-C1 antiserum were shown by in situ hybridization also to coexpress the ITP precursor transcript (Dirksen et al., 2008). The ITP antiserum was raised in rabbits and was generously provided by John E. Phillips (Vancouver, British Columbia, Canada) and Neil Audsley (CSL Sand Hutton, York, United Kingdom).

For PDF staining of all species except for *D. pseudoobscura*, we used a commercially available monoclonal anti-PDF serum (anti-PDF No. C7), which we obtained from the Developmental Studies Hybridoma Bank at the University of Iowa (DSHB; investigator: Justin Blau, New York University) and which was developed under the auspices of the NICHD. The antibody was raised after immunizing balb/c mice with the amidated *Drosophila* PDF peptide (NSELINSLLSLPKNMNDA-NH₂) by PickCell Laboratories B.V. (Amsterdam, The Netherlands; Cyran et al., 2005). The antibody reliably labels only PDF⁺ neurons in both adults and larvae. No staining is observed in *Pdf⁰¹* mutants.

PDF staining in *D. pseudoobscura* was conducted with a polyclonal antibody against *Uca pugilator* β PDH raised in rabbits. The antibody was generated against a synthetic β PDH (NSELINSILGLPKVMNDAamide) conjugated to bovine thyroglobulin via glutaraldehyde (Dirksen et al., 1987). This antibody was shown to stain PDF⁺ neurons reliably in *D. melanogaster* (see, e.g., Helfrich-Förster and Homberg, 1993). No staining was observed in *Drosophila melanogaster Pdf⁰¹* mutants.

The PDP1 α protein served as an antigen to produce the polyclonal anti-PDP1 serum, which was first described by Cyran et al. (2003) and was generously donated to us by Justin Blau. A recombinant GST-PDP1 α fusion protein after purification from bacteria was used by Covance Research Products (Denver, CO) to immunize rabbits. Specificity of the antiserum was demonstrated by Cyran

et al. (2003), showing that in-vitro-translated PDP1 protein is recognized by anti-PDP1 and that no PDP1 immunoreactivity was observed in homozygous *Pdp1^{P205}* larval pacemaker cells.

The anti-VRI serum was described by Glossop et al. (2003). For antibody generation, the coding region of VRI was first amplified from a *vri* EST clone (GenBank accession No. AI404327). Then the fragment was cloned into a pBlueBac4.5/V5-His-TOPO vector (Invitrogen, Carlsbad, CA), and the sequence was verified. After recombination into Bac-N-Blue viral DNA, Sf9 insect cells were transfected with the Bac-N-Blue VRI recombinants to produce VRI protein. Guinea pigs were then injected with purified VRI for antibody production (Cocalico Biological, Burlington, NC). Cyran et al. (2003) demonstrated the specificity of the antibody, showing that anti-VRI recognized in-vitro-translated VRI protein and that it reliably detected overexpression of *vri* with *tim(UAS)-Gal4*. The antibody was kindly provided by Paul E. Hardin (Texas A&M University).

Immunohistochemistry

Immunostaining was conducted on male adult brains. For VRI and PDP1 staining, flies were entrained to an LD 12:12-hour (500 lux) cycle at 20°C for at least 4 days and were collected 5 hours before lights-on (zeitgeber time [ZT] 19), a time at which clock protein staining is high and confined to the nucleus in *D. melanogaster* (Cyran et al., 2003). CRY staining was conducted after keeping the flies in constant darkness for 72 hours. Flies were fixed in 4% paraformaldehyde (PFA) in phosphate buffer (PB; 0.1 M; pH 7.4) with 0.1% Triton X-100 on a shaker in complete darkness at room temperature. Fixation times differed according to the flies' body size: *D. melanogaster*, *D. simulans*, *D. yakuba*, *D. ananassae*, and *D. willistoni* were fixed for 2.5 hours; *D. triauraria* and *D. pseudoobscura* for 3 hours; and *D. virilis*, *D. ezoana*, and *D. littoralis* for 4 hours. After fixation, the flies were washed three times in PB for 15 minutes and were dissected in PB. Five percent normal goat serum (NGS) in PB with 0.5% Triton X-100 was applied onto the brains as blocking solution at 4°C overnight. We subsequently incubated the brains in the primary antibody solution for 48 hours at 4°C. Primary antibodies were used in the following concentrations in PB with 5% NGS and 0.5% Triton X-100: anti-VRI 1:3,000, anti-PDP1 1:1,000, anti-CRY 1:1,000, anti-ScgITP-C1 1:4,000, anti-PDF 1:1,000, and anti- β PDH 1:2,000. After six washes in PB with 0.5% Triton X-100 for 10 minutes, secondary antibodies were applied in a dilution of 1:200 in PB with 5% NGS and 0.5% Triton X-100, and the brains were incubated for 3 hours at room temperature. We used fluorescence-conjugated Alexa Fluor antibodies (Molecular Probes, Carlsbad, CA) of 488 nm (goat anti-guinea pig, goat anti-rabbit), 532 nm (goat anti-rabbit,

TABLE 2.
Cryptochrome (CRY) and Neuropeptide (PDF, ITP) Protein Sequence Homologies (%) of Different *Drosophila* Species in Comparison With *D. melanogaster*

<i>Drosophila</i>	CRY-PA		PDF ¹		ITP ¹	
	Identity	Similarity	Identity	Similarity	Identity	Similarity
<i>simulans</i>	98.34	99.08	100	100	100	100
<i>yakuba</i>	96.5	97.97	100	100	100	100
<i>ananassae</i>	86.94	92.83	100	100	98.67	100
<i>triantaria</i>	n/a ²	n/a	n/a	n/a	n/a	n/a
<i>pseudoobscura</i>	84.92	90.62	88.89	100	100	100
<i>willistoni</i>	81.25	86.21	100	100	97.33	100
<i>virilis</i>	82.53	87.68	100	100	96	100
<i>ezoana</i>	n/a	n/a	n/a	n/a	n/a	n/a
<i>littoralis</i>	n/a	n/a	n/a	n/a	n/a	n/a

¹Identity and similarity were calculated for the mature peptide.

²n/a, Sequence not available.

goat anti-mouse), and 635 nm (goat anti-mouse). Brains were washed again six times in PB with 0.5% Triton X-100 for 10 minutes and were afterward embedded in Vectashield medium (Vector Laboratories, Burlingame, CA) and mounted on glass slides, all in the same orientation.

Microscopy and image analysis

We performed laser scanning confocal microscopy to analyze immunofluorescent brains (Leica TCS SPE; Leica, Wetzlar, Germany). Confocal stacks of 2 μ m thickness were obtained. We sequentially used three or two different diode laser lines for triple (488, 532, and 635 nm) and double (488 and 532 nm) immunolabeling, respectively, to excite the fluorophores of the secondary antibodies. To quantify the number of stained neurons, the hemispheres of seven to 13 brains were analyzed for each strain, and cell numbers were averaged for each brain and across fly strains. Complete confocal stacks were displayed in Leica Application Suite Advanced Fluorescence Lite Software (LAS AF Lite, 2.2.1 build 4842), and cells were counted in investigating single optical sections of each stack. Stacks were cropped and overlays were generated in the ImageJ distribution Fiji (<http://fiji.sc/wiki/index.php/Fiji> or <http://rsb.info.nih.gov/ij/>). We adjusted brightness and contrast and occasionally flipped an image on the horizontal axis to depict corresponding hemispheres. We performed no other manipulations of the images.

RESULTS

In silico analysis of clock protein sequences in different *Drosophila* species

To gain an idea of the evolutionary conservation of different clock proteins, we tested the extent to which amino acid sequences of the core clock proteins period (PER), timeless (TIM), VRI, and PDP1, as well as CRY and the neuropeptides PDF and ITP, are conserved in different

Drosophila species in comparison with sequences of *D. melanogaster*. In general, proteins and peptides of flies belonging to the *Sophophora* subgenus showed higher sequence similarities to *D. melanogaster* than those of flies belonging to the *Drosophila* subgenus. In particular, we found that CRY, PDF, and ITP are highly conserved in both subgenera, *Sophophora* and *Drosophila* (Table 2). Among the core clock proteins, both TIM and PDP1 are well conserved (Table 3), although not as well as CRY (Table 2). VRI seemed to be moderately well conserved (Table 3). Surprisingly, conservation of PER was rather low (Table 3). The complete PER sequence was not even found in all species of the *Sophophora* genus, including *D. melanogaster*'s closest relatives, *D. simulans* and *D. yakuba*.

Anti-VRI, anti-PDP1, and anti-CRY staining reveals clusters of clock neurons in different *Drosophila* species

VRI and PDP1 antibodies consistently labeled neurons in the lateral and dorsal protocerebrum of all *Sophophora* species except for *D. pseudoobscura* but were less reliable in the *Drosophila* subgenus (Table 4). The stained neurons largely resembled the clock neurons of *D. melanogaster* in number and location, and staining was similarly strong and restricted to the nucleus of the cells (no neuronal projections were stained by the antibodies). For species in which VRI and PDP1 antibodies worked, we did not observe single-stained neurons, but only neurons double labeled with both VRI and PDP1. Therefore, we named the stained cell clusters according to the appropriate nomenclature of the clock neuron clusters in *D. melanogaster* (Fig. 1). CRY expression was also similar throughout the whole *Drosophila* genus and overlapped with VRI and PDP1 staining in most subsets of lateral and dorsal neurons that had previously been described for *D. melanogaster* to be CRY⁺. Only the species of the

TABLE 3.
Core Clock Protein Sequence Homologies (%) of Different *Drosophila* Species in Comparison With *D. melanogaster* Proteins

<i>Drosophila</i>	PER-PA		TIM-PB		VRI-PA		PDP1 ¹	
	Identity	Similarity	Identity	Similarity	Identity	Similarity	Identity	Similarity
<i>simulans</i>	n/a ²	n/a	97.83	98.16	98.72	98.72	93.29	94.05
<i>yakuba</i>	n/a	n/a	94.02	95.33	97.97	98.72	93.01	93.26
<i>ananassae</i>	74.29	78.07	88.44	92.38	83.93	86.8	80.65	82.55
<i>triantaria</i>	n/a	n/a	n/a	n/a	n/a	n/a	n/a	n/a
<i>pseudoobscura</i>	n/a	n/a	66.25	71.96	75.85	78.4	85.16	86.4
<i>willistoni</i>	69.54	74.32	77.08	81.94	67.97	71.38	77.43	79.55
<i>virilis</i>	59.46	65.33	72.16	77.67	61.38	66.27	73.19	75.47
<i>ezoana</i>	n/a	n/a	n/a	n/a	n/a	n/a	n/a	n/a
<i>littoralis</i>	n/a	n/a	n/a	n/a	n/a	n/a	n/a	n/a

¹Highest sequence homology value to either *D. melanogaster* PDP1-PC or PDP1-PD.

²n/a, Sequence not available.

TABLE 4.
VRI, PDP1, and CRY Immunoreactivity in Adult *Drosophila* Brains

<i>Drosophila</i>		Average cell numbers per hemisphere ± SD								
		sLN _v	ILN _v	5.sLN _v	LN _d	DN1 _a	DN1 _p	DN2	DN3	LPN
<i>melanogaster</i>										
n ¹ = 10	VRI	3.9 ± 0.3	3.3 ± 0.6	1.0 ± 0	5.9 ± 0.2	1.8 ± 0.3	13.9 ± 0.6	2.0 ± 0.2	>50	3.1 ± 0.2
n = 10	PDP1	3.9 ± 0.3	3.3 ± 0.6	1.0 ± 0	5.0 ± 0.2	1.8 ± 0.3	13.9 ± 0.6	2.0 ± 0.2	>50	3.1 ± 0.2
n = 11	CRY	3.8 ± 0.3	3.5 ± 0.4	1.0 ± 0.2	3.0 ± 0.2	1.9 ± 0.2	5.7 ± 0.3	0 ± 0	0 ± 0	0 ± 0
<i>simulans</i>										
n = 12	VRI	4.0 ± 0	4.1 ± 0.3	1.0 ± 0.1	5.8 ± 0.3	1.9 ± 0.2	13.8 ± 0.7	1.9 ± 0.2	>50	3.0 ± 0
n = 12	PDP1	4.0 ± 0	4.1 ± 0.3	1.0 ± 0.1	5.8 ± 0.3	1.9 ± 0.2	13.8 ± 0.6	2.0 ± 0.1	>50	3.0 ± 0
n = 13	CRY	3.7 ± 0.6	4.4 ± 0.7	1.1 ± 0.4	3.3 ± 0.5	1.9 ± 0.2	5.9 ± 0.5	0 ± 0	0 ± 0	0 ± 0
<i>yakuba</i>										
n = 10	VRI	3.9 ± 0.3	3.9 ± 0.3	0.9 ± 0.2	6.0 ± 0.2	2.0 ± 0.2	14.0 ± 1.0	1.9 ± 0.2	>50	3.7 ± 0.5
n = 10	PDP1	3.9 ± 0.3	3.9 ± 0.3	0.9 ± 0.2	6.0 ± 0.2	2.0 ± 0.2	14.0 ± 1.0	1.9 ± 0.2	>50	3.7 ± 0.5
n = 10	CRY	2.9 ± 0.7	4.0 ± 0.7	1.0 ± 0.4	2.9 ± 0.2	1.8 ± 0.4	6.1 ± 0.8	0 ± 0	0 ± 0	0 ± 0
<i>ananassae</i>										
n = 11	VRI	4.0 ± 0.2	3.1 ± 0.4	0.9 ± 0.3	5.5 ± 0.8	1.9 ± 0.2	11.0 ± 0.8	2.0 ± 0.2	>50	2.8 ± 0.5
n = 11	PDP1	4.0 ± 0.2	3.1 ± 0.4	0.9 ± 0.3	5.5 ± 0.8	1.9 ± 0.2	11.0 ± 0.8	2.0 ± 0.2	>50	2.8 ± 0.5
n = 12	CRY	3.6 ± 0.4	3.6 ± 0.4	1.0 ± 0.1	2.7 ± 0.5	1.9 ± 0.2	5.2 ± 0.8	0 ± 0	0 ± 0	0 ± 0
<i>triantaria</i>										
n = 12	VRI	4.0 ± 0.1	4.0 ± 0.3	1.0 ± 0	4.9 ± 1.2	1.9 ± 0.2	13.3 ± 0.8	1.8 ± 0.4	>50	3.0 ± 0.1
n = 12	PDP1	4.0 ± 0.1	4.0 ± 0.3	1.0 ± 0	4.9 ± 1.2	1.9 ± 0.2	13.3 ± 0.8	1.8 ± 0.4	>50	3.0 ± 0.1
n = 13	CRY	3.8 ± 0.4	4.8 ± 0.6	0.9 ± 0.3	4.7 ± 0.6	1.8 ± 0.2	6.5 ± 0.9	0 ± 0	0 ± 0	0 ± 0
<i>pseudoobscura</i>										
n = 11	VRI	n.d.	n.d.	n.d.	n.d.	n.d.	n.d.	n.d.	n.d.	n.d.
	PDP1	n.d.	n.d.	n.d.	n.d.	n.d.	n.d.	n.d.	n.d.	n.d.
	CRY	3.8 ± 0.3	0 ± 0	0.8 ± 0.1	2.8 ± 0.3	1.8 ± 0.3	6.0 ± 0.7	0 ± 0	0 ± 0	0 ± 0
<i>willistoni</i>										
n = 12	VRI	3.8 ± 0.2	3.5 ± 0.9	1.1 ± 0.3	5.9 ± 0.2	2.0 ± 0.1	12.3 ± 0.9	1.5 ± 0.4	>50	3.0 ± 0.1
n = 12	PDP1	3.9 ± 0.2	3.8 ± 0.6	1.1 ± 0.3	5.9 ± 0.2	2.0 ± 0.1	12.3 ± 0.9	1.5 ± 0.3	>50	3.0 ± 0.1
n = 12	CRY	3.8 ± 0.4	3.8 ± 0.8	1.2 ± 0.3	4.5 ± 1.0	1.8 ± 0.3	7.0 ± 0.5	1.0 ± 0.7	0 ± 0	0 ± 0
<i>virilis</i>										
n = 7	VRI	n.d.	n.d.	n.d.	n.d.	n.d.	n.d.	n.d.	n.d.	n.d.
n = 13	PDP1	3.9 ± 0.2	4.0 ± 0	0.9 ± 0.2	5.9 ± 0.2	2.0 ± 0	11.7 ± 1.2	n.d.	>50	4.2 ± 0.6
	CRY	4.0 ± 0.2	0 ± 0	0.9 ± 0.2	2.8 ± 0.5	1.8 ± 0.2	6.3 ± 0.9	0 ± 0	0 ± 0	0 ± 0
<i>ezoana</i>										
n = 8	VRI	n.d.	n.d.	n.d.	n.d.	n.d.	n.d.	n.d.	n.d.	n.d.
n = 13	PDP1	3.9 ± 0.2	4.0 ± 0.3	1.0 ± 0	n.d.	n.d.	n.d.	n.d.	n.d.	n.d.
	CRY	4.0 ± 0.1	0 ± 0	0.8 ± 0.3	3.0 ± 0.4	1.8 ± 0.2	5.6 ± 0.4	0 ± 0	0 ± 0	0 ± 0
<i>littoralis</i>										
n = 10	VRI	n.d.	n.d.	n.d.	n.d.	n.d.	n.d.	n.d.	n.d.	n.d.
	PDP1	n.d.	n.d.	n.d.	n.d.	n.d.	n.d.	n.d.	n.d.	n.d.
	CRY	4.0 ± 0.2	0 ± 0	1.0 ± 0.3	2.6 ± 0.3	1.9 ± 0.3	5.8 ± 0.5	0 ± 0	0 ± 0	0 ± 0

¹n, No. of brains; n.d., nondetectable.

Drosophila subgenus as well as *D. pseudoobscura* of the *Sophophora* subgenus completely lacked CRY staining in the ILN_vs. Below we describe the staining patterns in the *Sophophora* and *Drosophila* subgenera in detail.

Sophophora subgenus

VRI, PDP1, and CRY staining patterns revealed that the clock network of *D. simulans* is indistinguishable from that of *D. melanogaster*. From among these two, we therefore depict confocal images of only *D. simulans* (Figs. 1, 3A–H, Table 4). The other two members of the melanogaster subgroup, *D. yakuba* (Fig. 3I–P, Table 4) and *D. ananassae* (Fig. 3Q–X, Table 4), showed mostly the same VRI, PDP1, and CRY expression as *D. melanogaster* and *D. simulans*. For *D. yakuba*, we observed strong staining only in glial cells with both anti-VRI and anti-PDP1 and in addition four LPNs per hemisphere instead of three in comparison with the other members of the melanogaster subgroup. The staining pattern in *D. triauraria* was in general similar to that of the species of the melanogaster subgroup but revealed rather variable LN_d cell numbers and occasionally strong PDP1 staining in glial cells (Fig. 4A–H, Table 4). Belonging to the willistoni group, the less closely related *D. willistoni* showed mostly the same staining pattern as we had observed in the other species of the *Sophophora* subgenus (Fig. 4I–P, Table 4). The only noticeable difference was the weak VRI signal in the ILN_vs (Fig. 4K) in contrast to normal PDP1 staining (Fig. 4L). The only *Sophophora* species that we were not able to stain against VRI and PDP1 reliably was *D. pseudoobscura*. With respect to CRY, *D. pseudoobscura* showed the same expression pattern as the other *Sophophora* species, except that they completely lacked CRY in the ILN_vs (Fig. 5A–C, Table 4).

Drosophila subgenus

The anti-VRI serum did not stain any cells in species of the *Drosophila* subgenus (confocal images not shown). Staining with anti-PDP1 was detectable in all clock neuron clusters in *D. virilis* and in the LN_vs of *D. ezoana* but completely undetectable in *D. littoralis* and *D. pseudoobscura*. The CRY antibody, however, reliably labeled neurons in the lateral and dorsal protocerebrum in these flies (excluding the ILN_vs). For *D. virilis*, PDP1 staining revealed the presence of all lateral and dorsal clock neuron clusters, which we observed in the *Sophophora* subgenus (Fig. 5D,F,G,I,J, Table 4). CRY staining in *D. virilis* was also consistently present in most cells, except the ILN_vs (Figs. 5E,H,K, 8K,L, Table 4). For *D. ezoana*, a quantitative analysis of the PDP1 staining was possible only in the LN_v clusters (Fig. 5L,N,O, Table 4), which resembled the LN_vs of the *Sophophora* species. We occasionally found *D. ezoana* brains with rather clear staining also in the dorsal

clock neuron clusters (Fig. 5Q,R), but we were not able to quantify the number of cells. *D. ezoana* brains did not express CRY in the ILN_vs either, but otherwise CRY staining was consistent as in the other species (Figs. 5M,P,S, 9E,F, Table 4). Although neither anti-VRI nor anti-PDP1 labeled any cells in *D. littoralis*, the CRY antibody stained the same neurons as in the other species of the *Drosophila* subgenus (Fig. 9K–M, Table 4).

In summary, we revealed the consistent presence of lateral and dorsal clock neuron clusters as described for *D. melanogaster* in all species of the *Drosophila* genus, by VRI, PDP1 and CRY staining. In addition, we have shown that CRY staining differs among species, in that *D. pseudoobscura* and species of the *Drosophila* subgenus lack CRY in the ILN_vs.

PDF expression and arborization patterns differ within the *Drosophila* genus

Next, we investigated the PDF and ITP content within the clock neurons of the different species as well as the expression pattern of both peptides outside the clock neurons. To do so, we performed triple staining against PDF, ITP, and VRI or double staining against PDF and ITP or PDF and CRY. We found that the overall expression pattern of PDF is similar in all investigated species. However, species of the *Drosophila* subgenus and *D. pseudoobscura* lacked PDF in some sLN_v neurons. Occasionally, it was even completely absent in these cells. In addition, we identified new PDF⁺ cell clusters in *D. triauraria* and *D. pseudoobscura* and a different cell cluster in the species of the *Drosophila* subgenus. Staining in these cells did not overlap with PDP1 or CRY staining, indicating that these cells are not clock neurons (Figs. 5J,K,R,S, 9M). The PDF staining revealed several differences among the species in the arborization patterns of the clock neurons, which are described below.

PDF⁺ clock neurons in the *Sophophora* subgenus

As in *D. melanogaster* (Fig. 1), we found in all other investigated species four or five PDF⁺ ILN_vs per hemisphere (Table 5), which send projections through the posterior optic tract (POT) to the contralateral hemisphere and arborize in the distal medulla. The ILN_v cell bodies of all species were located in close proximity to the accessory medulla, a small neuropil at the ventromedial edge of the medulla. Furthermore, all three species of the melanogaster subgroup had on average four PDF⁺ sLN_vs per hemisphere, which project into the dorsal protocerebrum. The PDF expression pattern of *D. simulans* appeared in fact to be indistinguishable from that of *D. melanogaster* (Fig. 6A,E,F, Table 5). For *D. yakuba* (Fig. 6G), we

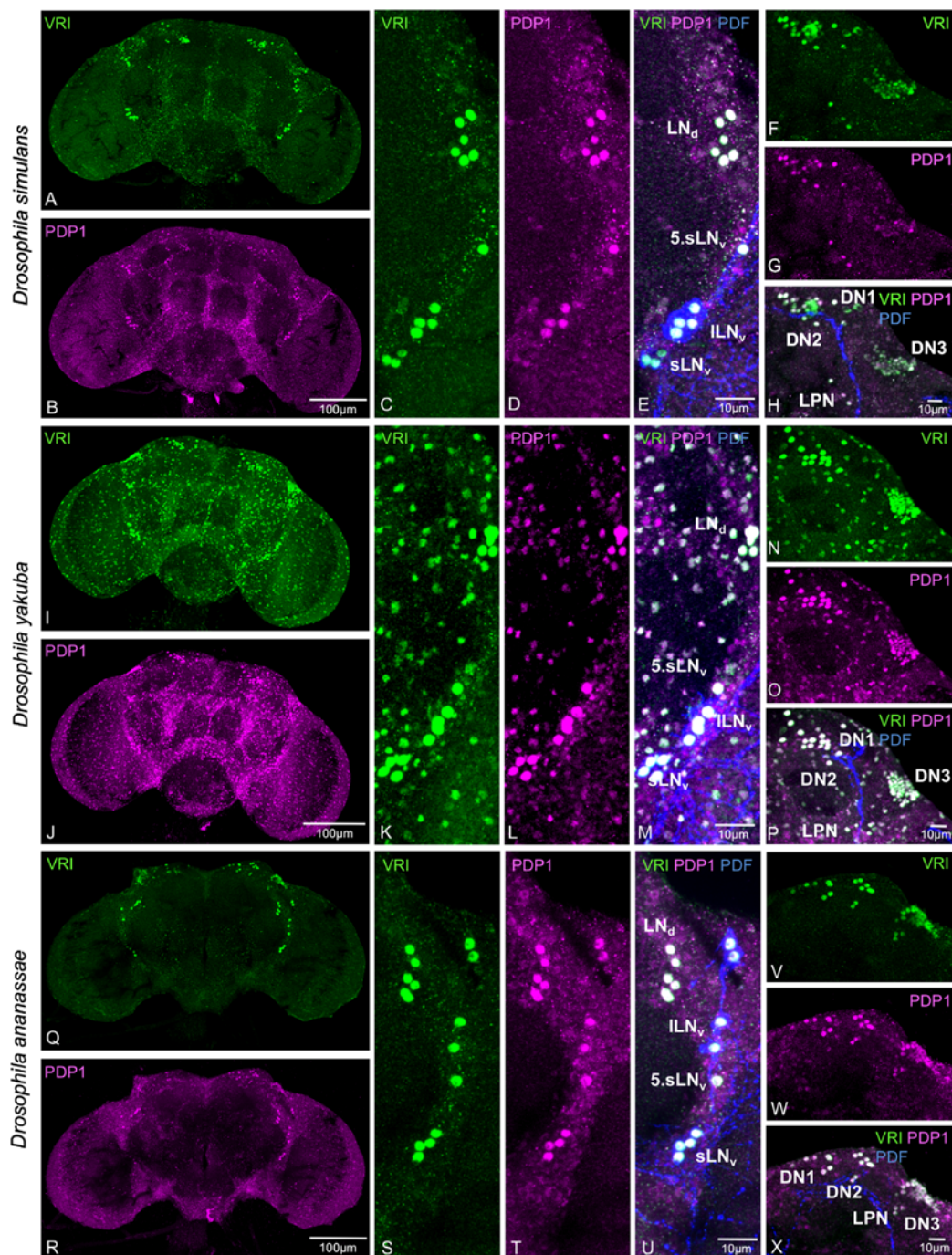


Figure 3. VRI, PDP1, and PDF expression in *D. simulans*, *D. yakuba*, and *D. ananassae*. To investigate the anatomy of the clock network, we stained male adult brains with anti-VRI (green), anti-PDP1 (magenta), and anti-PDF (blue) at ZT 19. *D. simulans* showed all clock neuron clusters with both anti-VRI (A) and anti-PDP1 (B) that are known from *D. melanogaster*. The LNs were present with the same cell numbers (C–E), as were the DNs (F–H). *D. yakuba* showed strong staining in glial cells with both anti-VRI (I) and anti-PDP1 (J) in addition to the staining in LN (K–M) and DN (N–P) clock neurons. VRI⁺ and PDP1⁺ LN and DN cell numbers in *D. ananassae* (S–U and V–X, respectively) were similar (see also Q and R). The fifth sLN_v can be distinguished in all three species, being PDF negative (E, M, U). Scale bars = 100 μm in B (applies to A, B); 10 μm in E (applies to C–E); 10 μm in H (applies to F–H); 100 μm in J (applies to J, I); 10 μm in M (applies to K–M); 10 μm in P (applies to N–P); 100 μm in R (applies to Q, R); 10 μm in U (applies to S–U); 10 μm in X (applies to V–X).

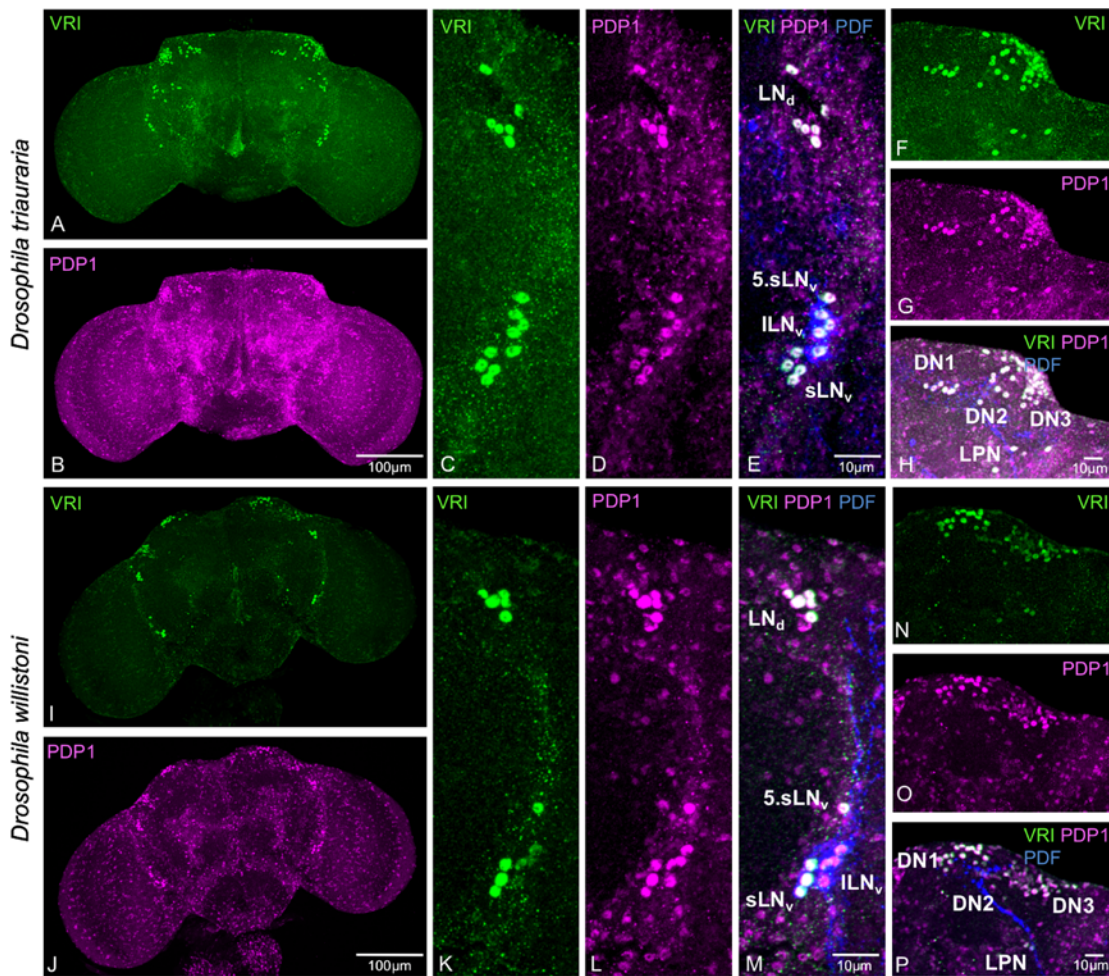


Figure 4. VRI, PDP1, and PDF expression in *D. triauraria* and *D. willistoni*. Anti-VRI (green) and anti-PDP1 (magenta) staining on male adult brains revealed that all known clock neuron clusters are present in *D. triauraria* (A,B) and *D. willistoni* (I,J). Anti-PDF (blue) labeled all LN_vs except for the fifth sLN_v in both species (*D. triauraria*, C–E; *D. willistoni*, K–M). All DN cell clusters were present as shown by anti-VRI and anti-PDP1 staining (*D. triauraria*, F–H; *D. willistoni*, N–P). Scale bars = 100 μ m in B (applies to A,B); 10 μ m in E (applies to C–E); 10 μ m in H (applies to F–H); 100 μ m in J (applies to J,I); 10 μ m in M (applies to K–M); 10 μ m in P (applies to N–P).

observed that the commissure through the POT formed by the ILN_v projection is clearly thicker than in *D. simulans* or *D. melanogaster*, and the dorsal projections of the sLN_vs lack their characteristic inwardly curved pathway in the dorsal brain (Fig. 6G, white arrow). In addition, the short branching extension of the sLN_v tract, the so-called dorsal horn, was clearly more pronounced in *D. yakuba* (Fig. 6G, yellow arrow) than in its sibling species (Fig. 6A, yellow arrow). *D. ananassae* was similar to the species of the melanogaster subgroup in PDF⁺ cell numbers (Fig. 7A,E,F, Table 5). However, in general, all PDF⁺ neuronal fibers, including the sLN_v tract to the dorsal brain, appeared thicker in this species, suggesting that maybe

also the ILN_vs send projections into the dorsal brain together with the sLN_vs (Fig. 7A).

The members of the montium and the obscura subgroups, *D. triauraria* and *D. pseudoobscura*, showed the most striking differences in the PDF expression pattern that we observed for the *Sophophora* subgenus. For *D. triauraria*, we found the same number of PDF⁺ sLN_vs (Fig. 7K,L, Table 5) as in the species of the melanogaster subgroup. There were, however, more varicose terminals stained in the dorsal brain, which derive probably mostly from the projection of these neurons (Fig. 7G, yellow arrow). In addition, we found multiple tangential PDF layers within the medulla deriving from ILN_v arborizations

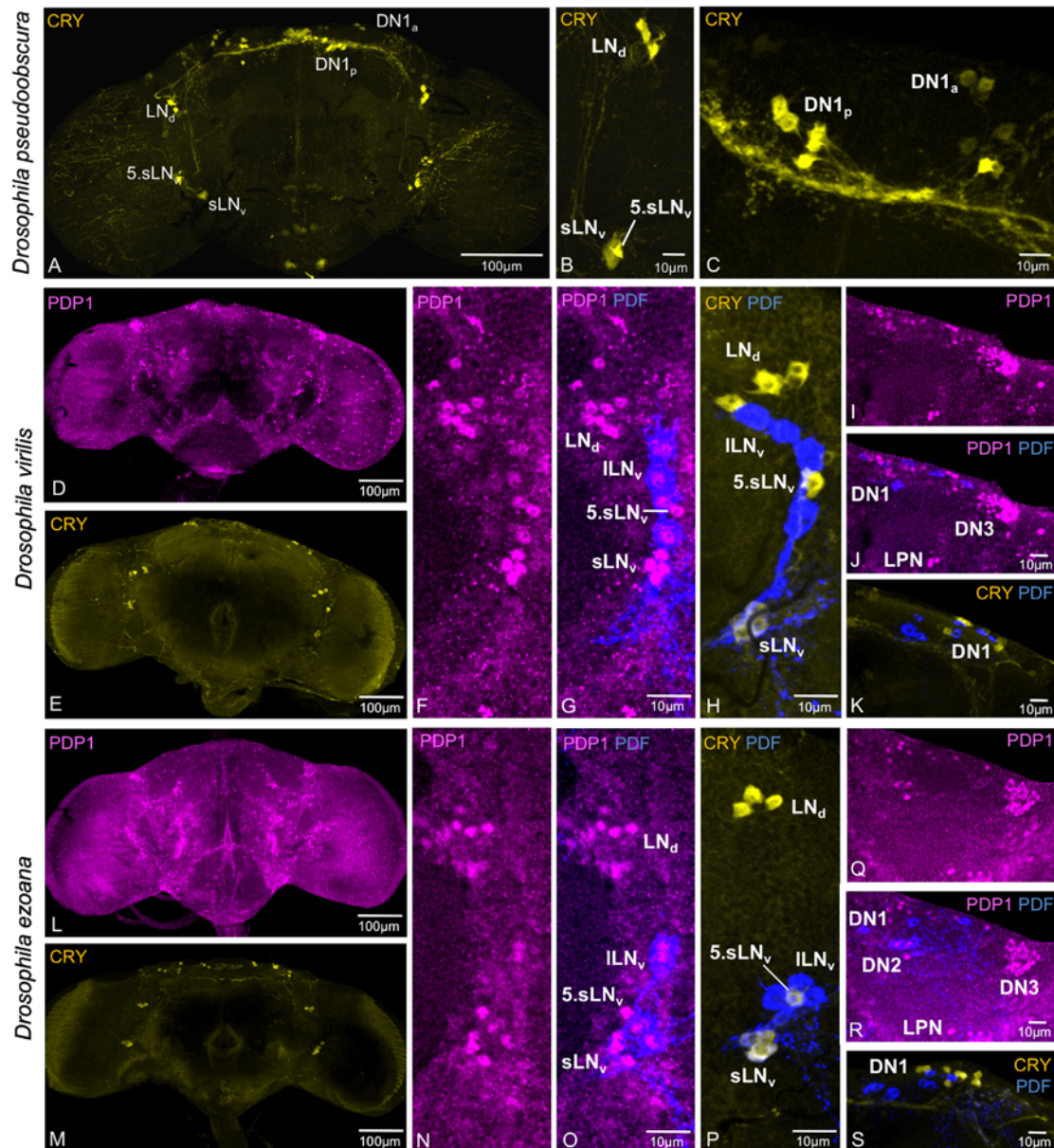


Figure 5. CRY, PDP1, and PDF expression in *D. pseudoobscura*, *D. virilis*, and *D. ezoana*. We performed CRY (yellow) single staining on *D. pseudoobscura* and anti-PDP1 (magenta)/anti-PDF (blue) and anti-CRY (yellow)/anti-PDF (blue) double staining on *D. virilis* and *D. ezoana*. CRY staining revealed lateral (A,B) and dorsal (A,C) clock neuron clusters in *D. pseudoobscura*. Anti-PDP1 staining showed that all clock neuron clusters are present in *D. virilis* (D). The LNs were present in normal cell numbers shown by anti-PDP1 (F,G) and anti-CRY staining (E,H). Anti-PDF staining allowed an identification of the fifth sLN_v, which is PDF⁻ (G,H). Except for the DN2, all DN clusters were stained with anti-PDP1 (I,J). Some DN1 neurons were CRY⁺ but different from the new cluster of PDF⁺ dorsal neurons (K). Anti-PDP1 staining attempts were only occasionally successful in *D. ezoana* (L). We found all LN clusters in normal cell numbers with anti-PDP1 (N,O), anti-CRY, and anti-PDF (M,P). Some brains showed PDP1 staining in all DN cell clusters (Q,R). CRY was present in a subset of the DN1, which was different from the newly identified PDF⁺ dorsal cell cluster (S). Scale bars = 100 μm in A,D,E,L,M; 10 μm in B,C,H,I,K,P,S; 10 μm in G (applies to F,G); 10 μm in J (applies to I,J); 10 μm in O (applies to N,O); 10 μm in R (applies to Q,R).

TABLE 5.

PDF Immunoreactivity in Adult *Drosophila* Brains

<i>Drosophila</i>	Average cell numbers per hemisphere \pm SD	
	sLN _v	ILN _v
<i>melanogaster</i> (n ¹ = 10)	3.6 \pm 0.6	4.0 \pm 0.4
<i>simulans</i> (n = 13)	3.7 \pm 0.6	4.4 \pm 0.7
<i>yakuba</i> (n = 10)	3.9 \pm 0.7	4.2 \pm 0.3
<i>ananassae</i> (n = 12)	3.6 \pm 0.4	3.7 \pm 0.3
<i>triauraria</i> (n = 13)	3.8 \pm 0.4	5.0 \pm 0.7
<i>pseudoobscura</i> (n = 13)	1.2 \pm 0.6	3.8 \pm 0.6
<i>willistoni</i> (n = 12)	3.8 \pm 0.4	4.6 \pm 0.4
<i>virilis</i> (n = 13)	1.7 \pm 2.0	4.0 \pm 0
<i>ezoana</i> (n = 13)	3.8 \pm 0.3	4.1 \pm 0.3
<i>littoralis</i> (n = 10)	2.1 \pm 1.5	4.1 \pm 0.3

¹n, No. of brains.

and additionally diffuse PDF staining in the lobula and in the antennal lobes (Fig. 7G, white arrows). In *D. pseudoobscura*, the monoclonal anti-PDF antibody only faintly stained PDF⁺ cell bodies and did not label any projections deriving from these neurons. Therefore, we utilized the polyclonal β -PDH antibody to stain PDF⁺ cells and fibers in this species. We found that only one (rarely two) of the four sLN_vs expressed PDF in *D. pseudoobscura* (Table 5, Fig. 7M). Surprisingly, *D. willistoni* as a member of the willistoni subgroup, which is more distantly related to *D. melanogaster*, was again more similar to the members of the melanogaster subgroup in both cell numbers and arborization pattern (Fig. 8A,E,F, Table 5). The latter was especially similar to *D. yakuba*, with its thick commissure through the POT and the shape of its dorsal sLN_v tract with pronounced terminals in the dorsal horn (Fig. 8A, white arrow).

PDF⁺ clock neurons in the *Drosophila* subgenus

PDF staining was very similar among the three investigated species of the *Drosophila* subgenus (Table 5, Figs. 8G, 9A,G) but revealed differences compared with the species of the *Sophophora* subgenus. The ILN_v arborizations in the medulla appeared less conspicuous than in the species of the *Sophophora* subgenus, more narrowly branched and located in deeper layers of the medulla. Interestingly, PDF immunostaining in the sLN_vs was reduced, ranging from a complete lack of PDF in these cells occasionally up to a normal number of four faintly stained PDF⁺ neurons (Table 5, note the large SD for *D. virilis* and *D. littoralis* sLN_vs; see Fig. 8I,J for *D. virilis* with only one PDF⁺ sLN_v, white arrow). This effect was not as pronounced in *D. ezoana* as in the other two species (Table 5). Again, CRY staining revealed that individuals with fewer PDF⁺ sLN_vs do not lack the neurons but simply do not express PDF in them (Figs. 8K,L [white arrow],

9E,F,K,L; see also PDP1 staining in sLN_vs of *D. virilis* in Fig. 5F,G and *D. ezoana* Fig. 5N,O). The PDF⁺ dorsal projection deriving from the sLN_vs was consequently less pronounced in the species of the *Drosophila* subgenus compared with the *Sophophora* subgenus (Figs. 8G, 9A,G, white arrows).

PDF⁺ nonclock neurons in both subgenera

For *D. triauraria* and *D. pseudoobscura* (*Sophophora* subgenus), we identified two new clusters of 10–15 PDF⁺ neurons per hemisphere in the central part of the brain, one being located more ventrally and the other one more dorsally (Fig. 7G,M, white arrowheads). We additionally detected PDF staining within the central complex in *D. pseudoobscura* (Fig. 7M, white arrow). For all three investigated species of the *Drosophila* subgenus, we identified one new cluster of PDF⁺ neurons, different from those of the *Sophophora* subgenus. It consists of about four to six cells per hemisphere, which are located in the dorsolateral brain above the calyces of the mushroom bodies (Figs. 8G, 9A,G, yellow arrows).

ITP expression is conserved within the clock neurons throughout the *Drosophila* genus

Triple staining of ITP, PDF, and VRI or double staining of ITP and PDF revealed that the ITP expression pattern is similar in all investigated fly species. The ITP neurons in *D. melanogaster* were divided into four subsets of neurons per hemisphere, four ipc-1, four ipc-2, three or four ipc-3, and two faintly stained ipc-4 neurons. Two neurons of the ipc-3 cluster are identical to clock neurons, the fifth sLN_v and one LN_d (Fig. 1). (Below we will refer to these two neurons as fifth sLN_v and LN_d and to the additional ipc-3 neurons as add.ipc-3 neurons.) ITP expression was especially well conserved within the two clock neurons and the four ipc-1 neurons (Table 6). The ITP antibody consistently labeled these cells in all investigated species. The staining in the other ipc clusters was not as consistent throughout the whole genus. We found less ITP⁺ neurons in the dorsal brain in the species more distantly related to *D. melanogaster*. Especially the species of the *Drosophila* genus more or less completely lacked ITP immunoreactivity in the dorsal ipc cell clusters (Table 6).

Detailed description of the ITP expression pattern

The ITP expression in *D. simulans* was identical to that in *D. melanogaster* (Fig. 6B). There were four very prominently stained ipc-1 neurons per hemisphere in a posterior dorsal or medial position, which project into central neuropils around the esophageal foramen. The fifth sLN_v as well as one LN_d were ITP⁺ (Fig. 6D,F, Table 6). Both

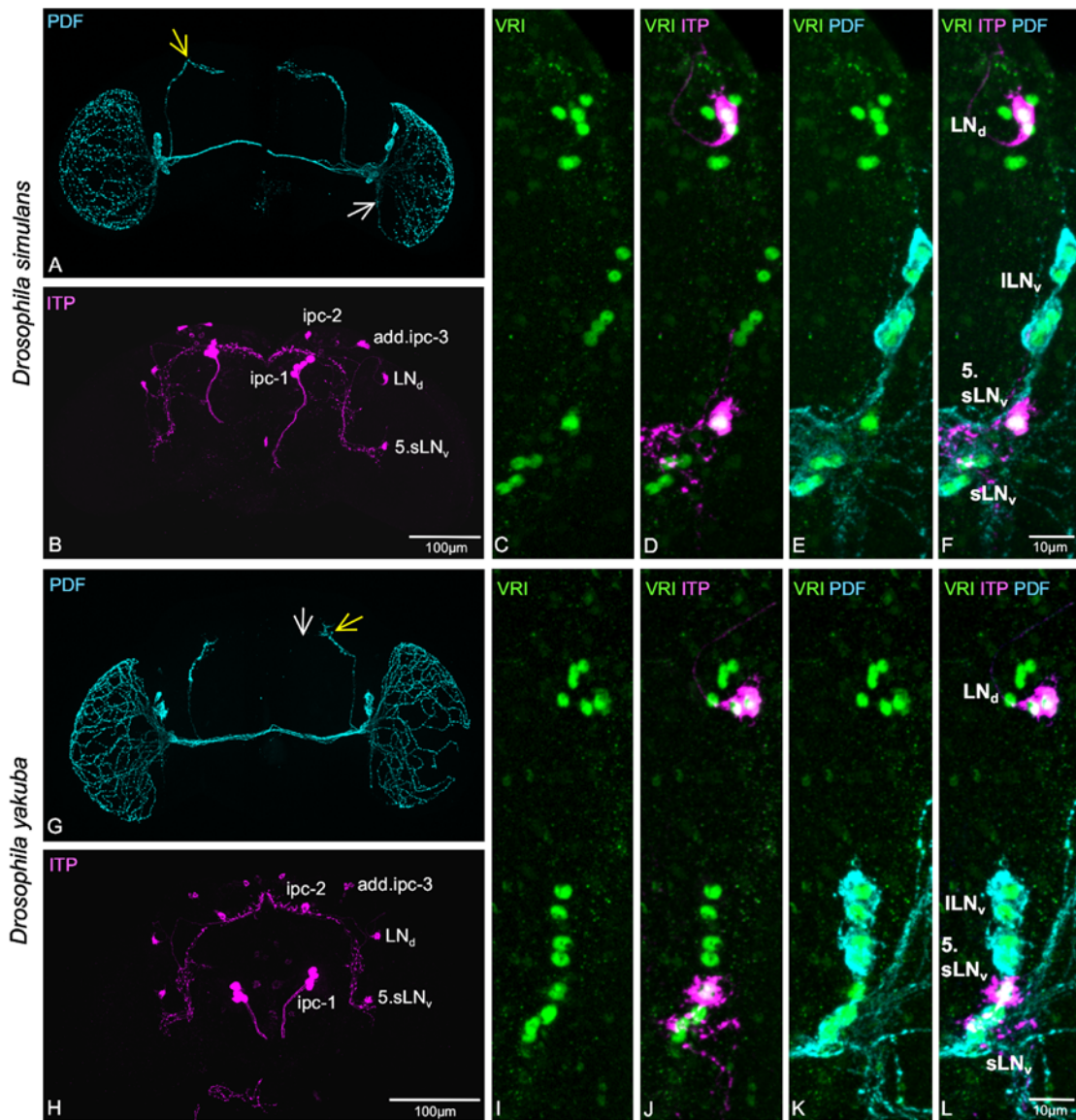


Figure 6. VRI, PDF, and ITP expression in *D. simulans* and *D. yakuba*. Male adult brains were triple stained with anti-VRI (green), anti-PDF (cyan), and anti-ITP (magenta). PDF and ITP expression in *D. simulans* was indistinguishable from that in *D. melanogaster* (A,B). PDF was present in all sLN_vs and ILN_vs but was absent in the fifth sLN_v, which was ITP⁺, with one ITP-expressing LN_d (C–F). The PDF neurons showed the same characteristic projection pattern as in *D. melanogaster* (A), i.e., ventral dendritic elongation of the accessory medulla (white arrow) and dorsal horn projections (yellow arrow). The PDF⁺ commissure through the POT in *D. yakuba* was more prominent than in *D. simulans*, and the dorsal projection of the sLN_vs was shaped differently from that in *D. melanogaster* (G, white and yellow arrows). ITP expression in *D. yakuba* and the peptide content within the LNs was similar to those in *D. simulans* (H–L). Scale bars = 100 μm in B (applies to A,B); 10 μm in F (applies to C–F); 100 μm in H (applies G,H); 10 μm in L (applies to I–L).

neurons send ITP⁺ fibers into the accessory medulla and branch in areas of the dorsal protocerebrum. ITP staining in the dorsal ipc clusters was also similar to that in *D. melanogaster* (Table 6). Except for more prominently stained neuronal fibers, *D. yakuba* showed the same ITP

expression pattern as its sibling species, *D. simulans* and *D. melanogaster* (Fig. 6H,J,L, Table 6). *D. ananassae* (Fig. 7B,D,F, Table 6), *D. triauraria* (Fig. 7H,J,L, Table 6), and *D. pseudoobscura* (Fig. 7N, Table 6) consistently showed ITP expression in the two clock neurons and the ipc-1

neurons. The *ipc-2* and *ipc-4* neurons were, however, reduced in number. In *D. willistoni*, all dorsal *ipc* neurons (*ipc-2*, *add.ipc-3*, and *ipc-4*) were mostly undetectable,

but *ipc-1*, fifth *sLN_v*, and *LN_d* were nicely stained (Fig. 8B,D,F, Table 6). *D. virilis* (Fig. 8H) and *D. ezoana* (Fig. 9B) of the *Drosophila* subgenus did not show any staining in

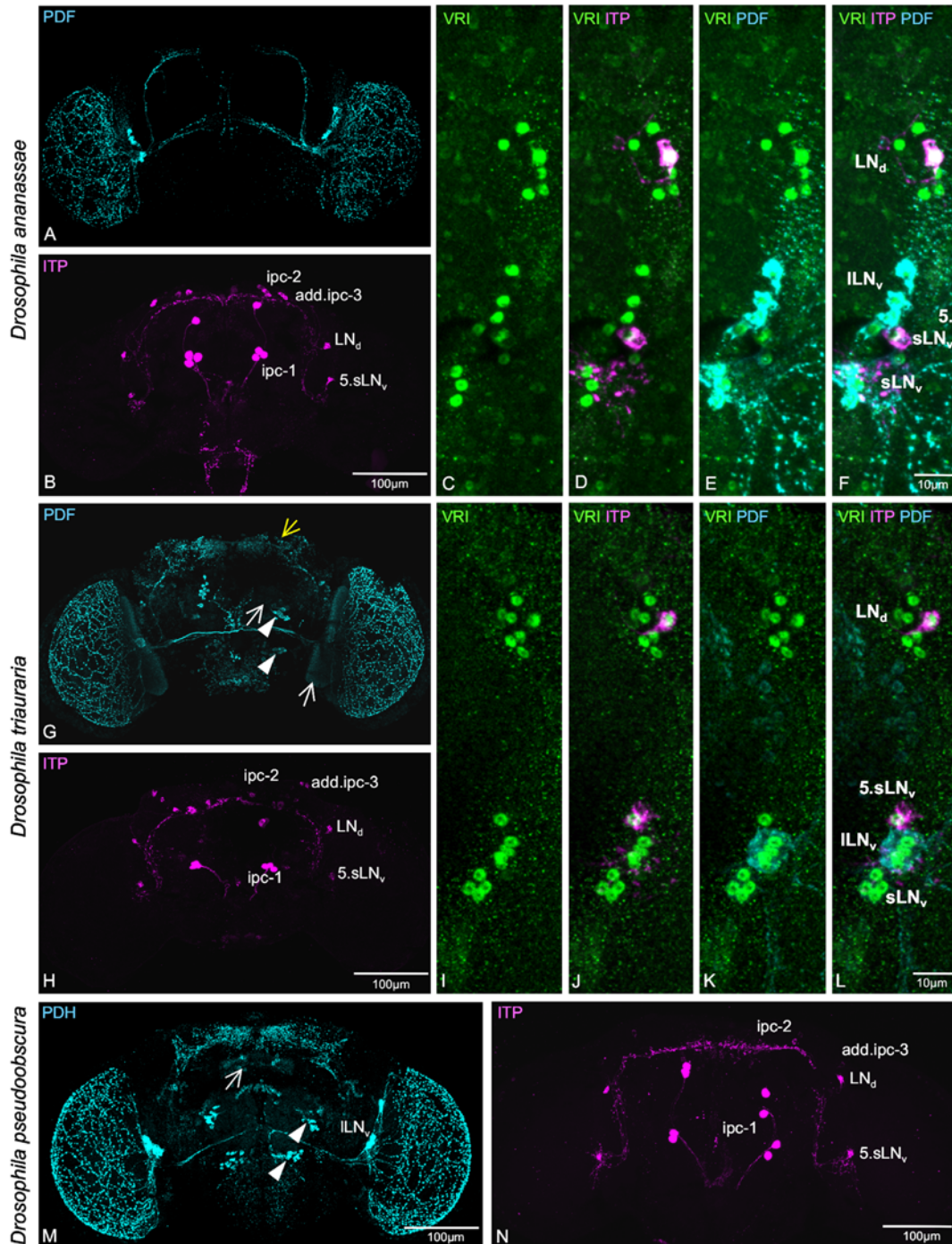


Figure 7

the dorsal ipc neurons (ipc-2, add.ipc-3, and ipc-4), but showed consistent staining in four ipc-1 neurons (Table 6). In addition, we found here two stained neurons in the lateral brain, which were both PDF⁻ (*D. virilis*, Fig. 8); *D. ezoana*, Fig. 9D, Table 6), indicating that, according to position and arborization pattern, these two neurons are identical to the fifth sLN_v and the LN_d, although counterstaining with a clock-neuron-specific antibody was not possible. We found the same expression pattern in *D. littoralis* (Fig. 9H,I) as in *D. ezoana*, but we occasionally observed ITP staining also in one ipc-2 or add.ipc-3 neuron (Fig. 9H, white arrow, Table 6).

DISCUSSION

This study compares sequences of different clock protein homologs and neuropeptide transmitters in silico as well as the morphology of the neuronal clock network of 10 different *Drosophila* species. We found that especially the neuropeptides ITP and PDF, but also the clock's photopigment CRY, are highly conserved in all *Drosophila* species. In contrast, the core clock proteins PER, VRI, and PDP1 seem to differ between the *Sophophora* and the *Drosophila* subgenera. This was most apparent for PER and less pronounced for PDP1. By PDP1 immunocytochemistry, we were able to reveal the clock neurons in all species and found that their number and location are highly conserved: all species had nine clusters of clock neurons distributed in the lateral and dorsal protocerebrum, as described in detail for *D. melanogaster* (Fig. 1; see, e.g., Helfrich-Förster et al., 2007). We further show that the expression of CRY in most species of the *Sophophora* subgenus also resembles the expression in *D. melanogaster* (Yoshii et al., 2008) but that flies of the *Drosophila* subgenus and *D. pseudoobscura* lack CRY within the ILN_s. Anti-PDF staining revealed the lack of PDF expression in some sLN_v clock neurons in species of the *Drosophila* subgenus and in *D. pseudoobscura*, which was previously shown for *D. virilis* by Bahn et al. (2009). In addition, we newly identified PDF⁺ cell clusters in some

of the species, which are not clock neurons. ITP expression within the fifth sLN_v and one LN_d was conserved throughout the whole *Drosophila* genus. We observed differences only in the number of ITP⁺ nonclock neurons. In general, expression patterns shown by the different antibodies were similar in all the species, indicating that our antibodies reliably labeled the proteins.

Gross anatomy of the clock neuron network is conserved within the *Drosophila* genus

To investigate the anatomical properties of the clock network in the different *Drosophila* species by immunohistochemistry, we searched for antibodies known for their specific labeling of all clock neuron clusters in *D. melanogaster* brains. We first applied antibodies against PER and TIM, but both completely failed to stain any cells in the other fly species (Hermann, Saccon, Helfrich-Förster, unpublished). Bahn et al. (2009) had previously reported the same for their anti-TIM serum. Failure of the PER antiserum is not surprising, considering the low PER conservation within the *Drosophila* genus, as revealed by our in silico analysis. Ousley et al. (1998) had previously shown a similar value for the conservation of the *D. virilis* PER in comparison with *D. melanogaster* PER. Despite the high overall level of similarity of the TIM protein within the *Drosophila* genus, differences in the protein region recognized by the anti-TIM serum may be crucial for the failure of the antibody to provide any staining results. Consequently, we switched to other clock-specific antibodies developed more recently and which are raised against larger parts of clock proteins, anti-VRI and anti-PDP1 (Reddy et al., 2000; Glossop et al., 2003). Both antibodies reliably labeled neuronal cells and some glial cells within the *Sophophora* subgenus, except in *D. pseudoobscura*, revealing the presence of all clock neuron clusters known from *D. melanogaster* in the different fly species. In general, we observed only minor differences in cell numbers of the different species compared with *D. melanogaster*. However, the anti-VRI serum completely failed to stain

Figure 7. VRI, PDF, and ITP expression in *D. ananassae*, *D. triauraria*, and *D. pseudoobscura*. Male adult brains of both *D. ananassae* and *D. triauraria* were triple stained with anti-VRI (green), anti-PDF (cyan), and anti-ITP (magenta), whereas *D. pseudoobscura* brains were separately stained with anti-β-PDH (cyan) and anti-ITP (magenta). Aside from thicker projections, the PDF expression pattern in *D. ananassae* resembled that in *D. simulans* (A). ITP was expressed in the fifth sLN_v, in one LN_d, and in dorsal ipc clusters (B–F). PDF expression in *D. triauraria* was different from that in *D. simulans* (G), showing diffuse staining in lobula and antennal lobes (G, white arrows) and several tangential PDF⁺ layers in the Me. We observed many varicose terminals in the dorsal brain (G, yellow arrow), and two new clusters of PDF⁺ neurons were present in each hemisphere (G, white arrowheads). Apart from a reduction in cell numbers in the dorsal ipc clusters, ITP expression was not different from that in *D. simulans* (H), as was the peptide expression in the LNs (I–L). PDF staining in *D. pseudoobscura* was similar to that in *D. triauraria*, revealing the presence of a new PDF⁺ cell cluster per hemisphere (M, white arrowheads). In addition, we observed PDF⁺ staining in the central complex (M, white arrow). ITP expression was consistent in the two lateral clock neurons as in the other species (N). Scale bars = 100 μm in B (applies to A,B); 10 μm in F (applies to C–F); 100 μm in H (applies G,H); 10 μm in L (applies to I–L); 100 μm in M,N.

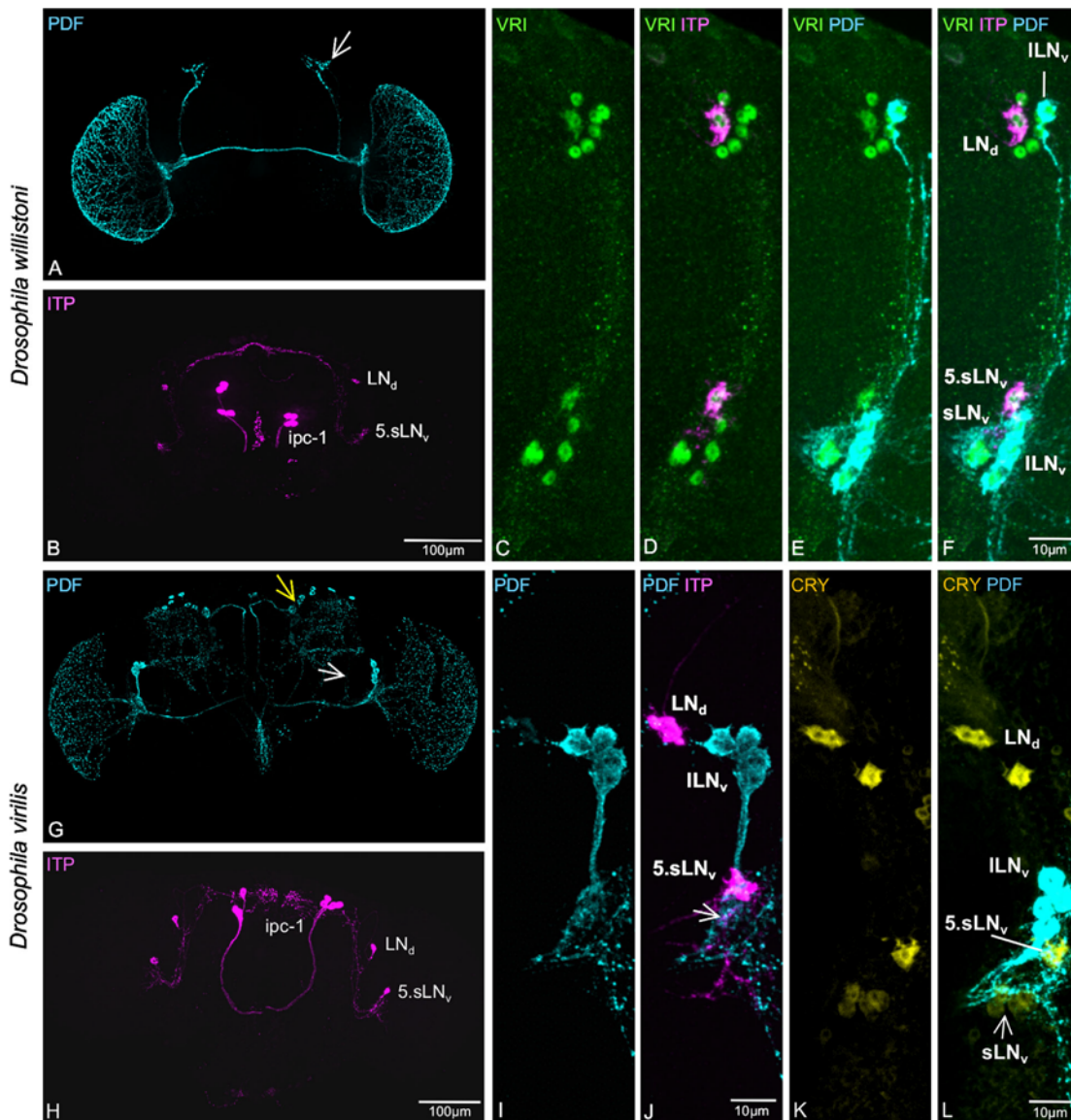


Figure 8. VRI, PDF, and ITP expression in *D. willistoni* and PDF, ITP, and CRY expression in *D. virilis*. Male adult brains of *D. willistoni* were triple stained with anti-VRI (green), anti-PDF (cyan), and anti-ITP (magenta). *D. virilis* brains were double stained with anti-PDF (cyan) and anti-ITP (magenta) and with anti-CRY (yellow) and anti-PDF (cyan). PDF expression of *D. willistoni* was very similar to that in *D. yakuba* (A, compare Fig. 6G), with prominent dorsal horn (A, white arrow) and thick fibers running through the POT. ITP was present in the fifth sLN_v and in one LN_d (B–F). We identified a new cluster of PDF⁺ neurons in the dorsal brain of *D. virilis* (G, yellow arrow). ITP was putatively expressed in the fifth sLN_v and one LN_d but was not found at all in the dorsal ipc clusters (H–J). PDF was expressed in a reduced number of sLN_vs, ranging from only one cell (I, J, white arrow) to the normal four cells. Consequently, the sLN_v tract to the dorsal brain was only weakly stained (G, white arrow). CRY staining proved the presence of all four CRY⁺ sLN_vs (K, L, white arrow). CRY was completely absent in all ILN_vs but was present in the fifth sLN_v and one LN_d (K, L). Scale bars = 100 μm in B (applies to A, B); 10 μm in F (applies to C–F); 100 μm in H (applies G, H); 10 μm in J (applies to I, J); 10 μm in L (applies to K, L).

any neurons in the *Drosophila* subgenus and in *D. pseudoobscura*, which probably is due to the relatively low sequence similarity of the VRI protein especially in the

Drosophila subgenus. In contrast, conservation of the PDP1 protein was higher within the whole genus, leading to a broader staining success with the PDP1 antiserum.

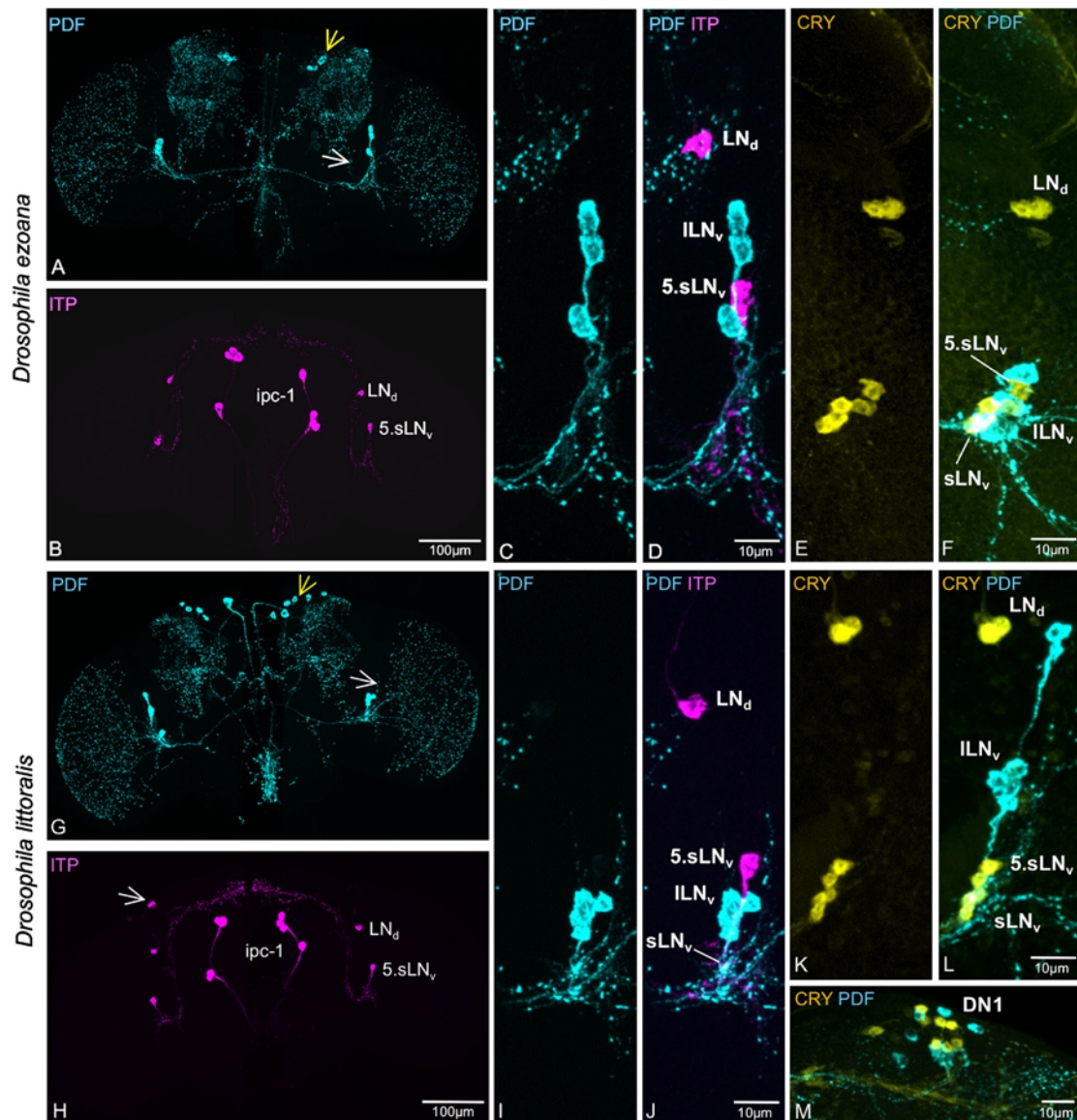


Figure 9. PDF, ITP, and CRY expression in *D. ezoana* and *D. littoralis*. Male adult brains of *D. ezoana* and *D. littoralis* were double stained with anti-PDF (cyan) and anti-ITP (magenta) and with anti-CRY (yellow) and anti-PDF (cyan). PDF expression in both species was similar to that in *D. virilis*, with a new PDF⁺ cell cluster in the dorsal brain (A,G, yellow arrow) and only weak staining in the sLN_v tract (A,G, white arrow). In *D. ezoana*, PDF was expressed in ILN_vs and in most cases in sLN_vs (C,D). ITP was absent in the dorsal ipc neurons (B) but was putatively expressed in the fifth sLN_v and one LN_d (C,D). PDF was irregularly expressed in the sLN_vs of *D. littoralis* (I,J), as was the case in *D. virilis* (compare Fig. 8J). ITP was present in the fifth sLN_v and one LN_d, as in the other species (H,I,J). Both *D. ezoana* (E,F) and *D. littoralis* (K,L) expressed CRY in four sLN_vs, in the fifth sLN_v, and in three LN_ds, but not in the ILN_vs. CRY staining showed the presence of the DN1 cell cluster in *D. littoralis* (M). Scale bars = 100 μm in B (applies to A,B); 10 μm in D (applies to C,D); 10 μm in F (applies to E,F); 100 μm in H (applies to G,H); 10 μm in J (applies to I,J); 10 μm in L (applies to K,L); 10 μm in M.

The antibody revealed that the different clock neuron clusters are present also in *D. virilis*. In *D. ezoana*, the antibody reliably labeled all LN cell clusters but only occasionally provided good staining in the other clock neuron

clusters. Because of these few exceptionally well-stained specimens, we are, nevertheless, convinced that the dorsal clock neuron clusters are also present in *D. ezoana*. Neither anti-VRI nor anti-PDP1 seemed to work properly

TABLE 6.
ITP Immunoreactivity in Adult *Drosophila* Brains

<i>Drosophila</i>	Average cell numbers per hemisphere \pm SD					
	5.sLN _v	ILN _d	ipc-1	ipc-2	add.ipc-3	ipc-4
<i>melanogaster</i> (n ¹ = 9)	1.0 \pm 0	1.0 \pm 0	4.0 \pm 0	3.9 \pm 0.5	1.8 \pm 0.3	3.2 \pm 1.6
<i>simulans</i> (n = 12)	1.0 \pm 0	1.0 \pm 0	4.0 \pm 0.2	3.4 \pm 0.5	1.8 \pm 0.6	0.8 \pm 0.8
<i>yakuba</i> (n = 14)	1.0 \pm 0.1	1.0 \pm 0.1	4.0 \pm 0.1	2.0 \pm 0.2	1.8 \pm 0.4	0.5 \pm 0.5
<i>ananassae</i> (n = 12)	1.0 \pm 0	1.0 \pm 0	4.0 \pm 0.3	1.6 \pm 0.7	1.6 \pm 0.5	0 \pm 0
<i>trauraria</i> (n = 14)	1.0 \pm 0	0.9 \pm 0.2	3.9 \pm 0.2	2.5 \pm 0.6	1.6 \pm 0.5	0 \pm 0
<i>pseudoobscura</i> (n = 14)	1.0 \pm 0.1	1.0 \pm 0.1	4.0 \pm 0	1.1 \pm 0.8	1.5 \pm 0.7	0.3 \pm 0.7
<i>willistoni</i> (n = 12)	1.0 \pm 0.1	1.0 \pm 0	4.0 \pm 0	0.6 \pm 0.5	0.7 \pm 0.7	0.4 \pm 1.0
<i>virilis</i> (n = 9)	0.9 \pm 0.2	1.0 \pm 0	3.9 \pm 0.2	0 \pm 0	0 \pm 0	0 \pm 0
<i>ezoana</i> (n = 10)	1.0 \pm 0	1.0 \pm 0	4.0 \pm 0.2	0 \pm 0	0 \pm 0	0 \pm 0
<i>littoralis</i> (n = 11)	0.9 \pm 0.2	1.0 \pm 0	4.0 \pm 0	0.2 \pm 0.4	0.1 \pm 0.3	0 \pm 0

¹n, No. of brains.

in *D. pseudoobscura* or *D. littoralis*. CRY staining, however, successfully labeled CRY⁺ putative clock neuron clusters in all investigated species. By this, we were able to detect subsets of lateral and dorsal clock neurons also in *D. pseudoobscura* and *D. littoralis*. Taking these results together, we conclude that the neuronal anatomy of the clock network is highly conserved throughout the *Drosophila* genus.

Clock network of different *Drosophila* species is modified by altered CRY and PDF expression

Within all investigated species of the *Sophophora* subgenus, except for *D. pseudoobscura*, CRY staining was remarkably similar to that in *D. melanogaster* (Fig. 1; Yoshii et al., 2008). Interestingly, we did not see any CRY staining in the ILN_vs in *D. pseudoobscura* or the species of the *Drosophila* subgenus. In *D. melanogaster*, the ILN_vs are assumed to be associated with the visual system and to be involved in coupling mechanisms between the pace-makers of the two hemispheres (Grima et al., 2004; Helfrich-Förster, 2004, 2005; Stoleru et al., 2004, 2005; Helfrich-Förster et al., 2007; Cao and Nitabach, 2008). Furthermore, the ILN_vs seem to modulate sleep and arousal in *D. melanogaster* (Parisky et al., 2008; Sheeba et al., 2008; Chung et al., 2009). Indeed, light-arousal and circadian-photoreception circuits appear to intersect at these neurons (Shang et al., 2008). CRY is crucially involved in the light input to the clock (Emery et al., 1998, 2000; Stanewsky et al., 1998; Ceriani et al., 1999; Rieger et al., 2003) and seems even to mediate a direct electrical activation of the ILN_vs upon light exposure (Fogle et al., 2011). Our *D. ezoana* and *D. littoralis* strains were collected in habitats of higher latitude (Finland), where summer days reach extremely long photoperiods, and the flies are consequently almost continuously exposed to light, a condition that renders *D. melanogaster* flies

arrhythmic (Emery et al., 2000). Reduction of CRY expression in those neurons that are most crucial for light arousal, such as the ILN_vs, may cause desensitization to light and might consequently be advantageous for proper clock function at high latitudes. The very high sequence similarities we found for the CRY protein homologues suggest that the differences that we found in the CRY staining probably do not derive from altered antibody specificity as a consequence of protein sequence variations but indeed derive from altered CRY protein expression in the ILN_vs.

The neuropeptide PDF was shown to be important for the function of the circadian clock in *D. melanogaster* acting as an output factor for circadian behavior and coupling neuromodulator among the different clock neuron clusters (see, e.g., Renn et al., 1999; Shafer et al., 2008; Shafer and Taghert, 2009; Yoshii et al., 2009). Direct information on its function within the clock network of other insect species is so far scarce. However, the fact that PDF is present in the circadian system of various insects such as cockroaches, crickets, blow flies, or blood-sucking bugs (Homberg et al., 1991, 2003; Stengl and Homberg, 1994; Petri et al., 1995; Lupien et al., 2003; Honda et al., 2006; Wen and Lee, 2008; Shiga and Numata, 2009; Vafopoulou et al., 2010; Wei et al., 2010; Vafopoulou and Steel, 2012) makes it probable that PDF is conserved in its function. In all insects, the PDF fibers project into the optic lobe as well as into the central brain, and the PDF projections are much more complex than in *D. melanogaster*. Even other Diptera such as houseflies and blowflies show a higher number of PDF neurons and more complex PDF projections (Nässel et al., 1991, 1993; Pyza and Meinertzhagen 1996, 1997, 2003; Pyza et al., 2003; Shiga and Numata, 2009). That is, larger flies possess additional PDF neurons in the dorsal brain, which invade the central brain, and their PDF neurons at the medulla invade several medulla layers, sometimes extending into the lamina. We found PDF

neurons in the dorsal protocerebrum in the flies of the *Drosophila* subgenus. Furthermore, the PDF projection patterns in the *Drosophila* subgenus resembled largely those of larger flies. This suggests that a common fly ancestor might have had more PDF⁺ neurons with more complex arborizations and that both got reduced during evolution. Interestingly, this reduction progressed in different directions within the Drosophilids. Whereas most flies of the *Sophophora* subgenus lost PDF in the neurons in the dorsal protocerebrum, the flies of the *Drosophila* subgenus retained PDF in the latter but lost PDF in the sLN_vs.

Bahn et al. (2009) had shown that the circadian locomotor behavior of *D. virilis* that lack PDF in the sLN_vs resembles the behavior of *D. melanogaster Pdf⁰¹* mutants, suggesting a correlation between rhythmic behavior and the presence of PDF in the sLN_vs. One possible explanation for this is the putative absence of the sLN_vs in this species. However, we were able to show now by VRI, PDP1 and CRY staining that this is not the case. All investigated species of the *Drosophila* subgenus and *D. pseudoobscura*, in which we observed a lack of PDF labeling in several of the sLN_vs, had in fact four sLN_vs per hemisphere but just did not express PDF in these cells. The high conservation of the peptide PDF itself rules out the possibility that the staining differences derive from altered peptide sequences; even the slightly deviating PDF sequence of *D. pseudoobscura* cannot account for this lack of immunoreactivity (although it may explain why the monoclonal anti-PDF antibody did not work). Thus, PDF might modulate circadian behavior in *D. virilis* in the same way as it does in *D. melanogaster*. The outcome of this modulation is then probably dependent on the extent to which PDF is expressed in the clock network, especially in the sLN_vs, which are important mostly for the morning activity of *D. melanogaster* flies and for maintaining rhythmicity under constant darkness (Grima et al., 2004; Stoleru et al., 2005). This might be the reason why *D. virilis* flies expressing no or less PDF in these neurons reduce evident morning activity and show arrhythmic behavior in constant darkness similarly to *D. melanogaster Pdf⁰¹* mutants. All these results together indicate that PDF is indeed conserved with regard to its function for the circadian clock but that there are differences in the expression pattern of this peptide that result in altered behavioral output. Activity in the morning is maladaptive for flies living in colder habitats or more northern regions, and such flies also do not need rhythmic behavior under constant darkness, because such conditions would anyway mean either winter or chilliness in their northern natural habitat. In addition to its role as a clock factor, PDF may play additional roles in the brain,

because it is expressed in several nonclock neurons in some of the investigated species.

ITP is a promising candidate for a conserved clock neuropeptide

According to peptide and mRNA structures and similar differential distributions in insects and crustaceans, ITP and crustacean hyperglycaemic hormones (CHH) are closely related, and the producing neurons likely share common phylogenetic ancestry (Audsley et al., 1992; Dirksen, 2009; Webster et al., 2012). In *D. melanogaster*, ITP occurs in three different isoforms after alternative splicing, and it is expressed in several central and peripheral neurons (Dirksen et al., 2008). The expression within clock neurons, the fifth sLN_v and one LN_d, in *D. melanogaster* was discovered by Johard et al. (2009). Both neurons send ITP⁺ fibers into the accessory medulla and the dorsal protocerebrum, where they can putatively contact other clock neurons or clock output sites, indicating possible roles for ITP within the clock network. Here we intended to reveal whether ITP is similarly present in clock neurons of other *Drosophila* species. In fact, we were able to show not only that the ITP peptide sequence is highly conserved within species of the whole *Drosophila* genus but also that expression within the two clock neurons is conserved in all investigated species of the *Sophophora* subgenus. Although we could not perform double labeling with anti-ITP and a clock-neuron-specific antibody in *D. virilis*, *D. ezoana*, *D. littoralis*, or *D. pseudoobscura* (anti-VRI does not work in these species, and anti-PDP1, anti-CRY, and anti-ITP are all raised in rabbits and could not be applied simultaneously), the position of the two ITP⁺ and PDF⁻ neurons in the lateral brain strongly suggests that they are identical with the fifth sLN_v and one LN_d. It will be very interesting for future work to investigate the role of ITP in *D. melanogaster* on the behavioral level. If ITP has a function in the circadian clock, it is quite probable that this function is conserved throughout the whole *Drosophila* genus. The extremely high sequence similarity throughout the whole genus further suggests the additional conservation of the as yet unknown receptor for ITP and possibly also its signaling cascade. A further analysis of the ITP expression pattern in the pacemaker centers of other insect species might even reveal a broader conservation of its function.

CONCLUSIONS

The distribution of the circadian pacemaker cells in the central nervous system is virtually identical throughout the *Drosophila* genus. This indicates that the general anatomy of the clock network within the two subgenera *Sophophora* and *Drosophila* is conserved from a common

ancestor species. Indeed, even the comparison of more distantly related animal groups such as flies, cockroaches, crickets, mollusks, and mammals showed that the circadian system is similarly organized not only on the molecular level but also on the cell and tissue levels (for review see Helfrich-Förster, 2004; Vansteensel et al., 2008; Tomioka and Matsumoto, 2010). Nevertheless, we have revealed differences in PDF transmitter usage and expression of the blue-light photopigment CRY among the clock neurons. The putative tropical ancestor species might have profited from morning activity (mediated by PDF in the sLN_s) and a highly light-sensitive clock (mediated by CRY in the lLN_s). However, in more northern climate zones, morning activity lost its selective advantage, and high light sensitivity even became maladaptive, because it would render the flies arrhythmic under long summer days. We did not check for other ecologically relevant changes in clock function, but these are most likely. Within the species *D. melanogaster*, latitudinal clines in clock gene polymorphisms are already present, highlighting the selective value of fine tuning the clock by the local environment (Kyriacou et al., 2008). Our present study provides the first basis for unraveling the clock organization in different *Drosophila* species as a consequence of successful adaptation to the environment.

ACKNOWLEDGMENTS

We thank Anneli Hoikkala, Hannele Kauranen (both University of Jyväskylä, Finland), Stephan Schnewly (University of Regensburg), and the *Drosophila* Species Stock Center (DSSC, San Diego) for fly strains; Paul Hardin (Texas A&M University) for the anti-VRI serum; Justin Blau (New York University) for anti-PDP1; John E. Phillips (Vancouver, British Columbia, Canada) and Neil Audsley (CSL Sand Hutton, York, United Kingdom) for anti-ScgITP-C1; and Takeshi Todo (Osaka University) for anti-CRY. In addition, we thank Federica Sandrelli and Rodolfo Costa for cosupervising R.S. and Matthias Schlichting for useful comments on the manuscript.

CONFLICT OF INTEREST STATEMENT

The authors declare that there are no conflicts of interest.

ROLE OF AUTHORS

All authors had full access to all the data in the study and take responsibility for the integrity of the data and the accuracy of the data analysis. Study concept and design: C.H.-F.; Acquisition of data: C.H., R.S., P.R.S., L.D.; Analysis and interpretation of data: C.H., P.R.S., T.Y.; Drafting of the manuscript: C.H., P.R.S., C.H.-F.; Critical revision of the manuscript and important intellectual contribution: T.Y., H.D.; Statistical analysis: C.H.; Study supervision: C.H.-F.

LITERATURE CITED

- Ashburner M. 1989. *Drosophila*. A laboratory Handbook. Cold Spring Harbor Laboratory Press.
- Audsley N, McIntosh C, Phillips JE. 1992. Isolation of a neuropeptide from locust corpus cardiacum which influences ileal transport. *J Exp Biol* 173:261–274.
- Bahn JH, Lee G, Park JH. 2009. Comparative analysis of Pdf-mediated circadian behaviors between *Drosophila melanogaster* and *D. virilis*. *Genetics* 181:965–975.
- Benito J, Houl JH, Roman GW, Hardin PE. 2008. The blue-light photoreceptor cryptochrome is expressed in a subset of circadian oscillator neurons in the *Drosophila* CNS. *J Biol Rhythms* 23:296–307.
- Beverly SM, Wilson AC. 1984. Molecular evolution in *Drosophila* and the higher Diptera II. A time scale for fly evolution. *J Mol Evol* 21:1–13.
- Beverly SM, Wilson AC. 1985. Ancient origin for Hawaiian *Drosophilinae* inferred from protein comparisons. *Proc Natl Acad Sci U S A* 82:4753–4757.
- Blau J, Young MW. 1999. Cyclic *vri* expression is required for a functional *Drosophila* clock. *Cell* 99:661–671.
- Cao G, Nitabach MN. 2008. Circadian control of membrane excitability in *Drosophila melanogaster* lateral ventral clock neurons. *J Neurosci* 28:6493–6501.
- Ceriani MF, Darlington TK, Staknis D, Mas P, Petti AA, Weitz CJ, Kay SA. 1999. Light-dependent sequestration of timeless by cryptochrome. *Science* 285:553–556.
- Chung BY, Kilman VL, Keath JR, Pitman JL, Allada R. 2009. The GABA_A receptor RDL acts in peptidergic PDF neurons to promote sleep in *Drosophila*. *Curr Biol* 19:386–390.
- Cyran SA, Buchsbaum AM, Reddy KL, Lin MC, Glossop NR, Hardin PE, Young MW, Storti RV, Blau J. 2003. *vri*, *Pdp1*, and *dClock* form a second feedback loop in the *Drosophila* circadian clock. *Cell* 112:329–341.
- Cyran SA, Yiannoulos G, Buchsbaum AM, Saez L, Young MW, Blau J. 2005. The double-time protein kinase regulates the subcellular localization of the *Drosophila* clock protein period. *J Neurosci* 25:5430–5437.
- Dereeper A, Guignon V, Blanc G, Audic S, Buffet S, Chevenet F, Dufayard JF, Guindon S, Lefort V, Lescot M, Claverie JM, Gascuel O. 2008. Phylogeny.fr: robust phylogenetic analysis for the non-specialist. *Nucleic Acids Res* 36:W465–469.
- Dirksen H. 2009. Insect ion transport peptides are derived from alternatively spliced genes and differentially expressed in the central and peripheral nervous system. *J Exp Biol* 212:401–412.
- Dirksen H, Zahn CA, Gaus G, Keller R, Rao KR, Riehm JP. 1987. The ultrastructure of nerve endings containing pigment dispersing hormone (PDH) in crustacean sinus glands: identification by an antiserum against synthetic PDH. *Cell Tissue Res* 250:377–387.
- Dirksen H, Tesfai LK, Albus C, Nässel DR. 2008. Ion transport peptide splice forms in central and peripheral neurons throughout postembryogenesis of *Drosophila melanogaster*. *J Comp Neurol* 509:23–41.
- Dushay MS, Rosbash M, Hall JC. 1989. The *disconnected* visual system mutations in *Drosophila melanogaster* drastically disrupt circadian rhythms. *J Biol Rhythms* 4:1–27.
- Emery P, So WV, Kaneko M, Hall JC, Rosbash M. 1998. CRY, a *Drosophila* clock and light-regulated cryptochrome, is a major contributor to circadian rhythm resetting and photosensitivity. *Cell* 95:669–679.
- Emery P, Stanewsky R, Helfrich-Förster C, Emery-Le M, Hall JC, Rosbash M. 2000. *Drosophila* CRY is a deep brain circadian photoreceptor. *Neuron* 26:493–504.
- Ewer J, Frisch B, Hamblen-Coyle MJ, Rosbash M, Hall JC. 1992. Expression of the period clock gene within different cell types in the brain of *Drosophila* adults and mosaic

- analysis of these cells' influence on circadian behavioral rhythms. *J Neurosci* 12:3321–3349.
- Fogle KJ, Parson KG, Dahm NA, Holmes TC. 2011. Cryptochrome is a blue-light sensor that regulates neuronal firing rate. *Science* 331:1409–1413.
- Glossop NR, Houl JH, Zheng H, Ng FS, Dudek SM, Hardin PE. 2003. *Vrille* feeds back to control circadian transcription of *Clock* in the *Drosophila* circadian oscillator. *Neuron* 37:249–261.
- Grima B, Chelot E, Xia R, Rouyer F. 2004. Morning and evening peaks of activity rely on different clock neurons of the *Drosophila* brain. *Nature* 431:869–873.
- Helfrich-Förster C. 1995. The period clock gene is expressed in central nervous system neurons which also produce a neuropeptide that reveals the projections of circadian pacemaker cells within the brain of *Drosophila melanogaster*. *Proc Natl Acad Sci U S A* 92:612–616.
- Helfrich-Förster C. 1998. Robust circadian rhythmicity of *Drosophila melanogaster* requires the presence of lateral neurons: a brain-behavioral study of *disconnected* mutants. *J Comp Physiol* 182:435–453.
- Helfrich-Förster C. 2004. The circadian clock in the brain: a structural and functional comparison between mammals and insects. *J Comp Physiol A* 190:601–613.
- Helfrich-Förster C. 2005. Organization of endogenous clocks in insects. *Biochem Soc Trans* 33:957–961.
- Helfrich-Förster C. 2009. Does the morning and evening oscillator model fit better for flies or mice? *J Biol Rhythms* 24:259–270.
- Helfrich-Förster C, Homberg U. 1993. Pigment-dispersing hormone-immunoreactive neurons in the nervous system of wild-type *Drosophila melanogaster* and of several mutants with altered circadian rhythmicity. *J Comp Neurol* 337:177–190.
- Helfrich-Förster C, Shafer OT, Wülbeck C, Grieshaber E, Rieger D, Taghert P. 2007. Development and morphology of the clock-gene-expressing lateral neurons of *Drosophila melanogaster*. *J Comp Neurol* 500:47–70.
- Hermann C, Yoshii T, Dusik V, Helfrich-Förster C. 2012. Neuropeptide F immunoreactive clock neurons modify evening locomotor activity and free-running period in *Drosophila melanogaster*. *J Comp Neurol* 520:970–987.
- Homberg U, Reischig T, Stengl M. 2003. Neural organization of the circadian system of the cockroach *Leucophaea maderae*. *Chronobiol Int* 20:577–591.
- Homberg U, Würden S, Dirksen H, Rao KR. 1991. Comparative anatomy of pigment-dispersing hormone-immunoreactive neurons in the brain of orthopteroïd insects. *Cell Tissue Res* 266:343–357.
- Honda T, Matsushima A, Sumida K, Chuman Y, Sakaguchi K, Onoue H, Meinertzhagen IA, Shimohigashi Y, Shimohigashi M. 2006. Structural isoforms of the circadian neuropeptide PDF expressed in the optic lobes of the cricket *Gryllus bimaculatus*: immunocytochemical evidence from specific monoclonal antibodies. *J Comp Neurol* 499:404–421.
- Johard HA, Yoshii T, Dirksen H, Cusumano P, Rouyer F, Helfrich-Förster C, Nässel DR. 2009. Peptidergic clock neurons in *Drosophila*: ion transport peptide and short neuropeptide F in subsets of dorsal and ventral lateral neurons. *J Comp Neurol* 516:59–73.
- Kaneko M, Hall JC. 2000. Neuroanatomy of cells expressing clock genes in *Drosophila*: transgenic manipulation of the *period* and *timeless* circadian pacemaker neurons and their projections. *J Comp Neurol* 422:66–94.
- Kaneko M, Helfrich-Förster C, Hall JC. 1997. Spatial and temporal expression of the *period* and *timeless* genes in the developing nervous system of *Drosophila*: newly identified pacemaker candidates and novel features of clock gene product cycling. *J Neurosci* 17:6745–6760.
- Kyriacou CP, Peixoto AA, Sandrelli F, Costa R, Tauber E. 2008. Clines in clock genes: fine-tuning circadian rhythms to the environment. *Trends Genet* 24:124–132.
- Lankinen P, Forsman P. 2006. Independence of genetic geographical variation between photoperiodic diapause, circadian eclosion rhythm, and Thr-Gly repeat region of the *period* gene in *Drosophila littoralis*. *J Biol Rhythms* 21:3–12.
- Lee G, Bahn JH, Park JH. 2006. Sex- and clock-controlled expression of the *neuropeptide F* gene in *Drosophila*. *Proc Natl Acad Sci U S A* 103:12580–12585.
- Lin Y, Stormo GD, Taghert PH. 2004. The neuropeptide pigment-dispersing factor coordinates pacemaker interactions in the *Drosophila* circadian system. *J Neurosci* 24:7951–7957.
- Low KH, Lim C, Ko HW, Edery I. 2008. Natural variation in the splice site strength of a clock gene and species-specific thermal adaptation. *Neuron* 60:1054–1067.
- Lupien M, Marshall S, Leser W, Pollack GS, Honegger HW. 2003. Antibodies against the PER protein of *Drosophila* label neurons in the optic lobe, central brain, and thoracic ganglia of the crickets *Teleogryllus commodus* and *Teleogryllus oceanicus*. *Cell Tissue Res* 312:377–391.
- Nässel DR, Wegener C. 2011. A comparative review of short and long neuropeptide F signaling in invertebrates: any similarities to vertebrate neuropeptide Y signaling? *Peptides* 32:1335–1355.
- Nässel DR, Shiga S, Wikstrand EM, Rao KR. 1991. Pigment-dispersing hormone-immunoreactive neurons and their relation to serotonergic neurons in the blowfly and cockroach visual system. *Cell Tissue Res* 266:511–523.
- Nässel DR, Shiga S, Mohrherr CJ, Rao KR. 1993. Pigment-dispersing hormone-like peptide in the nervous system of the flies *Phormia* and *Drosophila*: immunocytochemistry and partial characterization. *J Comp Neurol* 331:183–198.
- Nässel DR, Enell LE, Santos JG, Wegener C, Johard HA. 2008. A large population of diverse neurons in the *Drosophila* central nervous system expresses short neuropeptide F, suggesting multiple distributed peptide functions. *BMC Neurosci* 9:90.
- Nishinokubi I, Shimoda M, Ishida N. 2006. Mating rhythms of *Drosophila*: rescue of *tim01* mutants by *D. ananassae timeless*. *J Circadian Rhythms* 4:4.
- Ousley A, Zafarullah K, Chen Y, Emerson M, Hickman L, Sehgal A. 1998. Conserved regions of the *timeless* (*tim*) clock gene in *Drosophila* analyzed through phylogenetic and functional studies. *Genetics* 148:815–825.
- Parisky KM, Agosto J, Pulver SR, Shang Y, Kuklin E, Hodge JJ, Kang K, Liu X, Garrity PA, Rosbash M, Griffith LC. 2008. PDF cells are a GABA-responsive wake-promoting component of the *Drosophila* sleep circuit. *Neuron* 60:672–682.
- Peng Y, Stoleru D, Levine JD, Hall JC, Rosbash M. 2003. *Drosophila* free-running rhythms require intercellular communication. *PLoS Biol* 1:E13.
- Petri B, Stengl M, Würden S, Homberg U. 1995. Immunocytochemical characterization of the accessory medulla in the cockroach *Leucophaea maderae*. *Cell Tissue Res* 282:3–19.
- Pyza E, Meinertzhagen IA. 1996. Neurotransmitters regulate rhythmic size changes amongst cells in the fly's optic lobe. *J Comp Physiol A* 178:33–45.
- Pyza E, Meinertzhagen IA. 1997. Neurites of period-expressing PDH cells in the fly's optic lobe exhibit circadian oscillations in morphology. *Eur J Neurosci* 9:1784–1788.
- Pyza E, Meinertzhagen IA. 2003. The regulation of circadian rhythms in the fly's visual system: involvement of FMRFamide-like neuropeptides and their relationship to pigment dispersing factor in *Musca domestica* and *Drosophila melanogaster*. *Neuropeptides* 37:277–289.
- Pyza E, Siuta T, Tanimura T. 2003. Development of PDF-immunoreactive cells, possible clock neurons, in the housefly *Musca domestica*. *Microsc Res Techniq* 62:103–113.

- Reddy KL, Wohlwill A, Dzitoeva S, Lin MH, Holbrook S, Storti RV. 2000. The *Drosophila* PAR domain protein 1 (*Pdp1*) gene encodes multiple differentially expressed mRNAs and proteins through the use of multiple enhancers and promoters. *Dev Biol* 224:401–414.
- Renn SC, Park JH, Rosbash M, Hall JC, Taghert PH. 1999. A *pdf* neuropeptide gene mutation and ablation of PDF neurons each cause severe abnormalities of behavioral circadian rhythms in *Drosophila*. *Cell* 99:791–802.
- Ring M, Meredith J, Wiens C, Macins A, Brock HW, Phillis JE, Theilmann DA. 1998. *Insect Biochem Mol Biol* 28:51–58.
- Rieger D, Stanewsky R, Helfrich-Förster C. 2003. Cryptochrome, compound eyes, Hofbauer-Buchner eyelets, and ocelli play different roles in the entrainment and masking pathway of the locomotor activity rhythm in the fruit fly *Drosophila melanogaster*. *J Biol Rhythms* 18:377–391.
- Sakai T, Ishida N. 2001. Time, love and species. *Neuroendocrin Lett* 22:222–228.
- Shafer OT, Taghert PH. 2009. RNA-interference knockdown of *Drosophila* pigment dispersing factor in neuronal subsets: the anatomical basis of a neuropeptide's circadian functions. *PLoS One* 4:e8298.
- Shafer OT, Helfrich-Förster C, Renn SC, Taghert PH. 2006. Reevaluation of *Drosophila melanogaster's* neuronal circadian pacemakers reveals new neuronal classes. *J Comp Neurol* 498:180–193.
- Shafer OT, Kim DJ, Dunbar-Yaffe R, Nikolaev VO, Lohse MJ, Taghert PH. 2008. Widespread receptivity to neuropeptide PDF throughout the neuronal circadian clock network of *Drosophila* revealed by real-time cyclic AMP imaging. *Neuron* 58:223–237.
- Shang Y, Griffith LC, Rosbash M. 2008. Light-arousal and circadian photoreception circuits intersect at the large PDF cells of the *Drosophila* brain. *Proc Natl Acad Sci U S A* 105:19587–19594.
- Sheeba V, Fogle KJ, Kaneko M, Rashid S, Chou YT, Sharma VK, Holmes TC. 2008. Large ventral lateral neurons modulate arousal and sleep in *Drosophila*. *Curr Biol* 18:1537–1545.
- Shiga S, Numata H. 2009. Roles of PER immunoreactive neurons in circadian rhythms and photoperiodism in the blow fly, *Protophormia terraenovae*. *J Exp Biol* 212:867–877.
- Spicer GS. 1988. Molecular evolution among some *Drosophila* species groups as indicated by two-dimensional electrophoresis. *J Mol Evol* 27:250–260.
- Stanewsky R, Kaneko M, Emery P, Beretta B, Wager-Smith K, Kay SA, Rosbash M, Hall JC. 1998. The *cry^b* mutation identifies cryptochrome as a circadian photoreceptor in *Drosophila*. *Cell* 95:681–692.
- Stengl M, Homberg U. 1994. Pigment-dispersing hormone-immunoreactive neurons in the cockroach *Leucophaea maderae* share properties with circadian pacemaker neurons. *J Comp Physiol* 175:203–213.
- Stoleru D, Peng Y, Agosto J, Rosbash M. 2004. Coupled oscillators control morning and evening locomotor behaviour of *Drosophila*. *Nature* 431:862–868.
- Stoleru D, Peng Y, Nawathean P, Rosbash M. 2005. A resetting signal between *Drosophila* pacemakers synchronizes morning and evening activity. *Nature* 438:238–242.
- Tomioka K, Matsumoto A. 2010. A comparative view of insect circadian clock systems. *Cell Mol Life Sci* 67:1397–1406.
- Vafopoulou X, Steel CG. 2012. Metamorphosis of a clock: remodeling of the circadian timing system in the brain of *Rhodnius prolixus* (Hemiptera) during larval-adult development. *J Comp Neurol* 520:1146–1164.
- Vafopoulou X, Terry KL, Steel CG. 2010. The circadian timing system in the brain of the fifth larval instar of *Rhodnius prolixus* (hemiptera). *J Comp Neurol* 518:1264–1282.
- Vansteensel MJ, Michel S, Meijer JH. 2008. Organization of cell and tissue circadian pacemakers: a comparison among species. *Brain Res Rev* 58:18–47.
- Webster SG, Keller R, Dirksen H. 2012. The CHH-superfamily of multifunctional peptide hormones controlling crustacean metabolism, osmoregulation, moulting, and reproduction. *Gen Comp Endocrinol* 175:217–233.
- Wei H, el Jundi B, Homberg U, Stengl M. 2010. Implementation of pigment-dispersing factor-immunoreactive neurons in a standardized atlas of the brain of the cockroach *Leucophaea maderae*. *J Comp Neurol* 518:4113–4133.
- Wen CJ, Lee HJ. 2008. Mapping the cellular network of the circadian clock in two cockroach species. *Arch Insect Biochem Physiol* 68:215–231.
- Yamada H, Yamamoto MT. 2011. Association between circadian clock genes and diapause incidence in *Drosophila triauraria*. *PLoS One* 6:e27493.
- Yoshii T, Todo T, Wülbeck C, Stanewsky R, Helfrich-Förster C. 2008. Cryptochrome is present in the compound eyes and a subset of *Drosophila's* clock neurons. *J Comp Neurol* 508:952–966.
- Yoshii T, Wülbeck C, Sehadova H, Veleri S, Bichler D, Stanewsky R, Helfrich-Förster C. 2009. The neuropeptide pigment-dispersing factor adjusts period and phase of *Drosophila's* clock. *J Neurosci* 29:2597–2610.
- Yoshii T, Rieger D, Helfrich-Förster C. 2012. Two clocks in the brain—an update of the Morning and Evening oscillator model in *Drosophila*. *Prog Brain Res* (in press).

Neuropeptide F Immunoreactive Clock Neurons Modify Evening Locomotor Activity and Free-Running Period in *Drosophila melanogaster*

Christiane Hermann,¹ Taishi Yoshii,^{1,2} Verena Dusik,¹ and Charlotte Helfrich-Förster^{1*}

¹Department of Neurobiology and Genetics, Biocenter, University of Würzburg, D-97074, Germany

²Graduate School of Natural Science and Technology, Okayama University, Okayama 700-8530, Japan

ABSTRACT

Different subsets of *Drosophila melanogaster*'s clock neurons are characterized by their specific functions in daily locomotor rhythms and the differences in their neurotransmitter composition. We investigated the function of the neuropeptide F (NPF) immunoreactive clock neurons in the rhythmic locomotor behavior of adult flies. We newly identified the fifth s-LN_v and a subset of the l-LN_vs as NPF-positive in addition to the three LN_vs that have been described previously. We then selectively ablated different subsets of NPF-expressing neurons using *nprGal4*-targeted expression of the cell death gene *head involution defective* (*hid*) in combination with *cryGal80* and *pdfGal80*. By analyzing daily locomotor rhythms in these flies, we show that the NPF-positive clock neurons—especially the fifth s-LN_v

and the LN_vs—are involved in both the control of the free-running period in constant darkness (DD) and the phasing and amplitude of the evening activity in light-dark (LD) cycles. Furthermore, we show that the simultaneous ablation of NPF and pigment dispersing factor (PDF)-immunoreactive neurons has additive effects in LD, resulting in an evening peak phase that is even more advanced in comparison to PDF-ablated flies. We also found that this more advanced evening peak is additionally reduced in amplitude. To putatively assign the observed phenotypes to the action of NPF, we knocked it down in conjunction with PDF using RNA-interference (RNAi) and further suggest a possible role for NPF in the control of the flies' evening activity. *J. Comp. Neurol.* 520:970–987, 2012.

© 2011 Wiley Periodicals, Inc.

INDEXING TERMS: lateral neurons; circadian rhythms; cell ablation

Most organisms possess endogenous circadian clocks that allow them to adapt to daily alterations in the environment caused by the rotation of the earth. In animals, clocks are located in both peripheral tissues and the brain. Peripheral clocks control the particular functions of each tissue, while the clock in the brain controls not only a wide range of biological activities, including behavior, but governs in most cases also these peripheral clocks. Due to this dominance, the brain clock is regarded as a “master clock.”

In *Drosophila melanogaster* the master clock consists of about 150 clock neurons, which contain autonomous, self-sustained molecular oscillators that can be entrained by environmental time cues, so-called “zeitgebers.” However, the clock neurons do not act as individuals, but rather form a network to collaboratively control behavioral activity, in which different subgroups of clock neurons fulfill various functions.

In a light-dark (LD) cycle, *D. melanogaster* exhibits a typical diurnal activity pattern with a morning activity

peak around lights-on and an evening activity peak around lights-off. In 1976, Pittendrigh and Daan proposed a dual-oscillator model, suggesting that there are two different oscillators in nocturnal rodents: one controlling the morning activity and one controlling the evening activity. With regard to this hypothesis, it was first shown in *Drosophila* that different subgroups of clock neurons constitute anatomically separated morning (M) and evening (E) oscillators, respectively (Fig. 1).

Initial findings indicated that the four small ventral lateral neurons (s-LN_vs) that express the neuropeptide

Grant sponsor: Deutsche Forschungsgemeinschaft (DFG); Grant number: Fo207/12-1; Grant sponsor: European Commission; Grant number: FP6 IP EUCLOCK.

*CORRESPONDENCE TO: Charlotte Helfrich-Förster, Department of Neurobiology and Genetics, Biocenter, University of Würzburg, 97074 Würzburg, Germany. E-mail: charlotte.foerster@biozentrum.uni-wuerzburg.de

Received February 11, 2011; Revised July 13, 2011; Accepted August 3, 2011

DOI 10.1002/cne.22742

Published online August 8, 2011 in Wiley Online Library (wileyonlinelibrary.com)

© 2011 Wiley Periodicals, Inc.

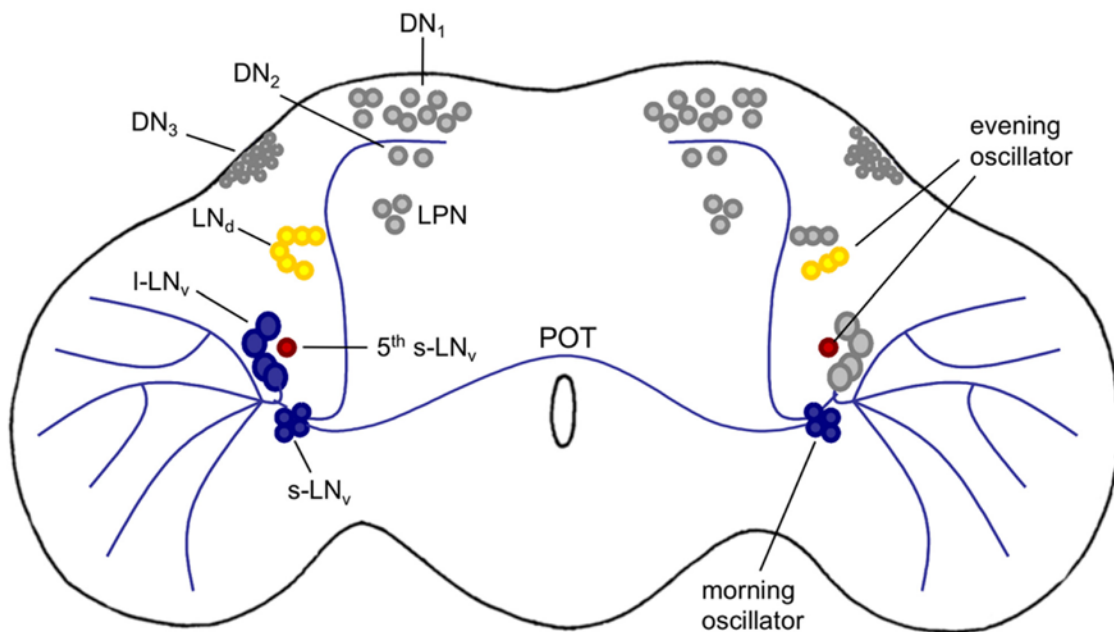


Figure 1. The neuronal network of the “master” clock in the adult *D. melanogaster* brain. The dorsally located clock neurons (DNs) consist of three different groups, the DN₁s, DN₂s, and the DN₃s. The lateral clock neurons (LNs) can be divided into a group of six dorsal lateral neurons (LN_ds, left side, yellow) and the more ventrally located LN_vs (left side, blue). There are four LN_vs per hemisphere with rather small cell bodies, the s-LN_vs, and four to six neurons with rather large soma, the I-LN_vs. Both s- and I-LN_vs express the neuropeptide PDF. Usually located among the I-LN_vs is another single neuron with smaller cell body, the fifth s-LN_v (red), which is PDF-negative. Another group of clock gene-expressing neurons, the LPNs, is located in the lateral posterior brain (Helfrich-Förster et al., 2007). According to the dual-oscillator model, three of the six LN_ds and the fifth s-LN_v were identified to be evening neurons (right side, yellow and red), whereas the s-LN_vs were found to be morning neurons (right side, blue). (Grima et al., 2004; Stoleru et al., 2004; Rieger et al., 2006; Picot et al., 2007).

pigment dispersing factor (PDF; Helfrich-Förster, 1995) control the morning activity, while the dorsal lateral neurons (LN_ds) control the evening activity (Grima et al., 2004; Stoleru et al., 2004). Later, the fifth s-LN_v joined the previously identified E oscillator neurons in their function (Rieger et al., 2006). Picot et al. (2007) further showed that the CRY-positive LN_ds and the fifth s-LN_v are sufficient to promote evening activity. Recent studies, however, suggest that the clock network is rather plastic and might be modulated by the environmental conditions: E neurons alone could produce both M and E activity under certain light conditions, even without functionality of the so far defined M neurons (Rieger et al., 2009; Sheeba et al., 2010). The same was reported for a subset of the dorsal clock neurons (DNs; Zhang et al., 2010). Thus, the dual-oscillator model is not as simple as first assumed and more information is required to understand the whole circadian network in *Drosophila*.

The *Drosophila* researchers have reaped great benefits from the establishment of the *Gal4-*uas** binary expression system (Brand and Perrimon, 1993). Using this system allows for ectopic expression of, for example, apoptotic

genes, such as *reaper* or *head-involution defective (hid)*, under the control of a tissue specific driver (*Gal4*) line, so that only *Gal4*-expressing neurons will express *reaper* or *hid* and will be genetically ablated (McNabb et al., 1997). This is a powerful approach to investigate the function of certain neurons. In the field of circadian research, Renn et al. (1999) first used this technique to ablate neurons that express *pdf*, which is a main output factor of the clock and exclusively expressed in small and large LN_vs (s-LN_vs and I-LN_vs) with the exception of the fifth s-LN_v (Helfrich-Förster, 1995). Flies expressing *uas-reaper* or *uas-hid* with *pdfGal4* displayed a phenocopy of the *Pdf* null-mutant, *Pdf⁰¹*: an advanced evening peak in LD cycles and a shorter free-running period in constant darkness (DD). Afterwards, *cryptochrome(cry)Gal4* along with a combination of *cryGal4* and *PdfGal80*, which suppresses *Gal4* activity and therefore prevents cell ablation in the *pdf*-positive neurons, were used to dissect the role of the *pdf*-negative clock neurons, revealing their importance for evening activity (Stoleru et al., 2004). One difficulty of this approach is the necessity of a *Gal4* line specifically driving expression in a subset of the clock neurons, which

should additionally allow the flies to survive development to the adult fly stage, when *reaper* or *hid* are used for targeted cell ablation.

Several members of neuropeptide Y (NPY)-like peptides were identified in different invertebrate species. In *Drosophila* a long neuropeptide F (NPF) and four different isoforms of short neuropeptide F (sNPF) have been described (Nässel et al., 2008; Nässel and Wegener, 2011). The long form of *Drosophila* NPF, which is more likely related to the vertebrate NPY than the sNPFs, is involved in various behavioral and physiological processes, such as feeding, courtship, and metabolism (Shen and Cai, 2001; Wu et al., 2003, 2005; Lee et al., 2006). Interestingly, NPF was also found to be expressed in three of the LN_d clock neurons in male flies (Lee et al., 2006). One of these NPF-positive LN_ds is also CRY-positive and might be the so-called “extra LN_d,” that was shown to be an important E component (Rieger et al., 2006, 2009; Johard et al., 2009). Lee et al. (2006) reported that the expression of *uas-reaper* with an *npfGal4* line leads to the ablation of all NPF neurons, including the three LN_ds. In another recent study by Hamasaka et al. (2010) the same *npfGal4* line was used to ablate the NPF neurons with *uas-hid*. Hamasaka et al. (2010) were able to confirm the ablation of at least two of the *npf*-positive LN_ds and suggested in addition the possible ablation of the PDF-negative fifth s-LN_v. Lee et al. (2006) showed that the ablation of all *npf*-positive neurons affects both phase and shape of the evening activity bout in male flies, suggesting that the *npf*-expressing neurons have a function in the control of the evening activity (Lee et al., 2006). However, NPF is expressed not only in clock neurons but also in many other non-clock cells, which were also ablated in these previous experiments. Therefore, the observed effect on evening activity might be due to the ablation of other NPF-cells that are not part of the clock network.

In this study we investigated the NPF distribution in the adult fly brain, both by specific antibody staining and *Gal4*-driven GFP expression, and newly show that NPF is expressed in both the fifth s-LN_v and in 3–4 I-LN_vs in both male and female flies, in addition to the three *npf*-positive LN_ds that have been described previously (Lee et al., 2006). We further show the complete ablation of all *npf*-positive clock neurons, when *uas-hid* is expressed using the same *npfGal4* line previously utilized by Lee et al. (2006) and Hamasaka et al. (2010). To reveal the function of the *npf*-positive clock neurons in circadian behavior, we refined the *npfGal4*-driven *hid* expression by the use of *cryGal80* and *pdfGal80*, so that only subsets of the *npf*-expressing cells were ablated. In addition, we compare the behavior of *npf*-ablated flies to *pdf*-ablated flies (*w; uas-hid/pdfGal4; +*) and flies with concurrent ablation of both *npf*- and *pdf*-positive neurons (*w; uas-hid/pdfGal4; npfGal4/+*). This allowed for a

better examination of how the *npf*-positive clock neurons contribute to the neuronal clock network in controlling rhythmic locomotor activity. To investigate the action of NPF in the observed phenotypes we simultaneously knocked it down together with PDF by RNA-interference (RNAi).

MATERIALS AND METHODS

Fly stocks

Flies were reared on standard cornmeal/agar medium with yeast at 20°C in an LD cycle. The *CantonS* (CS) wild-type strain served to reveal the NPF expression pattern.

Furthermore, a *y w; +; npfGal4* line containing an ≈1-kb upstream sequence including the 5' regulatory region and part of the first exon (generated by Wu et al., 2003; donated by Jae H. Park), which is a reliable reporter for NPF expression in larvae (Wu et al., 2003) and in adult flies (Lee et al., 2006), was used in combination with a *w; +; uas-gfp s65t*-line (Bloomington Stock Center, Bloomington, IN, #1522; donated by Karl Fischbach) to express green fluorescent protein (GFP) in the NPF neurons. To specifically ablate *npf* and *pdf*-expressing neurons, we crossed the *y w; +; npfGal4* line or a *y w; pdfGal4* line (kindly provided by Jae H. Park and Jeffrey C. Hall) to a *w; uas-hid¹⁴/CyO*-line (donated by Hermann Steller), which was generated by cloning the *hid* cDNA clone 5A1B into the EcoRI site of the pUAST vector (Zhou et al., 1997). We used the balancer-free progeny for behavioral analysis and immunocytochemistry. The *y w; pdfGal4* line contains 2.4 kb of 5'-flanking *pdf* DNA fused to *Gal4* and was described by Renn et al. (1999). To restrict the cell ablation to subsets of *npf*-expressing neurons, we first established a stable *w; uas-hid¹⁴/CyO; npfGal4/MKRS* line and crossed it to *y w; +; cryGal80_{2e3m}/TM6B, D³* and *y w; pdfGal80_{96A}/CyO* (both donated by Michael Rosbash). Both *Gal80* lines contain two inserts of the respective *Gal80*-constructs, in which a *pdf* 2.5 kb or a *cry* 5.5 kb promoter sequence was fused to the *Gal80* sequence, respectively (described by Stoleru et al., 2004). Furthermore, *w; uas-hid¹⁴/CyO, y w; +; npfGal4/+* and both *Gal80*-strains were crossed to *white¹¹¹⁸ (w)* females to get heterozygous control flies for behavioral experiments.

For RNAi-mediated gene silencing we used an X-chromosomal *uas-dicer2; +; +* line (Vienna *Drosophila* RNAi Center, #60012) and a *w; tim(uas)Gal4*-line (kindly provided by Michael W. Young, first described by Blau and Young, 1999) in combination with *w; +; uas-pdf^{RNAi}* and *w; uas-*npf*^{RNAi}* (Vienna *Drosophila* RNAi Center, #4380 and #108772, respectively).

Antibody characterization

Please see Table 1 for an overview of all primary antibodies that were used in this study.

TABLE 1.
Primary Antibodies Used

Antigen, antibody name	Immunogen	Species, dilution used
<i>Drosophila</i> NPF anti-NPF	Synthetic peptide deduced from mature <i>Drosophila</i> NPF, amino acids 1-36, amidated at the C-Terminus	Rabbit polyclonal, 1:300
TIM anti-TIM	Polyhistidine fused TIM fragment expressed in <i>E. coli</i> (amino acids 222-577)	Rat polyclonal, 1:1,000
PDF nb33 (IgG)	<i>Drosophila melanogaster</i> head extracts	Mouse monoclonal (hybridoma clone P3x63Ag8.653), 1:100

The rabbit anti-NPF serum (kindly donated by Jae H. Park) was generated against a 36-residue synthetic *Drosophila* NPF, amidated at the carboxyl terminus (SNSRPPRKN DVNTMADAYKFLQDLDTYYGDRARVRFamide; Shen and Cai, 2001). We show that the staining pattern of the antibody matches the expression pattern of the *npfGal4* line, ensuring the specificity of the NPF antiserum. Furthermore, when overexpressing *npf* by *Gal4*-driven expression of *uas-npf*, e.g., with *timGal4* or *pdfGal4*, the antibody reliably labeled all overexpressing cells (data not shown).

Polyclonal rat anti-TIM (kindly provided by Isaac Edery) was raised against a polyhistidine fused TIM fragment expressed in *E. coli* (amino acids 222-577; Sidote et al., 1998). The antigen was purified under denaturing conditions, using the TALON metal affinity resin from ClonTech (Palo Alto, CA), and the antibody was raised in rats by Cocalico (Biologicals, Reamstown, PA). The specificity of the TIM antiserum was demonstrated in western blots, where the antibody labeled one clear band of about 185 kD, which was absent in the knockout mutant *tim⁰¹* (Sidote et al., 1998). Furthermore, no labeling could be seen when the antisera were used to stain brains from *tim⁰¹* mutants (data not shown).

The mouse monoclonal antibody "nb33" (IgG; kindly donated by Alois Hofbauer) was derived from a hybridoma clone that was obtained after immunization of BALBc mice with homogenates of *D. melanogaster* heads and the subsequent fusion of spleen cells to mouse myeloma cells (P3x63Ag8.653; Hofbauer, 1991; Hofbauer et al., 2009). The clone was selected for its immunohistochemical specificity to all *pdf*-expressing cells in *D. melanogaster* (first described by Veleri et al., 2003, recognizing the PDF precursor peptide (PDFp)). No labeling is present in *pdf⁰¹* mutants (data not shown).

Immunocytochemistry

Flies were synchronized by 12:12-hour light/dark cycles (LD 12:12; 500 lux: 0 lux) for at least 4 days. Flies were collected at Zeitgeber Time 21 (ZT21) and were quickly fixed in 4% paraformaldehyde (PFA) in phosphate buffer (PB; pH 7.4) with 0.1% Triton X-100 at room temperature in the dark. For the fixation of flies expressing GFP, no Triton X-100 was used in the PFA solution. After

2.5 hours of fixation, the flies were rinsed three times for 15 minutes in PB and the brains were dissected in PB. The brains were blocked in 5% normal goat serum (NGS) in PB with 0.5% Triton X-100 at 4°C overnight and subsequently incubated in primary antibodies for 48 hours at 4°C. The primary antibodies rabbit anti-NPF, rat anti-TIM and mouse monoclonal nb33 directed against the precursor of PDF were diluted by 1:300, 1:1,000, and 1:100 in PB containing 5% NGS and 0.5% Triton X-100, respectively. After washing six times in PB with 0.5% Triton X-100, secondary fluorescence-conjugated antibodies were applied overnight at 4°C. For triple or double immunolabeling Alexa Fluor 488 (goat anti-rabbit), Alexa Fluor 555 (goat anti-rat), and Alexa Fluor 647 (goat anti-mouse; Molecular Probes, Carlsbad, CA) were used as secondary antibodies in a dilution of 1:200 in PB with 5% NGS and 0.5% Triton X-100. After the incubation in the secondary antibodies, the brains were washed six times in PB with 0.1% Triton X-100 and embedded in Vectashield mounting medium (Vector Laboratories, Burlingame, CA) in a way that the anterior surfaces were upside on the glass slide.

Microscopy and image analysis

Immunofluorescent brains were analyzed by laser scanning confocal microscopy (Zeiss LSM 510 Meta; Carl Zeiss MicroImaging, Jena, Germany). Confocal stacks of 2- μ m thickness were obtained at intervals of 2.4 μ m. In triple labeling GFP or NPF was visualized in the green channel, TIM in the red channel (converted to magenta), and PDF in the infrared channel (converted to blue). To exclude bleed through, we performed sequential scans of the three different laser lines. To quantify the number of NPF-expressing neurons or remaining cells after *hid* expression, the hemispheres of 8-15 brains were analyzed for each genotype. The complete confocal stacks were displayed in the Zeiss LSM Image Browser (v. 4,2,0,121) and after discriminating between the different groups of clock neurons according to their location and immunoreactivity, cells were counted investigating single optical sections of each stack.

Stacks were cropped and overlays were generated in the Zeiss LSM Image Browser (v. 4,2,0,121). These pictures were subsequently imported into ImageJ (freely

available at <http://rsb.info.nih.gov/ij/>) to adjust brightness and contrast. No other manipulations were performed on the images.

Behavioral analysis

Locomotor activity of individual flies was recorded photoelectrically using the *Drosophila* Activity Monitoring (DAM) System (Trikinetics, Waltham MA). Flies were raised on cornmeal medium at 25°C under a LD 12:12 cycle. At the age of 3–5 days individual male flies were transferred into the recording tubes, which were one-third filled with agar/sugar-medium (2% agar; 4% sucrose) and were closed by a plug, permeable to air. Activity monitors, containing an infrared light beam, were placed with 32 tubes each into a lightproof box inside an incubator to maintain a constant temperature of 20°C during the experiment. A computer recorded the activity of individual flies by counting the number of light-beam crosses per minute during the whole recording duration. White light LEDs (11000mcd, Lumitronix, LED-Technik, Hechingen, Germany) served as the light source and intensity was adjusted to 100 lux. To investigate behavior in LD we recorded the flies consecutively under LD 12:12 (12h light: 12h darkness) and LD 16:08 (16h light: 8h darkness) for 7 days each. Additionally, some genotypes were recorded for 7 days in LD 12:12, followed by at least 14 days of constant darkness (DD) to investigate the flies' behavior in constant conditions. Raw data of individual light beam crosses were collected in 1-minute bins by the DAMSystem Collection Software. Actograms were created using El Temps (Diez-Noguera, Barcelona, 1999; upper limit 5). For compiling daily activity profiles the raw data of day 2–7 were first averaged for every single fly in each photoperiod. Then the data were averaged across all entrained flies of each genotype. To smooth out short-term fluctuations (noise) from the raw datasets we applied a moving average of 11, i.e., each group of 11 consecutive data points was averaged to a new value. To optimally depict differences in the shape of the evening activity the data were finally normalized by the respective highest activity value in each genotype and photoperiod resulting in relative activity values. Additionally, we averaged the normalized LD 12:12 activity data of the last 6 hours of the light-phase into 1h-bins (b_{-6} to b_{-1} ; the index indicates the location relative to the light-to-dark transition) for each single fly and averaged them across each genotype. These data were depicted as overlays of line charts. Then we tested the relative amplitudes of the last two 1h-bins (b_{-2} and b_{-1}) of each genotype for significant differences.

Period lengths in DD were calculated by χ^2 -periodogram analysis.

Statistics

Data were tested for normal distribution by a one-sample Kolmogorov–Smirnov test (Lilliefors). Normally distributed data were statistically compared by a one-way analysis of variance (ANOVA) followed by a post-hoc test with Bonferroni correction for pairwise comparison. Not normally distributed data were compared by a Kruskal–Wallis test followed by Wilcoxon analysis (Systat 11, SPSS, Chicago, IL) with Bonferroni correction. Data were regarded as significantly different at $P < 0.05$ and as highly significant at $P < 0.001$.

RESULTS

NPF is expressed in subsets of LN_ds and l-LN_vs and in the fifth s-LN_v in both male and female adult flies

To confirm previous studies of *npf* distribution in the adult CNS (Lee et al., 2006; Johard et al., 2009), we expressed GFP with the very same *npfGal4* line that Lee et al. (2006) and Johard et al., (2009) had used in past studies. We detected all *npf*-positive cell groups in male adult brains that had been reported previously, and denominated them according to Lee et al. (2006) (Fig. 2A). To identify *npf*-positive clock neurons, we performed immunocytochemistry on GFP-expressing brains with anti-TIM and nb33 (against the precursor of PDF) at ZT 21, when the TIM level is at its maximum. We confirmed that the *npf*-positive L1-s group represents three of the six LN_ds, showing a colocalization of anti-TIM and GFP (Fig. 2B; Table 2). In some cases we could even observe four LN_ds expressing GFP (Fig. 2B1). Surprisingly, we additionally found colocalizations of GFP and anti-TIM staining in other clock cells: the fifth s-LN_v and 1–2 l-LN_vs, which have not been previously reported to be *npf*-positive (Fig. 2B; Table 2). To test whether the NPF peptide is indeed present in the *npfGal4*-expressing clock neurons, we additionally stained whole mounts of male wildtype brains with an anti-NPF antibody, which was raised against a 36-residue synthetic *Drosophila* NPF (Fig. 2C–E). The staining pattern of the antibody was very similar to the GFP expression driven by *npfGal4*, except for some stronger stained varicosities and axon terminals throughout the whole brain (Fig. 2C), suggesting the specificity of both the antibody and the *Gal4* line. In a triple staining with anti-NPF, anti-TIM, and nb33, on average three LN_ds were double-labeled with NPF and TIM antibodies (Fig. 2D; Table 2). The fifth s-LN_v was NPF-positive in almost all investigated brains, as were about 3–4 of the l-LN_vs (Fig. 2E; Table 2). Usually the LN_ds and the fifth s-LN_v showed a stronger NPF signal than the l-LN_vs, indicating that they contain more NPF peptide. In general, the clock neurons were stained weakly by anti-NPF compared

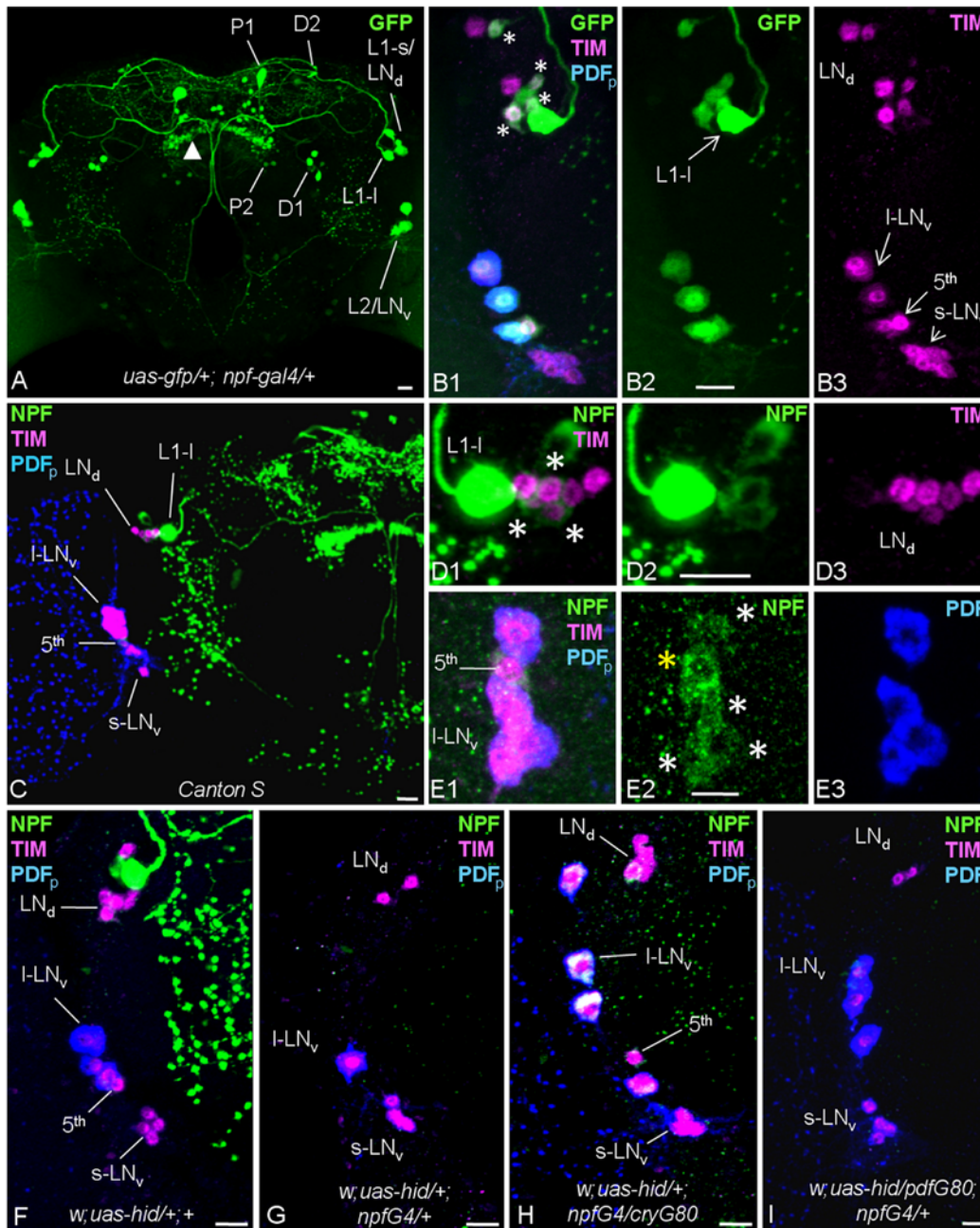


Figure 2. NPF expression pattern in adult male *D. melanogaster* brains. NPF distribution was investigated both by *npfGal4*-driven GFP expression (A,B) and antibody staining with anti-NPF (C–E). A: GFP was expressed in several cells in the central (D1, D2, P1, P2) and lateral (L1-I, L1-s, L2) part of the brain, as well as in the fan-shaped body (white arrowhead). B: A double labeling with anti-TIM (magenta) and nb33 (against the precursor of PDF (PDFp); blue) antibodies on GFP (green)-expressing brains revealed that 3–4 LN_ds (white stars), the fifth PDF-negative s-LN_v and 1–3 I-LN_vs express *npf*. C: The staining pattern with anti-NPF antibody (green) was comparable to the GFP expression, except for some stronger stained fibers and axon terminals. D: In a triple labeling together with anti-TIM (magenta) and nb33 (blue) the anti-NPF antibody stained three of the six LN_ds (white stars). The staining of the clock neurons was weaker than that of the non-clock cells, e.g., the L1-I, which is located closely to the LN_ds. E: The fifth s-LN_v was labeled with anti-NPF as well as 3–4 of the I-LN_vs (yellow and white stars, respectively). LN cell numbers in male fly brains after cell ablation and rescue were determined by anti-NPF, anti-TIM and nb33 staining (F–I). Wildtype cell numbers of clock neurons (F) were severely reduced in *uas-hid/+; npfGal4/+*-flies (G). The fifth s-LN_v was ablated in all brains, as well as 3–4 of the six LN_ds and 2–3 I-LN_vs. All *npf*-positive non-clock cells were ablated in these flies. Expression of *cryGal80* in *uas-hid/+; npfGal4/+*-flies rescued all clock neurons (H), expression of *pdfGal80* rescued only the I-LN_vs (I). Scale bars = 10 μm.

TABLE 2.
Mean Numbers of NPF-Positive Clock Neurons in Male and Female Adult Brains

	Males		Females	
	GFP <i>uas-gfp/npfG4</i> <i>n</i> = 11	Anti-NPF <i>Canton S</i> <i>n</i> = 17	GFP <i>uas-gfp/npfG4</i> <i>n</i> = 13	Anti-NPF <i>Canton S</i> <i>n</i> = 17
I-LN _v	1.6 ± 0.6	3.2 ± 0.7	1.4 ± 0.6	2.7 ± 0.6
fifth s-LN _v	1.0 ± 0	1.0 ± 0.1	1.0 ± 0	1.0 ± 0
LN _s	3.5 ± 0.5	3.0 ± 0.8	1.5 ± 0.3	2.7 ± 0.4

Values represent mean cell number ± SD per brain hemisphere. *n* indicates the number of examined brains.

TABLE 3.
Mean Numbers of Remaining Clock Neurons in Male and Female Adult Brains After Ablation of NPF or PDF Neurons

		<i>w; hid/+</i>	<i>w; hid/+;</i>	<i>w; hid/+;</i>	<i>w; hid/pdfG80;</i>	<i>w; hid/</i>	<i>w; hid/pdfG4;</i>
		<i>control</i>	<i>npfG4/+</i>	<i>npfG4/cryG80</i>	<i>npfG4/+</i>	<i>pdfG4; +</i>	<i>npfG4/+</i>
		<i>m n</i> = 10	<i>m n</i> = 10	<i>m n</i> = 16	<i>m n</i> = 15	<i>m n</i> = 8	<i>m n</i> = 11
		<i>fem n</i> = 8	<i>fem n</i> = 6	<i>fem n</i> = 15			
Males	I-LN _v	3.9 ± 0.2	2.1 ± 0.7	4.1 ± 0.3	3.8 ± 0.6	0 ± 0	0 ± 0
	fifth s-LN _v	1.0 ± 0.3	0	1 ± 0	0 ± 0.1	1 ± 0	0 ± 0
	LN _s	6.0 ± 0	2.2 ± 0.4	5.9 ± 0.2	2.0 ± 0	5.6 ± 0.4	2.1 ± 0.6
	s-LN _v	—	—	—	—	0 ± 0	0 ± 0
Females	I-LN _v	3.9 ± 0.2	3.1 ± 0.2	4.0 ± 0.4	—	—	—
	fifth s-LN _v	0.9 ± 0.2	0	1.0 ± 0	—	—	—
	LN _s	5.9 ± 0.2	3.8 ± 0.4	5.9 ± 0.2	—	—	—

Values represent mean cell number ± SD per brain lobe. *m n* and *fem n* indicate the number of examined male or female brains, respectively. —, not investigated.

to the other NPF-positive non-clock cells, e.g., the L1-I that is located in close proximity to the LN_s (Fig. 2D).

We additionally investigated the NPF expression in brains of adult female flies by the same methods that were used in male flies. Both *npfGal4*-driven GFP expression and anti-NPF staining revealed NPF expression in subsets of the LN_s and I-LN_vs and in the fifth s-LN_v. We found that, on average, females express NPF in one less LN_s and one less I-LN_v than males (Table 2).

Cry- and pdf-specific Gal80 mediate the rescue of certain clock neurons in *npf*-ablated flies

It has been reported that the *npfGal4*-driven expression of the apoptotic gene *reaper* leads to the ablation of all *npf*-expressing cells, including three LN_s, except for a few neurons with projections in the central complex (Lee et al., 2006). Recently, it has been suggested further by Hamasaka et al. (2010) that the *npfGal4*-driven expression of *hid* possibly also ablates the fifth s-LN_v. To investigate the function of the NPF neurons in the clock network of *Drosophila*, we ablated *npf*-positive cells using a *uas-hid*-construct that was expressed by the same *npfGal4* line. Immunocytochemical staining with anti-NPF, anti-TIM, and nb33 on whole mounts of male *w; uas-hid/+; npfGal4/+*-flies (later also referred to as *npf*-ablated flies) verified the successful ablation of all NPF cells, except for

some remaining cell body fragments of large NPF-positive non-clock cells in the central part of the brain. The fifth s-LN_v was ablated in all investigated brains. On average, two of the LN_s and two of the I-LN_vs remained intact in *npf*-ablated flies, indicating the ablation of 4 LN_s and 2–3 I-LN_vs (Fig. 2G; Table 3). The same was observed in female flies, except for slight differences in intact LN_s and I-LN_v cell numbers according to the differing *npf* expression (Table 3).

To restrict cell ablation to the *npfGal4*-expressing non-clock cells, we additionally introduced a *cryGal80*-construct, which is expressed in most clock neurons, including the NPF-positive ones, and consequently represses *Gal4*-function in these cells (Stoleru et al., 2004). Due to its strong promoter activity the expression pattern of the *cryGal80* line does not completely match the actual presence of the CRY protein (Yoshii et al., 2008). Thus, all six LN_s express *Gal80*, although only three of them are in fact CRY-positive. In both male and female *uas-hid/+; npfGal4/cryGal80* flies (hereafter also referred to as *cryGal80*-rescued flies) all subsets of clock neurons were present with wildtype cell numbers, according to the expression pattern of this *cryGal80* line, whereas the non-clock neurons, e.g., the L1-I, were ablated (Fig. 2H; Table 3).

To further dissect the function of different subsets of *npf*-expressing clock neurons, we combined *w; uas-hid/+; npfGal4/+*-flies with a *pdfGal80*-construct that prevents the ablation of the PDF neurons (Stoleru et al., 2004). *W;*

uas-hid/pdfGal80; npfGal4/+ male flies (from now on also referred to as *pdfGal80*-rescued flies) showed normal cell numbers in I-LN_vs but the fifth s-LN_v, the *npf*-positive LN_ds and all *npf*-expressing non-clock cells, were successfully ablated (Fig. 2I; Table 3).

Npf-ablated flies exhibit abnormalities in the shape of their evening activity bout in light-dark cycles

In LD cycles wildtype *D. melanogaster* flies depict a typical diurnal locomotor activity profile with an anticipatory morning and evening peak around lights-on and -off, respectively. To investigate the contributions NPF cells make to this rhythmic behavior, we tested the locomotor activity of *npf*-ablated flies in LD cycles in comparison to control flies containing either the *uas*- or the *Gal4*-construct (*w; uas-hid/+; +* and *w; +; npfGal4/+*) alone. In equinox or LD 12:12 the evening activity bout of *npf*-ablated flies was shaped differently in comparison to control flies, confirming previous observations made by Lee et al. (2006). The activity of both control genotypes increased linearly from the middle to the end of the light-phase, followed by a characteristic strong burst of activity, a so-called startle response, as a reaction to lights-off (Fig. 3A1,B1). *Npf*-ablated flies also showed an increase in activity from midday onwards, indicating that the onset of the evening activity was not different from control flies (Fig. 3C1). However, the late evening activity of *npf*-ablated flies was reduced in amplitude in comparison to control flies, resulting in an activity plateau before lights-off. Therefore, *npf*-ablated flies reached their maximum activity level earlier than control flies. To investigate this effect in detail, we tested the flies in a prolonged photoperiod with 16 hours of light (LD 16:08), in which wildtype flies clearly exhibit their evening peak before lights-off without interfering masking effect (Rieger et al., 2003). In LD 16:08, *npf*-ablated flies reached their maximum activity in the evening earlier than control flies and the activity plateau was more pronounced (Fig. 3A2–C2). In addition, we examined the LD 12:12 data in a 1h-resolution, confirming that *npf*-ablated flies have a reduced relative evening activity amplitude in comparison to control flies (Fig. 3D). By comparing the last two 1h-bins before the light-to-dark transition (b_{-1} and b_{-2}), we show that both control lines still show a significant increase in activity within 2 hours before lights-off, while *npf*-ablated flies do not (Fig. 3E), clearly indicating that the evening activity of *npf*-ablated flies had already reached its peak 2 hours before lights-off and remains then at the same level until lights-off.

We also investigated the behavior of *npf*-ablated females and found a comparable phenotype with slightly advanced and reduced evening activity peak in both LD 12:12 and LD 16:08 (data not shown).

Npf-positive clock neurons influence the shape of the evening activity

To investigate whether the observed effect on the evening activity derived from the ablation of the *npf*-positive clock neurons or non-clock neurons, we tested *cryGal80*-rescued flies, in which all clock neurons were excluded from the cell ablation, under the same conditions as *npf*-ablated flies. They exhibited the same gradual increase in activity before lights-off in LD 12:12 as the corresponding control flies (Fig. 4A1,B1,C,D). When we investigated the behavior of the flies in the longer photoperiod (LD 16:08), the shape of the evening activity bout in *cryGal80*-rescued flies appeared also very similar to control flies, with the presence of a clear peak of evening activity rather than a flat plateau, as in *npf*-ablated flies (Fig. 4A2,B2,E). The activity of *cryGal80*-rescued flies still increases significantly within 2 hours before lights-off (Fig. 4F), indicating that the activity level in the late evening is not reduced, as we had observed in *npf*-ablated flies. Thus, the wildtype-like evening activity was fully restored by the rescue of all clock neurons, indicating that the phenotypes observed in *npf*-ablated flies derived from the ablation of the *npf*-positive clock neurons.

Investigation of LD behavior in female *cryGal80*-rescued flies gave the same results as in male flies, indicating that female fly wildtype evening activity could also be restored by the rescue of the *npf*-positive clock neurons (data not shown).

Ablation of the fifth s-LN_v and the npf-positive LN_ds cause a reduction in the evening peak amplitude

To further dissect the function of different subsets of *npf*-expressing clock neurons, we investigated the LD behavior of *pdfGal80*-rescued flies, in which only the *npf*-positive I-LN_vs were rescued from the cell ablation. In contrast to *cryGal80*-rescued flies, the *pdfGal80*-mediated rescue was not sufficient to completely restore normal evening activity. In LD 12:12 *pdfGal80*-rescued flies also showed a small activity plateau in the very late evening (Fig. 5B1, compare to controls Fig. 5A1,C,D). However, this effect was not as pronounced as was observed in *npf*-ablated flies, as there was still a significant increase in activity within 2 hours before lights-off in *pdfGal80*-rescued flies (Fig. 5F, compare to Fig. 3C1,E). In LD 16:08 the evening activity of *pdfGal80*-rescued flies became clearly comparable to *npf*-ablated flies, which had shown the same activity plateau in this photoperiod (Fig. 5B2, compare to Fig. 3C2). The relative amplitude of the evening activity in *pdfGal80*-rescued flies was reduced, as we had observed in *npf*-ablated flies (see for LD 12:12, Fig. 5E). This indicates that the reducing effect on the activity amplitude in the late evening derives from the ablation of the *pdf*-negative, *npf*-positive clock neurons.

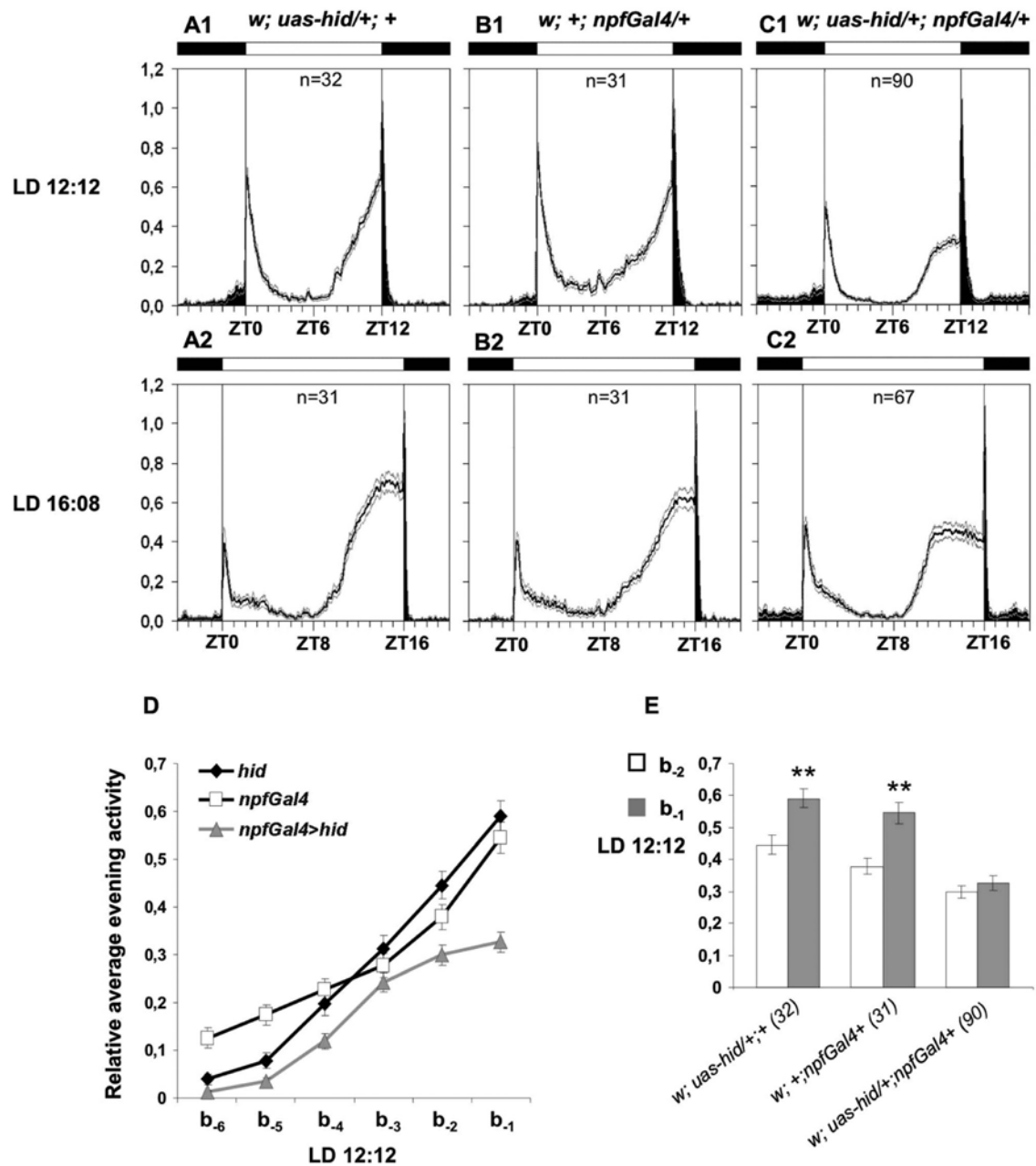


Figure 3. Activity data of *npf*-ablated flies and *uas/Gal4*-controls in LD 12:12 and LD 16:08. Flies were recorded subsequently for 7 days in each photoperiod and activity data were collected in 1-minute-bins. Data of days 2–7 were averaged for every single fly in each photoperiod and were further averaged over all flies of each genotype and smoothed by a moving average of 11. Data were normalized by the highest level of activity in each genotype and photoperiod resulting in relative activity values. Average activity profiles of control flies in LD 12:12 show normal evening anticipatory behavior with a gradual increase in activity before lights-off (A1,B1). The evening activity bout of *npf*-ablated flies, however, is clearly flattened and reduced in amplitude before lights-off (C1). In LD 16:08 the difference between controls (A2,B2) and *npf*-ablated flies (C2) was even more obvious. Normalized activity data of LD 12:12 were further averaged into 1h-bins for each genotype to depict differences in the last 6 hours before the light-to-dark transition (b_{-6} to b_{-1} , D). Comparison of the last two 1h-bins before lights-off (b_{-1} and b_{-2}) gave highly significant differences in control flies ($P < 0.001$), but not in *npf*-ablated flies (E). Black lines in A–C represent mean relative activity, gray lines represent SEM. Light regimes are depicted by black and white bars. Error bars in D,E represent SEM. Highly significant differences are indicated by **. Numbers in brackets in E indicate n .

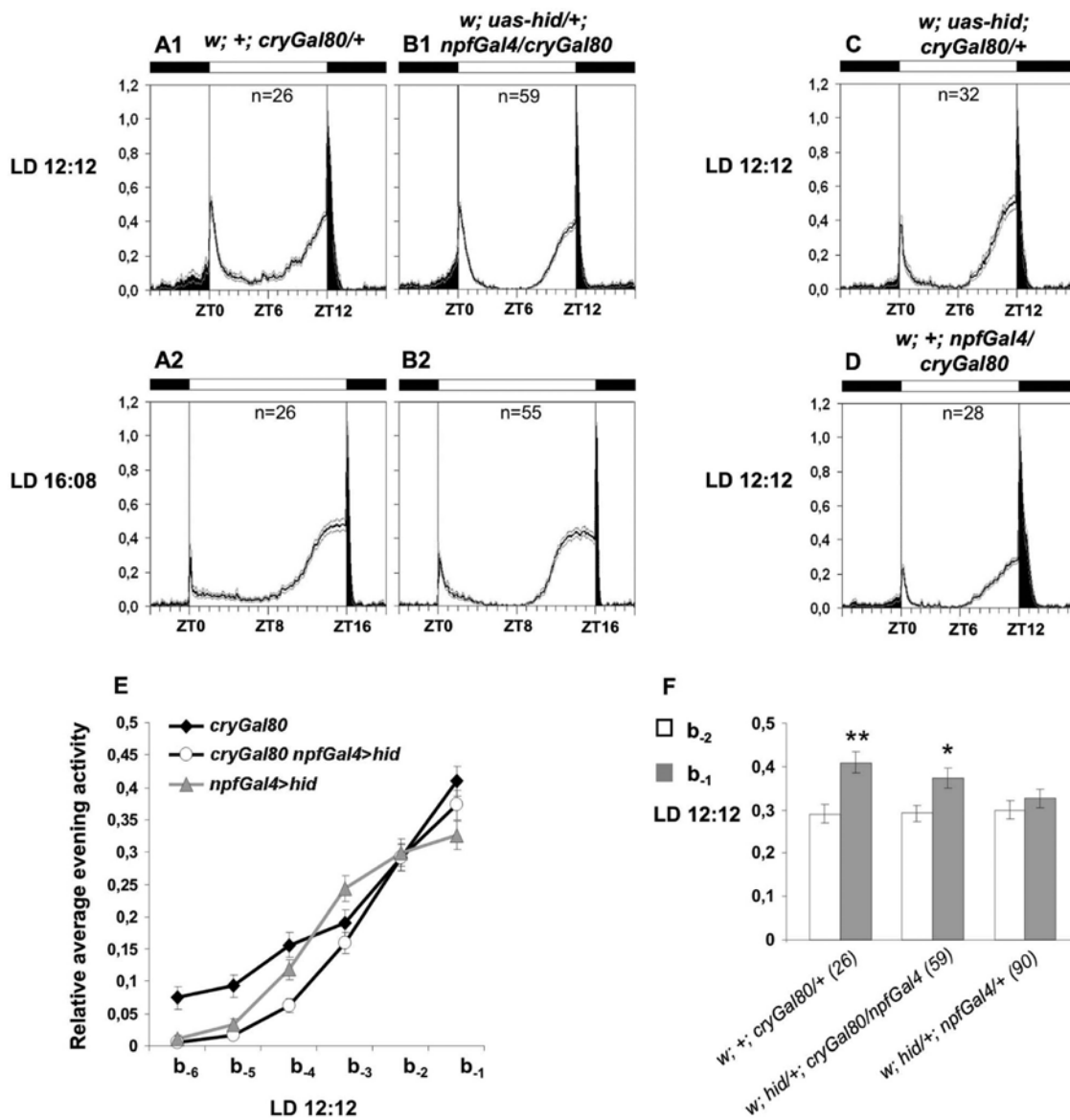


Figure 4. Activity data of *cryGal80* rescued flies and respective controls in LD 12:12 and LD 16:08. Activity data were processed as in Figure 3. In LD 12:12 all control flies (A1,C,D) and *w; uas-hid/+; npfGal4/cryGal80*-flies (B1) showed normal evening behavior, indicating that the action of *cryGal80* fully restored wildtype-like evening activity. The same was true for LD 16:08 (control A2, *cryGal80*-rescue B2). The shape of the evening activity bout and the relative amplitude in *cryGal80*-rescued flies was not different from control flies in the last 6 hours before the light-to-dark transition in LD 12:12, but from *npf*-ablated flies (E). In contrast to *npf*-ablated flies the activity of *cryGal80*-rescued flies was still significantly increasing ($P < 0.05$) within 2 hours before lights-off, as was the case in control flies ($P < 0.001$, F). Black lines in A–D represent mean relative activity, gray lines represent SEM. Light regimes are depicted by black and white bars. Error bars in E,F represent SEM. Significant differences are indicated by *, highly significant differences by **. Numbers in brackets in F indicate *n*.

Simultaneous ablation of *npf*- and *pdf*-positive neurons advances and slightly reduces evening activity in LD

Since it was shown by Renn et al. (1999) that the ablation of all *pdf*-positive neurons advances the phase of the

evening activity in LD-cycles just like in *Pdf^{D1}* mutant flies, we wondered after the above-described observations what effects a simultaneous ablation of *npf*- and *pdf*-positive neurons would have on the phase of the evening activity. We first expressed *hid* with a *pdfGal4* line, which

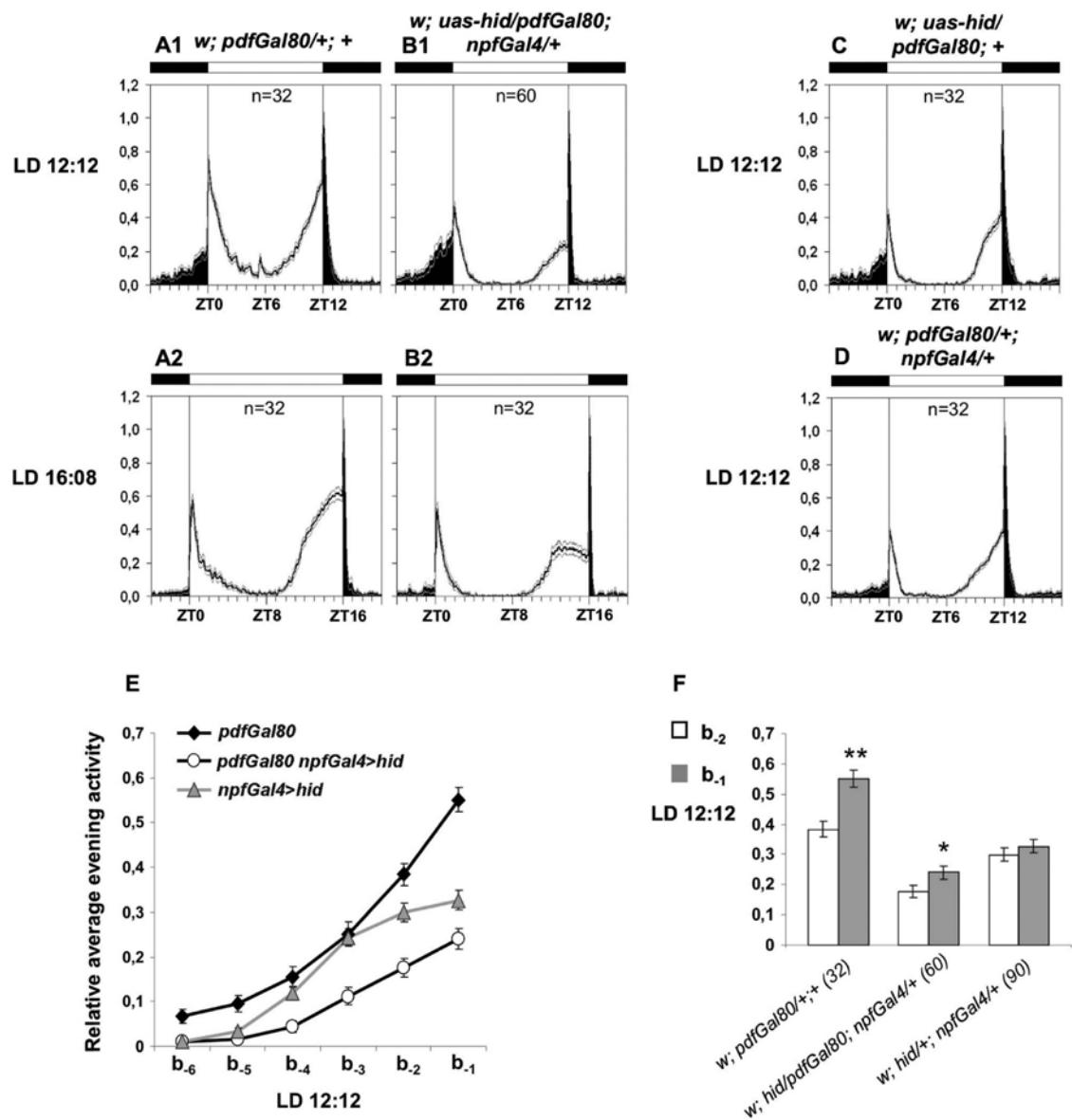


Figure 5. Activity data of *pdfGal80* rescued flies and respective controls in LD 12:12 and LD 16:08. Activity data were processed as in Figure 3. In LD 12:12 all control flies showed normal evening behavior (A1,C,D), whereas the evening activity bout in *pdfGal80*-rescued flies, although quite normally shaped, was reduced in relative amplitude (B1). In LD 16:08 control flies behaved normal (A2). *pdfGal80*-rescued flies (B2) showed, however, an evening activity plateau comparable to *npf*-ablated flies (Fig. 3, C2). Within the last 6 hours before the light-to-dark transition in LD 12:12 the relative activity of *pdfGal80*-rescued flies was reduced compared to control flies, but not differently shaped, as was the case in *npf*-ablated flies (E). The activity significantly increased within the last 2 hours before lights-off in *pdfGal80*-rescued flies ($P < 0.05$, F). Black lines in A–D represent mean relative activity, gray lines represent SEM. Light regimes are depicted by black and white bars. Error bars in E,F represent SEM. Significant differences are indicated by *, highly significant differences by **. Numbers in brackets in F indicate n .

led to the ablation of all *pdf*-positive neurons (Table 3), and investigated the flies' behavior in LD cycles. We confirmed that *pdf*-ablated flies (*w; uas-hid/pdfGal4; +*) clearly advance the phase of the evening activity in LD

12:12 (Fig. 6C1,E). This became even more obvious in LD 16:08 (Fig. 6C2). In contrast to *npf*-ablated flies, the relative amplitude of the evening activity, however, was not reduced (Fig. 6E). When we additionally expressed *hid* in

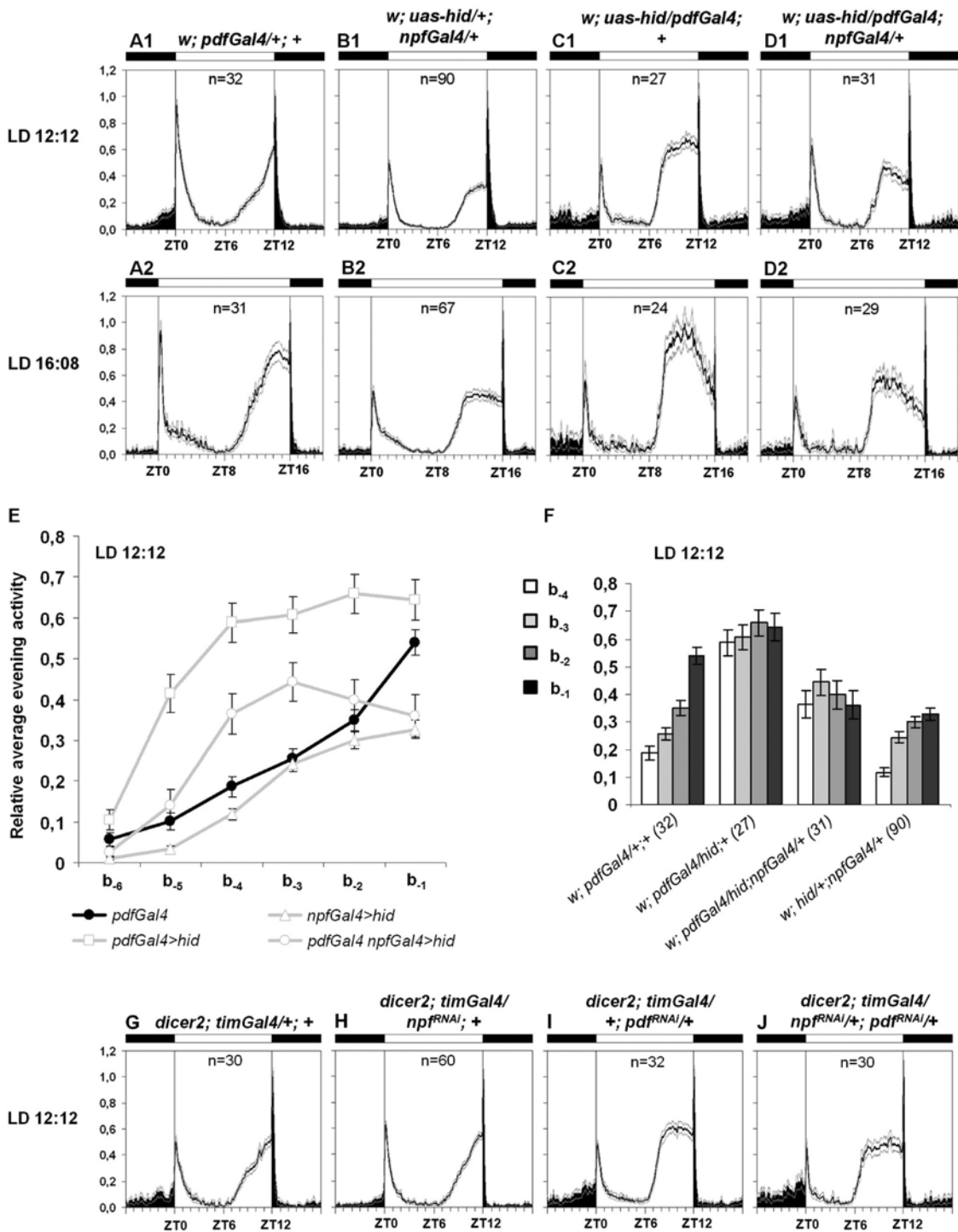


Figure 6

the *npf*-expressing neurons (*w; uas-hid/pdfGal4; npfGal4/+*, also referred to as *npf/pdf*-ablated flies), all lateral clock neurons, except for two *npf*-negative LN_s and the LPNs were ablated (Table 3). Already in LD 12:12, the evening activity of these flies even decreased before lights-off after reaching a peak (Fig. 6D1), indicating that the phase of the evening activity was even more advanced compared to *pdf*-ablated flies. In LD 16:08 the evening activity peak of *npf/pdf*-ablated flies (Fig. 6D2) occurred also clearly earlier than the peak of *pdf*-ablated flies (Fig. 6C2). In addition, the relative amplitude of the evening activity in *npf/pdf*-ablated flies was reduced in comparison to *pdf*-ablated flies (Fig. 6E,F).

Simultaneous knockdown of *pdf* and *npf* advances and slightly reduces evening activity in LD

To investigate the action of NPF in the above-described observations, we used a *uas-npf^{RNAi}*-construct and expressed it in combination with a *w; tim(uas)Gal4; +* and a *dicer2; +; +* line to knock down *npf* expression in the clock neurons. We checked the knockdown on the protein level by staining with anti-NPF and found that NPF was not reduced to an undetectable level (data not shown). As expected, we did not find any effect in LD behavior in *dicer2; timGal4/npf^{RNAi}; +* flies (also referred to as *npf*-knockdown flies, Fig. 6H). As Shafer et al. (2009) had described previously, *pdf* expression can be nearly completely knocked down by the expression of a *uas-pdf^{RNAi}*-construct in combination with *w; tim(uas)Gal4; +* and *dicer2; +; +*, which leads to a phenocopy of *Pdf⁰¹* mutant behavior. We used the same fly lines to knock down *pdf* expression in the clock neurons and found that PDF protein levels were reduced to an immunocytochemically undetectable level (data not shown). *Dicer2; timGal4/+; pdf^{RNAi}* flies (also referred to as *pdf*-knockdown flies) showed a clearly advanced phase of the evening activity peak in LD 12:12 (Fig. 6I, compare to controls Fig. 6G), which was comparable to *pdf*-ablated flies (Fig. 6C1).

Although the *npf* knockdown was incomplete, we additionally examined flies in which the *npf^{RNAi}*- and the

pdf^{RNAi}-constructs were expressed simultaneously (*dicer2; timGal4/npf^{RNAi}; pdf^{RNAi}/+*, also referred to as *npf/pdf*-knockdown flies). These flies also showed a complete reduction in PDF but not in NPF immunoreactivity. However, in LD 12:12 the evening activity peak of *npf/pdf*-knockdown flies was different from *pdf*-knockdown flies: it appeared broader and flatter (Fig. 6J, compare to Fig. 6I).

Ablation of the *npf*-positive clock neurons prolongs the free-running period in DD

To investigate whether the ablation of the NPF cells affects the internal free-running period of the flies' endogenous clock, we recorded their locomotor activity in constant darkness (DD) after entraining them to a standard LD 12:12 cycle. Most of the *npf*-ablated flies showed clear free-running rhythms in DD (Fig. 7C, compare to controls Fig. 7A,B, Table 4), but χ^2 -periodogram analysis revealed that they had a significantly prolonged free-running period compared to control flies ($P < 0.001$; Fig. 7J).

To determine again whether this effect derived from the ablation of the *npf*-positive clock neurons or the non-clock neurons, we rescued the clock neurons with *cryGal80*- and *pdfGal80*-constructs. The free-running period of *cryGal80*-rescued flies was significantly shorter than the period of *npf*-ablated flies ($P < 0.05$) and even shorter than in both corresponding controls (*w; uas-hid/+; cryGal80/+* and *w; +; npfGal4/cryGal80*; $P < 0.05$; Fig. 7D–F,K). This indicates that the prolongation of the period in *npf*-ablated flies was caused by the absence of the NPF-positive clock neurons, as the *cryGal80*-mediated rescue of these cells did not show a prolonged period any more. In contrast to that, the *pdfGal80*-mediated rescue of the *npf*-positive I-LN_s did not have the same effect. The free-running period of *pdfGal80*-rescued flies was not significantly different from the period of *npf*-ablated flies but was also not significantly different from one of the controls (Fig. 7I,L, compare to controls Fig. 7G,H), indicating that the rescue of the I-LN_s was not sufficient to completely abolish the free-running phenotype.

We additionally examined the free-running behavior of female *npf*-ablated flies and found that they similarly have

Figure 6. LD activity data of *npf*- and *pdf*-ablated flies with respective controls and RNA-interference (RNAi) experiments. Activity data were processed as in Fig. 3. Compared to control flies (A1,A2) *npf*-ablated flies showed a slightly advanced evening activity with a flattened plateau before lights-off in both LD 12:12 and LD 16:08 (B1,B2, see also Fig. 3C1,C2). *Pdf*-ablated flies clearly advanced the phase of the evening peak in both photoperiods (C1,C2). When both *npf* and *pdf*-expressing neurons were ablated simultaneously, the phase of the evening activity was even more advanced (D1,D2). The relative evening activity of *pdf*-ablated flies was not reduced in amplitude in contrast to *npf*-ablated and *npf/pdf*-ablated flies in LD 12:12 (E,F). Compared to control flies (G) the evening peak phase was unchanged in flies expressing an *npf^{RNAi}*-construct (H) and *dicer2* in the clock neurons. The evening peak phase, however, was clearly advanced, when *pdf* expression was knocked down by RNAi (I). When *npf* expression was simultaneously knocked down with *pdf* (J), flies showed an even broader evening activity bout, which was flattened in amplitude. Black lines in A–D,G–J represent mean relative activity, gray lines represent SEM. Light regimes are depicted by black and white bars. Error bars in E,F represent SEM.

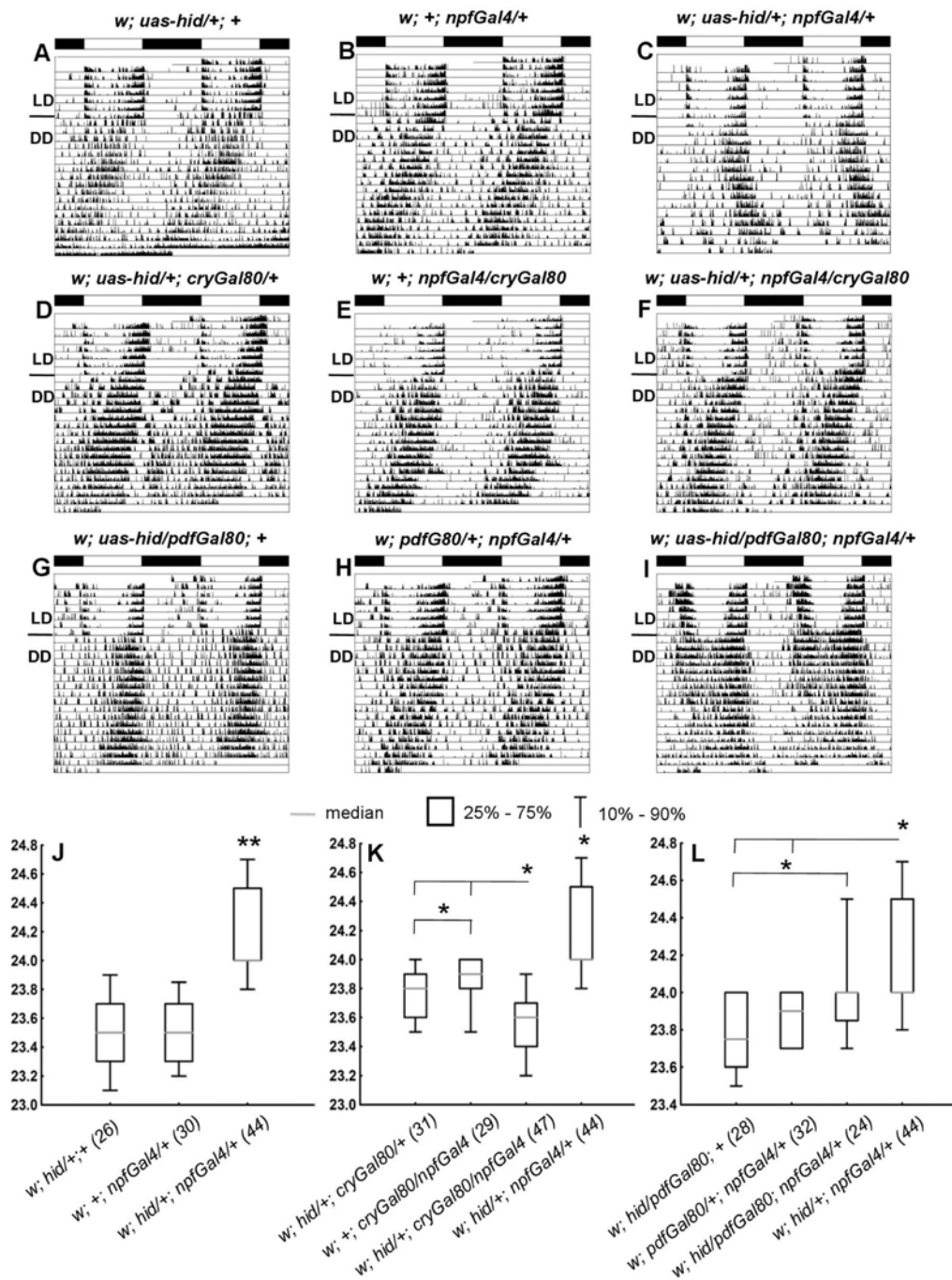


Figure 7. Free-running rhythms of *npf*-ablated and *Gal80*-rescued flies in constant darkness (DD). Flies were recorded in an LD 12:12 cycle for 7 days and subsequently in DD for at least 14 days. Experiments were conducted at a light intensity of 100 lux in LD and at 20°C. Representative single actograms are depicted as double-plots for different *uas/Gal4*-controls (A,B,D,E,G,H) and ablation genotypes (C,F,I). Boxplots show free-running periods in DD for the three different ablation genotypes with respective controls. *W; uas-hid/+; npfGal4/+*-flies showed a significantly prolonged free-running period in comparison to their respective *uas/Gal4*-controls (C,J). When all clock neurons were excluded from the cell ablation by the action of *cryGal80*, the free-running period was not prolonged compared to control flies (K). *PdfGal80*-mediated rescue of only the I-LN_s was not sufficient to abolish the free-running phenotype of *npf*-ablated flies (L). Bars above the actograms depict the light regime of the LD 12:12 cycle. Gray lines in J-L represent the median, boxes 25-75%, and whiskers 10-90% of the data. Significant differences are indicated by *, highly significant differences by **. Numbers in brackets in J-L indicate *n*.

TABLE 4.
Rhythmicity of All Investigated Genotypes in Constant Darkness (DD) According to Chi²-Periodogram Analysis

		<i>n</i>	Power in DD mean (SEM)	% rhythmic	Period in DD mean (SEM)
Males	<i>w; uas-hid/+; +</i>	26	29.3 (1.07)	100	23.5 (0.05)
	<i>w; +; npfG4/+</i>	30	29.5 (1.64)	96.8	23.5 (0.05)
	<i>w; uas-hid/+; npfG4/+</i>	44	34.8 (1.80)	91.7	24.2 (0.06)
	<i>w; uas-hid/+; cryG80/+</i>	31	49.6 (2.55)	96.9	23.7 (0.03)
	<i>w; +; npfG4/cryG80</i>	29	59.7 (2.26)	100	23.9 (0.03)
	<i>w; uas-hid/+; npfG4/cryG80</i>	47	47.7 (2.07)	97.9	23.6 (0.04)
	<i>w; uas-hid/pdfG80; +</i>	28	31.8 (2.24)	87.5	23.8 (0.05)
	<i>w; pdfG80/+; npfG4/+</i>	32	35.1 (1.91)	100	23.8 (0.03)
	<i>w; uas-hid/pdfG80; npfG4/+</i>	24	30.5 (2.28)	82.8	24.0 (0.06)
	Females	<i>w; uas-hid/+; +</i>	31	26.9 (1.6)	96.9
<i>w; +; npfG4/+</i>		25	22.3 (1.3)	87.5	24.1 (0.09)
<i>w; uas-hid/+; npfG4/+</i>		24	35.6 (2.2)	90	24.4 (0.05)
<i>w; uas-hid/+; npfG4/cryG80</i>		23	29.4 (2.3)	85.7	23.8 (0.8)

n indicates the number of investigated flies for each genotype. Power and period values were averaged over all rhythmic flies for each genotype.

a significantly prolonged period in DD, which can be rescued by the action of *cryGal80* (Table 4).

In general, all investigated genotypes were rhythmic in DD, indicating that the ablation of all NPF cells or subsets of them did not influence the rhythmicity of the flies (Table 4).

DISCUSSION

In the present study we have revealed the functional contribution of the *npf*-expressing neurons to *Drosophila*'s circadian behavior. We newly identified subsets of the I-LN_vs as well as the fifth s-LN_v as NPF-positive in both male and female flies, adding to the three NPF-positive LN_ds described by Lee et al. (2006). We found that *npf*-ablated flies of both sexes show a significantly prolonged free-running period in DD, a slightly advanced evening peak phase, and reduced evening peak amplitude. We showed that all phenotypes can be restored by *cryGal80*-mediated clock neuronal rescue; however, not by *pdfGal80*-mediated rescue of I-LN_vs, indicating that the fifth s-LN_v and the NPF-positive LN_ds are responsible for the observed effects. We further showed that the simultaneous ablation of *npf* and *pdf*-expressing neurons has additive effects, resulting in an evening peak phase that is even more advanced than in *pdf*-ablated flies and reduced in amplitude. Finally, we demonstrated that the simultaneous knockdown of *npf* and *pdf* leads to a similar phenotype suggesting that the observed effects are caused by the two peptides.

NPF is newly identified in the fifth s-LN_v and in subsets of the I-LN_vs in both male and female flies

In 2006, Lee et al. characterized the distribution of the NPF neurons in the brain of adult flies by utilizing *Gal4*-driven GFP-expression, in situ hybridization, and antibody staining to identify three of the six LN_d clock neurons as NPF-positive

in male flies. We confirmed these data, but additionally found NPF in the fifth s-LN_v as well as in a rather variable number of I-LN_vs (mostly 1–3 neurons). Since we obtained the same reproducible results with *npfGal4*-driven GFP expression and anti-NPF staining, it is most likely that these findings are indeed true. The staining intensity with the NPF antibody is rather weak, especially in the I-LN_vs, suggesting why they had not been discovered by previous studies to be NPF-positive. We also newly identified NPF expression in the fifth s-LN_v and in a subset of the I-LN_vs in female flies, and found that NPF is on average present in two LN_ds, i.e., in one LN_d more than was previously reported (Lee et al., 2006).

We show here that the expression of *hid* with *npfGal4* leads to the ablation of all NPF neurons, including all *npf*-positive clock neurons in both male and female flies. Recently, however, Hamasaka et al. (2010) found only an inconstant ablation of the fifth s-LN_v and no ablation of the I-LN_vs in *uas-hid/+; npfGal4/+*-flies, although they used the same *npfGal4* line. A reason for that might be that we used a *uas-hid/CyO* line (*w; uas-hid¹⁴/CyO*; Zhou et al., 1997) different from the one Hamasaka et al. (2010) used (*y w; uas-hid/CyO*; Renn et al., 1999) and ours might induce cell death more strongly.

Since *npfGal4* specifically covers subsets of the lateral clock neurons different from other clock-specific *Gal4*-drivers, such as *pdfGal4*, *cryGal4* and some recently characterized new *Gal4* lines (Emery et al., 2000; Park et al., 2000; Gummadova et al., 2009; Zhang et al., 2010), we regarded the *npfGal4* line as a useful tool to inquire the role of the *npf*-positive subset of clock neurons in circadian behavior.

Npf-positive fifth s-LN_v and LN_ds promote activity late in the day and influence the free-running period in DD

Lee et al. (2006) stated that the ablation of all NPF neurons by *reaper* expression affects the timing and

shape of the evening activity bout in male flies. It was, however, not clear in this previous study whether this phenotype derived from the ablation of the *npf*-positive clock neurons or non-clock neurons. We were able to rescue this evening peak phenotype by the expression of *cry-Gal80* and the subsequent rescue of all clock neurons, and therefore demonstrated that the observed phenotype was clearly due to the ablation of the *npf*-positive clock neurons. The rescue of the I-LN_vs with *pdfGal80*, however, still showed a reduction in the evening peak amplitude, indicating the importance of the *pdf*-negative NPF neurons—the fifth s-LN_v and the LN_ds—to promote activity late in the day. This fits into previous findings that the CRY-positive LN_ds as well as the fifth s-LN_v control evening activity in *Drosophila*'s circadian behavior (Grima et al., 2004; Stoleru et al., 2004; Rieger et al., 2006; Picot et al., 2007). *Npf*-positive and CRY-positive LN_ds overlap, however, in only one cell (Yoshii et al., 2008; Rieger et al., 2009), meaning that following cell ablation two putative evening cells remain intact, which are probably enough to promote some level of evening activity, albeit probably not at an amplitude consistent with wildtype activity levels. Interestingly, we found the same phenotypes in LD in female *npf*-ablated flies, in contrast to what was reported by Lee et al. (2006). This indicates that the effect on the evening activity is not sex-specific and might therefore not be due to alterations in courtship activity, as proposed by Lee et al. (2006).

Additionally, we newly found that the ablation of the NPF neurons results in a significantly prolonged free-running period in DD in both male and female flies. The *cry-Gal80*-rescue also confirmed here that this was not an effect of the ablated non-clock neurons, but of the *npf*-positive clock neurons. We further found that the rescue of only the I-LN_vs with *pdfGal80* was not sufficient to completely restore wildtype free-running period, indicating that the fifth s-LN_v and the *npf*-positive LN_ds are the cells that modulate the free-running period.

Most interestingly, the PDF-positive neurons have the opposite effect on the free-running period than the NPF-positive neurons (*pdf*-ablation leads to a short free-running period). This is compelling because both sets of neurons influence the phase of the evening activity in the same direction (advancing it after ablation). Previous studies have shown that an advanced phase of activity in LD usually correlates with a shortened free-running period in DD (e.g., Konopka and Benzer, 1971; Renn et al., 1999). This is clearly not the case in *npf*-ablated flies, which advanced the phase of the evening activity in LD while prolonging the free-running period in DD. One possible explanation is that there are two types of oscillating subsets among the *npf*-positive clock neurons separately controlling evening peak properties and free-

running period (Yoshii et al., 2004; Rieger et al., 2006), so that the cell ablation hits both subsets and yields the two phenotypes. This may also explain why the period changes are much more subtle after ablation of the NPF-neurons than after ablation of the PDF-neurons.

Phasing of the evening activity peak requires functionality of NPF- and PDF-positive lateral clock neurons

Pdf-ablated flies exhibit evening activity patterns very similar to *Pdf⁰¹* mutants, in which a clearly advanced evening peak phase is present in LD (Renn et al., 1999), and we therefore wondered what effects the simultaneous ablation of NPF- and PDF-positive neurons might have on fly behavior. We found that in flies, in which both *npf*- and *pdf*-positive neurons were ablated, the evening activity peak was even more advanced than in *pdf*-ablated flies and was additionally reduced in amplitude. Thus, the simultaneous ablation of NPF and PDF neurons seems to have additive effects on LD behavior. The correct phasing of the evening peak depends mostly on the action of the small PDF neurons (Renn et al., 1999; Shafer et al., 2009) and therefore the phase is more severely advanced in *pdf*-ablated flies than in *npf*-ablated flies. In our study, *npf*-ablated flies did not show an earlier activity onset compared to control flies. The evening activity level, however, was suppressed in the late evening. Thus, *npf*-ablated flies reached the activity maximum earlier than control flies. This indicates that the NPF-positive lateral neurons—especially the fifth sLN_v and the LN_ds—contribute to the right phasing of the evening activity probably by promoting activity late in the day. Since the ablation of the *pdf*-positive neurons advances the evening activity peak by speeding up the clock in the evening cells (Renn et al., 1999; Yoshii et al., 2009), we suggest that there might be different mechanisms by which *npf*-positive and *pdf*-positive lateral clock neurons modify the phasing of the evening activity.

NPF is putatively involved in the control of the evening activity

The functionality of a neuronal system such as the central clock network strongly depends on signaling mechanisms between different components of this system and the output signaling to downstream neurons. By the ablation of the *npf*-positive neurons we clearly disrupted the signaling circuit which is mediated by NPF. NPF in flies was shown to play a role in mating behavior (Lee et al., 2006; Hamasaka et al., 2010), aggression (Dierick et al., 2007), and also in feeding as its homolog NPY in mammals (Shen and Cai, 2001; Wu et al., 2003, 2005). Lee et al. (2006) suggested a possible role for NPF in

circadian rhythms. However, the critical point in that study was that the ablation of the NPF neurons is not a direct proof for the actual function of NPF. We therefore investigated whether the genetic knockdown of NPF by RNAi within the clock neurons has comparable effects to what we had observed in our cell ablation experiments. Unfortunately, we were not able to knockdown NPF to a level that was undetectable by immunocytochemistry, neither when the *npf^{RNAi}*-construct was expressed with *tim(uas)Gal4* nor when it was expressed with *npfGal4*. Since we separately tested two different *npf^{RNAi}*-constructs (data of the second RNAi line are not shown) in combination with *dicer2* and the driver lines, we assume that NPF cannot be completely knocked down by this method. We did not see any effect in circadian behavior in LD or DD in these flies (Fig. 6H).

Although we were not able to knockdown NPF completely, we investigated flies in which both the *pdf^{RNAi}*-construct and the *npf^{RNAi}*-construct were expressed in the clock neurons. These flies showed an advanced evening peak phase that was even slightly earlier than in *pdf*-knockdown and *npf*-knockdown flies. In addition, we observed a reduction of the evening peak amplitude compared to *pdf*-knockdown flies similar to the reducing effect we had observed when PDF and NPF neurons were ablated simultaneously. Thus, a slight reduction of NPF levels seemed to affect behavior, when *pdf* was additionally knocked down, indicating a possible function for NPF in the control of the evening activity. However, we suggest that the function of NPF in circadian rhythms needs to be subjected to further investigation, as the knockdown by RNAi was not complete. We additionally suggest that possible future work also includes the examination of the function of other neurotransmitters that are expressed in *npf*-positive clock neurons, such as the ion transport peptide (ITP) or acetylcholine (Audsley et al., 1992; Dirksen, 2009; Johard et al., 2009), to reveal their role in evening activity and free-running phenotypes that we observed in *npf*-ablated flies.

ACKNOWLEDGMENTS

We thank Isaac Edery, Karl Fischbach, Jeffrey C. Hall, Alois Hofbauer, Jae H. Park, Michael Rosbash, Hermann Steller, and Michael W. Young for providing antibodies and fly strains. We also thank Silvia Glotz for supplemental experiments, not shown in the article, and Charles A. Williams for English editing.

LITERATURE CITED

Audsley N, McIntosh C, Phillips JE. 1992. Isolation of a neuropeptide from locust corpus cardiacum which influences ileal transport. *J Exp Biol* 173:261–274.

- Blau J, Young MW. 1999. Cyclic *vri* expression is required for a functional *Drosophila* clock. *Cell* 99:661–671.
- Brand AH, Perrimon N. 1993. Targeted gene expression as a means of altering cell fates and generating dominant phenotypes. *Development* 118:401–415.
- Dierick HA, Greenspan RJ. 2007. Serotonin and neuropeptide F have opposite modulatory effects on fly aggression. *Nat Genet* 39:678–682.
- Dirksen H. 2009. Insect ion transport peptides are derived from alternatively spliced genes and differentially expressed in the central and peripheral nervous system. *J Exp Biol* 212(Pt 3):401–412.
- Emery P, Stanewsky R, Helfrich-Förster C, Emery-Le M, Hall JC, Rosbash M. 2000. *Drosophila* CRY is a deep brain circadian photoreceptor. *Neuron* 26:493–504.
- Grima B, Chelot E, Xia R, Rouyer F. 2004. Morning and evening peaks of activity rely on different clock neurons of the *Drosophila* brain. *Nature* 431:869–873.
- Gummadova JO, Coutts GA, Glossop NR. 2009. Analysis of the *Drosophila* Clock promoter reveals heterogeneity in expression between subgroups of central oscillator cells and identifies a novel enhancer region. *J Biol Rhythms* 24:353–367.
- Hamasaka Y, Suzuki T, Hanai S, Ishida N. 2010. Evening circadian oscillator as the primary determinant of rhythmic motivation for *Drosophila* courtship behavior. *Genes Cells* 15:1240–1248.
- Helfrich-Förster C. 1995. The *period* clock gene is expressed in central nervous system neurons which also produce a neuropeptide that reveals the projections of circadian pacemaker cells within the brain of *Drosophila melanogaster*. *Proc Natl Acad Sci U S A* 92:612–616.
- Helfrich-Förster C, Shafer OT, Wülbeck C, Grieshaber E, Rieger D, Taghert P. 2007. Development and morphology of the clock-gene-expressing lateral neurons of *Drosophila melanogaster*. *J Comp Neurol* 500:47–70.
- Hofbauer A. 1991. Eine Bibliothek monoclonaler Antikörper gegen das Gehirn von *Drosophila melanogaster*. Habilitation thesis, University of Würzburg, Würzburg, Germany.
- Hofbauer A, Ebel T, Waltenspiel B, Oswald P, Chen YC, Halder P, Biskup S, Lewandrowski U, Winkler C, Sickmann A, Buchner S, Buchner E. 2009. The Würzburg hybridoma library against *Drosophila* brain. *J Neurogenetics* 23:78–91.
- Johard HA, Yoishii T, Dirksen H, Cusumano P, Rouyer F, Helfrich-Förster C, Nässel DR. 2009. Peptidergic clock neurons in *Drosophila*: ion transport peptide and short neuropeptide F in subsets of dorsal and ventral lateral neurons. *J Comp Neurol* 516:59–73.
- Konopka RJ, Benzer S. 1971. Clock mutants of *Drosophila melanogaster*. *Proc Natl Acad Sci U S A* 68:2112–2116.
- Lee G, Bahn JH, Park JH. 2006. Sex- and clock-controlled expression of the *neuropeptide F* gene in *Drosophila*. *Proc Natl Acad Sci U S A* 103:12580–12585.
- Lin Y, Stormo GD, Taghert PH. 2004. The neuropeptide pigment-dispersing factor coordinates pacemaker interactions in the *Drosophila* circadian system. *J Neurosci* 24:7951–7957.
- McNabb SL, Baker JD, Agapite J, Steller H, Riddiford LM, Truman JW. 1997. Disruption of a behavioral sequence by targeted death of peptidergic neurons in *Drosophila*. *Neuron* 19:813–823.
- Nässel DR, Wegener C. 2011. A comparative review of short and long neuropeptide F signaling in invertebrates: any similarities to vertebrate neuropeptide Y signaling? *Peptides* 32:1335–1355.
- Nässel DR, Enell LE, Santos JG, Wegener C, Johard HA. 2008. A large population of diverse neurons in the *Drosophila* central nervous system expresses short neuropeptide F,

- suggesting multiple distributed peptide functions. *BMC Neurosci* 9:90.
- Park JH, Helfrich-Förster C, Lee G, Liu L, Rosbash M, Hall JC. 2000. Differential regulation of circadian pacemaker output by separate clock genes in *Drosophila*. *Proc Natl Acad Sci U S A* 97:3608–3613.
- Picot M, Cusumano P, Klarsfeld A, Ueda R, Rouyer F. 2007. Light activates output from evening neurons and inhibits output from morning neurons in the *Drosophila* circadian clock. *PLoS Biol* 5:e315.
- Pittendrigh CS, Daan S. 1976. A functional analysis of circadian pacemakers in nocturnal rodents. V. pacemaker structure: A clock for all seasons. *J Comp Physiol (A)* 106:333–355.
- Renn SC, Park JH, Rosbash M, Hall JC, Taghert PH. 1999. A *pdf neuropeptide* gene mutation and ablation of PDF neurons each cause severe abnormalities of behavioral circadian rhythms in *Drosophila*. *Cell* 99:791–802.
- Rieger D, Stanewsky R, Helfrich-Förster C. 2003. Cryptochrome, compound eyes, Hofbauer-Buchner eyelets, and ocelli play different roles in the entrainment and masking pathway of the locomotor activity rhythm in the fruit fly *Drosophila melanogaster*. *J Biol Rhythms* 18:377–391.
- Rieger D, Shafer OT, Tomioka K, Helfrich-Förster C. 2006. Functional analysis of circadian pacemaker neurons in *Drosophila melanogaster*. *J Neurosci* 26:2531–2543.
- Rieger D, Wülbeck C, Rouyer F, Helfrich-Förster C. 2009. *Period* gene expression in four neurons is sufficient for rhythmic activity of *Drosophila melanogaster* under dim light conditions. *J Biol Rhythms* 24:271–282.
- Shafer OT, Taghert PH. 2009. RNA-interference knockdown of *Drosophila* pigment dispersing factor in neuronal subsets: the anatomical basis of a neuropeptide's circadian functions. *PLoS One* 4:e8298.
- Sheeba V, Fogle KJ, Holmes TC. 2010. Persistence of morning anticipation behavior and high amplitude morning startle response following functional loss of small ventral lateral neurons in *Drosophila*. *PLoS One* 5:e11628.
- Shen P, Cai HN. 2001. *Drosophila* neuropeptide F mediates integration of chemosensory stimulation and conditioning of the nervous system by food. *J Neurobiol* 47:16–25.
- Sidote D, Majercak J, Parikh V, Edery I. 1998. Differential effects of light and heat on the *Drosophila* circadian clock proteins PER and TIM. *Mol Cell Biol* 18:2004–2013.
- Stoleru D, Peng Y, Agosto J, Rosbash M. 2004. Coupled oscillators control morning and evening locomotor behaviour of *Drosophila*. *Nature* 431:862–868.
- Veleri S, Brandes C, Helfrich-Förster C, Hall JC, Stanewsky R. 2003. A self-sustaining, light-entrainable circadian oscillator in the *Drosophila* brain. *Curr Biol* 13:1758–1767.
- Wu Q, Wen T, Lee G, Park JH, Cai HN, Shen P. 2003. Developmental control of foraging and social behavior by the *Drosophila* neuropeptide Y-like system. *Neuron* 39:147–161.
- Wu Q, Zhao Z, Shen P. 2005. Regulation of aversion to noxious food by *Drosophila* neuropeptide Y- and insulin-like systems. *Nature Neurosci* 8:1350–1355.
- Yoshii T, Funada Y, Ibuki-Ishibashi T, Matsumoto A, Tanimura T, Tomioka K. 2004. *Drosophila cry^b* mutation reveals two circadian clocks that drive locomotor rhythm and have different responsiveness to light. *J Insect Physiol* 50:479–488.
- Yoshii T, Todo T, Wülbeck C, Stanewsky R, Helfrich-Förster C. 2008. Cryptochrome is present in the compound eyes and a subset of *Drosophila*'s clock neurons. *J Comp Neurol* 508:952–966.
- Yoshii T, Wülbeck C, Sehadova H, Veleri S, Bichler D, Stanewsky R, Helfrich-Förster C. 2009. The neuropeptide pigment-dispersing factor adjusts period and phase of *Drosophila*'s clock. *J Neurosci* 29:2597–2610.
- Zhang Y, Liu Y, Bilodeau-Wentworth D, Hardin PE, Emery P. 2010. Light and temperature control the contribution of specific DN1 neurons to *Drosophila* circadian behavior. *Curr Biol* 20:600–605.
- Zhou L, Schnitzler A, Agapite J, Schwartz LM, Steller H, Nambu JR. 1997. Cooperative functions of the *reaper* and *head involution defective* genes in the programmed cell death of *Drosophila* central nervous system midline cells. *Proc Natl Acad Sci U S A* 94:5131–5136.

The following manuscript has been submitted to the Journal of Neuroscience

Dear Mrs. Hermann-Luibl,

On 10th Jan 2014, a manuscript entitled "The Ion Transport Peptide is a new functional clock neuropeptide in the fruit fly *Drosophila melanogaster*" by Christiane Hermann-Luibl, Taishi Yoshii, Pingkalai Senthilan, Heinrich Dirksen, and Charlotte Helfrich-Förster was submitted to the Journal of Neuroscience by Prof. Helfrich-Förster, pending payment of the submission fee (this applies to NEW and RESUBMITTED manuscripts only).

If this is a REVISION or FEATURE ARTICLE (Journal Club, etc.), then you do not have to pay the submission fee.

The manuscript has been assigned the paper number JN-RM-0111-14. To view the manuscript, please log into the system.

Sincerely,

Central Office Staff
The Journal of Neuroscience
jn@sfn.org

The Ion Transport Peptide is a new functional clock neuropeptide in the fruit fly *Drosophila melanogaster*

Christiane Hermann-Luibl¹, Taishi Yoshii², Pingkalai R. Senthilan¹, Heinrich Dircksen³ and Charlotte Helfrich-Förster^{1*}

¹ Neurobiology and Genetics, Theodor-Boveri Institute, Biocenter, University of Würzburg, Germany

² Graduate School of Natural Science and Technology, University of Okayama, Japan

³ Department of Zoology, Stockholm University, Sweden

* corresponding author: Charlotte Helfrich-Förster

Universität Würzburg, Lehrstuhl Neurobiologie und Genetik, Biozentrum, Am Hubland, 97074 Würzburg, Germany; email: charlotte.foerster@biozentrum.uni-wuerzburg.de

Abbreviated title: ITP acts in the clock of *Drosophila melanogaster*

Number of pages: 39

Number of figures: 10

Number of tables: 2

Number of words: abstract (235), introduction (488), discussion (1476)

Acknowledgements: This work was funded by the European Commission (FP6 IP EUCLOCK), the German Research Foundation (DFG, Fo-207/12-1; SFB-1047, INST 93/784-1) and Grants-in-Aid for Scientific Research (KAKENHI 25840121). We would like to thank the Bloomington stock center, the VDRC, J. C. Hall, M. W. Young, M. Kaneko, O. T. Shafer, F. Rouyer, and C. Wegener for providing fly lines. Further, we are grateful to Dick R. Nässel, Paul E. Hardin, R. Stanewsky and the DSHB for providing antibodies and to A. Fiala for the pUAST vector. The authors declare no competing financial interests.

Abstract

The clock network of *Drosophila melanogaster* expresses various neuropeptides, but a function in clock-mediated behavioral control was so far only found for the neuropeptide Pigment Dispersing Factor (PDF). Here we propose a role in the control of behavioral rhythms for the Ion Transport Peptide (ITP), which is expressed in the fifth sLNv, one LNd and in only few non-clock cells in the brain. Immunocytochemical analyses revealed that ITP, just like PDF, is most probably released in a rhythmic manner at projection terminals in the dorsal protocerebrum. Further, ITP expression is reduced in the hypomorph mutant *Clk^{AR}*, suggesting that the ITP expression is regulated by CLOCK. Using a genetically encoded RNAi construct we knocked down ITP in the two clock cells and found that these flies show reduced evening activity, increased nocturnal activity and a longer circadian free-running period. Overexpression of ITP with two independent *timeless-GAL4* lines completely disrupted behavioral rhythms, but only slightly dampened PER cycling in important pacemaker neurons, suggesting a role for ITP in clock output pathways rather than in the communication within the clock network. Simultaneous knockdown of ITP and PDF made the flies hyperactive and almost completely arrhythmic under constant conditions. Under light-dark conditions the double-knockdown combined the behavioral characteristics of the single-knockdown flies. In addition, it reduced the flies' sleep. We conclude that ITP and PDF are the clock's main output signals that cooperate in controlling the flies' activity rhythms.

Introduction

The fruit fly *Drosophila melanogaster* has served as model organism for the investigation of biological rhythms since decades. The master clock in the central brain of the fly consists of about 150 clock neurons, which can be divided into several subgroups: the sLN_v, fifth sLN_v, ILN_v, LNd and LPN in the lateral protocerebrum, and the DN1, DN2 and DN3 in the dorsal brain (Helfrich-Förster et al., 2007). These neurons are characterized by cell autonomous molecular oscillations of different clock proteins, which constitute the core clock mechanism (reviewed by Peschel and Helfrich-Förster, 2011). The most prominent circadian output in the fly is the rhythm in daily locomotor activity, which consists of a morning (M) and an evening (E) activity bout. Previous studies had shown that the M activity is mainly controlled by the sLN_v, while the fifth sLN_v and three of the LNd constitute the E oscillator cells (Grima et al., 2004; Stoleru et al., 2004; Rieger et al., 2006; Picot et al., 2007; reviewed by Yoshii et al., 2012).

M and E oscillator cells express different neuropeptides that seem to be involved in communication pathways within the clock network as well as in output signaling pathways. (reviewed by Peschel and Helfrich-Förster, 2011). The neuropeptide Pigment Dispersing Factor (PDF), which is expressed in the sLN_v and ILN_v, was shown to act as a synchronizing signal between different clock neurons (Shafer et al., 2008; Yoshii et al., 2009) and is important for the maintenance of rhythmicity in constant darkness (DD; Renn et al., 1999). In light-dark (LD) cycles, PDF was further shown to promote M activity, suggesting that it is the main output factor of the M oscillator cells (Renn et al., 1999; Shafer and Taghert, 2009).

The E oscillator cells are more heterogeneous with respect to their neuropeptide expression. Some contain the long form of neuropeptide F (NPF), others its short form (sNPF) and few neurons express the Ion Transport Peptide (ITP; Johard et al., 2009; Hermann et al., 2012). So far, only few clock-related functions of these neuropeptides have been demonstrated (Hermann et al., 2012; Damulewicz et al., 2013) and it is not clear, which of them is the main output factor of the E cells to control rhythmic behavior. Here, we have investigated the role of ITP, which is expressed in the fifth sLN_v and one LNd (Johard et al., 2009) and which has so far found most attention for its antidiuretic functions in the insect gut (Dircksen, 2009). Through RNA interference (RNAi) and

overexpression experiments we show for the first time that ITP participates in the control of locomotor rhythms. As part of the E oscillator neurons ITP promotes E activity and acts as a period shortening component in DD. We further demonstrate that its clock related functions may be mediated by rhythmic ITP release from the two clock cells into the Pars intercerebralis (PI), and that this occurs at different times than the PDF release.

Material and Methods

Fly stocks

All fly stocks were reared on standard cornmeal/agar medium in a humidity controlled climate chamber in LD 12:12 at 25°C. As wildtype we used the lab strain *Canton S* (CS), and *w¹¹¹⁸* was crossed to *GAL4*- and *UAS*-lines to obtain heterozygous control flies. We further used the mutants, *per⁰¹* and *Clk^{AR}* (M. Rosbash, Brandeis University, USA), and for the RNAi experiments *w¹¹¹⁸;UAS-dicer2;+;+* (#60012), *w¹¹¹⁸;+;UAS-itp-RNAi* (#43848) and *w¹¹¹⁸;+;UAS-pdf-RNAi* (#4380), which were all obtained from the Vienna *Drosophila* RNAi Center (VDRC). The utilized driver lines were the following: *yw;+;pdf-GAL4*, *w;tim-GAL4/CyO* and *yw;per-GAL4* (all from J. C. Hall and M Kaneko, Brandeis University, USA), *w;tim(UAS)-GAL4* (M. W. Young, Rockefeller University, USA), *w;clk856-GAL4* (O. T. Shafer, University of Michigan, USA; Gummadova et al., 2009), *w;cry-GAL4^{#39}* (F. Rouyer, CNRS, France), *w;elav-GAL4/CyO* (Bloomington Stock Center, #8765), and *386y(amon)-GAL4* (C. Wegener, University of Würzburg, Germany).

Generation of *UAS-ITP* flies

RNA was extracted from *Drosophila melanogaster Canton S* heads and was subsequently reversely transcribed into cDNA. The cDNA of the short ITP isoform (ITP-PE; DrmITP in Dirksen et al., 2008) was then amplified in its full length using a primer pair, which created EcoRI and XbaI restriction sites. (Forward primer from 5' to 3': ACG-AAT-TCG-TTT-CTG-CCC-CAC-AAC-AAC-AC; Reverse primer from 5' to 3': TCC-TCT-AGA-ATC-GCA-CTT-TAC-TTG-CGA-CC) The amplicon was ligated into the EcoRI-XbaI-digested pUAST vector (containing genes encoding Ampicillin resistance and *mini-white*; kindly donated by A. Fiala, University of Göttingen, Germany) and NEB 10-beta competent *E. coli* bacteria (New England BioLabs) were used for transformation with the ITP-pUAST vector. Positive clones

were selected on Ampicillin containing agar plates and one clone was chosen for vector amplification, sequencing and injection into *w¹¹¹⁸* flies by BestGene (BestGene Inc., *Drosophila* Embryo Injection Services, CA, USA). We obtained ten different red-eyed *UAS-ITP* lines, in which the construct was inserted either on the second or on the third chromosome.

Antibodies and Immunocytochemistry

Immunohistochemical analysis was performed to investigate the ITP expression pattern in the brain of wildtype and overexpressing flies, to confirm RNAi efficiency and to quantify clock protein cycling and ITP staining intensity.

The monoclonal mouse anti-PDF-C7 antibody was purchased from the Developmental Studies Hybridoma Bank at the University of Iowa (DSHB; investigator: Justin Blau, New York University). To counterstain all clock neurons we employed a polyclonal guinea pig antiserum against the clock protein Vriille (anti-VRI), which was described by Glossop et al. (2003) and kindly provided by Paul E. Hardin (Texas A&M University, USA). For the quantification of the PERIOD (PER) protein cycling we used a polyclonal rabbit anti-PER antibody (Stanewsky et al., 1997), which was a gift from R. Stanewsky (University College London, UK).

The polyclonal rabbit anti-ITP antibody was commercially generated against the C-terminal fragment of *Drosophila melanogaster* ITP, CEMDKYNEWRD₂-NH₂, coupled to bovine thyroglobulin via maleimide coupling methodology. Rabbits were repeatedly injected subcutaneously and were terminally bled after 110 days. Immunocytochemistry, antisera titrations and analyses of specificity were performed as described previously in Dircksen et al. (2008), i.e. via dilution series, preabsorption controls, Western Blots and combined HPLC-ELISA analysis.

The staining protocol for *Drosophila melanogaster* adult whole-mount brains was described in previous studies (Hermann et al., 2012, 2013). We used only male 3-5 days old flies, which were entrained for at least 4 days in LD 12:12, before they were collected at various Zeitgeber Times (ZTs) in LD or Circadian Times (CTs) on the third day in DD. Brains were embedded and confocal images were obtained using a Leica TCS SPE (Leica, Wetzlar, Germany) confocal microscope. Z-stack images were visualized and edited with the ImageJ distribution Fiji (<http://fiji.sc/wiki/index.php/Fiji> or <http://rsb.info.nih.gov/ij/>).

Stacks were cropped and compiled as maximum projections. Brightness and contrast were adjusted, but no other manipulations were performed on the images, if not explicitly stated otherwise.

For intensity quantification, samples were processed in exactly the same way during the staining protocol and were scanned with identical laser settings. The quantifications were conducted in ImageJ (Fiji). For quantification of PER or ITP in cell bodies, a square shaped area of 9 pixels (3x3 pixels) was placed on each cell of interest and the average pixel intensity was measured in the brightest focal plane. Cells of at least 5 different hemispheres were analyzed and the intensity values were first background corrected and then averaged for each neuronal group and genotypes. For quantification of ITP and PDF in the terminals, we compiled maximum projections containing the PI and the Pars lateralis (PL) and removed all staining besides the ITP- and PDF-terminals in this area (see Fig. 1C). All resulting images were consequently of the exact same size and contained only a defined part of the staining in the dorsal terminals. We then set the background of each image to 0 and measured the total intensity of the whole image, which then reflected the staining intensity in the dorsal projection terminals. We quantified at least 10 brains for each time point and ITP and PDF were analyzed in the same specimens.

Behavioral Assay

For analysis of daily locomotor rhythms we used 3-5 days old male flies, which were recorded using the commercially available *Drosophila* Activity Monitoring (DAM) System by TriKinetics. The exact procedure was described in Hermann et al. (2012). Experiments were performed in light-proof boxes, which were equipped with a computer controlled white light LED system. The whole setup was located in a climate chamber with controlled humidity and constant 20°C. Light intensity during light phases was set to 100 lux. We recorded the flies in LD 12:12 for seven days, followed by at least 14 days of DD. Experimental genotypes were always recorded together with their respective control genotypes in the same box and at the same time.

Analysis of LD behavioral data was performed using Microsoft Excel and the procedure of calculating normalized average activity profiles was in detail described in Hermann et al. (2012). Free-running period lengths in DD were determined using χ^2 -periodogram analysis and actograms were depicted using ElTemps (Diez-Noguera, Barcelona, 1999;

upper limit 5) and the ImageJ plugin ActogramJ (Schmid et al., 2011). Average activity levels were calculated from mean activity counts of single flies during daytime (ZT0 to ZT12) or nighttime (ZT12 to ZT24) relative to the average of activity counts over the whole day. We further calculated the average number of beam crosses during the evening (ZT06 to ZT18) relative to the average activity during the morning (ZT18 to ZT06). Sleep amount was defined as the sum of time, in which the flies did not cross the infrared light beam within 10 consecutive minutes. We calculated average sleep profiles in 1-hour bins over the whole day and quantified total sleep during the light phase and the dark phase.

Statistics

Data were tested for normal distribution applying a one-sample Kolmogorov-Smirnov test. To test for significant differences in normally distributed data sets we then applied a one-way ANOVA followed by a post-hoc pairwise comparison with Bonferroni correction. Not normally distributed data were tested for significant differences with a Kruskal-Wallis test followed by pairwise comparison with Wilcoxon analysis. Percentages of rhythmicity were compared by a χ^2 test. Data were considered as significantly different with $p < 0.05$ (*) and as highly significant with $p < 0.001$ (**). Significances are either indicated by asterisks or by a letter code within all graphical charts.

Results

ITP peptide levels cycle in dorsal projection terminals

ITP is expressed only in few brain neurons in the adult fly. The whole pattern was described in detail in Dirksen et al. (2008) and the original nomenclature of ITP-positive (ITP⁺) cells was mostly adopted into this work. We will, however, refer to the two ITP⁺ clock neurons as fifth sLN_v and LN_d, which were originally included in the ipc-3 neuronal group (Fig. 1A). According to this partly new nomenclature, the ITP⁺ cells in the brain can be divided into five groups: the two clock cells in the lateral brain, the ipc-1 in a posterior dorsal or medial position, the ipc-2 and the remaining ipc-3 cell(s) in the dorsal medial brain, and the ipc-4 in the dorsal central brain (Fig. 1A).

To investigate ITP peptide levels over the day, we immunostained brains of adult male CS flies every four hours in LD 12:12 with anti-ITP (Fig. 1A) and quantified the staining intensity in the cell bodies of the fifth sLNv and in the LNd (Fig. 1B). We did not see a significant cycling in staining intensity of the two cell bodies. Since the amount of PDF is also not cycling within the PDF⁺ cell bodies, but rather within the axon terminals in the dorsal protocerebrum indicating a rhythm in peptide release (Park et al., 2000), we pursued similar investigations concerning ITP. Male CS brains were immunostained every three hours in LD 12:12 and ITP staining intensity was quantified in the clock neuron terminals in the dorsal protocerebrum, which are close to the PI (Fig. 1C). We co-stained the same brains with anti-PDF and quantified also the PDF staining in the dorsal projection terminals of the sLNv. In accordance with Park et al. (2000), PDF immunostaining peaked at the beginning of the light phase, decreased during the rest of the day and was quite low during the night (Fig. 1D). ITP immunostaining in the projection terminals also showed significant differences during the LD cycle (Fig. 1D). The quantification revealed a peak in the middle of the light phase and a second peak around ZT20 during the night. Staining levels were minimal at around lights-on and lights-off. Decrease of immunostaining in the projection terminals may indicate a loss of peptide that is possibly mediated by peptide release from large dense core vesicles. Thus, our results suggest that PDF is released during the light phase, while ITP might be released in the end of the dark phase and the end of the light phase.

ITP levels are reduced in clock neurons of the hypomorph *Clk^{AR}* mutants

The next question was, whether ITP expression is depending on clock functionality. To answer this, we analyzed ITP staining intensity in the clock cell bodies in different clock-impaired mutants (Fig. 2A). We found that there is no difference in staining intensity in *per⁰¹* flies in comparison to wildtype CS (Fig. 2B). However, *per⁰¹* is thought to retain residual clock function, since only one of the two molecular feedback loops is impaired (Helfrich and Engelmann, 1987; Helfrich-Förster, 2001; Kempinger et al., 2009; Goda et al., 2011; Vanin et al., 2012; Bywalez et al., 2012; Menegazzi et al., 2012). In *Clk^{Jrk}* mutants clock function seems to be completely abolished (Allada et al., 1998); but besides its deficits in clock functionality, *Clk^{Jrk}* flies show strong developmental defects, which also

affect the presence of certain clock neurons (Park et al., 2000). We therefore decided to investigate ITP staining in the hypomorph clock mutant, *Clk^{AR}*. Interestingly, we found that the ITP staining intensity in the two clock cells is significantly reduced compared to wildtype and *per⁰¹*, suggesting that ITP expression is under clock regulation (Fig. 2B; Note that both ITP⁺ clock cells are only faintly stained, but clearly present in *Clk^{AR}*, Fig. 2A). When searching through the upstream region of the *itp* gene, we did not find any indications for the presence of E-boxes, whatsoever, indicating that ITP abundance is probably indirectly regulated by CLK.

ITP knockdown affects LD locomotor activity, especially the activity level during the night and during the evening.

In order to investigate the function of ITP for locomotor rhythms in the fly, we expressed a genetically encoded *itp-RNAi*-construct with the help of the *GAL4/UAS* system. We chose the very strong *tim(UAS)-GAL4* line (*tim(UAS)G4*; described in Blau and Young, 1999) to express both *UAS-dicer2* (*dcr2*) and the RNAi-construct, to knock down ITP (*itp-RNAi*) only in the ITP⁺ clock cells (ITP-knockdown). We used the same driver line to also manipulate PDF levels via *pdf-RNAi* (see below), as it was done previously (PDF-knockdown; Shafer and Taghert, 2009; Hermann et al., 2012). To verify the RNAi efficiency, we stained adult male brains of the respective genotypes with anti-ITP and anti-PDF and counterstained with anti-VRI (Fig. 3). PDF and ITP staining was wildtype-like in *tim(UAS)G4>dcr2* control flies (Fig. 3A) as well as in heterozygous RNAi-construct controls (*dcr2;itp-RNAi* and *dcr2;pdf-RNAi*; data not shown). ITP was, however, undetectable in both clock neurons in ITP-knockdown flies, but remained present in the ITP⁺ non-clock cells (Fig. 3B). PDF immunostaining was also completely lost, when *pdf-RNAi* was expressed in the clock neurons (Fig. 3C). When *itp-RNAi* and *pdf-RNAi* were expressed together, neither PDF nor ITP was present in the clock cells (Fig. 3D; ITP/PDF-knockdown). Thus, both RNAi constructs worked very efficiently, when expressed with *tim(UAS)G4* inside the clock neurons.

After assuring that the RNAi was working efficiently, we tested the locomotor rhythms of ITP-knockdown flies and corresponding controls in LD 12:12 cycles. We calculated normalized average activity profiles to better depict the general shape of the daily activity

pattern. The ITP-knockdown did not seem to have any severe effect on the shape of the bimodal activity profile (Fig. 4A). In particular the phasing of the activity peaks seemed to be normal. We also recorded these flies under longer and shorter photoperiods since changes in phase of M peak or E peak become more apparent, when the activity peaks do not occur at the exact time of the light transitions (e.g. Majercak et al., 1999, Rieger et al., 2003). But also these experiments did not reveal any impairment in activity peak timing (data not shown).

However, the knockdown of ITP had effects on relative activity levels. We calculated daytime and nighttime activity as the average number of beam crosses during the light phase and the dark phase relative to the average activity during the whole day (Fig. 4B). We found that ITP-knockdown flies show a significantly reduced relative daytime activity and a significantly enhanced nighttime activity. Furthermore, they seem to reduce E activity. When calculating the relation between average E activity (average beam crosses from ZT06 to ZT18) and average M activity (average beam crosses from ZT18 to ZT06), ITP-knockdown flies revealed a significant reduction in E activity relative to M activity (Fig. 4C).

ITP knockdown prolongs the free-running period in DD

To judge the effect of the ITP-knockdown on the free-running rhythm, we recorded ITP-knockdown flies together with their respective controls in LD 12:12 cycles followed by at least 2 weeks of constant darkness (DD). The ITP knockdown did not affect general rhythmicity of the flies, but slightly lengthened period (Table 1, see Fig. 8). We conclude that the presence of ITP is not necessary for maintaining rhythmicity under DD, but that ITP has a slight period shortening effect on the free-running period.

Overexpression of ITP with *timG4* impairs rhythmic behavior

Though the presence of ITP seems not to be necessary for robust free-running rhythms, this does not exclude the possibility that ITP influences rhythmicity. High ectopic levels of PDF in the dorsal brain (close to its usual terminals) have been shown to disrupt the internal communication among the clock neurons causing complex rhythms up to

arrhythmic behavior (Helfrich-Förster et al., 2000 and Wülbeck et al., 2008). Thus, we took a comparable approach as it was done for PDF and generated a *UAS-ITP* construct, which allowed the overexpression of ITP with different *GAL4 (G4)* lines. We chose several well-characterized driver lines that are specific to the neuronal clock system, but also broadly expressing drivers. The overexpression success was verified by antibody staining with anti-ITP (Fig. 5).

In general, we were able to overexpress ITP ectopically with all driver lines that we used (Fig. 5, confocal images). Focusing on the clock neurons, we counterstained ITP-overexpressing brains with anti-VRI and anti-PDF (data not shown) and found that all clock neuron clusters were able to synthesize ITP. Overexpression with *pdfG4*, *cryG4^{#39}* and *clk856G4* was rather specific to the neuronal clock network or a part of it (Fig. 5). Overexpression of ITP using *tim(UAS)G4*, *timG4* or *perG4* included not only clock neurons, but also structures like the antennal lobes, fan-shaped body or ellipsoid body (Fig. 5). The very broad driver lines *elav-GAL4* and *386y(amon)G4* showed even more, close to panneuronal overexpression of ITP (Fig. 5).

Interestingly, when we compared the locomotor rhythms in LD 12:12 and DD in the different ITP-overexpressing genotypes, we only found differences to control flies using *tim(UAS)G4* and *timG4*. These phenotypes were severe and identical in both driver lines, in that flies barely showed any M and E activity bouts in LD and were almost completely arrhythmic in DD (Fig. 5, Table 2; *tim(UAS)G4>ITP²* $\chi^2=73,5097$, $p<0.0001$; *timG4>ITP²* $\chi^2=56,7964$, $p<0.0001$). Overexpression with none of the other drivers had any effect on rhythmicity or period length.

We first tested whether these arrhythmic phenotypes derive from a disruption of the molecular clock mechanism, possibly mediated by the direct action of ITP on the clock network. To do so, we immunostained brains of *tim(UAS)G4>ITP²* flies and of the respective control genotypes with anti-PER every 4 hours in LD and the third day in DD. In LD, the oscillation in PER staining intensity in the different clock neuron clusters of *tim(UAS)G4>ITP²* flies was not different from controls (Fig. 6), indicating that the PER protein cycling is completely normal in LD in ITP-overexpressing flies. In DD, the amplitude of PER cycling was already reduced in some clock neurons of the control flies, but remained clearly cyclic in the sLN_v, the fifth sLN_v, and the LN_d (Fig. 6). In

tim(UAS)G4>ITP² flies, we also found significant PER cycling in these three groups of clock neurons, but the cycling amplitude was decreased in the sLNv and the LNd compared to controls (Fig. 6). Thus, PER cycling in DD wasn't completely abolished in ITP-overexpressing flies, but slightly dampened in its amplitude.

The rhythm of ITP and PDF release seems affected in behaviorally arrhythmic ITP-overexpressing flies

Since clock protein cycling within the clock neurons was not completely impaired in behaviorally arrhythmic ITP-overexpressing flies, we assume that ITP may mainly act downstream of the clock on behavior-controlling target structures inside the brain.

To localize putative ITP targets, which could possibly be responsible for the severe phenotype in ITP-overexpressing flies using *timG4* and *tim(UAS)G4*, we compared the anti-ITP staining pattern of these behaviorally arrhythmic flies with behaviorally rhythmic ITP-overexpressing flies. *386(amon)G4>ITP²* and *elavG4>ITP²* flies showed high ITP expression virtually everywhere in the brain, whereby staining was especially high in the mushroom bodies and in the subesophageal ganglion (Fig. 5). *perG4>ITP²* flies showed quite high ITP staining the central complex and the antennal lobes. Nevertheless, all these lines remained rhythmic, indicating that ITP does not evoke behavioral arrhythmicity by affecting these parts of the brain.

We then focused on the comparison of the arrhythmic *tim(UAS)G4>ITP²* flies with the rhythmic *perG4>ITP²* flies, because these had a similar strong ITP expression in the clock neurons and especially in the PI projections, where we had discovered a daily rhythm in ITP staining. To investigate, whether this rhythm is disturbed in the behaviorally arrhythmic but still present in the behaviorally rhythmic flies, we immunostained the two genotypes plus their relevant controls with anti-ITP and anti-PDF at ZT20 (when ITP levels had been high and PDF levels had been low in wildtype flies) and ZT02 (when ITP levels had been low, but PDF levels high in wildtype flies). We found that all control flies showed the expected significant differences in ITP and PDF staining intensity (Fig. 7A, B). The same was true for the *perG4>ITP²* flies; as expected these flies had very high ITP levels in the PI, but ITP-staining intensity was still cyclic (Fig. 7A). This was very different in *tim(UAS)G4>ITP²* flies, in which we could not detect any significant difference in ITP

staining at the two time points. ITP remained always similarly high (Fig. 7A). We conclude that a constant high release of ITP into the PI may disturb circadian rhythmicity. Interestingly, PDF-cycling seemed also to be affected in *tim(UAS)G4>ITP²* flies. The staining difference between ZT2 and ZT20 was smaller than in the other strains. PDF remained rather high in the middle of the night, when it was low in the controls (Fig. 6B). This may be partly caused by a changed projection pattern of the ILNv (Fig. 7C, D). In about 60% of *tim(UAS)G4>ITP²* flies some fibers from the l-LNv followed the projections of the s-LNv into the dorsal brain and terminated in the PI (Fig. 7C). PDF in these terminals remained constantly high and may have diminished the PDF rhythm (compare Helfrich-Förster et al., 2000; Wülbeck et al., 2008). Putatively, the arrhythmicity of *tim(UAS)G4>ITP²* flies is caused by a combination of constant high ITP and PDF release into the dorsal brain.

ITP/PDF-double-knockdown makes flies arrhythmic and hyperactive in DD

Since the results with *tim(UAS)G4>ITP²* flies already point to an interaction of ITP and PDF in the control of rhythmic behavior, we generated ITP/PDF-double-knockdown flies (*tim(UAS)G4>dcr2;itp-RNAi/pdf-RNAi*) and compared their rhythmic behavior with the single-knockdown flies. As mentioned earlier, the single ITP-knockdown had only mild effects on the free-running rhythms of the flies (Fig. 8): The percentage of rhythmic flies was the same as in the controls, only period was slightly but significantly longer (see also Table 1). In agreement with previous studies (Shafer and Taghert, 2009), the single PDF-knockdown had much more severe effects on rhythmicity than the ITP-knockdown: *tim(UAS)G4>dcr2;pdf-RNAi* flies were to a significantly lower amount rhythmic compared to *tim(UAS)G4>dcr2* ($p<0.0001$) and *dcr2;pdf-RNAi* ($p<0.0001$) flies, and the remaining rhythmic flies showed weak short free-running periods (Fig. 8, Table 1). This behavior largely mimicked that of *Pdf⁰* mutants (Renn et al., 1999). The simultaneous knockdown of PDF and ITP further reduced rhythmicity (Fig. 8). Periodogram analysis revealed residual rhythms in only about 30% of the ITP/PDF-double-knockdown flies, and these were clearly different from the PDF-knockdown flies. Usually, the activity of the double-knockdown flies was clustered in irregular activity bouts (Fig. 8C) with several rhythmic components appearing in the periodograms (not shown). Therefore, we could not

calculate an average period from the few rhythmic flies. Furthermore, the ITP/PDF-double-knockdown flies showed a significantly higher activity level than all other lines (Fig. 8E).

In LD, ITP/PDF-double-knockdown flies combine the behavioral characteristics of the single knockdown flies, but show in addition effects on sleep

In LD conditions, the behavior of ITP/PDF-double-knockdown flies was less disturbed than under DD conditions. Most flies did still show a kind of M and E activity, though with clearly altered characteristics (Fig. 8, 9). Their E peak was advanced as that of single PDF-knockdown flies (Fig. 9A, lower row right panel). Further, they revealed a reduced E peak and higher nocturnal activity as did single ITP-knockdown flies (Fig. 9B, C). Thus, the effects of the single-knockdowns seem to add up in the double-knockdown flies. Nevertheless, we did also observe effects that were not present in the single-knockdown flies: ITP/PDF-double-knockdown flies have a less pronounced siesta, which is the typical midday break in activity observed in wildtype flies. In the double-knockdown flies, the activity after lights-on decreases only slowly, whereas in all other genotypes (including ITP- and PDF-single-knockdown flies) the activity quickly decreases after the lights-on reaction and stays at a relatively low level until the beginning of the E activity.

The lacking siesta and the higher nocturnal activity suggests that ITP/PDF-double-knockdown flies do almost not sleep. To investigate this, we analyzed sleep in LD (Fig. 10) in the same data set that was used to calculate the LD activity profiles (Fig. 9). Neither ITP-knockdown nor PDF-knockdown alone did affect the sleep profile, but the simultaneous knockdown of ITP and PDF clearly reduced sleep during the siesta and during the night (Fig. 10A). Consequently, the total amount of sleep during the light and the dark phase was significantly reduced in ITP/PDF-double-knockdown flies, but in none of the other strains (Fig. 10B), although the ITP-knockdown flies showed higher nocturnal activity (see Fig. 4, 9).

Discussion

In the present study, we show that the activity rhythms of fruit flies are not only dependent on the neuropeptide PDF (Renn et al., 1999), but also clearly affected by the neuropeptide ITP. ITP promotes E activity and may therefore act as an output signal of the E oscillator cells. Under DD conditions, ITP has a mild period-shortening effect. Thus, ITP somehow opposes the effects of PDF, which promotes M activity and has a predominantly period-lengthening effect under DD (Renn et al., 1999; Shafer and Taghert, 2009). Nevertheless, the effects of ITP under DD are relatively mild as compared to PDF, which is necessary for robust rhythmicity. Notably, the double-knockdown of ITP and PDF completely disrupts circadian rhythmicity under DD, suggesting that the two neuropeptides are the clock's main output factors essential for rhythmicity under constant conditions. The two neuropeptides are also important for normal LD rhythms, whereby they seem to control different behavioral aspects: Whereas PDF strongly influences the activity phase of the flies promoting their adaptation to long photoperiods (Yoshii et al., 2009), ITP has no such effects. ITP mainly influences the activity level of the flies, reducing nocturnal activity and enhancing diurnal E activity. Most interestingly, both peptides cooperate in controlling the flies' sleep. Whereas the single-knockdown of either PDF or ITP did not affect sleep at all, the double PDF/ITP-knockdown strongly reduced sleep during the flies' siesta and night. In the following we will discuss specific points in more detail.

ITP's rhythmic way of action

In order to function in a circadian fashion, the synthesis of a neuropeptide, its stability or its receptor sensitivity can be under clock control. We have shown that ITP immunostaining is dramatically decreased inside the clock neurons in *Clk^{AR}* mutants, suggesting that the transcription of the *itp* gene might be regulated by CLK in the ITP⁺ clock neurons. Park and colleagues (2000) found a similar reduction in PDF immunostaining in *Clk^{Jrk}* mutants and identified an E-box (CACGTG) within the upstream regulatory region of the *pdf* gene. Nevertheless, *pdf* expression was independent of this E-box and *pdf*-mRNA levels were not cycling. We did not find any indications for the presence of E-boxes in the upstream region of the *itp* gene, indicating that ITP abundance

is probably indirectly regulated by CLK as is PDF. Similar to what was found for PDF (Park et al., 2000), we did also not find any significant cycling in ITP staining intensity in clock neuron cell bodies, but significant oscillations in staining intensity in the projection terminals. This suggests that PDF and ITP are continuously produced but rhythmically released from the axon terminals. ITP peaks in the middle of the night and the middle of the day. Assuming that peptide release occurs, when staining intensity decreases, we propose that ITP is most probably released from the clock neurons in the second half of the night and the second half of the day. Simultaneous analysis of PDF staining intensity in dorsal projection terminals of the same brains showed that PDF appears to be released in the middle of the day coinciding with previous studies (Park et al. (2000).

Notably, PDF and ITP appear not only to have different release times, but also different release sites. Whereas the PDF fibers terminate in the pars lateralis (PL) close to the calyces of the mushroom bodies (Helfrich-Förster and Homberg, 1993), most ITP fibers terminate medially to the PDF fibers in the PI (see also Johard et al. 2009). Both, the mushroom bodies and the PI have been previously shown to control sleep (Joiner et al., Pitman et al., 2006; Yuan et al., 2006; Foltenyi et al., 2007; Crocker, 2010). Thus, PDF and ITP may well interfere in the rhythmic control of sleep.

Clock derived ITP promotes E activity and reduces nocturnal activity

RNA interference in combination with the *GAL4/UAS*-system is a powerful tool to disrupt gene expression in a spatially specified way. Both the knockdown of ITP and the knockdown of PDF were very efficient in our experiments, leaving both peptides undetectable by the antibodies. To reduce ITP-knockdown exclusively in the clock neurons we used the *tim(UAS)G4* line to drive the RNAi-construct, that left ITP levels in ITP⁺ non-clock neurons unaffected. It is worth to mention that the complete knockdown of ITP in all ITP⁺ neurons is lethal (data not shown), while ITP-knockdown only in the clock neurons didn't seem to affect viability.

We did not find any effects of ITP-knockdown on the timing of M and E activity bouts in LD, not even under long and short photoperiods (data not shown). Thus, ITP seems not to be involved in general entrainment mechanisms and the adaptation to changing photoperiods. We found, however, effects of ITP-knockdown on activity levels, especially

during the evening and the night. The E activity of a wildtype fly occurs mainly during the light phase before lights-off, while the M anticipation before lights-on constitutes a large portion of the fly's M activity. Activity of ITP-knockdown flies was reduced during daytime and increased during nighttime relative to their overall average activity. In accordance with this, ITP-knockdown flies showed significantly less E activity in relation to their M activity compared to controls. Thus, we conclude that ITP, deriving from the E oscillator cells, normally promotes E activity and reduces nighttime activity.

Knocking down ITP and PDF together phenocopied both characteristics of PDF-knockdown flies and ITP-knockdown flies. On the one hand ITP/PDF-double-knockdown flies showed the same advance in E peak phase as it was typical for PDF-knockdown flies. On the other hand the E peak amplitude was decreased and nocturnal activity increased compared to PDF-knockdown flies as it was the case when ITP was knocked down alone. Thus, we conclude that PDF and ITP - independently of each other – control activity phase and levels, respectively.

ITP shortens the circadian free-running period in DD

In a previous study, we had shown that the ablation of the NPF⁺ clock neurons lengthens the circadian free-running period in DD and advances the E activity in LD (Hermann et al., 2012). Knocking down NPF via RNAi was not completely efficient and had thus not shown any effect on LD or DD behavior (Hermann et al., 2012). The *npfG4* line that we had used for the cell ablation experiments in this former study had included the two ITP⁺ clock neurons. Interestingly, we demonstrated now that the knockdown of ITP within these cells also slightly, but significantly prolongs the circadian free-running period in DD. This indicates that in fact the lack of ITP was probably responsible for the period lengthening, when the NPF⁺ cells were ablated. Thus, ITP normally acts as a period shortening factor, leading to a prolonged rhythm, when the ITP signaling is disrupted. *Pdf⁰¹* or PDF-knockdown flies on the other hand show shortened free-running rhythms in DD (Renn et al., 1999; Shafer and Taghert, 2009). Thus, both peptides have opposing effects on the period length, which could be a mechanism of fine-tuning clock neuron synchronization or rhythm output.

ITP might target mainly clock output sites to control rhythmic behavior

The ITP-receptor and its expression pattern are so far unknown. Thus, it is unclear whether ITP works within the clock network as was revealed for PDF (Im and Taghert, 2010) or on clock output sites. Here, we investigated whether ITP overexpression with *timG4* and *tim(UAS)G4* that led to behavioral arrhythmicity influenced the cycling of PER in the clock neurons. We found that solely PER cycling in the sLN_v and the LN_d seemed to be reduced in amplitude compared to control flies in DD, indicating a slow dampening of the circadian rhythm in these cells, which is possibly evoked by the action of ITP. However, *tim(UAS)G4>ITP²* flies were already arrhythmic from the first day in DD. Since there was still PER cycling on the third day in DD, albeit with reduced amplitude, we assume that ITP has its main targets in the clock output pathways.

Surprisingly, ITP could be highly overexpressed in the entire brain without provoking arrhythmicity indicating that the mushroom bodies, the central complex, the subesophageal ganglion, the antennal lobes and other brain regions do not contain ITP targets that are important for rhythmic behavior. Here, we show that a cyclic ITP release into the PI might be essential for behavioral rhythms, perhaps combined with a rhythmic PDF release into the PL, because both rhythms seemed to be disturbed in *tim(UAS)G4>ITP²* flies. Future studies have to reveal which neurons in the brain express the ITP-receptor and whether the sLN_v and the LN_d - the molecular PER-cycling of which is reduced in *tim(UAS)G4>ITP²* flies - are among them.

Taking all findings together, this is the first study demonstrating a role of ITP in the control of behavioral rhythms in *Drosophila melanogaster*. We propose a role for ITP in the output pathway of the clock which is partly complementary and partly cooperative to PDF.

Literature

- Allada R, White NE, So WV, Hall JC and Rosbash M (1998) A mutant *Drosophila* homolog of mammalian *Clock* disrupts circadian rhythms and transcription of *period* and *timeless*. *Cell* 93:791-804.
- Blau J and Young MW (1999) Cyclic *vriille* expression is required for a functional *Drosophila* clock. *Cell* 99:661-671.
- Bywalez W, Menegazzi P, Rieger D, Schmid B, Helfrich-Förster C and Yoshii T (2012) The dual-oscillator system of *Drosophila melanogaster* under natural-like temperature cycles. *Chronobiol Int* 29:395-407.
- Crocker A, Shahidullah M, Levitan IB and Sehgal A (2010) Identification of a neural circuit that underlies the effects of octopamine on sleep:wake behavior. *Neuron* 65:670-681.
- Damulewicz M, Rosato E and Pyza E (2013) Circadian regulation of the Na⁺/K⁺-ATPase alpha subunit in the visual system is mediated by the pacemaker and by retina photoreceptors in *Drosophila melanogaster*. *PLoS One* 8:e73690.
- Dircksen H (2009) Insect ion transport peptides are derived from alternatively spliced genes and differentially expressed in the central and peripheral nervous system. *J Exp Biol* 212:401-412.
- Dircksen H, Tesfai LK, Albus C and Nässel DR (2008) Ion transport peptide splice forms in central and peripheral neurons throughout postembryogenesis of *Drosophila melanogaster*. *J Comp Neurol* 509:23-41.
- Foltenyi K, Greenspan RJ and Newport JW (2007) Activation of EGFR and ERK by rhomboid signaling regulates the consolidation and maintenance of sleep in *Drosophila*. *Nat Neurosci* 10:1160-1167.
- Glossop NR, Houl JH, Zheng H, Ng FS, Dudek SM and Hardin PE (2003) VRILLE feeds back to control circadian transcription of *Clock* in the *Drosophila* circadian oscillator. *Neuron* 37:249-261.
- Goda T, Mirowska K, Currie J, Kim MH, Rao NV, Bonilla G and Wijnen H (2011) Adult circadian behavior in *Drosophila* requires developmental expression of *cycle*, but not *period*. *PLoS Genetics* 7:e1002167.
- Grima B, Chelot E, Xia R and Rouyer F (2004) Morning and evening peaks of activity rely on different clock neurons of the *Drosophila* brain. *Nature* 431:869-873.
- Gummadova JO, Coutts GA and Glossop NR (2009) Analysis of the *Drosophila Clock* promoter reveals heterogeneity in expression between subgroups of central oscillator cells and identifies a novel enhancer region. *J Biol Rhythms* 24:353-367.

- Helfrich C and Engelmann W (1987) Evidences for circadian rhythmicity in the *per⁰* mutant of *Drosophila melanogaster*. *Z Naturforsch* 42c:1335-1338.
- Helfrich-Förster C (2001) The locomotor activity rhythm of *Drosophila melanogaster* is controlled by a dual oscillator system. *J Insect Physio* 47:877-887.
- Helfrich-Förster C, Shafer OT, Wülbeck C, Grieshaber E, Rieger D and Taghert P (2007) Development and morphology of the clock-gene-expressing lateral neurons of *Drosophila melanogaster*. *J Comp Neurol* 500:47-70.
- Helfrich-Förster C, Tauber M, Park JH, Mühlig-Versen M, Schneuwly S and Hofbauer A (2000) Ectopic expression of the neuropeptide pigment-dispersing factor alters behavioral rhythms in *Drosophila melanogaster*. *J Neurosci* 20:3339-3353.
- Hermann C, Saccon R, Senthilan PR, Domnik L, Dirksen H, Yoshii T and Helfrich-Förster C (2013) The circadian clock network in the brain of different *Drosophila* species. *J Comp Neurol* 521:367-388.
- Hermann C, Yoshii T, Dusik V and Helfrich-Förster C (2012) Neuropeptide F immunoreactive clock neurons modify evening locomotor activity and free-running period in *Drosophila melanogaster*. *J Comp Neurol* 520:970-987.
- Im SH and Taghert PH (2010) PDF receptor expression reveals direct interactions between circadian oscillators in *Drosophila*. *J Comp Neurol* 518:1925-1945.
- Johard HA, Yoshii T, Dirksen H, Cusumano P, Rouyer F, Helfrich-Förster C and Nässel DR (2009) Peptidergic clock neurons in *Drosophila*: ion transport peptide and short neuropeptide F in subsets of dorsal and ventral lateral neurons. *J Comp Neurol* 516:59-73.
- Joiner WJ, Crocker A, White BH and Sehgal A (2006) Sleep in *Drosophila* is regulated by adult mushroom bodies. *Nature* 441:757-760.
- Kempinger L, Dittmann R, Rieger D and Helfrich-Förster C (2009) The nocturnal activity of fruit flies exposed to artificial moonlight is partly caused by direct light effects on the activity level that bypass the endogenous clock. *Chronobio Int* 26:151-166.
- Majercak J, Sidote D, Hardin PE and Edery I (1999). How a circadian clock adapts to seasonal decreases in temperature and day length. *Neuron* 24:219-230.
- Menegazzi P, Yoshii T and Helfrich-Förster C (2012) Laboratory versus nature: the two sides of the *Drosophila* circadian clock. *J Biol Rhythms* 27:433-442.
- Park JH, Helfrich-Förster C, Lee G, Liu L, Rosbash M and Hall JC (2000) Differential regulation of circadian pacemaker output by separate clock genes in *Drosophila*. *Proc Natl Acad Sc U S A* 97:3608-3613.
- Peschel N and Helfrich-Förster C (2011) Setting the clock--by nature: circadian rhythm in the fruitfly *Drosophila melanogaster*. *FEBS letters* 585:1435-1442.

- Picot M, Cusumano P, Klarsfeld A, Ueda R and Rouyer F (2007) Light activates output from evening neurons and inhibits output from morning neurons in the *Drosophila* circadian clock. PLoS Biol 5:e315.
- Pirez N, Christmann BL and Griffith LC (2013) Daily rhythms in locomotor circuits in *Drosophila* involve PDF. J Neurophysiol 110:700-708.
- Pitman JL, McGill JJ, Keegan KP and Allada R (2006) A dynamic role for the mushroom bodies in promoting sleep in *Drosophila*. Nature 441:753-756.
- Renn SC, Park JH, Rosbash M, Hall JC and Taghert PH (1999) A pdf neuropeptide gene mutation and ablation of PDF neurons each cause severe abnormalities of behavioral circadian rhythms in *Drosophila*. Cell 99:791-802.
- Rieger D, Shafer OT, Tomioka K and Helfrich-Förster C (2006) Functional analysis of circadian pacemaker neurons in *Drosophila melanogaster*. J Neurosci 26:2531-2543.
- Rieger D, Stanewsky R and Helfrich-Förster C (2003) Cryptochrome, compound eyes, Hofbauer-Buchner eyelets, and ocelli play different roles in the entrainment and masking pathway of the locomotor activity rhythm in the fruit fly *Drosophila melanogaster*. J Biol Rhythms 18:377-391.
- Schmid B, Helfrich-Förster C and Yoshii T (2011) A new ImageJ plug-in "ActogramJ" for chronobiological analyses. J Biol Rhythms 26:464-467.
- Shafer OT, Kim DJ, Dunbar-Yaffe R, Nikolaev VO, Lohse MJ and Taghert PH (2008) Widespread receptivity to neuropeptide PDF throughout the neuronal circadian clock network of *Drosophila* revealed by real-time cyclic AMP imaging. Neuron 58:223-237.
- Shafer OT and Taghert PH (2009) RNA-interference knockdown of *Drosophila* pigment dispersing factor in neuronal subsets: the anatomical basis of a neuropeptide's circadian functions. PloS One 4:e8298.
- Stanewsky R, Frisch B, Brandes C, Hamblen-Coyle MJ, Rosbash M and Hall JC (1997) Temporal and spatial expression patterns of transgenes containing increasing amounts of the *Drosophila* clock gene *period* and a *lacZ* reporter: mapping elements of the PER protein involved in circadian cycling. J Neurosci 17:676-696.
- Stoleru D, Peng Y, Agosto J and Rosbash M (2004) Coupled oscillators control morning and evening locomotor behaviour of *Drosophila*. Nature 431:862-868.
- Vanin S, Bhutani S, Montelli S, Menegazzi P, Green EW, Pegoraro M, Sandrelli F, Costa R and Kyriacou CP (2012) Unexpected features of *Drosophila* circadian behavioral rhythms under natural conditions. Nature 484:371-375.

- Wülbeck C, Grieshaber E and Helfrich-Förster C (2008) Pigment-dispersing factor (PDF) has different effects on *Drosophila's* circadian clocks in the accessory medulla and the dorsal brain. *J Biol Rhythms* 23(5):409-24.
- Yoshii T, Rieger D and Helfrich-Förster C (2012) Two clocks in the brain: an update of the morning and evening oscillator model in *Drosophila*. *Progr Brain Research* 199:59-82.
- Yoshii T, Todo T, Wülbeck C, Stanewsky R and Helfrich-Förster C (2008) Cryptochrome is present in the compound eyes and a subset of *Drosophila's* clock neurons. *J Comp Neurol* 508:952-966.
- Yoshii T, Wülbeck C, Sehadova H, Veleri S, Bichler D, Stanewsky R and Helfrich-Förster C (2009) The neuropeptide pigment-dispersing factor adjusts period and phase of *Drosophila's* clock. *J Neurosci* 29:2597-2610.
- Yuan Q, Joiner WJ and Sehgal A (2006) A sleep-promoting role for the *Drosophila* serotonin receptor 1A. *Curr Biol* 16:1051-1062.

Figure legends

Figure 1: ITP staining intensity in clock neuron cell bodies and projection terminals in LD 12:12. (A) Anti-ITP staining on male *Canton S* brains at different ZTs in LD 12:12 (20°C). **(B)** Quantification of the ITP staining intensity at different ZTs in the fifth sLNv (upper panel) and the LNd (lower panel). We found no significant oscillation in staining intensity in the ITP⁺ cell bodies (fifth sLNv ANOVA $F_{(6,65)}=0.685$; $p=0.663$; LNd ANOVA $F_{(6,65)}=0.484$; $p=0.818$). **(C)** Terminals of the ITP and PDF clock neurons in the dorsal protocerebrum. The ipc-1, ipc-2 and ipc-3 neurons were removed for better clarity. The two ITP neurons (LNd and 5th sLNv, magenta) terminate predominantly in the Pars intercerebralis (PI), whereas the PDF-expressing sLNv (blue) terminate in the Pars lateralis (PL). The PDF terminals were maximally stained at ZT2 and the ITP terminals at ZT20. For quantification of staining intensity everything in the picture was erased except the terminals in between the yellow bars as indicated for PDF in the upper and for ITP in the lower picture. **(D)** ITP and PDF staining intensities in the terminals depicted in **C**. PDF staining intensity significantly peaks at ZT2, decreases during the rest of the light phase and remains low during the night (ANOVA $F_{(7,111)}=25.64$; $p<0.0001$). Quantification of the ITP staining intensity revealed two statistically significant peaks: one around noon and one around midnight (ANOVA $F_{(7,111)}=8,86$; $p<0.0001$). The troughs occurred at the time of lights-on and lights-off. Error bars depict SEM; small letters indicate significant differences between time points; black and white bars indicate light regime; scale bars = 10µm.

Figure 2: ITP staining intensity in clock neuron cell bodies in *Canton S* (CS) compared to the clock mutants *per*⁰¹ and *Clk*^{AR}. (A) Anti-ITP staining on male adult brains of CS, *per*⁰¹ and *Clk*^{AR} at ZT02 in LD 12:12. **(B)** Quantification of the ITP staining intensity in the fifth sLNv (left panel) and the LNd (right panel) in the different genotypes. Anti-ITP staining intensity was significantly reduced in both cells in *Clk*^{AR} mutants compared to CS and *per*⁰¹ (fifth sLNv ANOVA $F_{(2,31)}=30,469$; $p<0.001$; LNd ANOVA $F_{(2,33)}=37,900$; $p<0.001$). Error bars depict SEM; scale bars = 10µm; ** indicates $p<0.001$ in pairwise comparisons.

Figure 3: Immunohistochemistry on RNAi expressing flies to validate RNAi efficiency. RNAi constructs were expressed with *tim(UAS)G4*. Male adult brains were stained with anti-ITP (magenta), anti-VRI (green) and anti-PDF (cyan). **(A)** Control flies (*tim(UAS)G4>dcr2*) show wildtype-like expression pattern of ITP and PDF in the clock neurons. **(B)** ITP is undetectable in the fifth sLNv and the LNd in ITP-knockdown flies (*tim(UAS)G4>dcr2;itp-RNAi*), while it is still present in the ITP⁺ non-clock neurons (*ipc-1*). **(C)** PDF is undetectable in sLNv and ILNv in PDF-knockdown flies (*tim(UAS)G4>dcr2;pdf-RNAi*). **(D)** Both ITP and PDF are undetectable in the clock neurons in ITP/PDF-double-knockdown flies (*tim(UAS)G4>dcr2;itp-RNAi/pdf-RNAi*). Scale bars = 10µm.

Figure 4: Locomotor activity of ITP-knockdown flies and controls in LD 12:12. **(A)** Average activity profiles were calculated for each genotype and light condition and were normalized to the highest activity value to better visualize the shape of the profile. No obvious differences in the shape of the bimodal activity pattern of ITP-knockdown flies (*tim(UAS)G4>dcr2;itp-RNAi*) were visible compared to controls. n = number of investigated flies; black areas indicate darkness, gray areas indicate light of 100 lux; black line = mean, gray lines = SEM. **(B)** Relative activity levels for day (left panel) or night (right panel) were calculated as mean beam crosses per minute during the light phase or the dark phase relative to the average of beam crosses during the whole day. ITP-knockdown flies (light gray) showed significantly less daytime activity in comparison to both controls (darker grays; Kruskal Wallis $H_{(2)}=37.637$; $p<0.001$) and significantly higher nighttime activity (Kruskal Wallis $H_{(2)}=37.637$; $p<0.001$). **(C)** When calculating mean E activity (ZT06 to ZT18) relative to mean M activity (ZT18 to ZT06), ITP-knockdown flies show a reduction in relative E amplitude compared to both controls (Kruskal Wallis $H_{(2)}=30.345$; $p<0.001$). T = 20°C; error bars depict SEM; * indicates $p<0.05$ and ** indicates $p<0.001$ in pairwise comparisons; n.s. = not significant.

Figure 5: Overexpression of ITP with different driver lines. Confocal pictures depict anti-ITP staining in heterozygous *UAS-ITP²* controls (top) and ITP-overexpressing adult male brains. One individual representative double plotted actogram is depicted for each genotype (black line indicates the transition from LD 12:12 to DD). Overexpression of ITP

with *tim(UAS)G4* and *timG4* impaired rhythmicity, while overexpression with all other driver lines did not affect rhythmicity. T = 20°C; black and white bars indicate the light regime in LD 12:12 (100 lux); scale bars = 10µm.

Figure 6: Period (PER) staining intensity in clock neurons in LD 12:12 and DD in ITP-overexpressing flies and controls. Adult male brains were stained with anti-PER after entrainment to LD 12:12 (100 lux, 20°C). Flies were collected at different ZTs in LD 12:12 and at different CTs on the third day in DD. CTs indicate the time points, when the light would have been on or off with respect to the previous LD cycle. Staining intensity in different clock neuron clusters was quantified in at least 5 brains per time point. PER cycling in behaviorally arrhythmic ITP-overexpressing flies (*tim(UAS)G4>ITP²*; light gray) did not differ from controls (darker grays) in any of the investigated clock neuron clusters in LD. PER protein was still clearly cycling in sLNv (*tim(UAS)G4*: ANOVA $F_{(5,24)}=27.114$; $p<0.001$; *UAS-ITP²*: ANOVA $F_{(5,24)}=26.478$; $p<0.001$), fifth sLNv (*tim(UAS)G4*: ANOVA $F_{(5,24)}=63.311$; $p<0.001$; *UAS-ITP²*: ANOVA $F_{(5,24)}=14.065$; $p<0.001$) and LNd (*tim(UAS)G4*: ANOVA $F_{(5,24)}=14.764$; $p<0.001$; *UAS-ITP²*: ANOVA $F_{(5,24)}=43.876$; $p<0.001$) in both control flies in DD. In ITP-overexpressing flies, we also found cycling in PER staining intensity in the sLNv (ANOVA $F_{(5,23)}=6.664$; $p<0.001$), the fifth sLNv (ANOVA $F_{(5,23)}=20.428$; $p<0.001$) and in the LNd (ANOVA $F_{(5,23)}=10.199$; $p<0.001$), however the amplitude of these oscillations seemed to be slightly reduced. Black and light gray bars indicate the LD light regime; black and dark gray bars indicate subjective night and day in DD; error bars depict SEM.

Figure 7: ITP and PDF cycling in the dorsal brain terminals in ITP-overexpression flies. (A) *tim(UAS)G4>ITP²* flies lack a significant difference in ITP staining at ZT2 and ZT20 in the Pars intercerebralis (PI). **(B)** Also the difference in PDF-staining intensity between the two time points is reduced in *tim(UAS)G4>ITP²* flies. **(C)** *tim(UAS)G4>ITP²* flies show a higher percentage of aberrant PDF-fibers in the PI than the other fly strains ($\chi^2=25.55$; $p<0.001$). **(D)** Typical brain of a *tim(UAS)G4>ITP²* fly stained with anti-PDF at ZT2 showing aberrant fibers stemming from the ILNv in the PI (cell bodies not in the picture).

Figure 8: Representative individual double plotted actograms of ITP-, PDF- and ITP/PDF-knockdown flies and controls in LD 12:12 followed by DD. ITP-knockdown flies (*tim(UAS)G4>dcr2;itp-RNAi*) (**B**) have significantly longer free-running periods in DD as compared to the relevant controls (**A**) (Kruskal Wallis $H_{(2)}=15.447$; $p<0.001$; pairwise comparisons: ITP-knockdown to *timG4>dcr2* $p<0.001$; ITP-knockdown to *dcr2;itp-RNAi* $p<0.05$). Many of the PDF-knockdown flies (*tim(UAS)G4>dcr2;pdf-RNAi*) were arrhythmic in DD (**D**) ($\chi^2=30.072$; $p<0.0001$); the still rhythmic individuals free-run with a short period (**B**) that was significantly different from the relevant controls (**A**) (Kruskal Wallis $H_{(2)}=16.506$; $p<0.001$; Wilcoxon pairwise comparisons: PDF-knockdown to *tim(UAS)G4>dcr2* $p=0.021$; PDF-knockdown to *dcr2;pdf-RNAi* $p=0.003$). The majority of the ITP/PDF-double-knockdown flies (*tim(UAS)G4>dcr2;itp-RNAi/pdf-RNAi*) were arrhythmic (**C** right actogram, **D**) ($\chi^2=19.354$; $p<0.0001$). The remaining flies showed several free-running components in DD (**C** left actogram), the period of which was impossible to determine. Furthermore, all ITP/PDF-double-knockdown flies had a high activity level that was significantly different to all other genotypes (**E**) (Kruskal Wallis $H_{(5)}=54.746$; $p<0.001$). Black and white bars indicate the light regime in LD 12:12 (100 lux, 20°C). The control strains in (**D**) and (**E**) (dark gray bars) are in the following order from left to right: *tim(UAS)G4>dcr2*, *dc2;itp-RNAi*, *dcr2;pdf-RNAi*. Error bars depict SEM.

Figure 9: Locomotor activity of ITP/PDF-double-knockdown flies and controls in LD 12:12. (**A**) Average activity profiles were calculated for each genotype and were normalized to the highest activity value. PDF-knockdown flies (*tim(UAS)G4>dcr2;pdf-RNAi*) show the typical advanced E activity and reduced M activity. The same phenotypes can be seen in ITP/PDF-double-knockdown flies (*tim(UAS)G4>dcr2;itp-RNAi/pdf-RNAi*). In addition, these flies show a less pronounced siesta compared to the other genotypes. n = number of investigated flies; black areas indicates darkness, gray areas indicates light of 100 lux; black line = mean, gray lines = SEM; $T = 20^\circ\text{C}$ (**B**) Relative activity levels for day (left panel) and night (right panel) were calculated as mean beam crosses per minute during the light phase or the dark phase relative to the average of beam crosses during the whole day. Relative daytime and nighttime activities were significantly dependent on the genotype (day: ANOVA $F_{(5,171)}=16.787$, $p<0.001$; night: ANOVA $F_{(5,171)}=27.802$,

$p < 0.001$). In particular, ITP/PDF-double-knockdown flies showed a slight reduction in daytime activity. The tendency towards reduced daytime activity in ITP-knockdown flies (*tim(UAS)G4>dcr2;itp-RNAi*) was similar to the results of Fig. 4B. Both ITP-knockdown flies and ITP/PDF-double-knockdown flies showed a significant increase in nighttime activity. **(C)** Mean E activity (ZT06 to ZT18) was calculated in relation to mean M activity (ZT18 to ZT06) as in Fig. 4C and was significantly dependent on the genotype (Kruskal Wallis $H_{(5)}=73,298$, $p < 0.001$). ITP-knockdown flies showed significantly less E activity than the controls and PDF-knockdown flies (compare also to Fig. 4C). E activity in ITP/PDF-double-knockdown flies was similarly reduced. The control strains in **B** and **C** (dark gray bars) are in the following order from left to right: *tim(UAS)G4>dcr2*, *dc2;itp-RNAi*, *dcr2;pdf-RNAi*. Error bars depict SEM.

Figure 10: Daily averaged sleep profile and total sleep of ITP/PDF-double-knockdown flies and controls in LD 12:12. Sleep was defined as the average amount of time, in which the flies did not cross the infrared light beam for at least 10 consecutive minutes. **(A)** Daily average sleep profiles of ITP-knockdown flies (red), PDF-knockdown flies (blue), ITP/PDF-double-knockdown flies (magenta) and controls (different grays). ITP-knockdown flies don't show any differences in the sleep profile compared to controls. ITP/PDF-double-knockdown flies clearly sleep less during the night and during the first half of the day. **(B)** Total amount of sleep during nighttime (full bars) and daytime (empty bars). ITP-knockdown flies do not differ from controls in total sleep. ITP/PDF-double-knockdown flies show significantly decreased nighttime (Kruskal Wallis $H_{(5)}=38.709$, $p < 0.001$) and daytime (Kruskal Wallis $H_{(5)}=42.811$, $p < 0.001$) sleep compared to all other genotypes. * indicates $p < 0.05$, ** indicates $p < 0.001$, n.s. = not significant; error bars depict SEM.

FIGURE 1

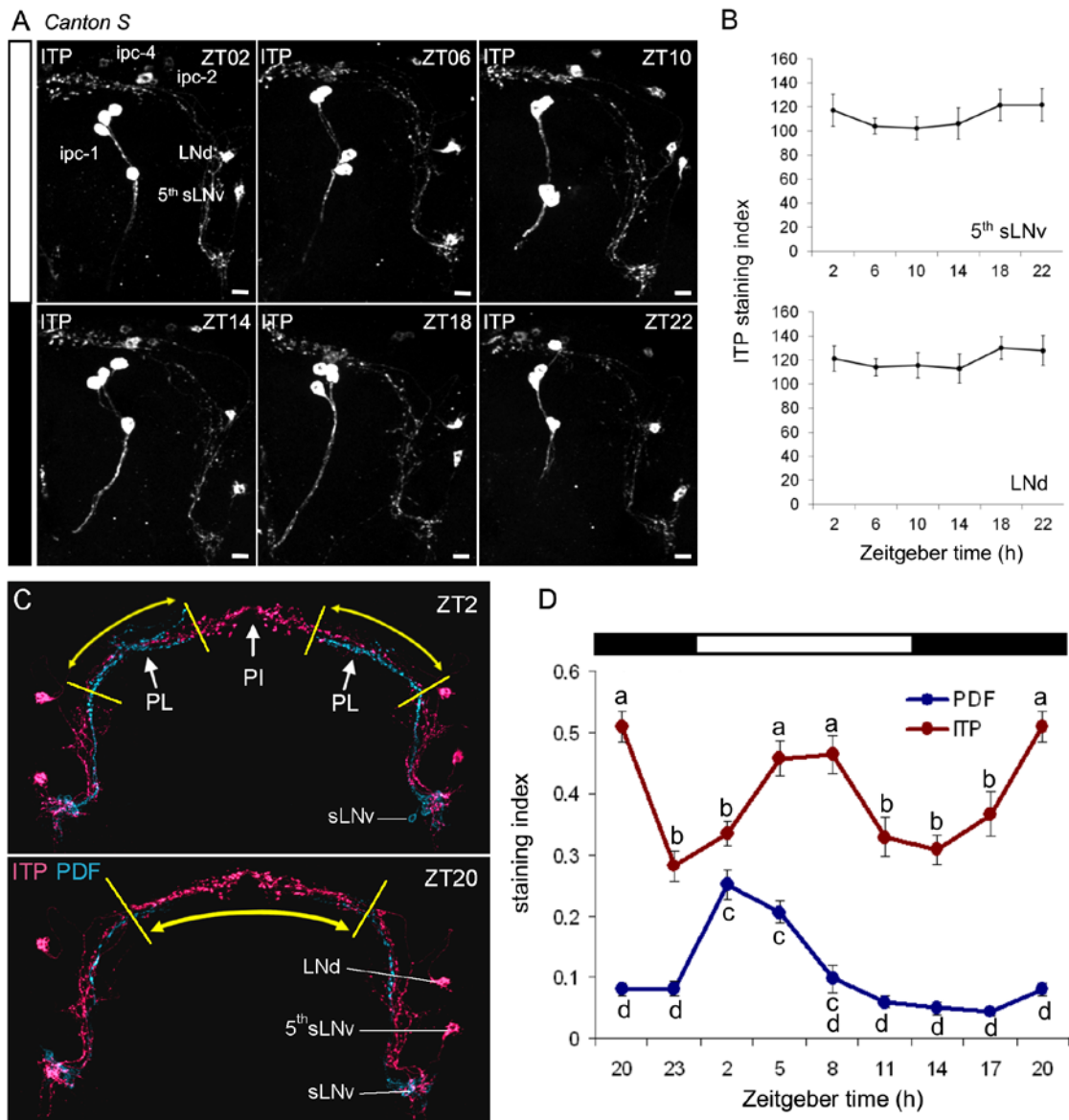


FIGURE 2

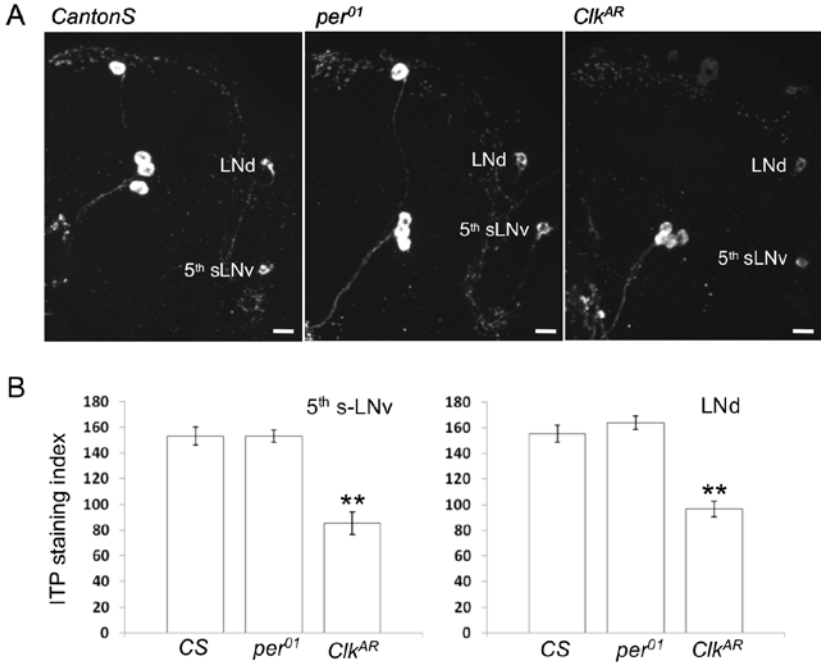


FIGURE 3

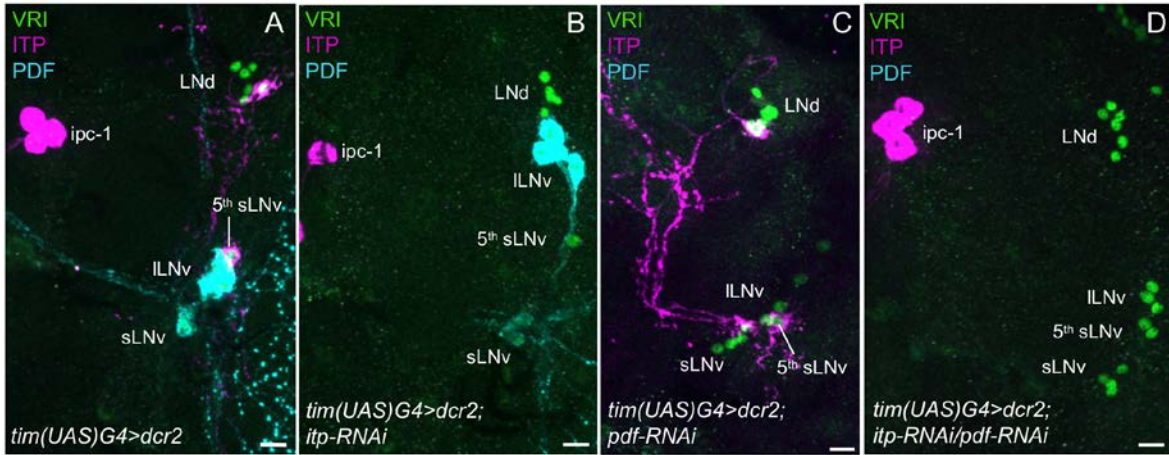


FIGURE 4

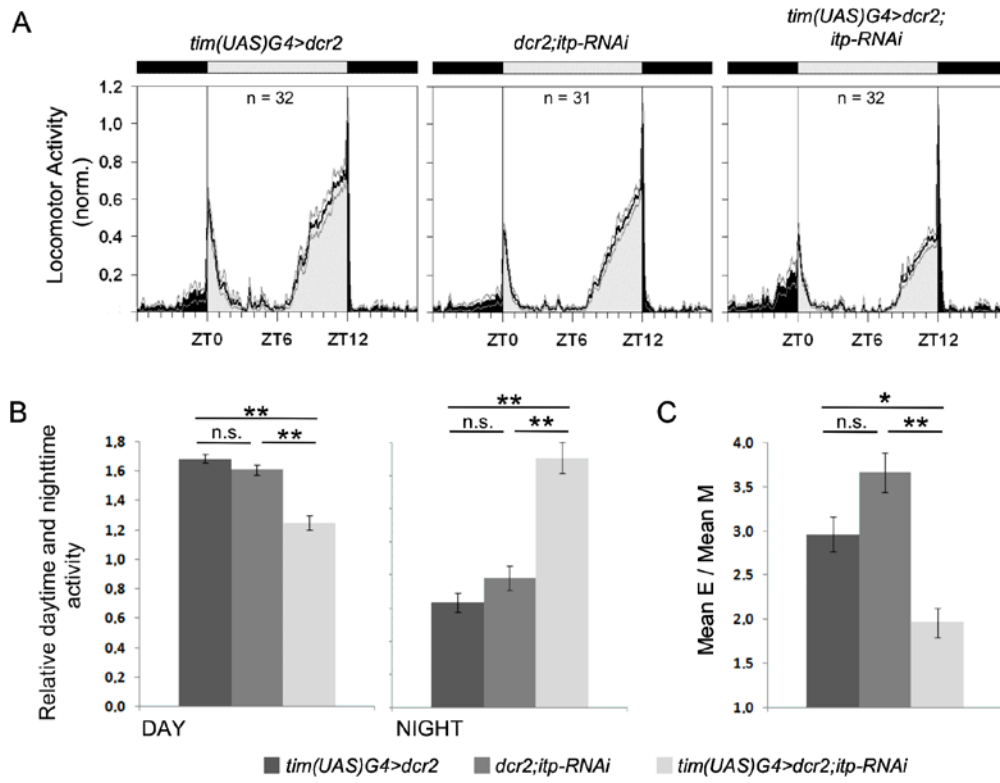


FIGURE 5

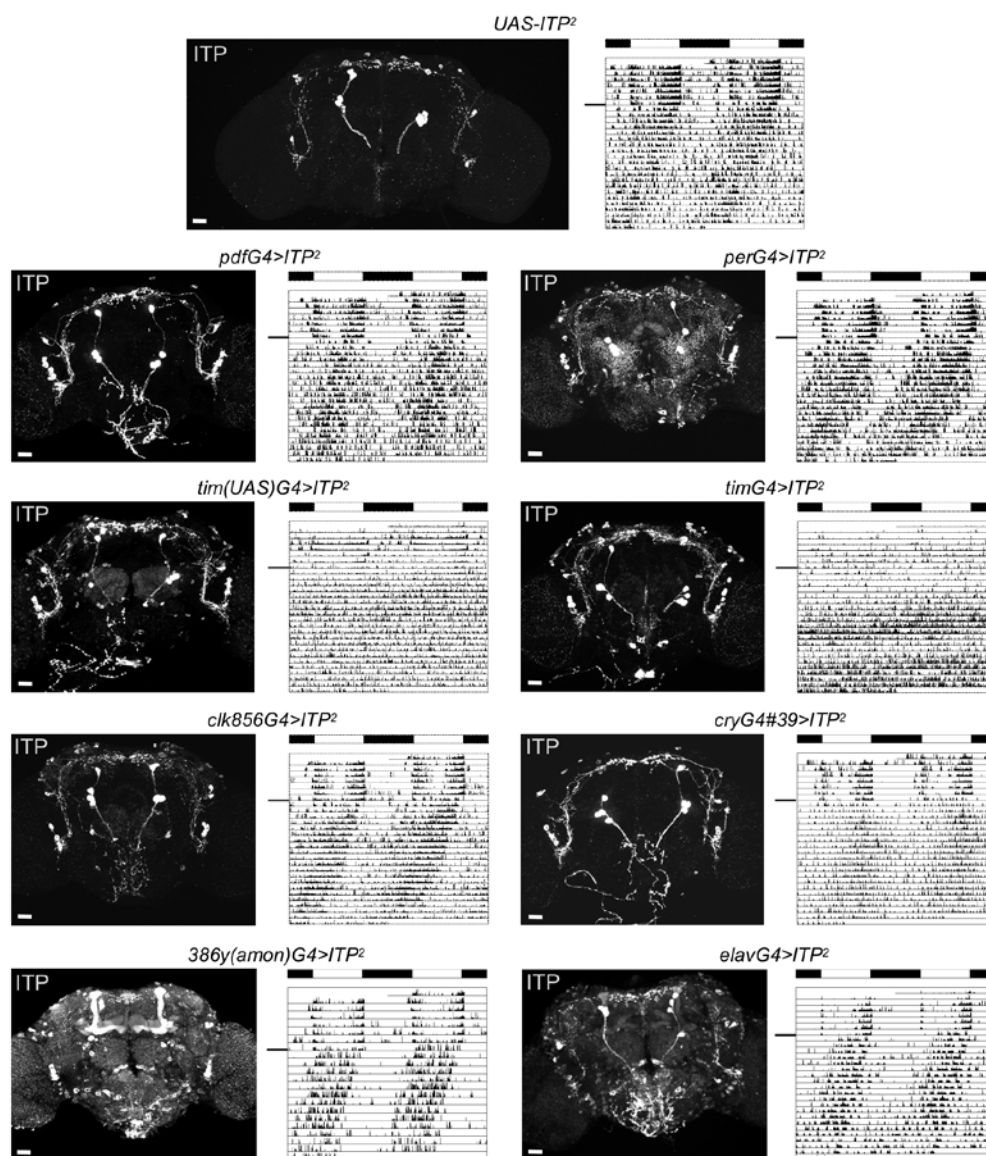


FIGURE 6

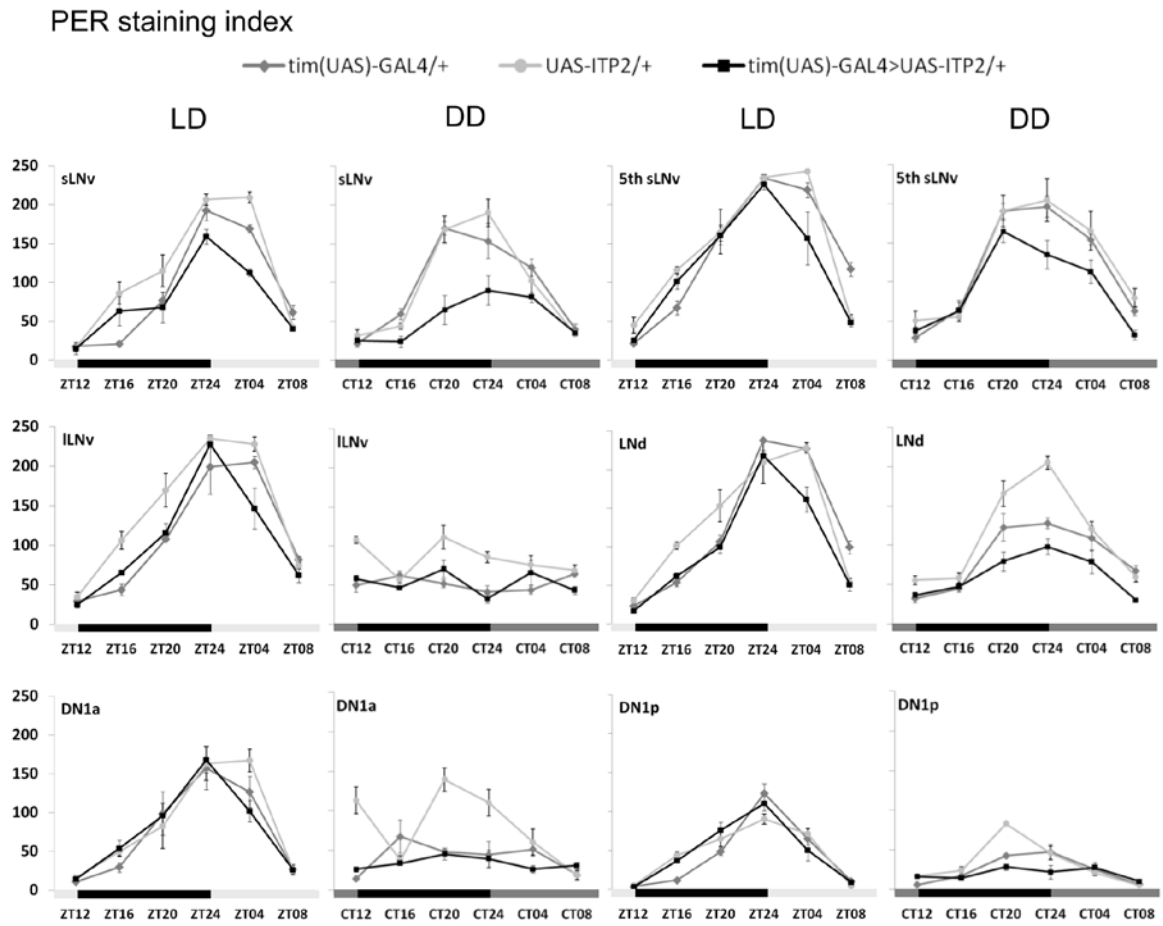


FIGURE 7

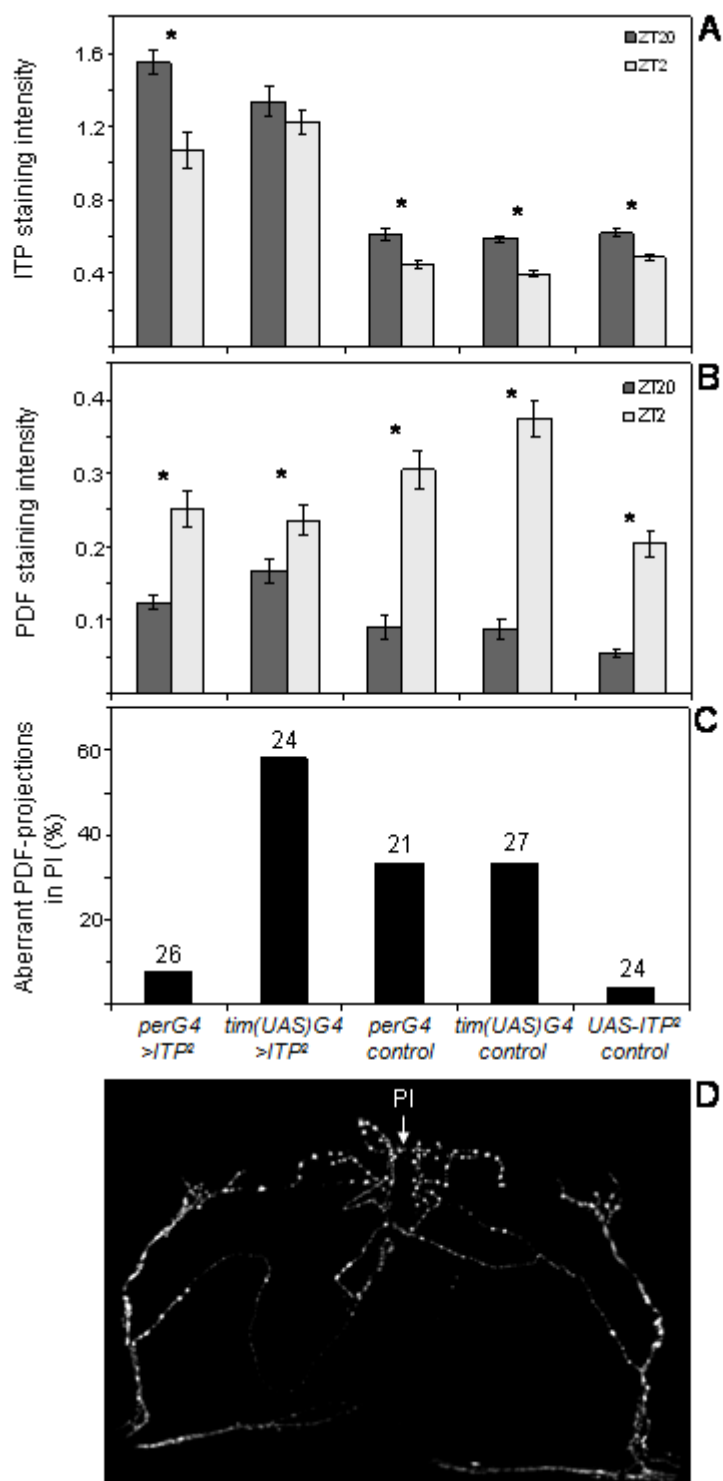


FIGURE 8

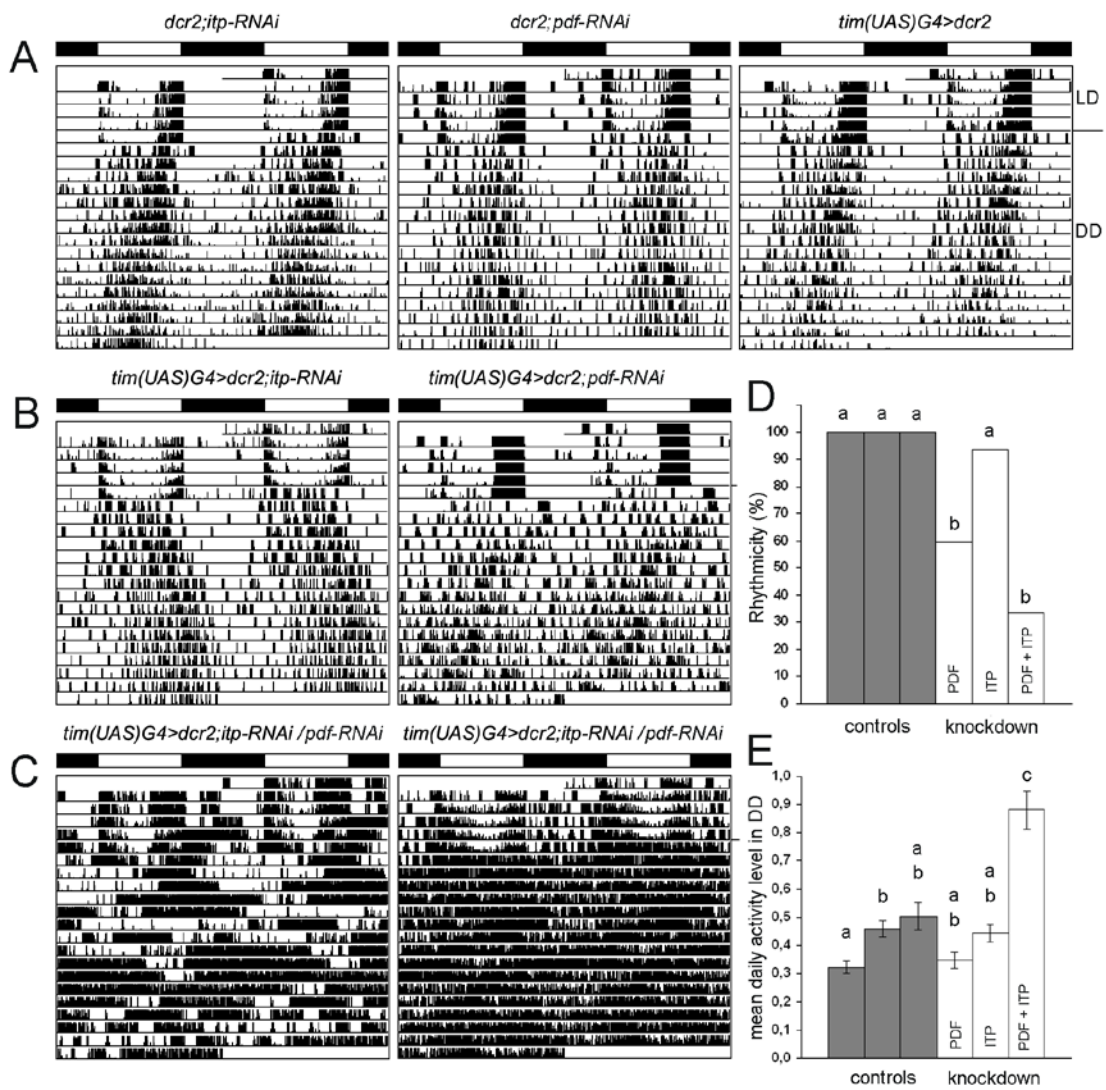


FIGURE 9

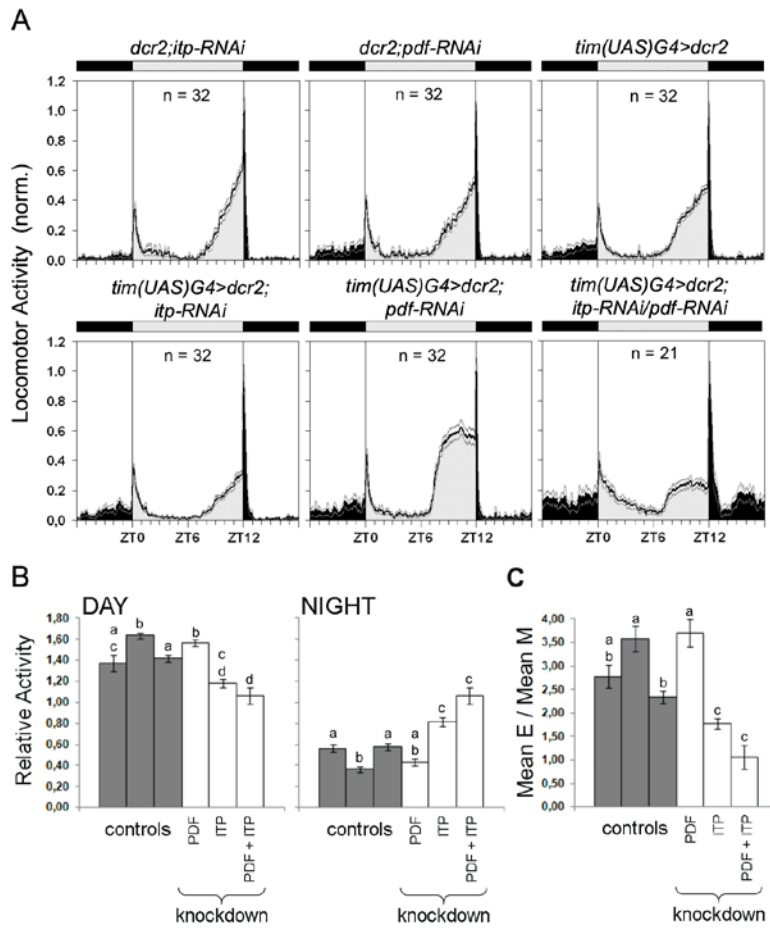


FIGURE 10

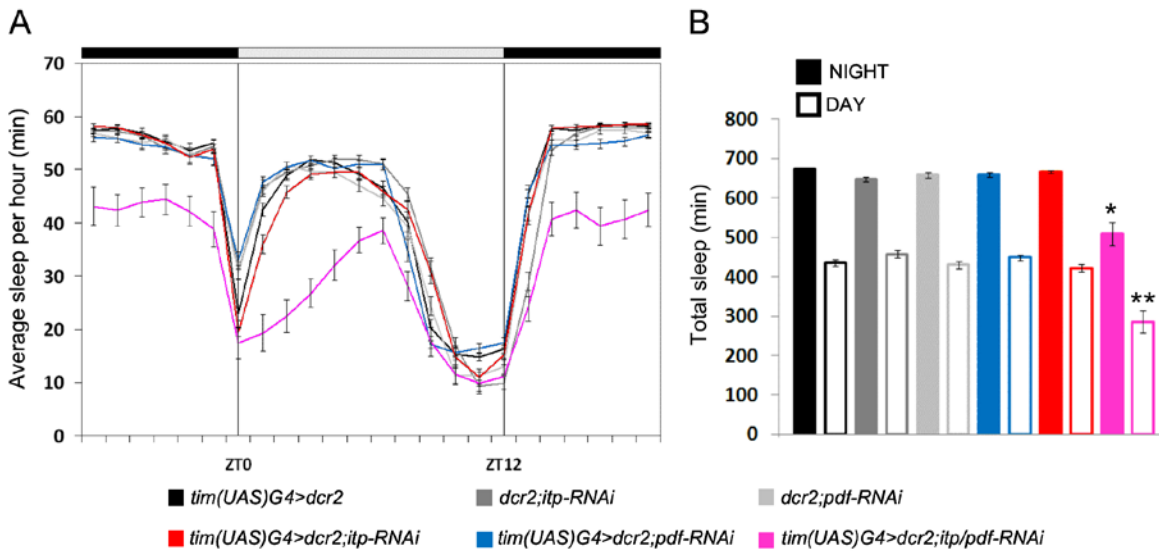


Table 1: Rhythmicity data of ITP-knockdown flies, PDF-knockdown flies and ITP/PDF-double-knockdown flies and controls in constant darkness (DD). Percentage of rhythmicity and period lengths of ITP-knockdown flies and PDF-knockdown flies were statistically compared to the data of the two respective genetic controls. * indicate significant differences in period length (for statistical values, see Figure legend 8). ** indicate highly significant differences in the percentage of rhythmic flies (for statistical values, see Figure legend 8).

Genotype	period (SEM) in h (n rhythmic flies)	power (SEM)	% rhythmic flies
tim(UAS)G4>dcr2	23.7 (0.05) (32)	22.8 (0.68)	100
dcr2;itp-RNAi	23.9 (0.05) (28)	35.1 (2.00)	100
tim(UAS)G4>dcr2;itp-RNAi	24.1 (0.08) (30)*	34.1 (1.96)	94
dcr2;pdf-RNAi	23.8 (0.06) (32)	36.1 (2.29)	100
tim(UAS)G4>dcr2;pdf-RNAi	23.4 (0.09) (19)*	16.4 (0.44)	59**
tim(UAS)G4>dcr2;pdf-RNAi/itp-RNAi	- (-) (8)	- (-)	38**

Table 2: Rhythmicity data of ITP-overexpressing flies and controls in constant darkness (DD).

Percentages of rhythmicity and period lengths of ITP-overexpressing strains were always compared with the respective *GAL4*-control and *UAS-ITP²*-control. ** indicate highly significant differences (*tim(UAS)-G4>ITP²* $\chi^2=73,5097$, $p<0.0001$; *tim-G4>ITP²* $\chi^2=56,7964$, $p<0.0001$).

genotype	period (SEM) in h (n rhythmic flies)	power (SEM)	% rhythmic flies
UAS-ITP2/+ (ITP2)	23.4 (0.07) (30)	29.6 (1.2)	100
tim(UAS)G4/+	24.1 (0.04) (30)	39.9 (2.30)	97
tim(UAS)G4>ITP2	25.0 (0.25) (2)	19.8 (2.16)	7**
timG4/+	24.6 (0.11) (23)	22.2 (1.18)	74
timG4>ITP2	- (-) (0)	- (-)	0**
pdfG4/+	24.4 (0.06) (30)	31.7 (1.59)	97
pdfG4>ITP2	23.7 (0.10) (31)	21.4 (0.70)	97
perG4	25.3 (0.16) (31)	32.1 (2.03)	97
perG4>ITP2	23.7 (0.04) (29)	29.1 (1.66)	100
clk856G4/+	23.8 (0.04) (32)	41.0 (1.89)	100
clk856G4>ITP2	23.3 (0.04) (32)	35.2 (1.82)	100
cryG439/+	25.2 (0.16) (24)	22.9 (1.60)	75
cryG439>ITP2	23.9 (0.06) (26)	21.5 (1.21)	81
elavG4/+	23.7 (0.06) (25)	23.8 (1.73)	83
elavG4>ITP2	23.6 (0.06) (20)	28.7 (2.53)	100
386y(amon)G4/+	23.1 (0.77) (31)	29.1 (2.04)	97
386y(amon)G4>ITP2	23.5 (0.05) (27)	26.7 (1.19)	100

Appendix

Additional Material

Table 9: Buffers and Media.

Buffer/Medium name	Ingredients/Source
TAE (Tris Acetate-EDTA)	0.5x, SIGMA-Aldrich (10x stock)
Na-Acetate	3M, pH 5.2
Phosphate Buffer (PB)	0.1 M Na ₂ HPO ₄ / NaH ₂ PO ₄ ; at the ratio of 4:1 for pH 7.2-7.4
Phosphate Buffered Saline (PBS)	1x, pH 7.4, SIGMA-Aldrich (10x stock)
Phosphate Buffer + TrX-100 (PBT)	0.1M PB + TrX-100 (0.1% or 0.5%), pH 7.4
Phosphate Buffered Saline + TrX-100	1x PBS + TrX-100 (0.1% or 0.5%), pH 7.4
Na-Azide (NaN ₃)	0.02% in 1x PBS (from 2% stock, SIGMA-Aldrich)
Squishing buffer	50 mM NaOH, 1 M Tris-HCl, pH 8.0
Paraformaldehyde	4%, in 0.1M PBT (0.1% TrX-100)
Hemolymph-like Saline (HL3)	70mM NaCl, 5mM KCl, 1.5mM CaCl ₂ , 20mM MgCl ₂ , 10mM NaHCO ₃ , 5mM trehalose, 115mM sucrose, 5mM HEPES, pH 7.1
TriKinetics medium	4% sucrose; 2% agar-agar (Danish)
LB ₀ liquid medium	1% bacto-tryptone; 0.5% bacto-yeast extract; 1% NaCl; 0.3% NaOH; pH 7.0
LB _{Amp} liquid medium	LB ₀ with 50-100 µg/ml Ampicillin
LB _{Amp} agar plates	LB _{Amp} liquid medium (100 µg/ml Ampicillin) with 1.5% bacto-agar

Table 10: Commercially available kits used in this thesis.

Kit	Application	Source
ZYMO Quick-RNA™ MicroPrep	RNA extraction	ZYMO Research Corporation
gDNA wipe-out	removal of genomic DNA	QIAGEN
VWR Taq DNA Polymerase Master Mix Kit	PCR	VWR
QuantiTect Reverse Transcription Kit	Reverse Transcription	QIAGEN
innuPREP DOUBLEpure Kit	DNA extraction from agarose gel slices	Biometra, analytikJena
SIGMA GenElute™ Plasmid Midiprep Kit	Plasmid DNA extraction (mid-preparation)	SIGMA-Aldrich
MSB®Spin PCRapace (250)	DNA purification	INVITEK
SensiFAST™ SYBR No-ROX Kit	qPCR	BIOLINE

Table 11: Primer pairs used for PCR and qPCR.

Primer	Sequence from 5' to 3'	Application/Source
ITP-PE Fw (5')	ACGAATTCGTTTCTGCCCCACAACAACAC	ITP-PE cDNA cloning; SIGMA-Aldrich
ITP-PE Rev (3')	TCCTCTAGAATCGCACTTTACTTGCGACC	
ITP-gene part Fw (5')	ATAAACTCGAGTGCCAGAGAATC	sequencing of genomic <i>itp</i> gene part; SIGMA-Aldrich
ITP-gene part Rev (3')	GCTTACCTTAGGCGCTTGTTTCG	
ITP-pUAST Fw (5')	CGCAGCTGAACAAGCTAAACAATC	sequencing of ITP-pUAST vector; SIGMA-Aldrich
sNPF Fw (5')	TCAGCTTTATGCTCGCTTGCCTC	qPCR to determine snpf-RNAi efficiency; SIGMA-Aldrich
sNPF Rev (3')	ACATAGAGGCCCGAAAGCTGTA	
Tub Fw (5')	TCTGCGATTCGATGGTGCCCTTAAC	qPCR reference; SIGMA-Aldrich
Tub Rev (3')	GGATCGCACTTGACCATCTGGTTGGC	qPCR reference; SIGMA-Aldrich

Table 12: Other Reagents and Substances.

Reagent	Application	Source
pUAST vector	UAS-line generation	A. Fiala
NEB 10-beta competent <i>E. coli</i>	Transformation of large DNA plasmids	New England BioLabs
RNAse free water	Molecular Biology	SIGMA-Aldrich
GelRed [®] Nucleic Acid Gel Stain	DNA Staining in Gel Electrophoresis	Biotium
Medori Green Advanced DNA Stain	DNA Staining in Gel Electrophoresis	NIPPON Genetics EUROPE
Isopropanol (100%)	DNA precipitation	SIGMA-Aldrich
Ethanol (70%)	DNA precipitation	SIGMA-Aldrich
Fast Digest [®] EcoRI	Restriction Enzyme	Fermentas
Fast Digest [®] XbaI	Restriction Enzyme	Fermentas
T4 DNA Ligase, 5u/μl	DNA Ligation	Fermentas
Fast AP [™] Thermosensitive Alkaline Phosphatase	Phosphatase Reaction	Fermentas
10x DNA Loading Dye	Gel Electrophoresis	
GeneRuler 1kb DNA Ladder	DNA Ladder	Fermentas
peqGOLD Universal Agarose	Gel Electrophoresis	Peqlab
Normal Goat Serum	4% in PB/PBS, Blocking solution	SIGMA-Aldrich
Fixogum	Removable cover slip sealing	Marabu
Vectashield	mounting medium for fluorescence microscopy	Vector Laboratories
Dimethylsulfoxide (DMSO)	peptide dilution	SIGMA-Aldrich
Forskolin	positive control (cAMP Imaging)	SIGMA-Aldrich
Carbamylcholine (Carbachol)	positive control (Ca ²⁺ imaging)	SIGMA-Aldrich

Abbreviations

aa	amino acid(s)	NGS	Normal Goat Serum
AcCh	Acetylcholine	LED	light emitting diode
AMP	Adenosine Monophosphate	LN	Lateral Neurons
BL	Bloomington Stock Center	NPF	Neuropeptide F
°C	degree Celsius	NPFR	NPF receptor
Ca ²⁺	Calcium	PB	Phosphate Buffer
cAMP	cyclic AMP	PBS	Phosphate Buffered Saline
cDNA	complementary DNA	PCR	Polymerase Chain Reaction
CFP	Cyan Fluorescent Protein	PDF	Pigment Dispersing Factor
CRY	Cryptochrome	PDFR	PDF receptor
CT	Circadian Time	PDP1	Par Domain Protein 1
DD	constant darkness	PER	Period
Δ	delta/difference	PFA	Paraformaldehyde
DGRC	<i>Drosophila</i> Genetic Resource Center	+	positive
DN	Dorsal Neurons	qPCR	quantitative PCR
DNA	Deoxyribonucleic Acid	RNA	Ribonucleic Acid
DSSC	<i>Drosophila</i> Species Stock Center	RNAi	RNA interference
E	Evening	Rev	Reverse
e.g.	for example	s	second
et al.	et alii (and others)	SD	Standard Deviation
F	Fluorescence	SEM	Standard Error of the Mean
FRET	Fluorescence Resonance Energy Transfer	sNPF	short Neuropeptide F
Fw	Forward	sNPFR	sNPF receptor
GFP	Green Fluorescent Protein	TIM	Timeless
GPCR	G-protein coupled receptor	TrX	Triton-X 100
h	hour	UAS	Upstream Activating Sequence
ITP	Ion Transport Peptide	VDRC	Vienna <i>Drosophila</i> RNAi Center
LD	light/dark	VRI	Vrille
M	Morning	YFP	Yellow Fluorescent Protein
μm	micrometer	ZT	Zeitgeber Time
μl	microliter		
ml	milliliter		
min	minute		
NaN ₃	Sodium Azide		
-	negative		

Acknowledgements

First of all, I would like to thank Prof. Dr. Charlotte Förster for allowing me to conduct this research project under her supervision, for always giving me as much of her valuable time as she could spare and for her encouragement and support.

I am grateful to Prof. Dr. Thomas Raabe for being the second referee of this doctoral thesis and for fruitful discussions at our meetings; and to Assistant Prof. Ori T. Shafer for being my external supervisor, who welcomed me in his group of friendly people at the University of Michigan, where I was allowed to spend three labor intensive, but awesome months.

My very special thanks go to Assistant Prof. Taishi Yoshii, who took care of me from the very beginning, teaching me what it means to be a good scientist always being an example of organized and creative scientific practice. Although being almost ten thousand kilometers away, he never seemed far (thanks to Skype!) and I will always appreciate him not only for being a great colleague, but also for being a friend.

Further, I would like to thank all coauthors for their contributions to the publications included in this thesis.

A very big THANK YOU to all people of the Department of Neurobiology and Genetics for the pleasant atmosphere in the lab, for the great teamwork when experiments seemed too huge to master them on your own, and for numerous entertaining hours we enjoyed off work.

And finally, I would like to thank my husband, Sebastian, and my parents for always being supportive in any imaginable kind of way.

Curriculum vitae

Personal Profile

Name	Christiane Luibl, née Hermann
Date/Place of Birth	18. December 1984; 84307 Eggenfelden, Germany
Nationality	German

Academic Education

Jan 2014	Doctoral Thesis Submission
Apr-Jul 2011	Visiting Scholar at the Department of Molecular, Cellular and Developmental Biology at the University of Michigan, USA (Ass. Prof. PhD Orié T. Shafer)
2010-present	Doctoral student in the Graduate School of Life Sciences at the University of Würzburg (Department of Neurobiology and Genetics, Prof. Dr. Charlotte Förster)
2009	Diploma thesis at the Department of Cellular and Developmental Biology at the University of Regensburg and Graduation with a Dipl. biol. degree (Prof. Dr. Charlotte Förster)
Apr-Jul 2008	Enrolment into the Practicum Program of the University of New South Wales, Sydney, Australia; Internship in ecological field work at the Fowlers Gap Arid Zone Field Station (Prof. David Croft); partly funded by the DAAD
2004-2009	Undergraduate studies of Biology at the University of Regensburg with focus on Zoology, Cellular and Developmental Biology and Microbiology

Würzburg, 13. Jan 2014

Place, Date

Signature

Declarations

“Dissertation Based on Several Published Manuscripts“

Statement of individual author contributions and of legal second publication rights

Publication (complete reference): **Christiane Hermann**, Taishi Yoshii, Verena Dusik and Charlotte Helfrich-Förster. (2012) The neuropeptide F immunoreactive clock neurons modify evening locomotor activity and free-running period in *Drosophila melanogaster*. J Comp Neurol 520: 970-987

Participated in	Author Initials, Responsibility decreasing from left to right				
Study Design	C. H.-F.	T. Y.	C. H.		
Data Collection	C. H.	V. D.			
Data Analysis and Interpretation	C. H.	T. Y.	C.H.F.		
Manuscript Writing	C. H.	C. H.-F.	T. Y.		

Publication (complete reference): **Christiane Hermann**, Rachele Saccon, Pingkalai R. Senthilan, Lilith Domnik, Heinrich Dirksen, Taishi Yoshii and Charlotte Helfrich-Förster. (2013) The circadian clock network in the brain of different *Drosophila* species. J Comp Neurol 521(2): 367-388

Participated in	Author Initials, Responsibility decreasing from left to right				
Study Design	C. H.-F.	C. H.	T. Y.		
Data Collection	C. H.	P. R. S.	R. S.	L. D.	
Data Analysis and Interpretation	C. H.	P. R. S.	C. H.-F.	T. Y.	H. D.
Manuscript Writing	C. H.	C. H.-F.			

Publication (complete reference): **Christiane Hermann-Luibl**, Taishi Yoshii, Pingkalai R. Senthilan, Heinrich Dirksen and Charlotte Helfrich-Förster. (2013) The Ion Transport Peptide is a new functional clock neuropeptide in *Drosophila melanogaster*. *submitted*

Participated in	Author Initials, Responsibility decreasing from left to right				
Study Design	C. H.-F.	T. Y.	C. H.-L.	P. R. S.	H. D.
Data Collection	C. H.-L.	T. Y.	P. R. S.	H. D.	
Data Analysis and Interpretation	C. H.-L.	C. H.-F.	T. Y.	H. D.	
Manuscript Writing	C. H.-F.	C. H.-L.	T. Y.		

Explanations (if applicable): Manuscript was submitted to Journal of Neuroscience.

I confirm that I have obtained permission from both the publishers and the co-authors for legal second publication.

I also confirm my primary supervisor's acceptance.

Christiane Luibl (née Hermann) 13. Jan 2014 Würzburg

Doctoral Researcher's Name

Date

Place

Signature

Affidavit

I hereby confirm that my thesis "The Role of the Neuropeptides NPF, sNPF, ITP and PDF in the Circadian Clock of *Drosophila melanogaster*" is the result of my own work. I did not receive any help or support from commercial consultants. All sources and/or materials applied are listed and specified in the thesis.

Furthermore, I confirm that this thesis has not yet been submitted as part of another examination process neither in identical nor in similar form.

Würzburg, 13. Jan 2014

Place, Date

Signature

Eidesstattliche Erklärung

Hiermit erkläre ich an Eides statt, die Dissertation „Die Rolle der Neuropeptide NPF, sNPF, ITP und PDF in der Circadianen Uhr von *Drosophila melanogaster*“ eigenhändig, d.h. insbesondere selbständig und ohne Hilfe eines kommerziellen Promotionsberaters, angefertigt und keine anderen als die von mir angegebenen Quellen und Hilfsmittel verwendet zu haben.

Ich erkläre außerdem, dass die Dissertation weder in gleicher noch in ähnlicher Form bereits in einem anderen Prüfungsverfahren vorgelegen hat.

Würzburg, 13. Januar 2014

Ort, Datum

Unterschrift